



R. M. FARMER

PH. D.



107  
890  
THS

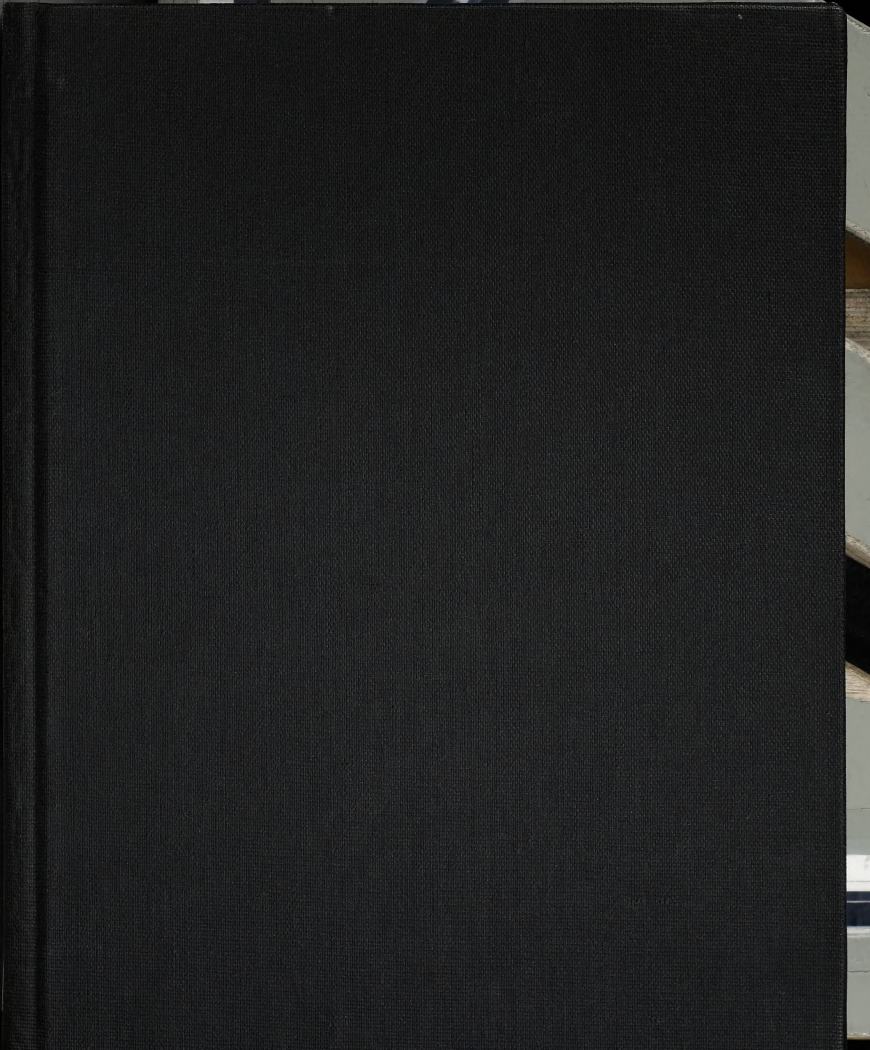
PH. D.

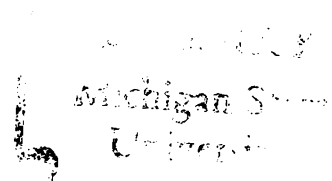
PH. D.

107  
890  
THS









This is to certify that the  
thesis entitled

Spectroscopic and Electrochemical Studies of  
Ion Solvation and Complexation in Various Solvents

presented by

Richard M. Farmer

has been accepted towards fulfillment  
of the requirements for

Ph.D. degree in Chemistry

A handwritten signature in cursive script, which appears to read "Richard M. Farmer", is written over a horizontal line.

Major professor

Date August 6, 1981



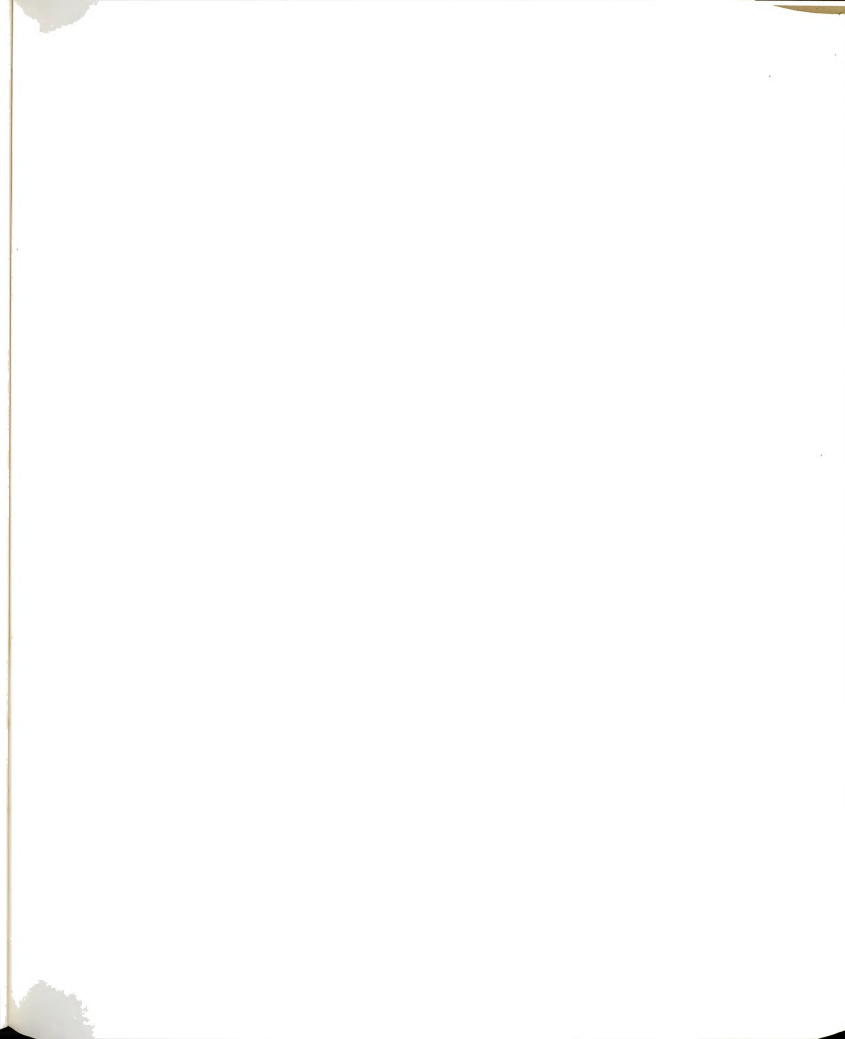
OVERDUE FINES:

25¢ per day per item

RETURNING LIBRARY MATERIALS:

Place in book return to remove  
charge from circulation records

Two vertical lines are drawn on the page, one on the left and one on the right, extending downwards from the text area. These lines appear to be part of a form or a placeholder for information.





SPECTROSCOPIC AND ELECTROCHEMICAL STUDIES OF  
ION SOLVATION AND COMPLEXATION  
IN VARIOUS SOLVENTS

By

Richard M. Farmer

A DISSERTATION

Submitted to  
Michigan State University  
in partial fulfillment of the requirements  
for the degree of

DOCTOR OF PHILOSOPHY

Department of Chemistry

1981



ABSTRACT

SPECTROSCOPIC AND ELECTROCHEMICAL STUDIES OF  
ION SOLVATION AND COMPLEXATION  
IN VARIOUS SOLVENTS

By

Richard M. Farmer

Calcium-43 nuclear magnetic resonance (NMR) behavior of a number of calcium salts was studied in acetone, dimethylsulfoxide, dimethylformamide (DMF), ethylene glycol, formamide, methanol, propylene carbonate, tetramethylguanidine, and water as a function of salt concentration. There was evidence for ion-pairing for the chlorides, bromides, perchlorates, and nitrates in all solvents except DMF. The complexation of  $\text{Ca}^{2+}$  ion with ethylenediaminetetraacetic acid (EDTA), and crown ethers 18-crown-6 (18C6) and 15-crown-5 (15C5) was also studied. The complexes with EDTA and 18C6 exhibited a slow exchange of the  $^{43}\text{Ca}$  ion between the free and complexed state, resulting in two resonances. There was no evidence for  $\text{Ca}^{2+}$  ion complexation with 15C5.

The tetraphenylarsonium (and tetraphenylphosphonium)

Sept 1964

17  
18  
19  
20  
21  
22  
23  
24  
25  
26  
27  
28  
29  
30  
31  
32  
33  
34  
35  
36  
37  
38  
39  
40  
41  
42  
43  
44  
45  
46  
47  
48  
49  
50  
51  
52  
53  
54  
55  
56  
57  
58  
59  
60  
61  
62  
63  
64  
65  
66  
67  
68  
69  
70  
71  
72  
73  
74  
75  
76  
77  
78  
79  
80  
81  
82  
83  
84  
85  
86  
87  
88  
89  
90  
91  
92  
93  
94  
95  
96  
97  
98  
99  
100

tetraphenylborate single ion assumption was studied using  $^{75}\text{As}$ ,  $^{31}\text{P}$ ,  $^{11}\text{B}$ ,  $^{13}\text{C}$ , and proton NMR. Due to broad resonance lines (1000 Hz),  $^{75}\text{As}$  NMR was not sufficiently precise to test the validity of the assumption. Phosphorous-31 and boron-11 NMR data show that the central ion is not entirely shielded from the solvent, although ion-ion interactions are negligible. Carbon-13 data indicate that the charge is not localized on the central atom. Both carbon-13 and proton data indicate that tetraphenylarsonium, tetraphenylphosphonium, and tetraphenylborate ion are not solvated equivalently. Ion-ion interactions, as seen by  $^{13}\text{C}$  and proton NMR, are negligible. Care is advised when using this assumption to calculate free energies of transfer for single ions.

Complexation of phosphonoacetic acid (PAA) with calcium ion was studied potentiometrically in aqueous solution. The thermodynamic formation constants for the deprotonated and monoprotinated PAA complexes with  $\text{Ca}^{2+}$  were found to be:  $\log K_f = 4.68 \pm 0.03$  and  $\log K_f = 2.68 \pm 0.08$ , respectively. The thermodynamic quantities

$$\Delta G^\circ = -6.38 \quad 0.07 \text{ kcal/mole}$$

$$\Delta H^\circ = 0.6 \quad 0.2 \text{ kcal/mole}$$

$$\Delta S^\circ = 21.4 \quad 0.7 \text{ cal/}^\circ\text{K-mole}$$

were calculated from the temperature dependence of the formation constant for the deprotonated PAA complex with

$\text{Ca}^{2+}$  ion. The formation constant of manganese(II) ion with PAA was determined using electron spin resonance, while the complexation constants of copper(II), lead(II), and thallium(I) with PAA were determined using cyclic voltammetry. The silver(I) ion complexation constant with PAA was measured potentiometrically. The complexation of calcium(II), manganese(II), and thallium(I) ion was studied with the ligands 3-phosphonopropionic acid and phosphonoformic acid, resulting in the determination of formation constants for these ligands.



To Jane

"Love is patient, love is kind, and is not jealous;  
love does not brag and is not arrogant,

does not act unbecomingly; it does not seek its own, is  
not provoked, does not take into account a wrong suffered,  
does not rejoice in unrighteousness, but rejoices with  
the truth;

bears all things, believes all things, hopes all things,  
endures all things.

1 Cor. 13:4-7





## ACKNOWLEDGMENTS

The author wishes to thank Professor Alexander I. Popov for his guidance, counsel, and patience in the field of chemical research and scientific writing.

The contributions of Professor Stanley R. Crouch as second reader are gratefully appreciated.

The author wishes to acknowledge the advice and assistance of the following individuals: Dr. Thomas V. Atkinson, in the area of computer programming and usage, Professor Michael J. Weaver in electrochemistry, and Professor Gerald T. Babcock in the field of electron spin resonance.

The friendship and help of Dr. A. I. Popov's group is greatly appreciated, as it made life at Michigan State University infinitely easier and more pleasant.

The help of Frank Bennis, Wayne Burkhardt, and Tom Clark in the maintenance of the NMR instruments is acknowledged.

Financial aid from the Department of Chemistry, Michigan State University, the National Science Foundation, and Union Carbide was appreciated.

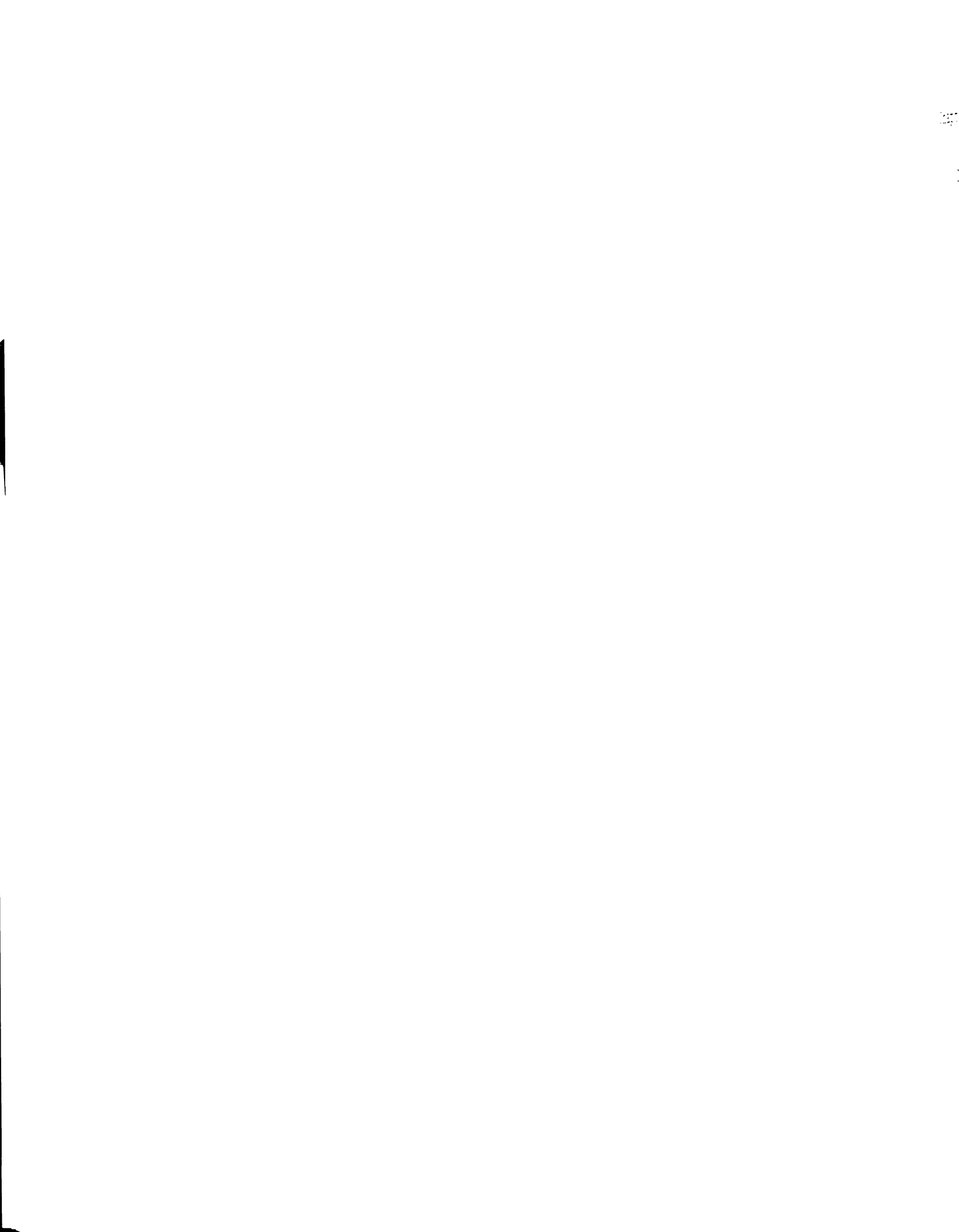
Finally, to my wife, Jane, whose love, encouragement, and patience were major factors in the successful completion of this research project, thank you.

## TABLE OF CONTENTS

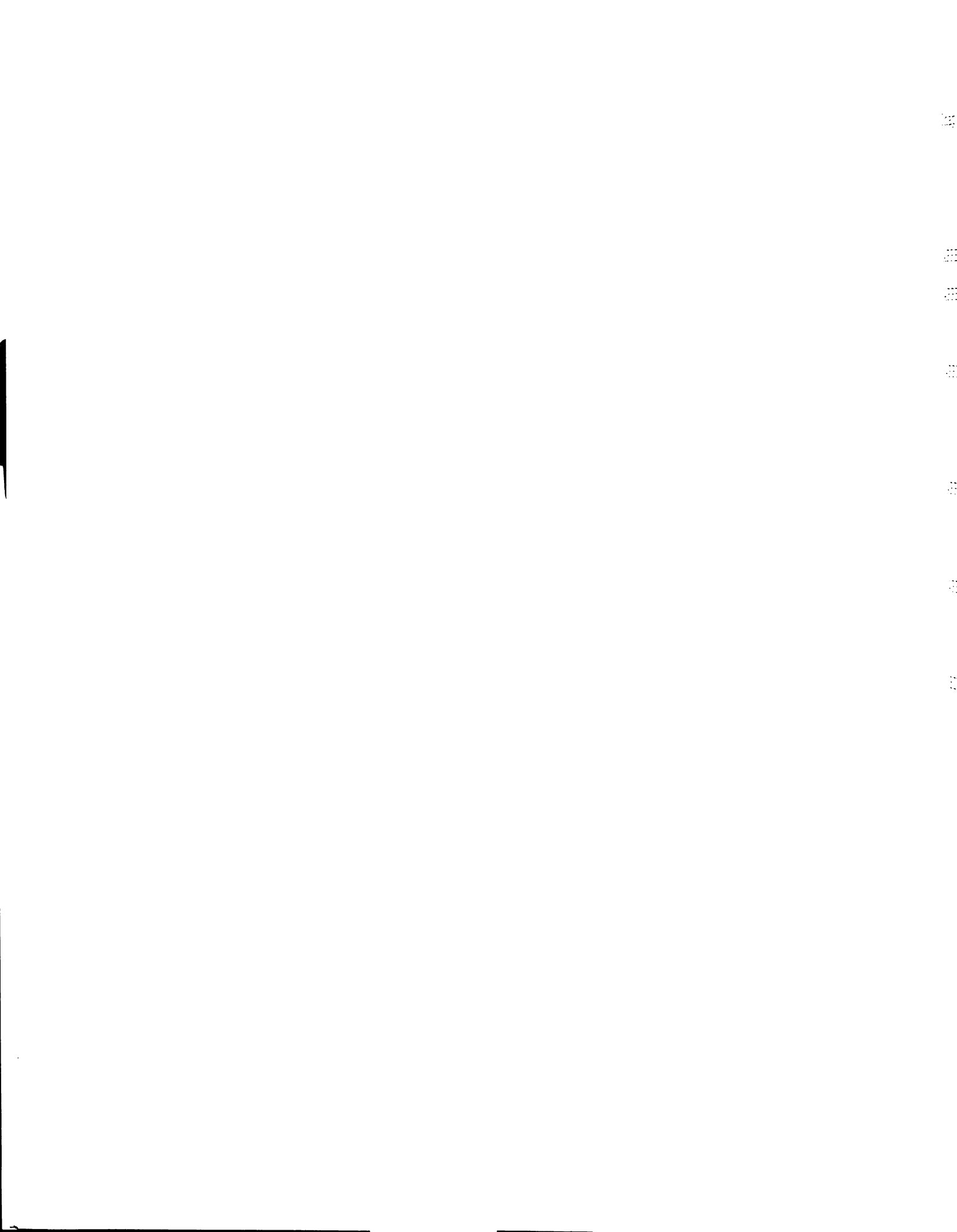
Chapter	Page
LIST OF TABLES. . . . .	ix
LIST OF FIGURES . . . . .	xvii
PART I - Calcium-43 NMR Studies . . . . .	1
CHAPTER I - HISTORICAL REVIEW . . . . .	2
1.1. Introduction. . . . .	3
1.2. Calcium-43 NMR. . . . .	4
1.3. Ligands . . . . .	8
1.4. Conclusions . . . . .	10
CHAPTER II - MATERIALS AND METHODS. . . . .	12
2.1. Reagents. . . . .	13
2.1.1. Salts . . . . .	13
2.1.2. Purification Procedures . . . . .	14
2.1.3. Drying Procedures . . . . .	14
2.2. Ligands . . . . .	15
2.3. Solvents. . . . .	16
2.4. Molecular Sieves. . . . .	17
2.5. Nuclear Magnetic Resonance. . . . .	17
2.5.1. Varian CFT-20 NMR Spectrometer. . . . .	17
2.5.2. Bruker WH-180 Superconducting NMR Spectrometer. . . . .	18
2.5.3. Bruker WM-250 Superconducting NMR Spectrometer. . . . .	18
2.5.4. Operating Procedures. . . . .	18

Chapter	Page
2.6. Miscellaneous Instrumentation . . . . .	20
2.7. Data Handling . . . . .	20
CHAPTER III - Results and Discussion. . . . .	21
3.1. Introduction. . . . .	22
3.2. General Information on Calcium-43 NMR . . . . .	23
3.3. Aqueous Studies - Chemical Shifts. . . . .	26
3.4. Linewidths. . . . .	33
3.5. Studies in Nonaqueous Solutions . . . . .	33
3.5.1. Chemical Shifts . . . . .	33
3.5.2. Linewidths. . . . .	43
3.6. Gutmann Donor Number Cor- relation. . . . .	47
3.7. Complexation. . . . .	49
3.8. Conclusions . . . . .	55
PART II - AN NMR INVESTIGATION OF THE REFERENCE ELECTROLYTE ASSUMPTION FOR THE DETERMINATION OF SINGLE ION MEDIUM EFFECTS. . . . .	56
CHAPTER I - INTRODUCTION AND HISTORICAL . . . . .	57
1.1. Introduction. . . . .	58
1.2. Historical. . . . .	61
1.3. Reference Electrolyte Assumption. . . . .	62
1.4. A Nuclear Magnetic Resonance Study . . . . .	69
1.4.1. Arsenic-75 NMR. . . . .	69
1.4.2. Phosphorous-31 NMR. . . . .	70

Chapter	Page
1.4.3. Boron-11 NMR. . . . .	71
1.4.4. Carbon-13 and Proton. . . . .	72
1.5. Conclusions . . . . .	73
CHAPTER II - RESULTS AND DISCUSSION . . . . .	75
2.1. Introduction. . . . .	76
2.2. Phosphorous-31 NMR Results. . . . .	77
2.3. Arsenic-75 NMR Results. . . . .	81
2.4. Boron-11 NMR Results. . . . .	87
2.5. Carbon-13 NMR Results . . . . .	88
2.6. Proton NMR Results. . . . .	112
2.7. Summary and Conclusions . . . . .	140
PART III - PHOSPHONOACETIC ACID STUDIES . . . . .	142
CHAPTER I - HISTORICAL REVIEW . . . . .	143
1.1. Introduction. . . . .	144
1.1.1. Viral Replication . . . . .	146
1.1.2. Inhibition of the Viral Replication Path by PAA. . . . .	147
1.2. Toxicity of PAA . . . . .	150
1.3. Analogs of Phosphonoacetic Acid . . . . .	151
1.4. Chemical Properties of PAA and its Analogs . . . . .	152
1.5. Experimental Techniques . . . . .	153
1.5.1. Calcium Ion Selective Electrodes. . . . .	153
1.5.2. Manganese Electron Spin Resonance . . . . .	155
1.6. Conclusions . . . . .	158



Chapter	Page
CHAPTER II - MATERIALS AND METHODS. . . . .	159
2.1. Reagents. . . . .	160
2.2. Experimental Methods. . . . .	160
2.2.1. Electron Spin Resonance Spectroscopy. . . . .	160
2.2.2. Cyclic Voltammetry. . . . .	161
2.2.3. Potentiometry . . . . .	162
2.2.4. Coulometer. . . . .	165
2.3. Sample Preparation. . . . .	166
2.3.1. Manganese Electron Spin Resonance. . . . .	166
2.3.2. Cyclic Voltammetry. . . . .	168
2.3.3. Potentiometry . . . . .	169
2.4. Data Handling . . . . .	171
CHAPTER III - RESULTS AND DISCUSSION. . . . .	173
3.1. Complexation Studies of PAA . . . . .	174
3.1.1. Manganese Electron Spin Resonance . . . . .	174
3.1.2. Cyclic Voltammetry. . . . .	185
3.1.3. Potentiometric Studies. . . . .	196
3.2. Thermodynamics of Calcium Complexation with PAA . . . . .	202
3.3. Summary and Discussion. . . . .	206
3.4. Phosphono Acetic Acid Analogs . . . . .	209
3.4.1. Manganese Electron Spin Resonance. . . . .	210
3.4.2. Cyclic Voltammetry. . . . .	210
3.4.3. Potentiometry . . . . .	213
3.5. Thermodynamic Studies of 3-PAA Complexes . . . . .	218





Chapter	Page
3.6. Summary and Discussion. . . . .	219
3.7. Conclusion. . . . .	219
APPENDICES. . . . .	222
APPENDIX A - THE GENERAL USE OF THE NON- LINEAR CURVE FITTING ROUTINE KINFIT4. . . . .	222
APPENDIX B - DATA REDUCTION OF A POTEN- TIOMETRIC TITRATION FOR THE DETERMINATION OF COMPLEX FORMA- TION CONSTANTS USING THE COMPUTER PROGRAM MINIQVAD . . . . .	225
APPENDIX C - THE USE OF THE PROGRAM FARM2.TSK FOR THE DETERMINATION OF MONO- PROTONATED PAA-CALCIUM FORMATION CONSTANTS FROM POTENTIOMETRIC DATA . .	234
APPENDIX D - SOME CROWN AND CRYPTAND COMPLEX FORMATION CONSTANTS WITH MANGANESE (II) ION DETERMINED BY ELECTRON SPIN RESONANCE . . . . .	238
BIBLIOGRAPHY . . . . .	241

LIST OF TABLES

Table		Page
I	Properties of Selected Nuclei in NMR Spectroscopy. . . . .	24
II	Some Solvent Properties and Magnetic Susceptibility Corrections. . . . .	35
III	Linewidths of the Calcium-43 Resonance Signal in Some Solvents . . . . .	44
IV	A Comparison of the Transfer Ac- tivity Coefficients from Water to Methanol of Silver and Sodium Based on Different Single Ion Assumptions . . . . .	63
V	The $^{31}\text{P}$ Chemical Shifts in ppm for Tetraphenylphosphonium Salts as a Function of Counterion, Solvent, and Concentration . . . . .	78
VI	The $^{75}\text{As}$ Chemical Shift in ppm ( $\pm 7$ ppm) for Tetraphenylarsonium Ion as a Function of Concentration, Counterion, and Solvent . . . . .	82
VII	Some Representative $^{75}\text{As}$ Linewidths for Tetraphenylarsonium Chloride	

Table	Page
	in Various Solvents ( $\pm 80$ Hz) . . . . . 83
VIII	The $^{11}\text{B}$ Chemical Shifts of Sodium Tetraphenylborate as a Function of Concentration and Solvent in Various Solvents. . . . . 84
IX	The Infinite Dilution $^{11}\text{B}$ Chemical Shifts, Corrected for Bulk Mag- netic Susceptibilities, as a Function of Solvent . . . . . 86
X	Carbon-13 Chemical Shift Changes with Concentration for Tetraphenylarsonium ( $\text{As}(\text{Ph})_4^+$ ) and Tetraphenylphos- phonium ( $\text{P}(\text{Ph})_4^+$ ) Salts in $\text{H}_2\text{O}$ . . . . . 89
XI	Carbon-13 Chemical Shift Changes with Concentration for Tetraphenyl- arsonium ( $\text{As}(\text{Ph})_4^+$ ) and Tetra- phenylphosphonium ( $\text{P}(\text{Ph})_4^+$ ) Salts in $\text{MeOH}$ . . . . . 90
XII	Carbon-13 Chemical Shift Changes with Concentration for Tetraphenyl- arsonium and Tetraphenylphosphonium Salts in $\text{DMSO}$ . . . . . 91
XIII	Carbon-13 Chemical Shift Changes with Concentration for Tetraphenyl- arsonium and Tetraphenylphosphonium



Table	Page
	Salts in DMF. . . . . 93
XIV	Carbon-13 Chemical Shift Changes with Concentration for Tetraphenyl- arsonium and Tetraphenylphosphon- ium Salts in Nitromethane . . . . . 95
XV	Carbon-13 Chemical Shift Changes with Concentration for Tetraphenyl- arsonium and Tetraphenylphosphonium Salts in Propylene Carbonate. . . . . 96
XVI	Carbon-13 Chemical Shift Changes with Concentration for Tetraphenyl- arsonium and Tetraphenylphosphonium Salts in Acetonitrile . . . . . 97
XVII	Carbon-13 Chemical Shift Changes for Sodium Tetraphenylborate in Various Solvents as a Function of Concentration. . . . . 98
XVIII	Bulk Magnetic Susceptibility Cor- rections as a Function of Tetra- phenylphosphonium Chloride Concen- tration in DMSO . . . . . 103
XIX	The Infinite Dilution <sup>13</sup> C Chemical Shifts for Tetraphenylborate, Tetraphenylphosphonium, and Tetraphenylarsonium Ions as a

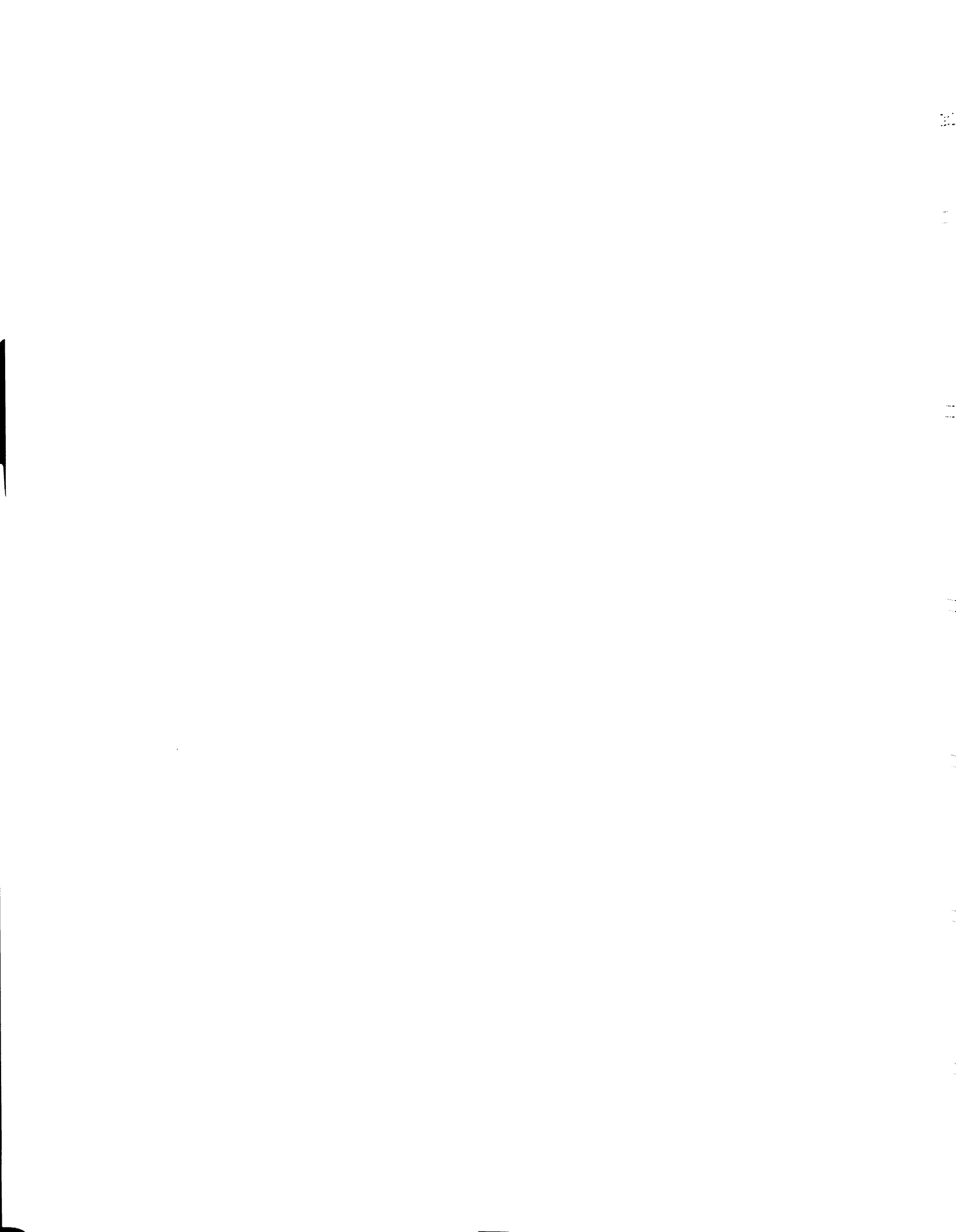


Table	Page
	Function of Solvent . . . . . 105
XX	The Difference in $^{13}\text{C}$ Infinite Dilution Chemical of Tetraphenyl- arsonium (and Tetraphenylphos- phonium) <u>vs</u> Tetraphenylborate Ion as a Function of Solvent. . . . . 107
XXI	The $^{13}\text{C}$ Chemical Shifts of Tetra- phenylgermanium and Tetraphenyl- arsonium Chloride in Dichloro- methane and Deuterated Chloro- form. . . . . 113
XXII	Proton Chemical Shift Data for Tetraphenylarsonium Chloride, Tetraphenylphosphonium Chloride and Tetraphenylborate in Water. . . . . 114
XXIII	Proton Chemical Shifts of Tetra- phenylarsonium Chloride as a Function of the Total Chloride Ion Concentration . . . . . 115
XXIV	Proton Chemical Shift Data for Tetraphenylarsonium Chloride and Some Tetraphenylphosphonium Salts in Methanol . . . . . 116
XXV	Proton Chemical Shift Data for Tetraphenylarsonium Chloride,

Table	Page
	Some Tetraphenylphosphonium Salts and Sodium Tetraphenylborate in DMSO. . . . . 117
XXVI	Proton Chemical Shift Data for Tetraphenylarsonium Chloride, Some Tetraphenylphosphonium Salts, and Sodium Tetraphenyl- borate in DMF . . . . . 119
XXVII	Proton Chemical Shift Data for Tetraphenylarsonium Chloride, Some Tetraphenylphosphonium Salts, and Sodium Tetraphenylborate in Acetonitrile. . . . . 121
XXVIII	Proton Chemical Shift Data for Tetraphenylarsonium Chloride, Some Tetraphenylphosphonium Salts, and Sodium Tetraphenylborate in Nitromethane. . . . . 122
XXIX	Proton Chemical Shift Data for Tetraphenylarsonium Chloride, Some Tetraphenylphosphonium Salts, and Sodium Tetraphenylborate in Propylene Carbonate . . . . . 123
XXX	The Infinite Dilution Proton Chemical Shifts for Tetraphenyl-



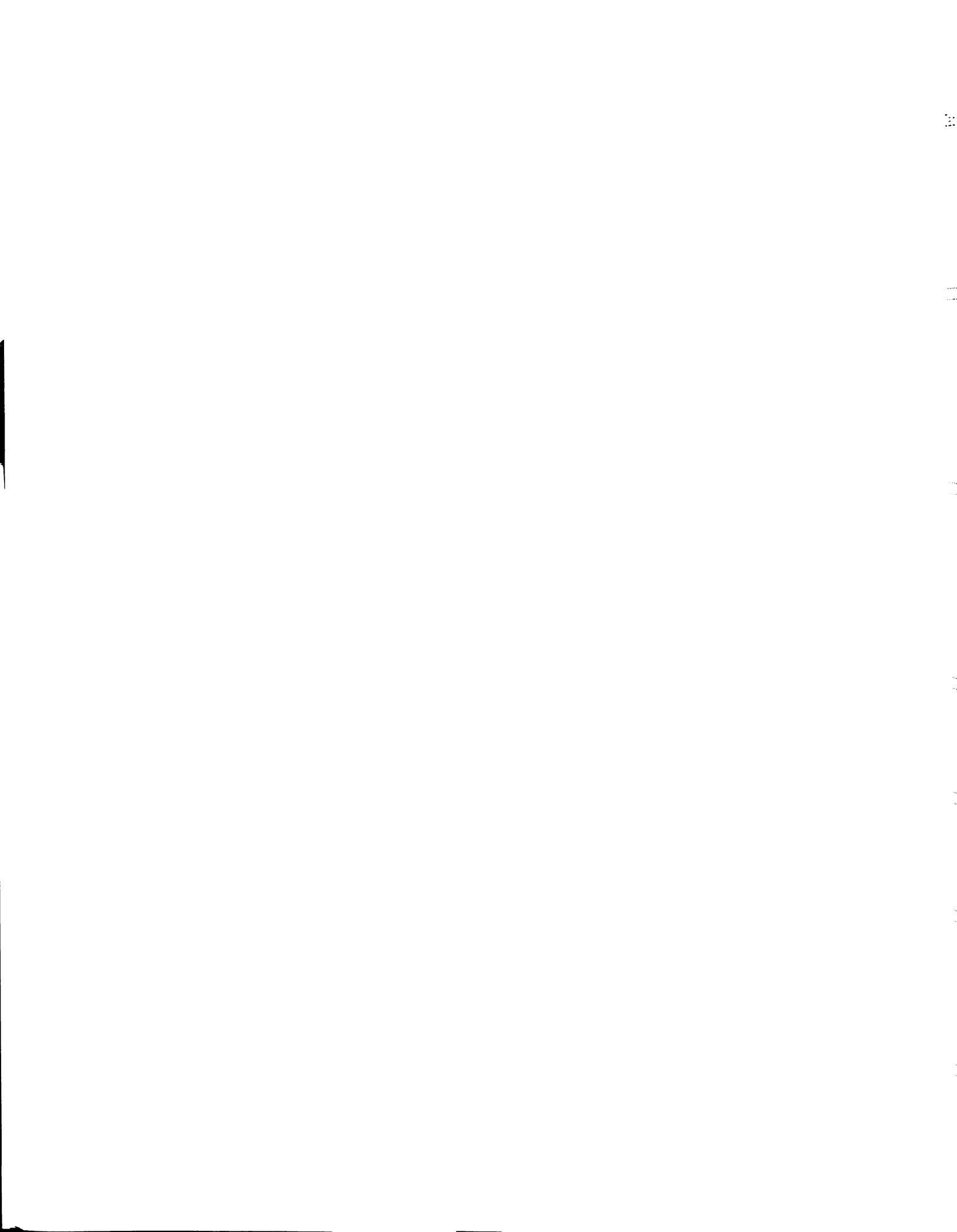


Table	Page
	arsonium, Tetraphenylphosphonium, and Tetraphenylborate Ion as a Function of the Solvent . . . . . 134
XXXI	The Difference in Proton Infinite Dilution Chemical Shifts of Tetraphenylarsonium <u>vs</u> Tetra- phenylborate Ion as a Function of Solvent. . . . . 137
XXXII	The Proton Chemical Shifts of Tetraphenylgermanium and Tetra- phenylarsonium Chloride in Di- chloromethane and Deuterated Chloroform. . . . . 139
XXXIII	Formation Constants of a De- protonated Manganese-Citrate Complex . . . . . 177
XXXIV	Formation Constants of Manganese- (II) Ion-PAA Complexes at Dif- ferent Ionic Strengths and 25°C . . . . . 185
XXXV	The Change in the Emf of a Pb- PAA Complex as a Function of the Negative log [PAA] at 25°C, I = 0.05. . . . . 192
XXXVI	The Change in the Emf of a Cu-PAA Complex as a Function of the

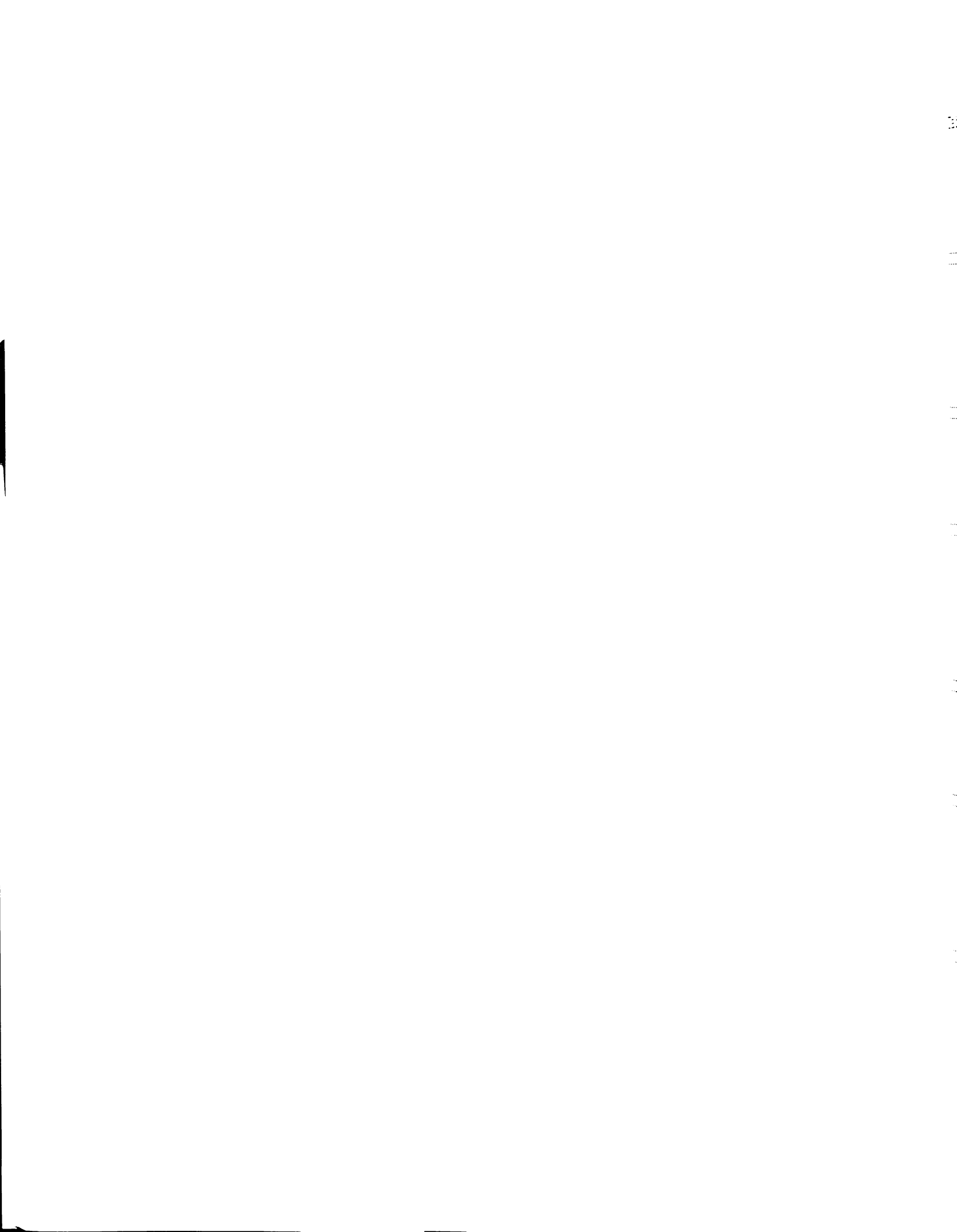


Table	Page
	Negative log [PAA] at 25°C, I = 0.05. . . . . 192
XXXVII	The Change in the Emf of a Tl- PAA Complex as a Function of the Negative log [PAA] at 25°C, I = 0.05. . . . . 193
XXXVIII	Formation Constants of Thallium(I)- PAA Complexes at Different Ionic Strengths and 25°C. . . . . 194
XXXIX	Formation Constants for Cal- cium(II) Ion-PAA Complexes as a Function of the Ionic Strength at 25°C . . . . . 201
XL	Thermodynamic Quantities for Metal Ion Complexation with PAA. . . . . 205
XLI	The Solvation Entropy, Radius, and Formation Constants of Some Metal Ions with PAA at 25°C and an Ionic Strength of 0.05 . . . . . 207
XLII	Formation Constants of Thallium- (I)-PFA Complexes at Different Ionic Strengths and 25°C. . . . . 212



Table		Page
XLIII	Formation Constants of Calcium- (II)-PFA Complexes as a Function of the Ionic Strength at 25°C . . . . .	216
XLIV	Formation Constants of Calcium (II)-3-PPA Complexes as a Function of the Ionic Strength at 25°C . . . . .	217
XLV	Formation Constants for Some Metal Ions with PAA, PFA, and 3-PPA at 25°C and $I = 0.05$ . . . . .	220

LIST OF FIGURES

Figure	Page
1	5
The structure of some crown ethers and a cryptand. . . . .	
2	27
Concentration and anion dependence of the $^{43}\text{Ca}$ chemical shift in aqueous solution measured with a 60 MHz NMR spectrometer (triangles - $\text{CaCl}_2$ , squares - $\text{CaBr}_2$ , circles - $\text{Ca}(\text{ClO}_4)_2$ , and crosses - $\text{Ca}(\text{NO}_3)_2$ ), . . . . .	
3	28
Concentration and anion dependence of the $^{43}\text{Ca}$ chemical shift in aqueous solution measured with a 180 MHz NMR spectrometer. . . . .	
4	36
Concentration and anion dependence of the $^{43}\text{Ca}$ chemical shift in TMG, methanol, and ethylene glycol. . . . .	
5	37
Concentration and anion dependence of the $^{43}\text{Ca}$ chemical shift in DMSO, formamide, DMF, acetone, and propylene carbonate . . . . .	

Figure		Page
6	A plot of the Gutmann donor number <u>vs</u> the $^{43}\text{Ca}$ infinite dilution chemical shift. . . . .	48
7	A plot of the observed $^{43}\text{Ca}$ chemical shift <u>vs</u> the mole ratio of EDTA to calcium . . . . .	50
8	Calcium-43 resonance of a solution 0.4M in $\text{CaCl}_2$ and 0.2M in EDTA at pH $\sim$ 10. Peak A - complexed $\text{Ca}^{2+}$ , peak B - free $\text{Ca}^{2+}$ . . . . .	52
9	The structure of tetraphenylarsonium, tetraphenylphosphonium, and tetraphenylborate ion. . . . .	64
10	The $^{13}\text{C}$ NMR spectra of: upper - tetraphenylarsonium chloride, middle - tetraphenylphosphonium chloride, and lower - sodium tetraphenylborate in DMSO. . . . .	99
11	The $^{13}\text{C}$ NMR spectra of tetraphenylarsonium tetraphenylborate in DMSO and DMF. . . . .	101
12	Some resonance structures of tetraphenylarsonium ion. . . . .	109



13	A plot of the difference in chemical shift between the cation and anion <u>vs</u> the dielectric constant. . . . .	111
14	A plot of the proton chemical shift <u>vs</u> the total salt concentration in water (squares - para protons, triangles - meta protons, circles - ortho protons, open symbols - tetraphenylarsonium chloride, closed symbols - sodium tetraphenylborate). . . .	124
15	A plot of the proton chemical shift <u>vs</u> total salt concentration in DMSO . . . . .	125
16	A plot of the proton chemical shift <u>vs</u> total salt concentration in DMF . . . .	126
17	A plot of the proton chemical shift <u>vs</u> total salt concentration in acetonitrile. . . . .	127
18	A plot of the proton chemical shift <u>vs</u> total salt concentration in nitromethane . . . . .	128
19	A plot of the proton chemical shift - <u>vs</u> total salt concentration in propylene carbonate. . . . .	129



Figure	Page
20	A plot of the proton chemical shift <u>vs</u> total chloride ion concentration for tetraphenylarsonium chloride in water. . . . . 131
21	The proton NMR spectra of sodium tetraphenylborate, tetraphenylarsonium chloride, and tetraphenylphosphonium chloride in DMSO . . . . . 132
22	The proton NMR spectra of tetraphenylarsonium chloride in different solvents. . . . . 135
23	The structures of phosphonoacetic acid (PAA), phosphonoformic acid (PFA), 2-phosphonopropionic acid, and 3-phosphonopropionic acid. . . . . 145
24	DNA synthesis and the proposed PAA inhibition mechanism . . . . . 148
25	A schematic representation of the Orion 90-20 calcium ion selective electrode. . . . . 154
26	A schematic representation of the pyrex glass cells used for A - cyclic voltametric studies, and B - potentiometric studies . . . . . 164

- 27 A calibration plot of the observed ESR intensity as a function of  $\text{MnCl}_2$  concentration . . . . . 175
- 28 A plot of the log formation constant of Mn-PAA as a function of the ionic strength (upper curve - deprotonated PAA, lower curve - monoprotonated PAA). . . . . 184
- 29 A plot of the change in Emf vs the negative log [PAA] to determine the formation constant of a Pb-PAA complex (upper curve - deprotonated PAA, lower curve - monoprotonated PAA). . . . . 189
- 30 A plot of the change in Emf vs the negative log [PAA] to determine the formation constant of a Cu-PAA complex (upper curve - deprotonated PAA, lower curve - monoprotonated PAA). . . . . 190
- 31 A plot of the change in Emf vs the negative log [PAA] to determine the formation constant of a monoprotonated PAA-Tl complex. . . . . 191

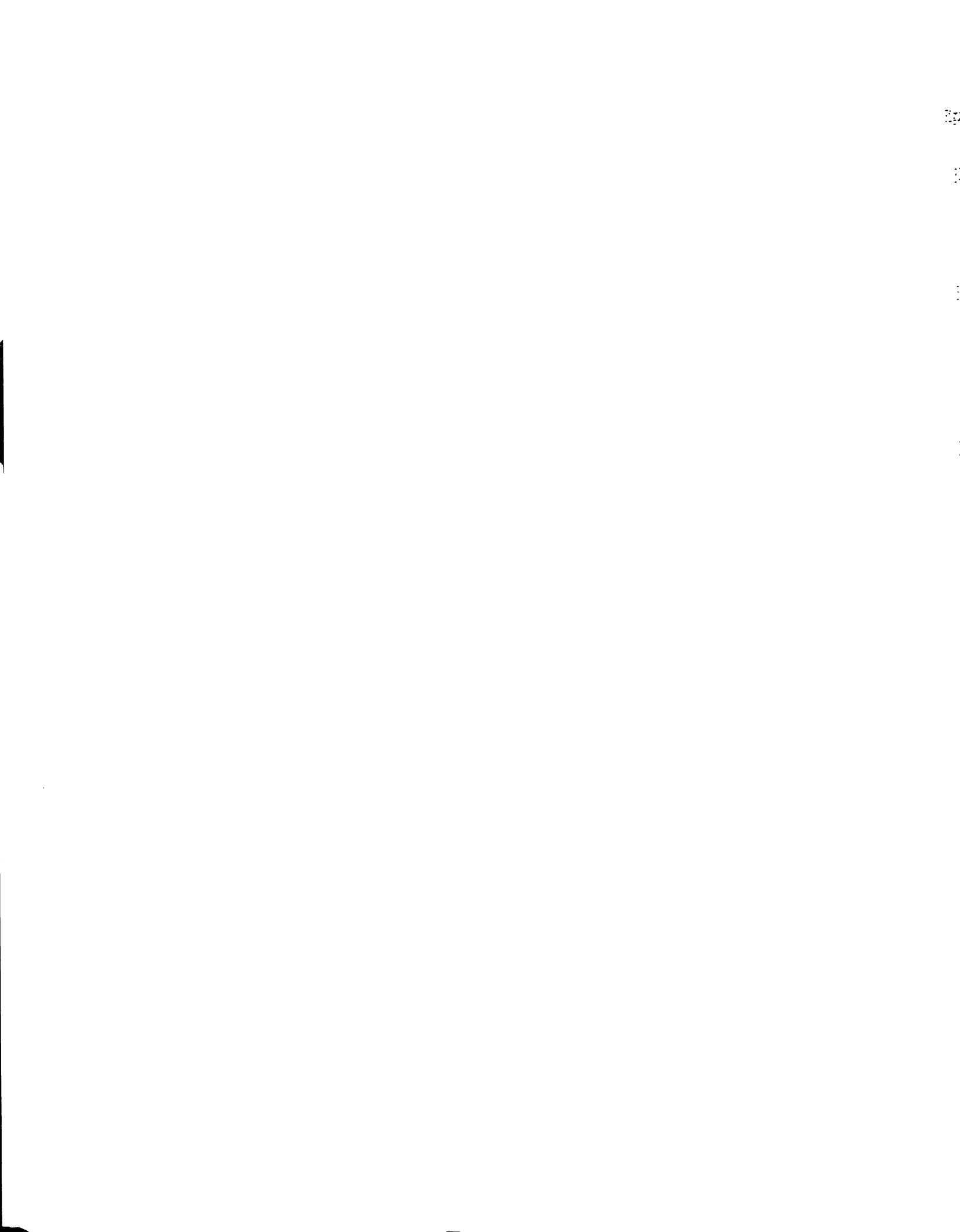


Figure	Page
32	A plot of log formation constant of deprotonated PAA-Tl complex as a function of the ionic strength . . . . . 195
33	A sample calibration plot and titration curve of silver ion with deprotonated PAA using a silver ion specific electrode. . . . . 197
34	A sample calibration plot and titration curve of calcium ion with deprotonated PAA using a calcium ion selective electrode. . . . . 199
35	A plot of log formation constant of Ca-PAA as a function of the ionic strength (upper curve - deprotonated PAA, lower curve - monoprotinated PAA). . . . . 200
36	A plot of $\log K_t$ vs $1000 \times \text{Temperature}^{-1}$ to determine the entropy and enthalpy of a deprotonated $\text{Ca}^{+2}$ complex with deprotonated PAA (upper curve) and 3-PPA (lower curve) . . . . . 204
37	A plot of the entropy of solvation (e.u.) vs the log formation constant of some metal ion complexes

Figure	Page
	with deprotonated PAA. . . . . 208
38	A plot of the log formation constant of a deprotonated PFA-Tl complex as a function of the ionic strength. . . 211
39	A plot of the log formation constant of Ca-PFA as a function of the ionic strength (upper curve - deprotonated PAA, lower curve - monoprotonated PAA). . . . . 214
40	A plot of the log formation constant of Ca-3-PPA as a function of the ionic strength (upper curve - deprotonated PAA, lower curve - monoprotonated PAA). . . . . 215

PART I

CALCIUM-43 NMR STUDIES



CHAPTER I

HISTORICAL REVIEW



## 1.1. Introduction

Multinuclear NMR has been shown to be a sensitive technique for probing the immediate chemical environment of metal ions in solution. This sensitivity, coupled with the non-destructive nature of the method, renders multinuclear NMR a desirable technique for the study of a wide variety of chemical and biological systems. As the scope of this investigation encompasses a range of metal-ligand interactions, e.g., calcium complexes with phosphonocarboxylic acids, it was of interest to determine the suitability of natural abundance calcium- $^{43}$  NMR as a probe of the complexation phenomena. Prior to such a study, however, fundamental work on the NMR of calcium salt solutions was necessary to characterize such solution interactions as ion-pairing and solvation. These interactions are important to the extent that they influence complexation (e.g., ion-pairing will compete for the free calcium ions in solution, which will have a definite effect on complexation.)

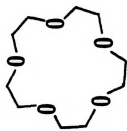
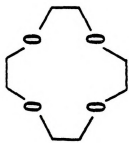
It was also of interest to us to investigate a possible use of  $^{43}\text{Ca}$  NMR for studies of calcium complexes in aqueous and nonaqueous solutions. We chose to study  $\text{Ca}^{2+}$  complexes with the well known EDTA ligand as well as with

some crown ethers. The latter ligands have been a subject of intense interest since their introduction by Pederson (12,13). The ligands 15C5 and 18C6 (Figure 1) were chosen because the calcium diameter most closely matches the ring cavity size (13) for these ligands; 18C6 has a slightly larger cavity size than would be indicated for a "best fit" with the calcium ion, but studies (16-18) have shown that ions will also complex with the next larger ring size.

These ligands should provide a range of environments which would effect the observed calcium-43 resonance, thereby indicating the suitability of calcium NMR for the investigation of complexation reactions.

## 1.2. Calcium-43 NMR

The calcium-43 resonance signal was first observed by Jeffries (1) in 1953 at a frequency of 2.85 Mc/sec with a 10 kG magnet operating in a continuous wave mode. A 0.7 M  $\text{CaBr}_2$  aqueous solution (68% enriched in  $^{43}\text{Ca}$ ) was used to obtain the value of 7/2 for the spin and a magnetic moment of -1.3152 nm for this nuclei. Further studies were not conducted until 1969 when Bryant (2) studied calcium-ATP complexes in water. A continuous wave Varian V-4210A spectrometer was used to study 0.9 M aqueous calcium solutions (31.68% enriched in  $^{43}\text{Ca}$ ) with variable ATP concentrations. The exchange rate was observed to be fast on the

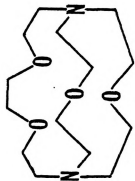
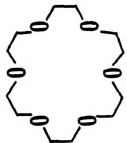


12C4

1.2-1.6A

15C5

1.7-2.2A



18C6

2.6-3.2A

C211

1.6A

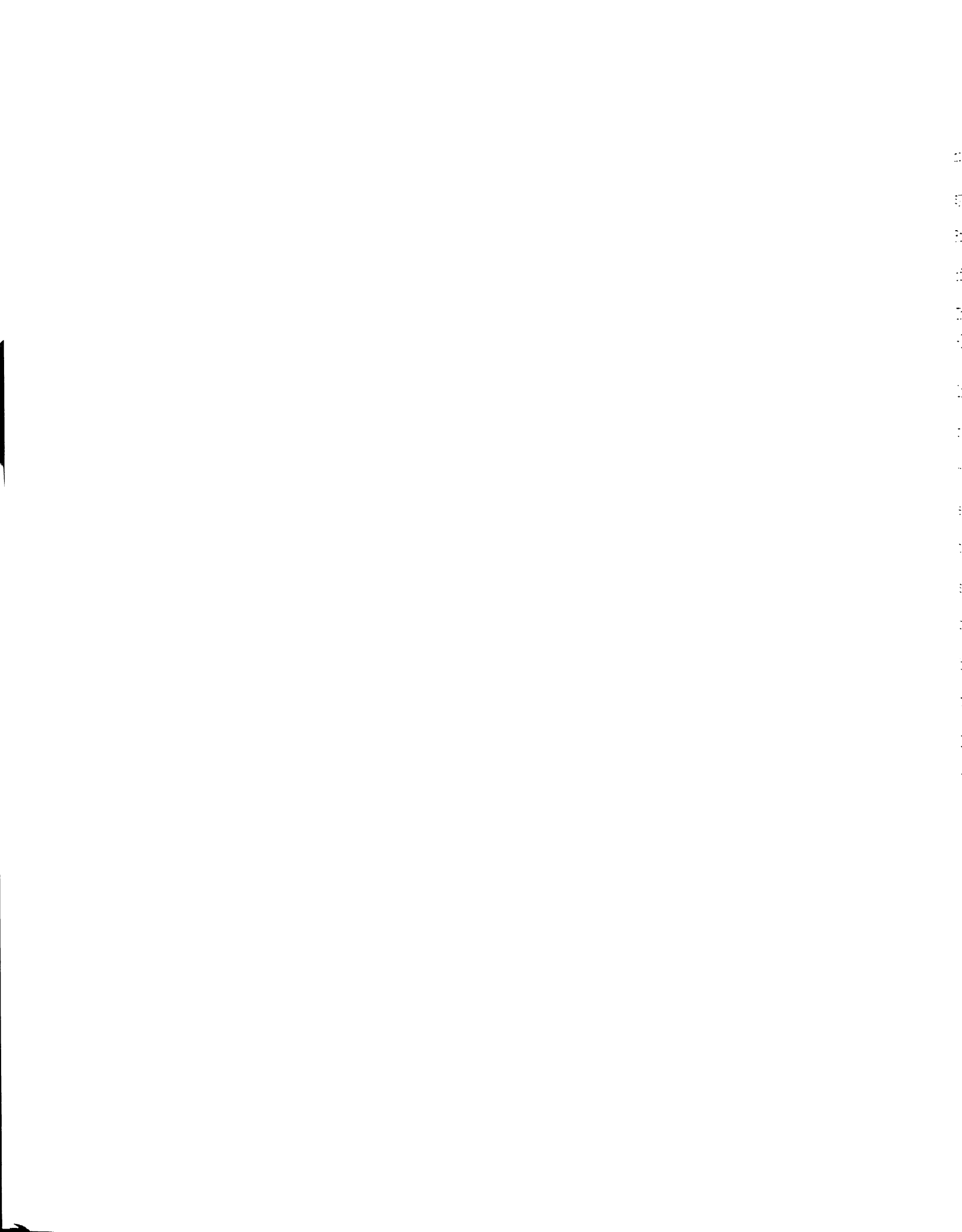
Figure 1. The structure of some crown ethers and a cryptand.



NMR time scale, resulting in a single resonance with a typical spin-lattice relaxation time  $T_2 = 0.85$  s. The author concluded that calcium-43 NMR would be a powerful tool for investigating calcium interactions with large biological molecules.

The calcium-43 NMR of solid compounds has been investigated by Bleich and Redfield (3). It was found that a double resonance technique with solid state decoupling allowed the measurement of a  $^{43}\text{Ca}$  resonance for a  $\text{CaF}_2$  sample with natural abundance of  $^{43}\text{Ca}$ . The full width at half intensity was 130 Hz at 77°K. A similar study on  $\text{CaF}_2$  was conducted by Jacquinet, et al. (4).

The most fundamental study of calcium ion interactions, though, was published by Lutz, et al. (5) in 1973 and continued in 1975 (6). Using a 18.07 kG Bruker BKR32 spectrometer at a resonance frequency of 5.178 MHz, Lutz investigated the aqueous behavior of some calcium chloride, bromide, nitrate, and perchlorate solutions. The effect of concentration and counter-ion on the observed calcium resonance was studied for solutions ranging from 0.5 to 7.2 M. Also of fundamental importance was the determination of the quadrupole moment for  $^{43}\text{Ca}$  by Grundeuk, et al. (7). An atomic beam magnetic resonance technique with laser detection was used to determine a quadrupole moment of -0.065 b. The bare calcium-43 nucleus was generated by means of a plasma discharge source.





The bulk of calcium-43 NMR investigations since 1970, however, followed Bryant's suggestion that biological systems were particularly amenable to this technique. Robertson, Hiskey, and Koehler (8) studied the binding of  $\gamma$ -carboxylglutamic acid containing peptides to calcium. The calcium salt used in this study was 79.98% enriched in  $^{43}\text{Ca}$ . The dissociation constant of calcium ion with the ligand was found to be 0.6 mM with a total chemical shift range upon complexation of 2 ppm. Calcium binding to parvalbumins was investigated by Parello, et al. (9). The effects of pH, temperature, and calcium/protein ratio on the full width at half-height of the resonance band were studied with a 100 MHz spectrometer using a 61.63% enriched calcium salt. The exchange rate between free and bound calcium was found in all cases to be fast on the NMR time scale. The interaction of the calcium ion with calf DNA was studied by Reimarsson (10) using enriched samples. The average lifetime for calcium ion bound to DNA was estimated as 9ms at 25°C and 3 ms at 50°C. Marsh, et al. (11) studied calcium ion-bovine prothrombin fragment 1 interactions with enriched calcium-43 NMR, in conjunction with circular dichroism and fluorescence techniques and found that calcium ion induces a helical structure in the prothrombin as a function of pH. The linewidth of the calcium resonance varied between 2 and 10 Hz.

### 1.3. Ligands

The complexation properties of 15C5 in aqueous solutions have been studied calorimetrically by Izatt, et al. (19) with the alkali, alkaline earth, and some post transition elements. It was found that, within experimental error, there was no evidence for complexation with the calcium ion. This does not preclude completely the possibility of such a complex, as calorimetric techniques require a measurable  $\Delta H$  of complexation in order to determine a formation constant. A low  $\Delta H$  would indicate no complex according to calorimetric studies, although the  $\Delta S$  term and subsequent  $\Delta G$  might be favorable to complexation. A study by Lamb (20) in methanol yielded a  $\text{Ca}^{2+}$  - 15C5 formation constant of  $\log K_f = 2.18$ . Crystallographic studies of  $\text{Ca}^{2+}$  - 15C5 complexes have not been done due to the difficulty of obtaining crystals. However, structures of  $\text{Ca}^{2+} \cdot \text{Benzo 15C5}$  (21) and  $\text{Ca}^{2+} \cdot \text{Dibenzo 15C5}$  (22) complexes indicate the calcium ion is not positioned in the plane of the ring. This suggests that the complexation with the benzo derivatives of 15C5 is weak. These results, together with Izatt's work, indicate that in aqueous solutions, at best only a weak complex can exist.

The toxic effects of 15C5 have been studied by Hendrixson et al. (23). The acute and chronic effects of oral administration of 15C5 was studied in mice. The  $\text{LD}_{50}$  (the lethal dose required to kill 50% of the mice) was found



to be 1.02 g/kg body weight of the mouse. There was no cumulative effect from daily ingestion of small amounts of 15C5 over a period of two weeks. The ligand is a strong topical irritant which is readily absorbed through the skin.

Complexation studies of 18C6 with calcium ion have been conducted by Izatt in water (24), 70% aqueous methanol (25), and pure methanol (20). There is no evidence for complexation in water, while  $\log K_f$  (formation constant) values are 2.51 in 70% methanol, and 3.86 in methanol. These data, along with those for calcium - 15C5 complexes, indicate that water solvates  $\text{Ca}^{2+}$  ion much stronger than methanol. In water, therefore, the solvent effectively competes with the ligand for the calcium ion, leading to little or no complex formation. In methanol, the stability of the complex is greater than the solvation enthalpy (26). A crystallographic study of the  $\text{Ca}^{2+}$ .18C6.SCN complex (27) revealed a disordered structure in which calcium lies in the mean plane of the ring. The thiocyanate anions are associated with the calcium above and below the plane of the ring. The inclusion of calcium within the ring is indicative of a stronger interaction than that of  $\text{Ca}^{2+}$ . (di)benzo 15C5 where calcium is outside the cavity. These data indicate that  $\text{Ca}^{2+}$  ion forms a stronger complex with the next larger crown than would be predicted from the best fit of an ion into the crown cavity.

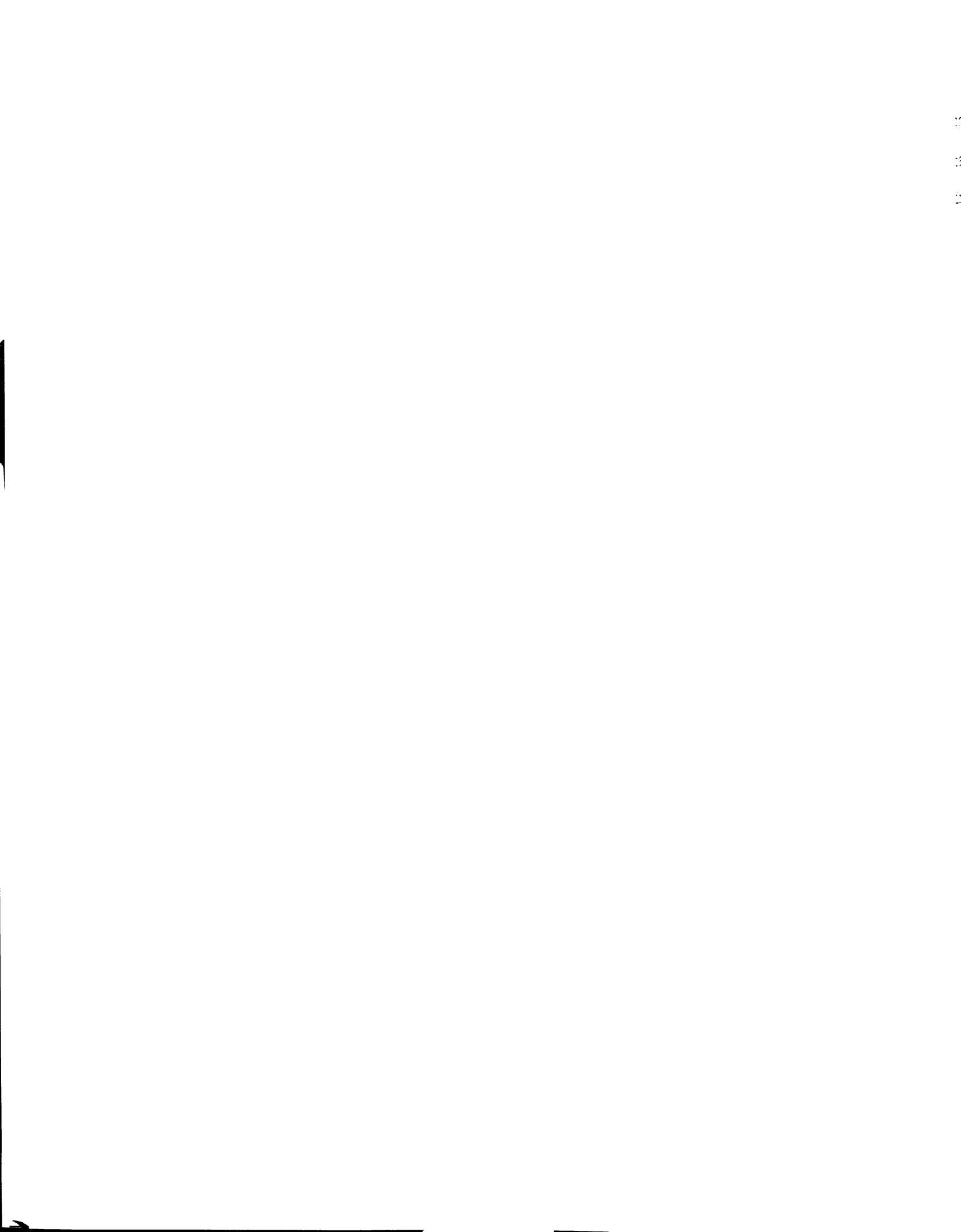
Toxicological studies of 18C6 on mice (23) have led to the determination of an LD<sub>50</sub> of 0.71 g/kg body weight. Again, no cumulative effects were observed with daily ingestion over a period of two weeks. This study concluded that the toxic effects of crown ethers increased with increasing ring size.

The above brief survey is by no means an attempt at a complete compilation of crown ether chemistry. The reader is referred to several books (28-30) and review articles (14,31-33) for a more complete study of macrocyclic chemistry.

Complex compounds with EDTA are too well known to warrant an historical survey. It seems sufficient to note that the formation constant of the calcium ion complex with EDTA was found to be  $5.0 \times 10^8$  at 25°C and an ionic strength of 0.1 (15).

#### 1.4. Conclusions

Thus far, the use of calcium-43 NMR for the investigation of complexation and ion-ion interactions has been restricted to aqueous solutions, usually using an isotopically enriched calcium salt. The behavior of calcium salts in nonaqueous solvents has not been investigated by calcium-43 NMR. The purpose of this portion of the thesis was to study the technique of natural abundance calcium-43 NMR, especially as it applies to the solution

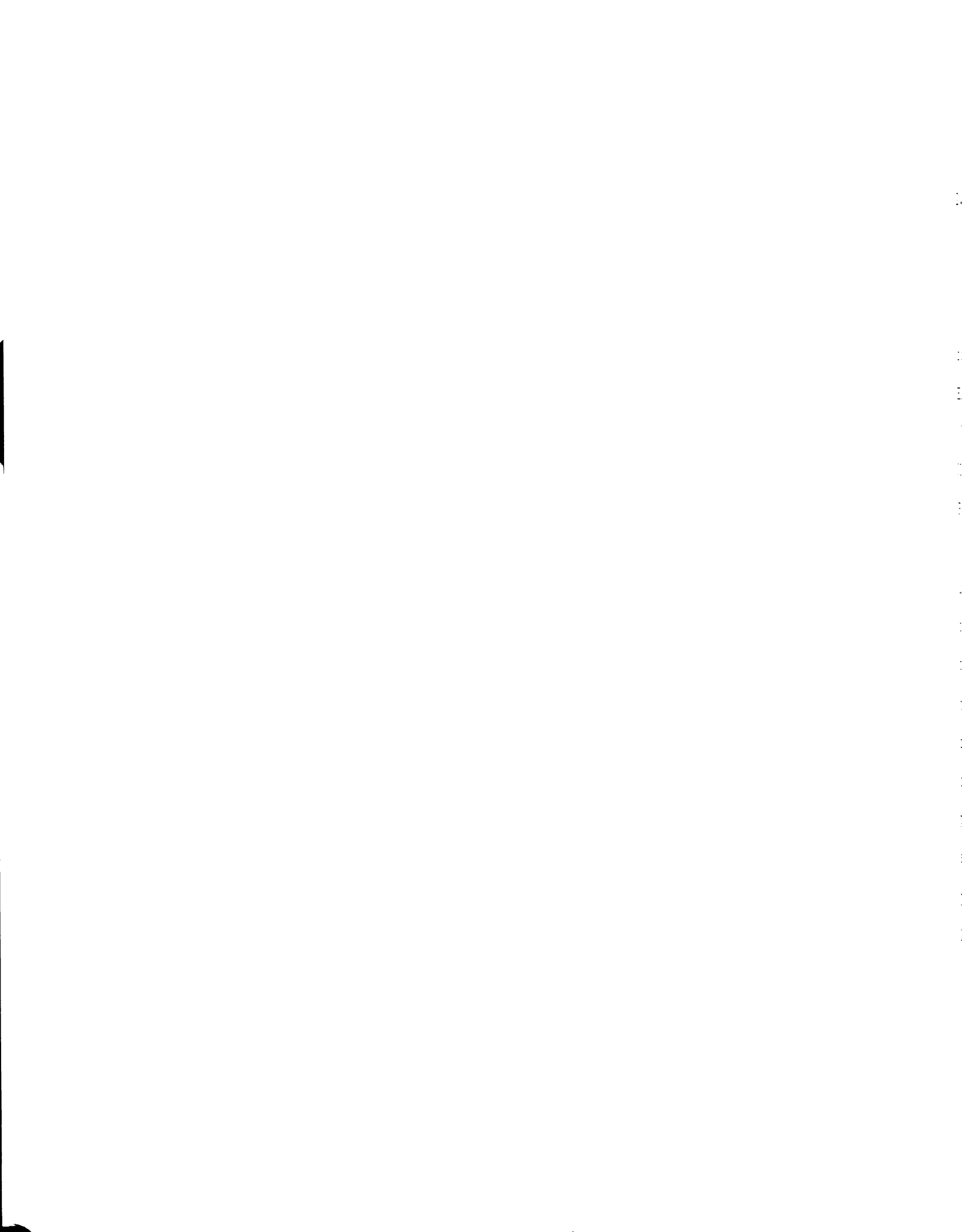


chemistry of calcium salts. This work should serve as a basis for future studies involving complexation reactions in aqueous and nonaqueous solvents.

CHAPTER 2

MATERIALS AND METHODS





## 2.1. Reagents

### 2.1.1. Salts

The chemical manufacturer of each compound has been coded as follows: Aldrich (A), Alfa (Al), J. T. Baker (B), Eastman Organics (E), Fischer Scientific Co. (F), K & K (K), Mallinckrodt (M), Matheson, Coleman, and Bell (MCB), Merck & Co. (Mc), Ozark Mahoning (O), Pfaltz & Bayer (PB), Parish (P), Richmond Organics (R), and G. F. Smith Co. (S).

The following chemicals were of reagent grade and were used without further purification (except for drying) calcium bromide dihydrate (MCB), calcium chloride (MCB), calcium nitrate tetrahydrate (F), calcium perchlorate tetrahydrate (S), cupric chloride dihydrate (MCB), ferrous chloride hydrate (MCB), lead nitrate (F), lithium perchlorate (K), manganous chloride hexahydrate (B), nickel perchlorate hexahydrate (B), potassium bromide (M), potassium hexafluorophosphate (PB), potassium hydroxide (MCB), potassium nitrate (MCB), potassium phosphate dibasic trihydrate (M), silver nitrate (MCB), sodium chloride (M), sodium hexafluoroarsenate (O), sodium para-toluene sulfonate (E), sodium perchlorate (F), thallium nitrate (Al), 3-trimethylsilyl propionate sodium salt (known as TSP, the water soluble analog of TMS for use as an external

standard in  $D_2O$ ), and zinc chloride (M). Tetramethylammonium hydroxide (E) was obtained as a 10% solution in water. A tris buffer was made with gold label tris-(hydroxymethyl)amino methane (A1) and perchloric acid (B).

### 2.1.2. Purification Procedures

Tetraethylammonium perchlorate (TEAP) was recrystallized twice by dissolving in a minimum amount of boiling water. The solution was filtered hot, then recrystallized upon gradual cooling to  $0^\circ C$ . The crystals were filtered and washed with cold water. Tetraphenylarsonium (S) and tetraphenylphosphonium chloride (A1) were precipitated from an isopropyl alcohol-acetone solution upon the addition of benzene (92). Tetraphenyl phosphonium bromide (A1) and iodide (A1) were recrystallized from water following the procedure used for tetraethylammonium perchlorate. Tetraphenylarsonium tetraphenylborate was synthesized by mixing aqueous solutions of tetraphenylarsonium chloride and gold label sodium tetraphenylborate (A) in equal proportions. Tetraphenylarsonium iodide was synthesized by mixing aqueous solutions of tetraphenylarsonium chloride and reagent grade sodium iodide (M) in equal proportions.

### 2.1.3. Drying Procedures

The following chemicals were dried in a vacuum oven (except where noted), with the drying time and temperature

in parenthesis: calcium chloride (\*), calcium nitrate (96 h, 140°C) (32), calcium perchlorate (96 h, 140°C) (32), lithium perchlorate (\*), manganese chloride tetrahydrate (48 h, 210°C, regular oven), tetraphenylarsonium salts (24 h, 100°C), tetraphenylphosphonium salts (24 h, 100°C), and tetraethylammonium perchlorate (24 h, 50°C).

## 2.2. Ligands

Ethylenediamine tetraacetate disodium salt (B) and citric acid (M) were of reagent grade, requiring only drying (\*) prior to usage. Crown ether 18C6 (A or P) was recrystallized from acetonitrile by forming the 18C6 acetonitrile complex (33) at an acetone-ice bath temperature. The solution was filtered and dried (48 h, ambient). The melting point of the purified product was approximately one degree below that of the literature value (33). The 15C5 (A) was fractionally distilled under reduced pressure and vacuum dried. The 12C4 (A) was used without further purification.

Phosphonoacetic acid (PAA, R) was dissolved in a minimal amount of glacial acetic acid near its boiling point. The solution was gradually cooled to room temperature. A minimal amount of ethyl ether was then added

---

\*(24 h, 110°C, regular oven)

to aid in recrystallization. The crystals were filtered and rinsed with ethyl ether, followed by vacuum drying (48 h, 60°C). The melting point of 141-142 agrees well with the literature value of 142-143°C (34). Phosphonopropionic acid (3-PPA, R) was recrystallized similarly. The melting point was 176-178°C compared to a literature value of 178-180°C (35). The phosphonoformic acid (PFA) was donated by Dr. Boezi's group and was used without further purification.

### 2.3. Solvents

The following solvents were used during the course of experimentation: acetone (F), acetonitrile (M), dimethylformamide (DMF, M), dimethylsulfoxide (DMSO, F), ethylene glycol (MCB), formamide (F), methanol (M), nitromethane (A), propylene carbonate (PC, A), pyridine (M), tetramethylguanidine (TMG, E), and water.

The following purification and drying procedures were common to all solvents: the solvent was refluxed and fractionally distilled for 48 hours over a chemical drying agent, with only the middle fraction retained. The solvent was stored over molecular sieves (Davison Chemical Co., 3Å pore size) under a nitrogen atmosphere. Unless stated, the chemical drying agent used was calcium hydride.

Acetone, ethylene glycol, propylene carbonate, and TMG were distilled using molecular sieves as a drying agent.

Methanol was distilled over Mg turnings, while pyridine was distilled using KOH and molecular sieves as drying agents. Conductance water was obtained through the courtesy of Dr. Weaver's laboratory and was used without further purification.

#### 2.4. Molecular Sieves

Molecular sieves of pore size  $3\text{\AA}$  were dried at  $110^\circ\text{C}$  for 24 h prior to activation. Activation was accomplished by drying at  $500^\circ\text{C}$  for 24 h under nitrogen (dried by passage through sulfuric acid).

#### 2.5. Nuclear Magnetic Resonance

The nuclear magnetic resonance spectra were collected on three instruments, all operating in the Fourier transform mode.

##### 2.5.1. Varian CFT-20 NMR Spectrometer

The CFT-20 spectrometer was used to measure some  $^{13}\text{C}$  spectra. The resonance frequency of  $^{13}\text{C}$  is 20 MHz at a field strength of 18.7 kG. Spinning tubes of 10 mm OD with a 3 mm OD capillary containing 0.3 M TSP in  $\text{D}_2\text{O}$  as a reference held in the center with teflon spacers.



### 2.5.2. Bruker WH-180 Superconducting NMR Spectrometer

Phosphorous-31, arsenic-75, and calcium-43 spectra were obtained using this instrument. Their resonance frequencies are 72.88 MHz, 30.82 MHz, and 12.12 MHz, respectively at a field of 42.28 kG. Calcium-43 and arsenic-75 were run in 20 mm OD non-spinning tubes with a 5 mm OD reference tube held in the center. The loss of sample homogeneity was negligible when comparing spectra obtained using spinning vs non-spinning tubes. The phosphorous-31 studies were conducted using a 10 mm OD spinning tube with a 5 mm reference held in the center with teflon spacers.

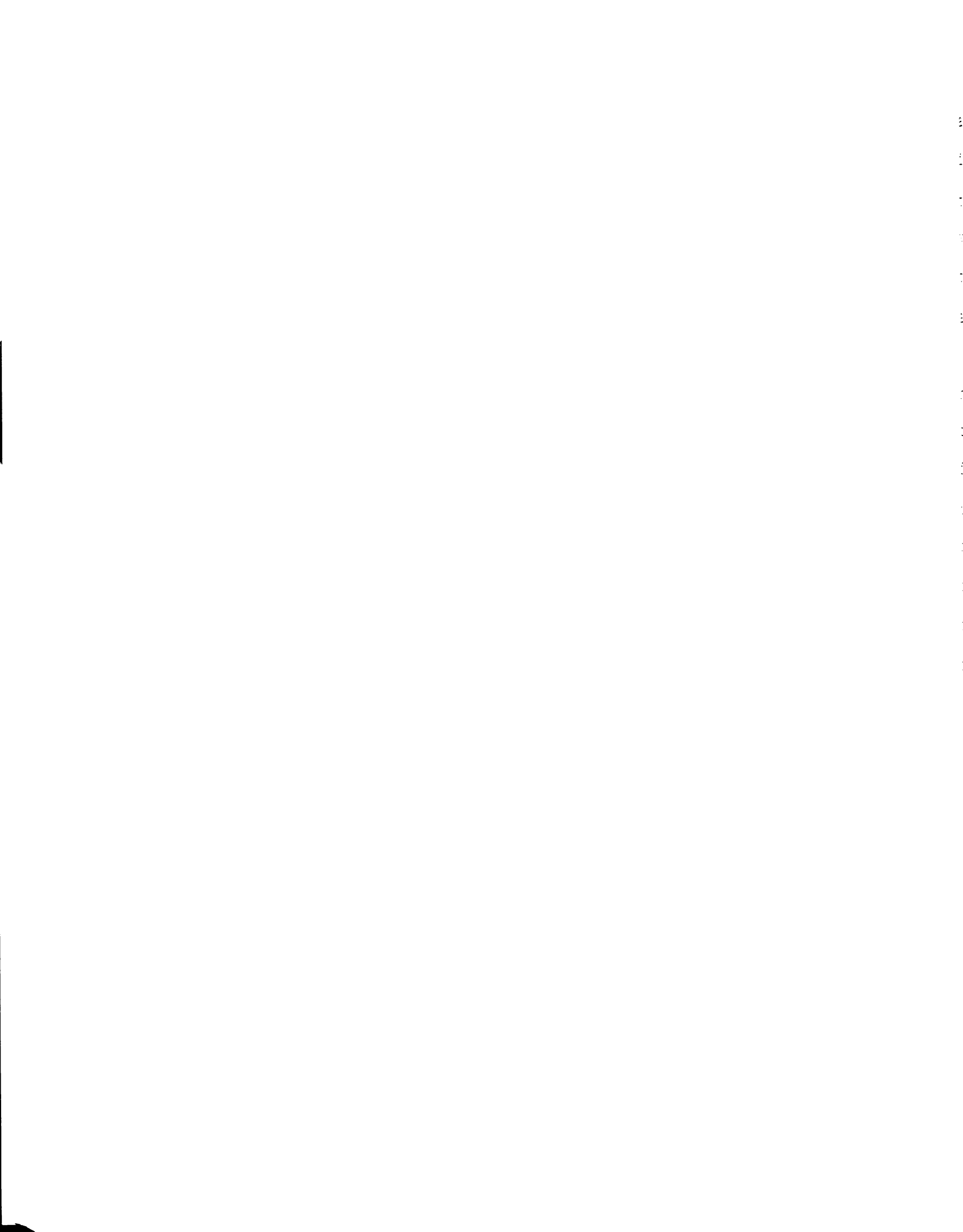
### 2.5.3. Bruker WM-250 Superconducting NMR Spectrometer

Proton and carbon-13 spectra were obtained primarily with the WM-250 spectrometer at resonance frequencies of 250 MHz and 62.894 MHz in a 58.72 kG field. The sample preparation is the same as that for the CFT-20 spectrometer.

### 2.5.4. Operating Procedures

All chemical shifts were measured with respect to an external standard and are as follows: Proton and carbon-13 - a 0.3 M solution of TSP in  $D_2O$ , arsenic-75 - a 0.1 M  $KAsF_6$  solution in  $D_2O$ , phosphorous-31 - A 85% phosphoric





acid in  $D_2O$  solution, boron-11 - A 0.1 M  $(CH_3O)_3B$  solution in  $D_2O$ , and calcium-43 - an infinitely dilute aqueous solution (a 5.071 M  $CaCl_2$  was used as a standard). The solutes were weighed under normal atmospheric conditions, then transferred to a dry box for dilution with a given non-aqueous solvent.

Chemical shifts downfield from the reference (paramagnetic are designated as positive. All chemical shifts have been corrected for the bulk magnetic susceptibility differences between pure water and the given non-aqueous solvent. The correction due to the solute is assumed to be negligible except in the case of proton NMR (36). The corrections have been calculated based on the equations of Live and Chan (37) for normal magnets (Equation (1)) and superconducting magnets (Equation (2)),

$$\delta_{\text{corr}} = \delta_{\text{obs}}^N - \frac{4\pi}{3} (X_{\text{ref}} - X_{\text{sample}}) \quad (1)$$

$$\delta_{\text{corr}} = \delta_{\text{obs}}^S + \frac{2\pi}{3} (X_{\text{ref}} - X_{\text{sample}}) \quad (2)$$

where  $\delta_{\text{corr}}$  is the actual chemical shift (independent of the type of magnet used),  $\delta_{\text{obs}}^N$  and  $\delta_{\text{obs}}^S$  are the observed chemical shifts for normal and superconducting magnets, and  $X_{\text{ref}}$  and  $X_{\text{sample}}$  are the magnetic susceptibility of the reference and sample.

## 2.6. Miscellaneous Instrumentation

Melting points were determined with a Fischer-John melting point apparatus. The water content of the non-aqueous solvents was measured with an Aqua Test II Karl-Fischer apparatus. The purity of selected solvents was determined using a Varian Aerograph Model 920 gas chromatograph.

## 2.7. Data Handling

Extensive use was made of the CDC-7501 computer for equilibrium calculations. The programs KINFIT4 (Appendix A, 38) and MINIQAD (Appendix B, 39) were used for equilibrium and thermodynamic parameter calculations. Some complex equilibrium data required further treatment using a PDP-11 minicomputer and the program in Appendix C.

CHAPTER 3

RESULTS AND DISCUSSION



### 3.1. Introduction

The purpose of this investigation was to determine the suitability of calcium-43 NMR spectroscopy to the study of  $\text{Ca}^{2+}$  ion solution chemistry in aqueous and nonaqueous solvents. It has been shown that alkali metal NMR is a very sensitive probe of the immediate environment around an alkali ion in solution (40,41), yielding both structural and thermodynamic information (17,18). Calcium is an ion of both biological and chemical interest. Its chemical behavior is more representative of the chemistry of alkaline earth metals than magnesium, while its role in living organisms is well known. It was desirable, therefore, to use the sensitivity of multinuclear NMR in the study of calcium interactions in solution. Due to the high cost of enrichment, natural abundance studies seemed to be of more practical value as a preliminary effort.

The system which generated interest in this technique was the aqueous solution complexation of calcium with phosphonoacetic acid (PAA). However, basic solution interactions, such as ion-pairing, were studied first, as they influence the complexation behavior. The applicability of calcium-43 NMR to the complexation phenomena itself was then tested with three known systems. Finally, a study

of the calcium-PAA system was then attempted.

### 3.2. General Information on Calcium-43 NMR

The properties of the calcium-43 nuclei (the only stable odd spin calcium nuclei) are not as favorable as some of the alkali metal nuclei for the use as a probe nucleus in NMR. The natural abundance of the calcium-43 isotope is 0.13%. The sensitivity of NMR towards calcium-43 is 0.064 (at a constant field), relative to a proton NMR sensitivity of one. A more accurate reflection of the difficulties associated with calcium NMR is a comparison of the product of sensitivity and natural abundance with other nuclei, as shown in Table I. Calcium-43 has a lower overall NMR sensitivity than any of the alkali metals. In fact, it has a lower sensitivity than most nuclei studied today. The nucleus has a spin of  $7/2$  and a quadrupole moment of  $-0.065b$ ; these factors lead to a fairly narrow natural line width ( $\sim 10$  Hz). The resonance frequency is somewhat low at 12.12 MHz (at a field of 42.88 kG), which is experimentally exacerbated by the fact that it is on the borderline between the frequency ranges of two probes we used to observe this nucleus.

Calcium salts do have an advantage (as opposed to Li or Mg) in that they do not have a high affinity for water. The attainment of water-free salts for nonaqueous studies is then rendered a difficult, but not an impossible task.

Table I. Properties of Selected Nuclei in NMR Spectroscopy.

Nuclei	Spin	Quadrupole Moment	Natural Abundance	Sensitivity	Overall Sensitivity
${}^7\text{Li}$	3/2	-0.040	93	0.29	27
${}^{23}\text{Na}$	3/2	0.11	100	0.093	9.3
${}^{39}\text{K}$	3/2	0.09	93	0.0005	0.047
${}^{87}\text{Rb}$	3/2	0.14	27	0.18	4.9
${}^{133}\text{Cs}$	7/2	-0.003	100	0.047	4.7
${}^{25}\text{Mg}$	5/2	0.22	10	0.027	0.27
${}^{43}\text{Ca}$	7/2	-0.003	0.13	0.064	0.0083
${}^{67}\text{Zn}$	5/2	0.16	41	0.0029	0.12
${}^{75}\text{As}$	3/2	0.3	100	0.025	2.5
${}^{31}\text{P}$	1/2	---	100	0.066	6.6



Once dried, the salts are sufficiently non-hygroscopic to assure that water is not producing a measurable contamination effect when solutions of these salts are studied in nonaqueous solvents.

This study has elucidated general trends in the solubility of calcium salts in nonaqueous solvents. The trends tend to follow the "hard, soft" concept of solvent donicity (42), rather than a Gutmann donor number (43) or dielectric constant relationship. That is, the "hard" calcium (relatively high charge to mass ratio) will prefer to bind to the "hard" oxygen donating solvents rather than the "soft" nitrogen donating solvents. This trend can be seen when considering the solubility of calcium nitrate in acetone, pyridine, and acetonitrile. Calcium nitrate is more soluble in acetone (donor number = 17.0, dielectric constant  $\epsilon = 20.7$ ) than in pyridine DN = 33.1,  $\epsilon = 12.3$ ) or acetonitrile (DN = 14.1,  $\epsilon = 38.0$ ), even though pyridine has a higher donor number and acetonitrile a higher dielectric constant than acetone. Within a given solvent the nitrates and perchlorates are more soluble than the halides, due to their bulky size and lower charge-to-mass ratio. With respect to calcium salts, it may be generalized that the lower surface charge density counterions ( $\text{ClO}_4^-$  and  $\text{NO}_3^-$ ) tend to be more soluble due to less ion-ion interaction.

### 3.3. Aqueous Studies - Chemical Shifts

The study by Lutz (5,6) represents the only previous natural abundance calcium-43 NMR investigation of the behavior of some calcium salts in aqueous solutions. The results are shown in Figure 2, where the units of concentration have been changed from the author's original units of moles solute/mole water to the more familiar molarity scale. The results of aqueous NMR studies of calcium salts in this work are shown in Figure 3. It is important to note that in Lutz' study the lowest limit of detection is 0.56 M calcium salt, while the lower limit of detection for this study is 0.15 M  $\text{Ca}(\text{ClO}_4)_2$ . This was obtained after approximately 15,000 scans ( $\sim 4$  h) at 8K memory and 5000 Hz sweepwidth. The minimum signal-to-noise ratio necessary before a chemical shift was recorded was 3. The signal-to-noise ratio was calculated by measuring the average noise around the baseline and comparing it to the height of the  $^{43}\text{Ca}$  resonance peak from that baseline.

The difference in detection limits is due to the use of a different magnetic field strength in the two studies. Lutz used a 1.807 T field whereas this study was done on a 4.288 T instrument. The increase in sensitivity of approximately 3.5, as measured by comparing the lower limits of detection, was due to the higher field, as well as the increased field stability of a superconducting magnet vs an iron core magnet. The greater stability of the



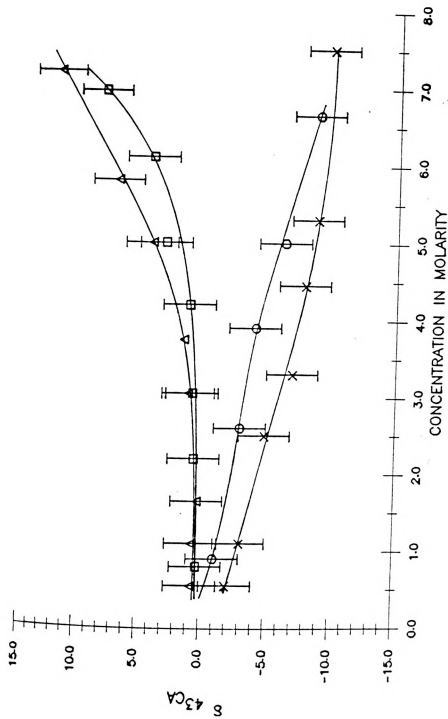


Figure 2. Concentration and anion dependence of the  $^{43}\text{Ca}$  chemical shift in aqueous solution measured with a 60 MHz NMR spectrometer (triangles -  $\text{CaCl}_2$ , squares -  $\text{CaBr}_2$ , circles -  $\text{Ca}(\text{ClO}_4)_2$ , and crosses -  $\text{Ca}(\text{NO}_3)_2$ ).

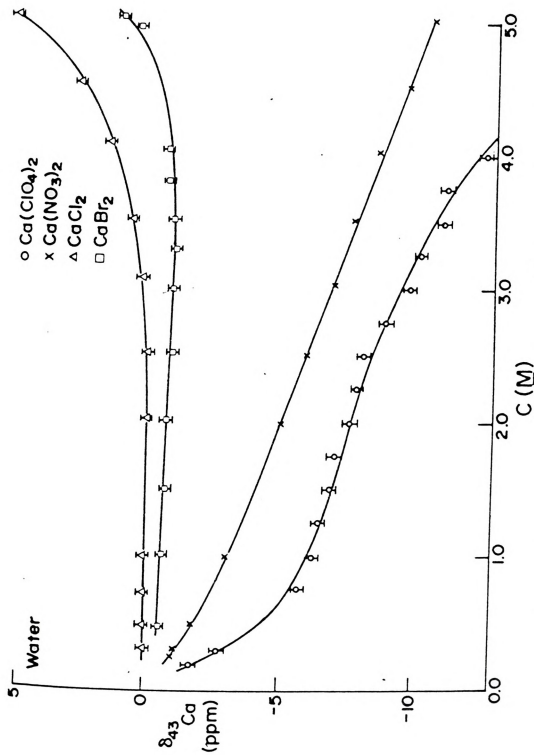


Figure 3. Concentration and anion dependence of the  $^{43}\text{Ca}$  chemical shift in aqueous solution measured with a 180 MHz NMR spectrometer.

magnetic field in this study also resulted in a lower error associated with a given measurement. The estimated error for any given chemical shift by repetitive measurement, in this study was  $\pm 0.2$  ppm, while Lutz found errors of approximately  $\pm 2$  ppm.

Aside from these differences, the experimental data of the two studies agree very well. For example, the concentration dependence of the chemical shift was identical within the experimental error. The conclusion drawn from this comparison is that the behavior of the resonance signal was reproducible, even if a different instrument was used. The demonstration of such reproducibility was necessary before the technique could be accepted as scientifically and analytically valid.

The relationship between the observed resonance signal and concentration in a system characterized by fast exchange of the cation between the two sites (the free ion and the ion-pair) is given by the expression

$$\delta_{\text{obs}} = X_f \delta_f + X_{\text{ip}} \delta_{\text{ip}} \quad (3)$$

where  $\delta_{\text{obs}}$ ,  $\delta_f$ , and  $\delta_{\text{ip}}$  are the observed, free, and ion-paired chemical shifts, respectively, while  $X_f$  and  $X_{\text{ip}}$  are the mole fraction of calcium ions in the free and ion-paired state. In the case of the chloride and bromide salts, the halogens are better electron donors than water.

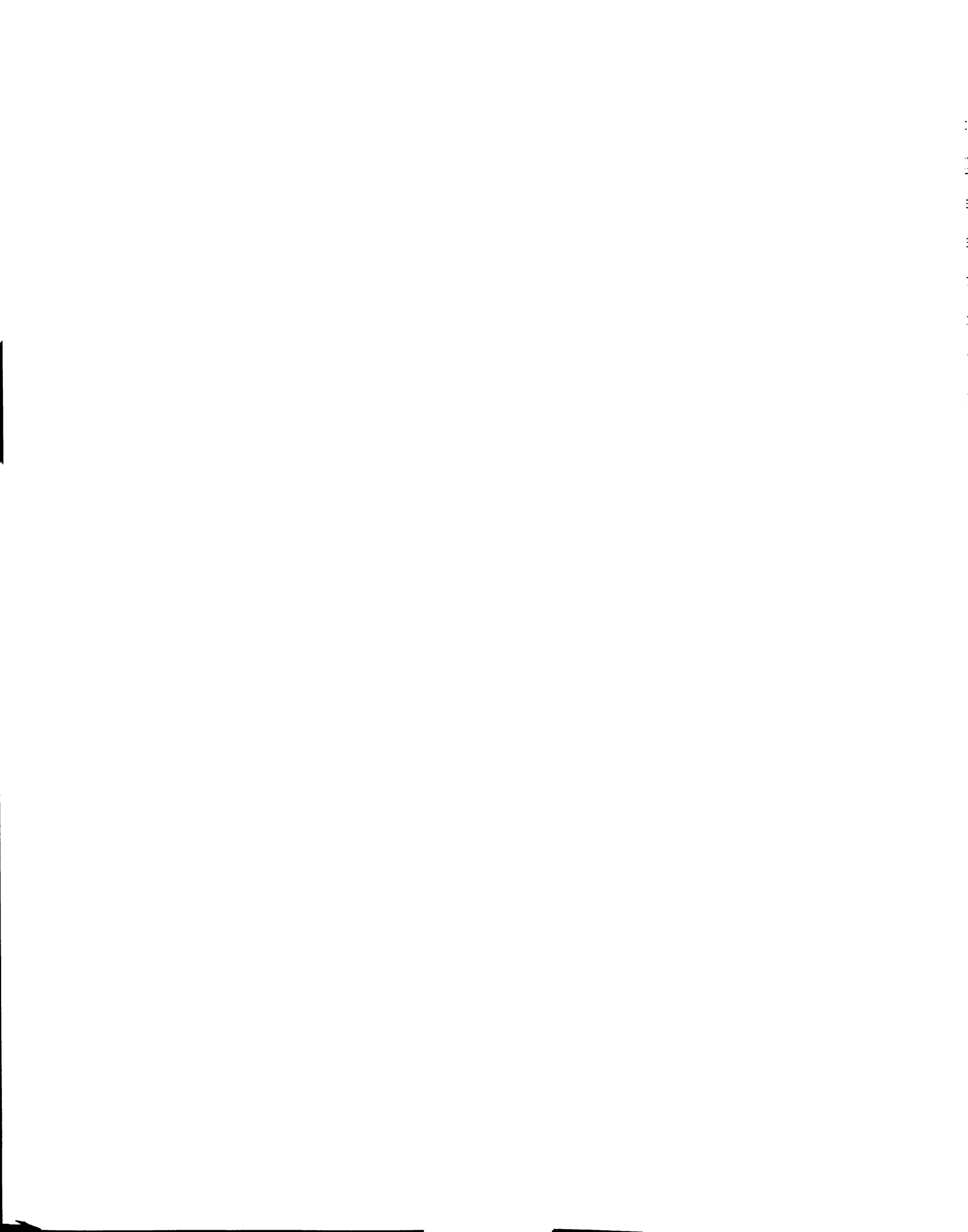


An ion-pair with a halogen will have a  $\delta_{ip}$  further downfield than that of the water-solvated, free calcium ion, due to the increase in electron density around the nucleus when the halogen replaces water. At infinite dilution the  $X_{ip}$  is essentially zero (no ion-pairing), increasing with increasing salt concentration. The result is a gradual shift in the resonance signal downfield with increasing concentration. The nitrate and perchlorate curves can be similarly predicted with the exception that the nitrate and perchlorate ions are worse electron donors than water, leading to a gradual upfield shift with increasing concentration.

Aqueous conductance studies of  $\text{CaCl}_2$  (44,45) and  $\text{Ca}(\text{NO}_3)_2$  (45), as well as a Raman study of  $\text{Ca}(\text{NO}_3)_2$  (46) tend to confirm the calcium-43 NMR evidence for ion-pairing. The conductance of aqueous  $\text{CaCl}_2$  and  $\text{Ca}(\text{NO}_3)_2$  solutions decreases with increasing concentration of salt. This behavior has been attributed to the formation of a neutral ion-pair as the salt concentration increases. The Raman evidence for ion-pairing is more direct, as the intensity of a band assigned to the ion-pair was observed to increase in intensity (as a free  $\text{NO}_3^-$  signal decreased) with increasing concentration.

While the NMR, conductance and Raman studies predict the presence of ion-pairing, the  $\text{CaCl}_2$  conductance studies indicate that ion-pairing occurs to a greater extent than seen by NMR studies. Conductance data indicate ion-pairing





of  $\text{CaCl}_2$  in solutions with a salt concentration of 0.01  $\text{M}$ , whereas the NMR results indicate ion-pairing becomes significant only at concentrations of approximately 2.5  $\text{M}$  and larger. This apparent contradiction can be rationalized through the realization that NMR and conductance techniques measure different phenomena. Conductance data measure the total amount of ion-pairing, while NMR data will only measure "contact" ion-pairing (47,48). Nuclear magnetic resonance spectroscopy, observing predominantly nearest neighbor effects, would be insensitive to solvent-separated ion-pairs. Hence the extent of ion-pairing in  $\text{CaCl}_2$  as observed by calcium-43 NMR is less than the extent of total ion-pairing observed by conductance experiments. A similar argument applies to  $\text{Ca}(\text{NO}_3)_2$ , although the agreement between conductance, Raman, and NMR data is better.

Equation (3) may be rewritten through the use of equilibrium and mass balance equations, to yield

$$\delta_{\text{obs}} = \left[ \frac{-1 \pm (1 + 4K_a C_T^M)^{1/2}}{2K_a C_T^M} \right] (\delta_f - \delta_{\text{ip}}) + \delta_{\text{ip}} \quad (4)$$

where  $K_a$  is the ion-pair formation constant and  $C_T^M$  the total salt concentration. As the total salt concentration is increased, the term in brackets approaches zero, or

$$\lim_{C_T^M \rightarrow \infty} \delta_{\text{obs}} = \delta_{\text{ip}} \quad (5)$$

This is somewhat at odds with the aqueous data, as there is no sign of a limiting behavior in the observed chemical shift. However, since the  $K_a$  for these ion-pairs is assumed to be small (46), the attainment of limiting behavior would not occur until a concentration exceeding the solubility of the salt.

Another consequence of Equation (4) is that the conductance data are not directly comparable to the NMR data. In Equation (4) the  $K_a$  is the contact ion-pair formation constant; hence there are two unknowns,  $K_a$  and  $\delta_{ip}$ . Attempts to fit Equation (4) to the data using a non-linear curve fitting computer program (38) with two unknowns have failed due to a lack of points in the limiting region. This is why only qualitative comparisons can be made between the methods.

The behavior of  $\text{Ca}(\text{ClO}_4)_2$  in aqueous solutions is anomalous, with two processes apparently occurring in solution. From infinite dilution to  $\sim 1.5 \text{ M}$ , ion-pairing occurs, with the chemical shift remaining constant from about 1-2  $\text{M}$ . The resonance signal then shifts upfield, apparently not reaching a constant value. A possible explanation is the formation of a  $\text{Ca}(\text{ClO}_4)_2$  ion triplet at  $\sim 2 \text{ M}$ . This would shift the resonance further upfield with increasing concentration, just as an ion-pair did initially. Aqueous conductance data are lacking to support such a hypothesis.

The conclusion reached from this study is that  $\text{CaCl}_2$

is the salt of choice in aqueous solutions when it is desired to minimize ion-ion interactions. The influence of the chloride ion on the calcium resonance signal behavior is less than that of the other salts studied.

#### 3.4. Linewidths

The linewidths (the full width at half-height of a  $^{43}\text{Ca}$  resonance signal) do not vary appreciably for the aqueous calcium salts studied. The bromide and chloride salts exhibited a linewidth of  $5 \pm 2$  Hz over the entire concentration range. This agrees, within the experimental error, with the values of Lutz (6) and Parello (9). The linewidth for the nitrate and perchlorate salts increases with increasing concentration from 5 Hz to approximately 15 Hz. This increase is probably due to viscosity broadening, as the solutions above 3 M tended to be viscous. The same behavior was observed by Lutz (6).

#### 3.5. Studies in Nonaqueous Solutions

##### 3.5.1. Chemical Shifts

The behavior of calcium salts in nonaqueous solvents was studied by  $^{43}\text{Ca}$  NMR in the following media: acetone, dimethylformamide (DMF), dimethylsulfoxide (DMSO), ethylene glycol, formamide, methanol (MeOH), propylene carbonate (PC), and tetramethylguanidine (TMG). Some pertinent



properties of the above solvents are shown in Table II. The solvents chosen represent a wide range of solution properties such as, dielectric constant ( $\epsilon_{\text{TMG}} = 11.0$  to  $\epsilon_{\text{formamide}} = 109.5$ ), viscosity (15 cp for EG to 0.32 cp for methanol at 25°C), and the Gutmann donor number (15.1 for PC to 29.8 for DMSO). The Gutmann donor number (43) is an empirical scale of the donor ability of solvents. It is based on the enthalpy of the 1:1 complex formation of the solvent molecule, S, with antimony pentachloride, both dissolved in 1,2-dichloroethane as the solvent. The degree of contact ion-pairing, as measured by multinuclear NMR spectroscopy, has been found to be dependent on bulk solution properties such as the donor number and dielectric constant (49-51). Ions in solvents with low donicity and/or low dielectric constants tend to show an increasing tendency towards ion-pairing.

The chemical shift results in the calcium-43 NMR studies of nonaqueous systems are presented in Figures 4 and 5. The studies were limited in the number of salts investigated due to solubility restrictions. The study of some calcium salts in methanol is shown in Figure 4. The behavior of  $^{43}\text{Ca}$  chemical shifts for the chloride, nitrate, and perchlorate is qualitatively similar to that observed for these salts in water. An increase in concentration produces a downfield shift for chloride salt, but an upfield shift for nitrate and perchlorate salts. As

Table II. Some Solvent Properties and Magnetic Susceptibility Corrections.

Solvent	Gutmann's Donor Number	Dielectric Constant	Viscosities at 25°C in cp	Magnetic suscept. Correction on WH-180 in ppm
Acetone	17.0	20.7	0.32	+1.1
Dimethylformamide (DMF)	26.6	36.7	0.80	+0.6
Dimethylsulfoxide (DMSO)	29.8	46.7	2.0	+0.5
Ethylene Glycol	----	37.7	10	---
Formamide	29.0	109.5	3.3	+0.7
Methanol (MeOH)	25.7	32.7	0.55	+0.9
Propylene Carbonate (PC)	15.1	65.0	2.5	+0.4
Tetramethylguanidino (TMG)	----	11.0	1.4	+0.5
Water	33.0	78.5	0.89	0.0

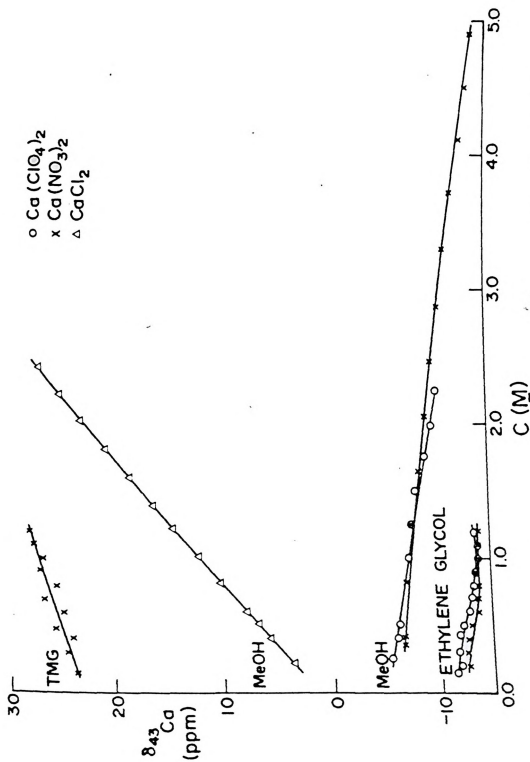


Figure 4. Concentration and anion dependence of the  $^{43}\text{Ca}$  chemical shift in TMG, methanol, and ethylene glycol.



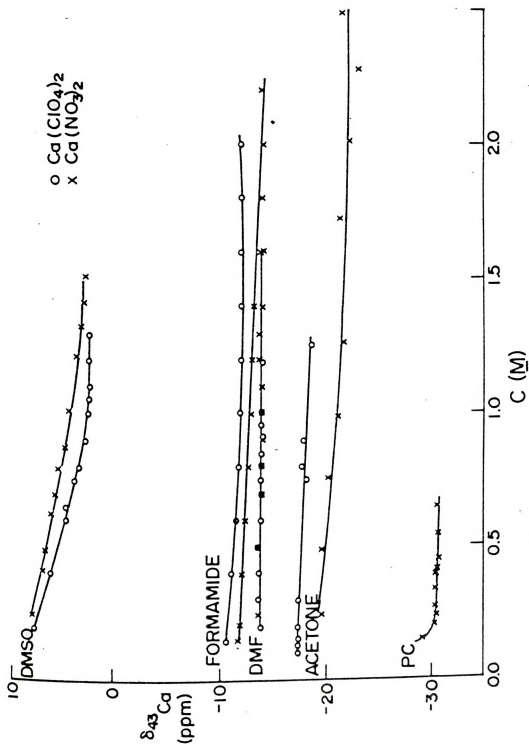


Figure 5. Concentration and anion dependence of the  $^{43}\text{Ca}$  chemical shift in DMSO, formamide, DMF, acetone, and propylene carbonate.



the concentration increases, perchlorate shifts further upfield than the nitrate which is similar to its aqueous behavior. Methanol is generally a weaker donor solvent than water, although there is some disagreement as to the donor number of water (43,52). The extent of ion-pairing should be greater in methanol, and this can be seen by the behavior of the chloride salt. The chemical shift of calcium chloride moves downfield even at low concentrations, indicating a greater tendency towards ion-pairing than in water.

In aqueous solutions, the chemical shifts for all salts upon infinite dilution tended to the same value, which is indicative of the free hydrated species (54). Similarly, the infinite dilution chemical shifts in methanol should converge to one value. This can be qualitatively seen in Figure 4. It seems likely that, near infinite dilution, the calcium nitrate and perchlorate shifts will vere sharply downfield, much the same as in water. In methanol, this shift would occur below the limit of detection. The linear extrapolation of the calcium chloride line to infinite dilution will probably more nearly represent the infinite dilution chemical shift in methanol (estimated at 1 ppm).

The variation in the chemical shift with concentration for calcium nitrate and perchlorate in ethylene glycol solution indicates the formation of stable ion-pairs.



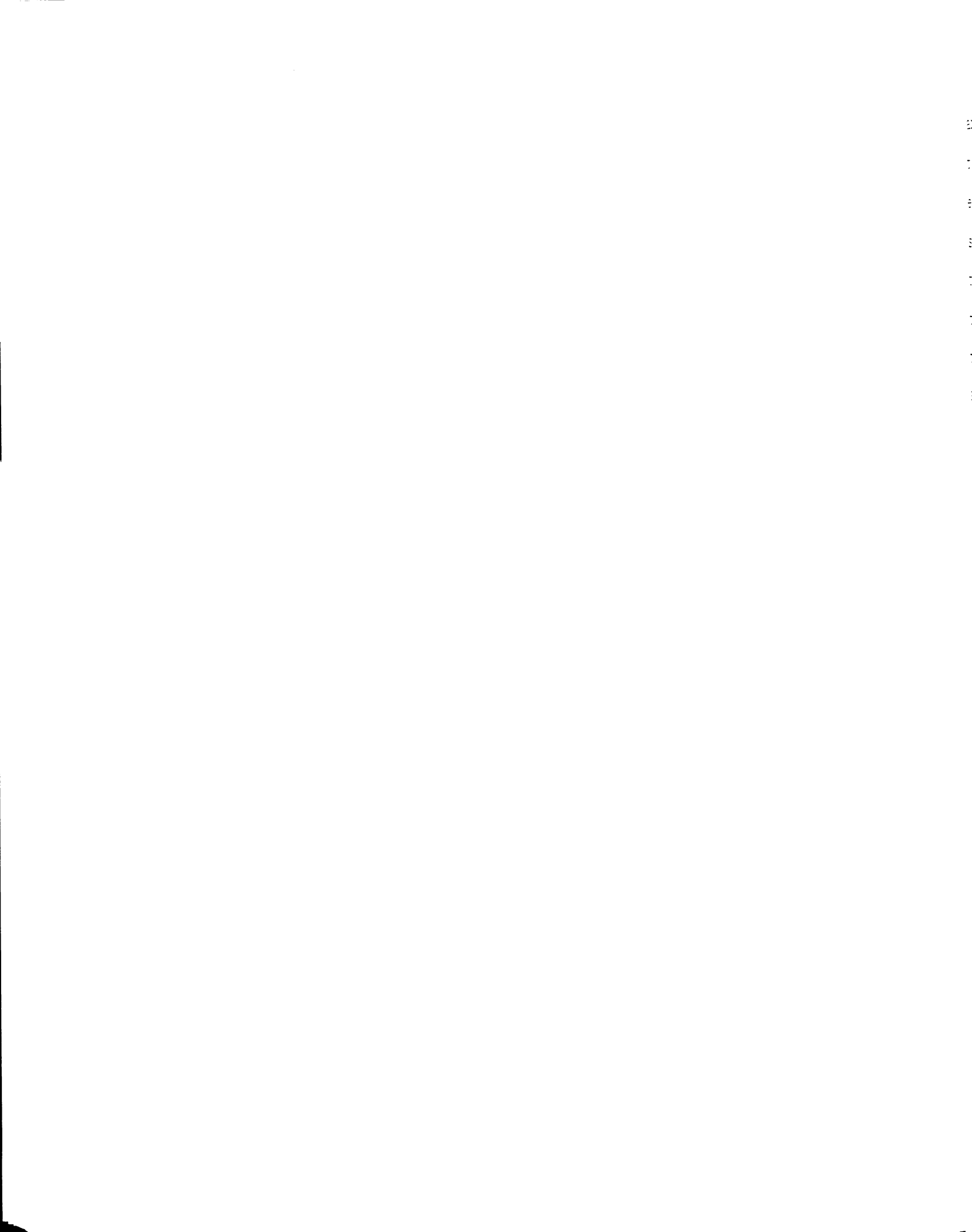
There is an upfield chemical shift with increasing concentration, with an apparent limiting value of the chemical shift reached at approximately 1 M. While variation in the chemical shift with concentration is too slight to computer fit to Equation (4) (the computed errors in the calculated  $K_a$  and  $\delta_{ip}$  are much larger than the computed values), it is apparent that most of the calcium ions are ion-paired by 1.0 M. Similar behavior has also been observed in calcium nitrate solutions in PC. Again, the trend is not large enough to analyze the data quantitatively, but it appears that the calcium nitrate is completely ion-paired at concentrations  $\geq 0.25$  M. From a consideration of the low donor number of PC and low dielectric constant of ethylene glycol (donor number of which has not been measured), the extent of ion-pairing is not unexpected.

Significant ion-pair formation is also indicated by studies in DMSO solution. A limiting chemical shift was obtained at approximately 1 M salt concentration. The chemical shift data have been more amenable to computer fitting to derive  $K_a$  and  $\delta_{ip}$ . The  $K_a^{NO_3}$  was found to be  $0.8 \pm 0.2$  and  $\delta_{ip}$  is  $-9 \pm 1$  ppm, while the  $K_a^{ClO_4} = 4 \pm 2$  and  $\delta_{ip} = -2 \pm 1$  ppm. The errors are large, but it can be seen qualitatively in Figure 5 that the perchlorate reaches a limiting behavior before the nitrate. A secondary source of error, not considered in the computer analysis, is in the estimation of  $\delta_f$ , with the total error rendering the

values trustworthy only to an order of magnitude. It must be emphasized that in these studies the  $K_a$  determined is a concentration ion-pair formation constant.

The study in dimethylformamide (DMF) and formamide solution are interesting in that interactions with the calcium ion should be present in each solvent, but in DMF these are modified by the presence of the two methyl groups. In the case of formamide, contact ion-pair formation is indicated, although the extent of formation is small. The overall chemical shift range for the concentration study was 1 ppm for the perchlorate and 2 ppm for the nitrate. The counter-ion dependency is also indicated by the presence of two distinct curves representing the concentration dependence of the chemical shift, separated by 2 ppm. This behavior is due to the strong solvating ability of the formamide. It has a high dielectric constant, which would tend to minimize ion-ion interactions. The study in DMF produced somewhat unexpected results. There was found to be no concentration or counter-ion dependence of the chemical shift in the 0.2 - 1.5 M concentration range. Therefore, either there is a quantitative formation of contact ion-pairs, or complete dissociation throughout the concentration range.

The co-linearity of the lines representing the concentration dependence of the chemical shift would tend to eliminate the first possibility, as the electron density



around the nitrate and perchlorate ions are different; this difference would lead to a different environment experienced by the calcium ion for each ion-pair. The second possibility is somewhat at odds with the current theories of solvation. Bulk solvent properties, such as the dielectric constant and Gutmann donor number, would tend to indicate that DMF will not solvate the calcium ion as well as water or DMSO. Hence, one would expect more ion-ion interactions as the solvating ability decreases. However, neither the Gutmann donor number nor the dielectric constant is, of itself, the best indication of the solvating ability of a given solvent. The anomalous behavior in DMF could indicate that the solvent forms a strong complex with the calcium ion. The keto group of DMF would have a higher electron density than formamide, due to the inductive effects of the methyl groups. This could lead to a strong complex which would be resistant to replacement of a DMF molecule by the nitrate or perchlorate.

Calcium nitrate in tetramethylguanidine solution also shows somewhat anomalous behavior. The linear behavior of the calcium-43 chemical shift with concentration can be explained by ion-pairing, and it has been seen previously in formamide and methanol. However, the direction of the chemical shift change with increasing concentration is anomalous. Replacement of the solvent by the nitrate ion is expected to produce an upfield shift, yet in TMG



the shift is downfield with increasing concentration. This may be explained by the structure of TMG vs that of the nitrate ion. TMG is a pure nitrogen donor (as opposed to a nitrogen and oxygen donor such as formamide), which would have a lower electron density around the coordinating group than an oxygen donor. Hence, although the negative charge is spread over three oxygen atoms, the donating oxygens of the nitrate group have a higher electron density than the solvent. The result is a downfield shift with increasing concentration.

Calcium ion solutions in acetone were also studied. There is evidence for ion-pairing, as seen by the concentration dependence of the chemical shift, but the overall change is slight. Counterion dependency is seen in the different lines obtained for the perchlorate and the nitrate. Conductance studies on calcium perchlorate solutions in acetone (55) indicate the formation of ion-pairs, although such studies predict a greater degree of ion-pairing than is seen by  $^{43}\text{Ca}$  NMR.

In conclusion, calcium-43 NMR studies show the technique to be very sensitive to the immediate environment of the calcium ion. Near-neighbor effects are minimal, which renders the technique sensitive to contact ion-pairing only. This lack of sensitivity to long range interactions is confirmed by comparing the extent of ion-pair formation as seen by conductance (studies are sadly lacking in most

nonaqueous solvents) and NMR. Conductance studies frequently indicate a greater extent of ion-pairing than NMR studies. Raman spectroscopy studies of  $\text{Ca}(\text{NO}_3)_2$  solutions (46) indicate that this technique is sensitive only to contact ion-pairing. The degree of ion-pairing predicted from Raman spectroscopy studies is closer to that predicted from  $^{43}\text{Ca}$  NMR than conductance ion-pairing data.

### 3.5.2. Linewidths

Representative linewidths for all solvents studied are presented in Table III. The linewidth is related to the spin-spin relaxation time through

$$\Delta\nu_{1/2} = 1/\pi T_2^* \quad (6)$$

and

$$1/T_2 = 1/T_2^* + \gamma \Delta H_0/2 \quad (7)$$

where  $T_2^*$  is the apparent spin-spin relaxation obtained from the linewidth,  $T_2$  is the actual spin-spin relaxation time,  $\Delta\nu_{1/2}$  is the full width at half height of the resonance signal,  $\gamma$  is the gyromagnetic ratio for a given nuclei, and  $\Delta H_0$  is the contribution to the linewidth due to field inhomogeneity. The contribution due to the field inhomogeneity is usually negligible for super conducting magnets.

Table III. Linewidths of the Calcium-43 Resonance Signal in Some Solvents.

Solvent	Conc. (M)	Full Width at 1/2 Height (Hz)	
		Ca(NO <sub>3</sub> ) <sub>2</sub>	Ca(ClO <sub>4</sub> ) <sub>2</sub>
Acetone	0.25	22	14
	1.25	49	53
	2.7	205	--
DMF	0.3	7	7
	1.1	10	15
DMSO	0.4	14	12
	1.3	28	51
Ethylene glycol	0.4	40	13
	1.2	53	26
Formamide	0.2	17	8
	2.0	34	25
Methanol	0.4	6	6
	2.2	15	10
PC	0.4	30	--
	0.7	36	--
TMG	0.4	37	--
Water	0.3	5	5
	4.0	9	12

Since extreme narrowing conditions exist for this nuclei under the conditions of this study (which implies  $T_1 = T_2$ ), the observed linewidth is then related to  $T_1$  (the spin-lattice relaxation time) by

$$\Delta\nu_{1/2} = 1/\pi T_1 \quad (8)$$

Of the five principle relaxation processes: dipole-dipole relaxation, chemical shift anisotropy, scalar coupling, spin rotation, and quadrupole relaxation, the latter has been found to be dominant for nuclei with a spin greater than 1/2 (56). The rate of relaxation is then given by

$$R_1 = \left(\frac{3}{40}\right) \left(\frac{2I+3}{I^2(2I-1)}\right) \left(1 + \frac{\eta^2}{3}\right) (e^2 Q_q / h)^2 \tau_c \quad (9)$$

where  $R_1$  is the relaxation rate,  $I$  the spin of the nucleus,  $\eta$  the assymetry parameter,  $Q$  the quadrupole coupling constant, and  $\tau_c$  the translational correlation time. A change in linewidth due to ion-pairing is usually caused by changing the molecular symmetry ( $\eta$ ) and quadrupole coupling constant. The correlation time is related more to a difference in solvation of the ion from one solvent to another. It can be thought of as the time required for a translational movement through the distance of a molecular diameter and is hence related to the solvent structure as well as ion

solvation. Solvents which are strongly bound to an ion tend to have low correlation times with a subsequent narrow linewidth (57).

The lack of ion-pairing information from chemical shift data in acetone is compensated by a wealth of linewidth information. Acetone will weakly solvate the calcium ion leading to fairly large linewidths at low concentrations, where little ion-pairing is expected. A contact ion-pair, however, drastically alters the symmetry and quadrupole coupling constant, leading to a large increase in linewidth with increasing concentration. Hence, while chemical shift data do not seem to indicate significant ion-pairing, changes in the linewidth with concentration appear to indicate that it is substantial. Such studies underline the importance of obtaining both linewidth and chemical shift information in an NMR study.

The narrow linewidth of the calcium resonance signal in DMSO, methanol, DMF, and water solutions all indicate a symmetrical, as well as relatively tight, solvation. The linewidth data are further evidence for a strong solvation/complexation of DMF with calcium. The study in tetramethylguanidine indicate weak solvation (resulting in a broad resonance signal) with an influence of ion-pairing as the concentration increases. Propylene carbonate, formamide, and ethylene glycol are also weakly solvated, although how much this effect contributes to the linewidth

13

12

11

10

9

8

7

6

5

4

3

2

1

is unknown. The other contribution in the case of these three solvents is line broadening due to viscosity. The viscosity of ethylene glycol is approximately .10 cp, that of PC 2.5 cp, and that of formamide 3.3 cp at 25°C. When salt solutions are made on the order of 0.5 M in these solvents, the viscosity is further increased. In these three cases, viscosity is certainly a dominant factor in the resultant broad linewidth.

### 3.6. Gutmann Donor Number Correlation

Previous studies in this laboratory (51,58,59) have shown a correlation between the solvent donicity scale of Gutmann (43) and the infinite dilution chemical shift of given nuclei. Since the infinite dilution chemical shift represents the solvation of the bare calcium ion, its value would be a measure of the donating ability of a solvent. The infinite dilution chemical shifts for a series of solvents should then reflect the relative donating ability of a given solvent with respect to others. The correlation between the relative donicities expressed by NMR and those formulated by Gutmann are shown in Figure 6.

The relatively large errors associated with the estimation of infinite dilution chemical shifts in acetone, DMSO, ethylene glycol, formamide, PC, and TMG are due to an uncertainty in the behavior below the limits of





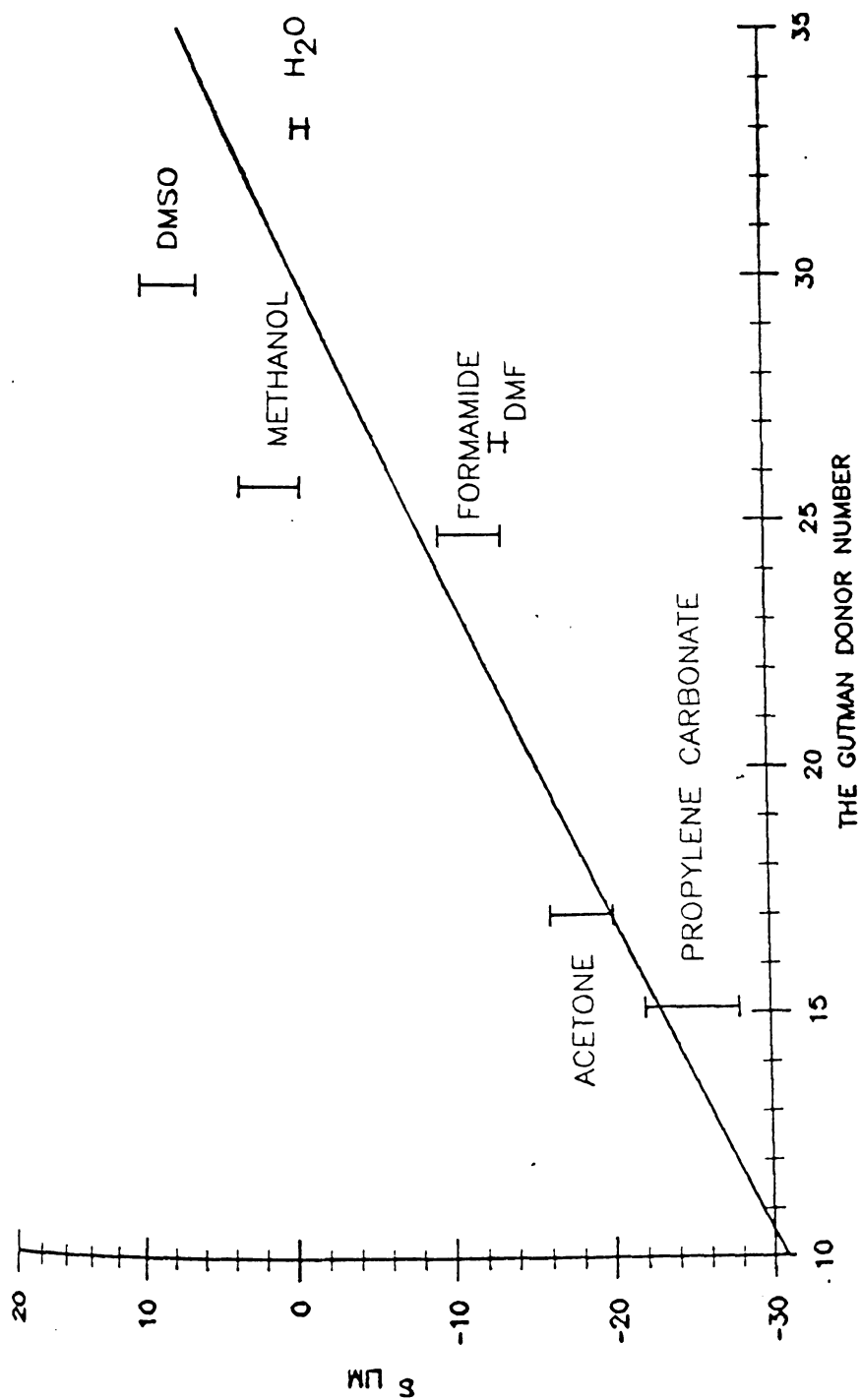


Figure 6. A plot of the Gutmann donor number vs the  $^{43}\text{Ca}$  infinite dilution chemical shift.

sensitivity. The concentration dependence of the  $^{43}\text{Ca}$  chemical shift for  $\text{Ca}(\text{NO}_3)_2$  and  $\text{Ca}(\text{ClO}_4)_2$  solutions in water shows that the chemical shift may change by 2 or 3 ppm between the infinite dilution and the lower detection limits. In fact, the infinite dilution  $^{43}\text{Ca}$  chemical shift could only be obtained by studying  $\text{CaCl}_2$  solutions in water. The downfield (higher electron density) trend in the chemical shift at infinite dilution with increasing donor number is logical, since a higher donating ability implies a greater electron donation to the calcium ion. However, the scatter of the points (a correlation coefficient for the two parameters of 0.83), would indicate that the Gutmann donor number is perhaps not the best indication of solvent donicity. The donor numbers of TMG and ethylene glycol are predicted graphically to be 44 and 23, respectively. These numbers are qualitative, but useful for the prediction of chemical shift behavior for other nuclei.

### 3.7. Complexation

Complexation studies were exploratory, being limited in both scope and depth. The calcium-ethylenediamine tetraacetate system was studied using  $^{43}\text{Ca}$  NMR in aqueous solution at a pH of 10. A plot of ligand-to-metal mole ratio vs the chemical shift of the calcium-43 resonance is shown in Figure 7. There is a slight downfield shift

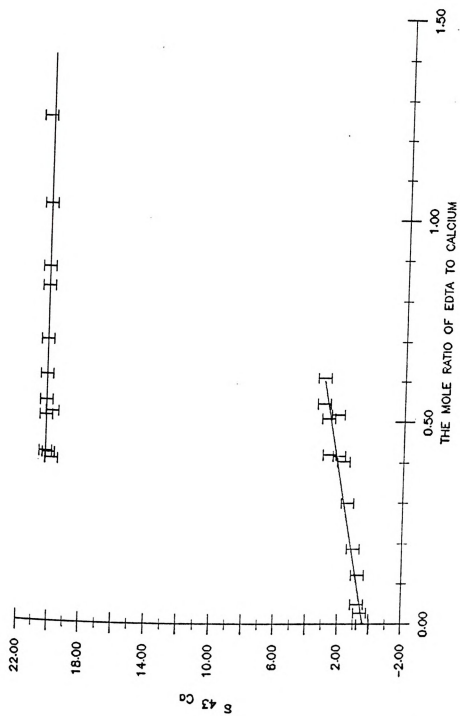


Figure 7. A plot of the observed  $^{43}\text{Ca}$  chemical shift vs the mole ratio of EDTA to calcium.

of the calcium resonance between a mole ratio of zero to 0.4. In the 0.4 to 0.6 range a new resonance signal appears approximately 18 ppm downfield. This signal increases in intensity, while that of the free calcium signal decreases, but the resonance frequency remains constant. Beyond a mole ratio of 0.6, the free calcium signal is no longer detectable. The linewidth of the free (7 Hz) and complexed (8 Hz) calcium resonance remained fairly constant over the entire mole ratio range. The presence of two distinct signals indicates that the exchange process between solvated and complexed calcium is slow on the NMR time scale. Similar results were obtained by Heubel (51) in the study of the magnesium-EDTA system.

In principle the formation constant of the complex could be calculated from the areas under the curves, which are proportional to the relative concentrations of the free and complexed calcium ion. In this case, however, the signal-to-noise ratio was not high enough to allow the accurate determination of the area under the peak (see Figure 8). The areas can be approximated by a function of the height of the peak, with the ratio of areas equal to a ratio of peak heights (for approximately equal linewidths). From the ratio of peak heights, the formation constant must be large (it is approximately  $10^{10}$  under these conditions (15)). Within the experimental error, all of the EDTA was complexed by calcium below a mole ratio of one.

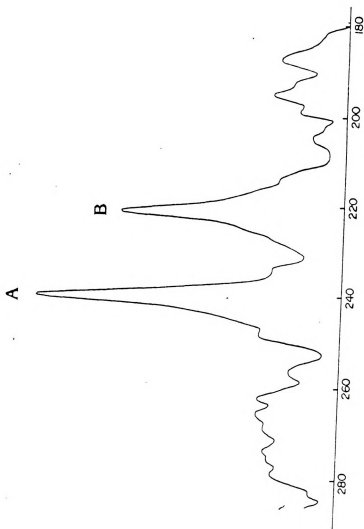


Figure 8. Calcium-43 resonance of a solution 0.4M in  $\text{CaCl}_2$  and 0.2M in EDTA at pH 10. Peak A - complexed  $\text{Ca}^{2+}$ , Peak B - free  $\text{Ca}^{2+}$ .

The complexation of 15C5 with calcium ion was investigated in aqueous solution. A mole ratio study showed no evidence for the formation of a 15C5-calcium complex. There was no change in the linewidth or the chemical shift over the mole ratio range 0-2. This result confirms the results of a calorimetric study of the calcium-15C5 system by Izatt (19), and the emf measurements by Hoviland (60).

In the case of the  $18C6 \cdot Ca^{2+}$  complex, the exchange of  $Ca^{2+}$  ion between the two sites - free solvated ion and complex - is slow, and two  $^{43}Ca$  resonances are observed in solutions containing an excess of  $Ca^{2+}$  ion. The resonance of the  $Ca^{2+}$  ion was approximately 40 ppm upfield from the free calcium resonance. This signal increased in intensity with increasing ligand-to-metal mole ratio, while showing no linewidth or chemical shift changes over the mole ratio range 0 to 1. Slow exchange between the complex and solvated calcium was also indicated by Dale and Kristiansen (61), who conducted a proton NMR study of the same system. No attempt was made to calculate the formation constant since the signal-to-noise ratio precluded either an accurate peak area or height measurement.

The chemical shifts of the complexed resonances for calcium-EDTA and calcium 18C6 can be qualitatively explained by the electron density of the ligand. The EDTA has negatively charged oxygen atoms chelating the calcium, which have a higher electron density than the water. The 18C6, on the other hand, has only ether atom bonding,

with a lower electron density than the solvent methanol. EDTA would then have a complex resonance downfield from the free aqueous calcium, whereas the 18C6 calcium complex has a resonance far upfield from the solvent methanol.

Calcium ion forms a sparingly soluble precipitate upon the addition of the deprotonated form of PAA. The solubility of this precipitate is less than 0.1  $\underline{M}$ , which means that the sensitivity of calcium- $^{43}$  NMR precludes its use for this system.

Routine determination of complexation formation constants using calcium- $^{43}$  NMR is limited by the low sensitivity of the method. Since the lower limit of detection is 0.2  $\underline{M}$ , any complexation study with calcium would have to be carried out at a very high ionic strength. Any concentration formation constants determined would have little physical significance, as the ion-ion interactions would abound, and these will complicate the system beyond a simple complex formation model. Although the chemical shift is a very sensitive probe of the immediate environment around the calcium, limits of detection render other techniques, e.g., potentiometry with an ion selective electrode, more applicable to the study of calcium ion complex.

### 3.8. Conclusions

The range of  $^{43}\text{Ca}$  chemical shifts due to complexation, ion-pairing, or nonaqueous solvent interactions is approximately 60 ppm. This indicates the sensitivity of the technique to the environment of the calcium ion. Extensive use of this method for the measurement of thermodynamic properties is inhibited chiefly by the low natural abundance of calcium-43. Enrichment is presently very expensive, while natural abundance studies do not have respectable detection limits. However, the trend towards higher magnetic fields will result in a dramatic improvement of detection limits for this technique. A comparison between the data of Lutz (5) and the present work reveal an increase in precision and sensitivity attained by higher fields. It is hoped that, as larger and more homogeneous fields evolve, the technique of calcium-43 NMR will prove to be useful in dilute solutions.



PART II

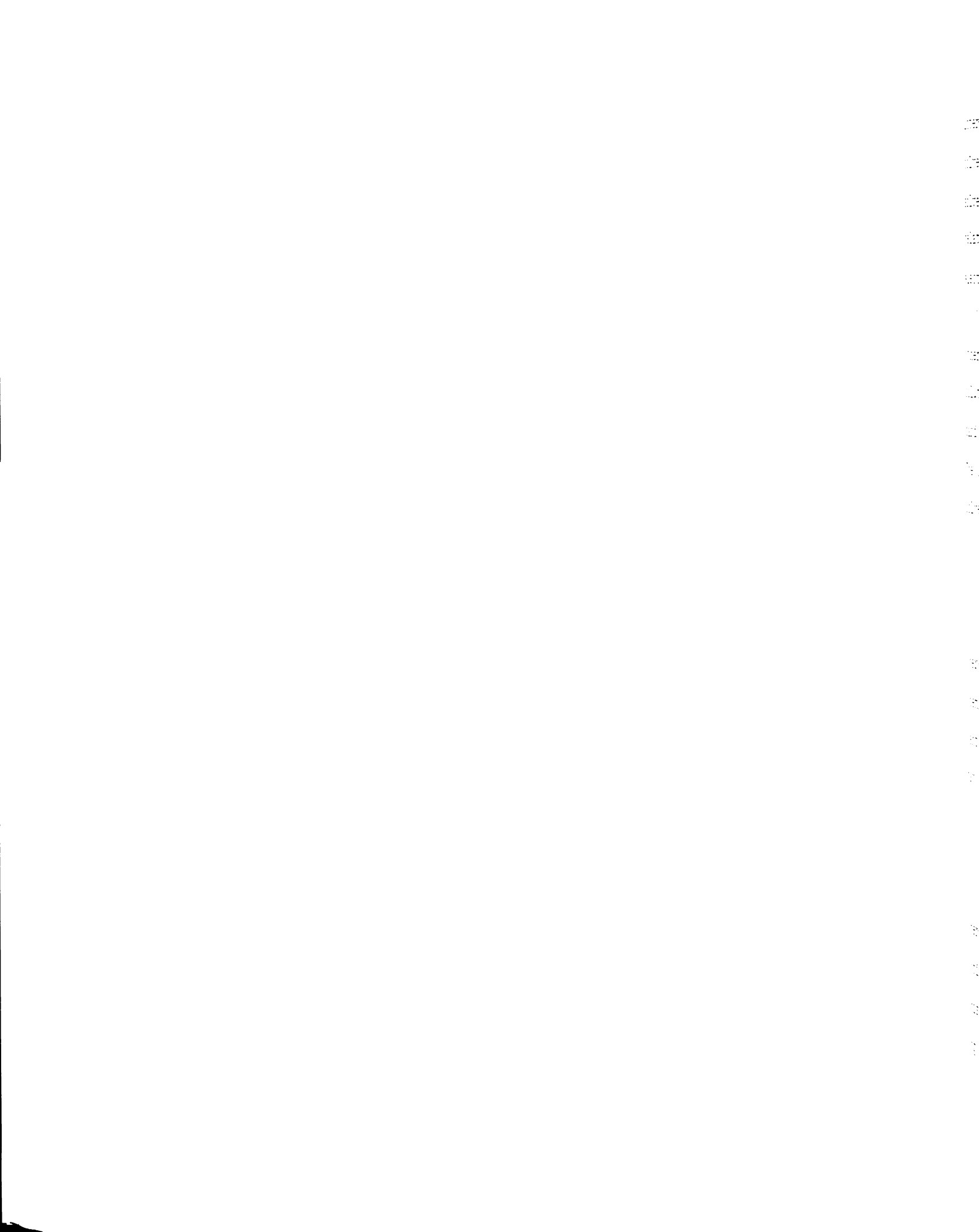
AN NMR INVESTIGATION OF THE REFERENCE ELECTROLYTE  
ASSUMPTION FOR THE DETERMINATION OF SINGLE  
ION MEDIUM EFFECTS

CHAPTER I

INTRODUCTION AND HISTORICAL

## 1.1. Introduction

Historically, most solution chemistry studies have been conducted in aqueous media. Convenient standard states evolved, e.g., an ideal one molal (or one molar) solution of an electrolyte for activity, the standard hydrogen electrode for electrochemistry, etc., which were used as references for solution properties when comparing them with another solution similarly referenced. There has been increasing interest, however, in the solution chemistry that occurs in nonaqueous solvents. Nonaqueous solvents are advantageous when compared to water in that the physical properties of the media (the acidity or basicity, the dielectric constant, the electrochemical potential window, temperature range, etc.) can be varied by changing solvents to facilitate the observation of an interested chemical phenomenon. The use of nonaqueous solvents necessitated the adoption of standard states in that solvent. In most cases for a given solvent, the standard state was adopted analogous to that in water, e.g., the hypothetical one molal solution, the standard hydrogen electrode in that solvent, etc. Such a system leads to as many standard states as there are solvents, with no a priori relationship between them. Since it is of



interest to compare the behavior of a system in different solvents, a means of relating the standard states of various solvents is necessary. If this could be done, fundamental relationships such as a solvent-independent pH scale or electrochemical potential scale, would be obtainable.

Water is usually chosen as the standard solvent, all other solvents being referred to the analogous aqueous solution. The problem then reduces to relating the standard states in water to those in the nonaqueous solvent. The chemical potential of an electrolyte in a nonaqueous solvent at a given concentration is given by

$$\bar{G}_i = {}_s\bar{G}_i^\circ + RT \ln {}_s a_i \quad (1)$$

where  $\bar{G}_i$  is the chemical potential,  ${}_s\bar{G}_i^\circ$  is the standard chemical potential, and  ${}_s a_i$  is the activity using the solvent standard state (17). Similarly, the same equation may be written using an aqueous standard state

$$\bar{G}_i = {}_w\bar{G}_i^\circ + RT \ln {}_w a_i \quad (2)$$

where  ${}_w\bar{G}_i^\circ$  and  ${}_w a_i$  refer to an aqueous standard state and activity. While  $\bar{G}_i$  is clearly the same in the two cases, this does not imply that  ${}_w\bar{G}_i^\circ = {}_s\bar{G}_i^\circ$ , or  ${}_w a_i = {}_s a_i$ . Equating (1) and (2) yields

$$\left( {}_s\bar{G}_i^\circ - {}_w\bar{G}_i^\circ \right) = \Delta\bar{G}_{tr}^\circ = RT \ln \frac{{}_w a_i}{{}_s a_i} \quad (3)$$

The activities can be expressed in terms of activity coefficients and molalities. Since we are dealing with one solution, Equation (3) becomes

$$\bar{G}_{tr}^{\circ} = RT \ln \frac{wY_i}{sY_i} \quad (4)$$

But  $sY_i$  approaches unity at infinite dilution, yielding

$$\Delta \bar{G}_{tr}^{\circ} = RT \ln (wY_i) \quad (5)$$

This factor  $wY_i$  is the activity coefficient of the electrolyte dissolved in a nonaqueous solvent, but based on an aqueous standard state. Its value depends on the difference in the molal standard chemical potentials between water and the nonaqueous solvent. This term is given the symbol  $mY_i$  and called the medium effect, or transfer activity coefficient. The quantity  $\Delta \bar{G}_{tr}^{\circ}$  is called the standard free energy of transfer. Conceptually, the transfer activity coefficient is a conversion factor which relates a solute's properties in water to those in some nonaqueous solvent.

Equation (5) is valid for neutral molecules as well as neutral combinations of electrolytes. This is as far as a rigorous thermodynamical treatment will allow the theory to proceed. However, Equation (5) is not in a form which is too terribly useful, as many experiments

(e.g., the measurement of pH, the determination of the SHE emf, etc.) require the knowledge of transfer activity coefficients of single ions. To obtain values for the transfer activity coefficients of a single ion requires the use of an extra-thermodynamic assumption.

## 1.2. Historical

The estimation of single ion activity coefficients has been attempted using a number of different methods. Bjerrum and Larsson (62) and later Iowa (63), and Parker et al. (64) estimated single ion activity coefficients electrochemically assuming a negligible liquid junction potential at an aqueous and nonaqueous interface. Extrapolation techniques, based on ion size parameters, were used by Izmaylou (65), Feakins and Watson (66), and Deligny, et al (67) to calculate transfer free energies from aqueous to nonaqueous solvents for some alkali metal ions. Similar extrapolation studies were conducted, based on Buckingham's theory of hydration (68), to determine transfer free energies from water to N-methylformamide (69) and to some mixed aqueous-nonaqueous solvents (70-72).

A major area of interest has been in the use of a standard reference, whose properties are solvent independent. Pleskov (73) was the first author to propose the use of this assumption when he proposed that the emf of a  $\text{Rb}^+/\text{Rb}$  half-cell was solvent independent. Other

proposals for reference standards have been: iron(III)-phenanthroline/iron(II)-phenanthroline (74,75), tetraphenylarsonium-tetraphenylgermanium (78), tetraphenylborate-tetraphenylmethane (79), Hammett indicator acids (80), triiodide-iodine (81). The most popular of these assumptions is that proposed by Koepp, et al (76), that the emf of a ferricene-ferrocinium (or cobaltocene-cobalticinium) half-cell is solvent independent.

A more complete review and critique of these assumptions may be found in the reviews by Popovych (77,82), Parker (83) and Kolthoff (84). The most disturbing aspect of these assumptions is their lack of agreement in calculated medium effects, as seen in Table IV.

### 1.3. Reference Electrolyte Assumption

The most popular of the standard reference assumptions is the reference electrolyte assumption (82). It postulates that the transfer free energy for a given 1:1 electrolyte can be equally apportioned between the cation and anion. Obviously, the choice of the appropriate salt is of critical importance. To date, three such reference electrolytes have been introduced: triisoamyl-n-butyl ammonium tetraphenylborate (85), tetraphenylphosphonium tetraphenylborate (86), and tetraphenylarsonium tetraphenylborate (87) (the latter two being the most popular, see Figure 9).

For a solid reference electrolyte in equilibrium with



Table IV. A Comparison of the Transfer Activity Coefficients from Water to Methanol of Silver and Sodium Based on Different Single Ion Assumptions.

Assumption	Ion	Log $\gamma_1^w$	Ref.
$MYAs(Ph)_4^+ = MyB(Ph)_4^-$	$Ag^+$	1.2	A
$MYAs(Ph)_4^+ = MyC(Ph)_4$		2.1	B,C
$MyB(Ph)_4^- = MyC(Ph)_4$		0.4	B,C
$My = MyARx$		2.6	B
$My = MyCH_3I$		2.0	B
Ferrocene-Ferricinium		-2.2	B
Ejunction = 0		1.5	B
Extrapolation $N^{-2} \rightarrow 0$		3.5	D
Extrapolation of $R^{-1} \rightarrow 0$ N	$Na^+$	2.2	E
Extrapolation $N^{-2} \rightarrow 0$		1.8	D
Extrapolation $R^{-1} \rightarrow 0$		-2.23	F
Extrapolation $f(R) \rightarrow 0$		-1.34	G
Ion-Quadrupole Extrapolation		0.4	H
Ion-Quadrupole Extrapolation		-2.0	I

<sup>a</sup>Popovych, O., A. Gibofsky, and D. H. Berne, Anal. Chem., 44, 811 (1972).

<sup>b</sup>Alexander, R., A. J. Parker, J. H. Sharp, and W. E. Waghorne, J. Amer. Chem. Soc., 94, 1148 (1972).

<sup>c</sup>Cox, B. G., and A. J. Parker, J. Amer. Chem. Soc., 94, 3674 (1972).

<sup>d</sup>Izmaylov, N. A., Dokl. Akad. Nauk. SSSR, 149, 884, 1103, 1364 (1963).

<sup>e</sup>Ibid, 126, 1033 (1959).

<sup>f</sup>Andrews, A. L., H. P. Bennetoo, D. Feakins, K. G. Lawrence, R.P.T. Tomkins, J. Chem. Soc., A, 1968, 1486.

<sup>g</sup>Alfenaar, M., and C. L. Deligny, Rec. Trav. Chim., 86, 929 (1967).

<sup>h</sup>Bax, D., C. L. Deligny, M. Alfenaar, Rec. Trav. Chim., 91, 452 (1972).

<sup>i</sup>Salomon, M., J. Electrochem. Soc. 118, 1609 (1971).

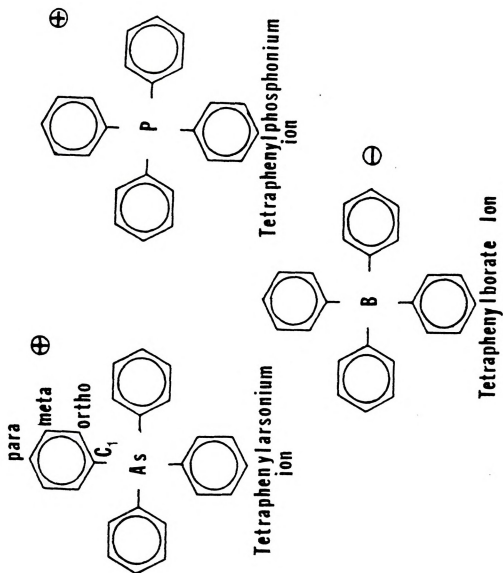


Figure 9. The structure of tetraphenylarsonium, tetraphenylphosphonium, and tetraphenylborate ion.

a saturated solution of reference electrolyte in solvent s, the chemical potential is

$${}_s\bar{G}_{\text{solid}} = {}_s\bar{G}_{\text{saturated}} = {}_s\bar{G}^{\circ}_{\text{saturated}} + RT \ln {}_s a_{+} a_{-} \quad (6)$$

and in water

$${}_s\bar{G}_{\text{solid}} = {}_w\bar{G}_{\text{saturated}} = {}_w\bar{G}^{\circ}_{\text{saturated}} + RT \ln {}_w a_{+} a_{-} \quad (7)$$

Equating the two yields

$$\Delta\bar{G}^{\circ}_{\text{tr}} = RT \ln {}_s K_{\text{sp}} / {}_w K_{\text{sp}} \quad (8)$$

where  ${}_s K_{\text{sp}}$  and  ${}_w K_{\text{sp}}$  are the thermodynamic solubility products in solvent s and water, respectively. If the solubility is low, activity corrections are negligible and  $\Delta\bar{G}^{\circ}_{\text{tr}}$  is obtained from a ratio of the concentration solubility products. From Equation (5), since the  $\Delta\bar{G}^{\circ}_{\text{tr}}$  is for the complete electrolyte, the medium effect is then

$$\Delta\bar{G}^{\circ}_{\text{tr}} = RT \ln \gamma_{+} \gamma_{-} \quad (9)$$

where  $\gamma_{+}$  and  $\gamma_{-}$  are the medium effects for the cation and anion respectively. According to the reference electrolyte assumption, the medium effects are equal, such that the medium effect for a single reference ion is the geometric mean of the cation and anion. By then using a different

anion (or cation), a  $\gamma_-$  (or  $\gamma_+$ ) may then be calculated for the new anion. This leads to an entire series of transfer free energies for single ions.

The  $\Delta\bar{G}_{tr}$  of a single ion may be broken down into

$$\Delta G_{tr}^{\circ} = \Delta G_{el} + \Delta G_N + \Delta G_{SI} \quad (10)$$

where  $\Delta G_{el}$  is the contribution due to electrostatic interactions,  $\Delta G_N$  is a neutral term, commonly associated with the energy required to produce a solvent cage the size of the ion, and  $\Delta G_{SI}$  is a specific term which accounts for all interactions of a non-electrostatic nature (77). Since the assumption involves the equivalent solvation of a cation and anion (implied by the assumption of equivalent  $\Delta G_{tr}^{\circ}$  for each ion) the  $\Delta G_{el}$  should be negligible or minimal. Unless the specific interaction terms are equivalent for cation and anion, these too should be minimal, leaving the  $\Delta G_N$  term dominant.

The validity of the reference electrolyte assumption has been tested both theoretically and experimentally. The first experimental test of this hypothesis was by Coetzee and Sharpe (88) in 1971. NMR investigations of primarily the solvent chemical shift in the presence of the reference electrolyte led Coetzee and Sharpe to conclude that caution is advised when using this assumption. Experimental data from this study cast doubt on the validity

of assuming equivalent solvation of the cation and anion. This method of investigation was continued by Caruso et al. (89-91).

The possibility of ion-pairing in solutions of tetraphenylarsonium chloride in water, acetonitrile, ethylene dichloride, 70% dioxane, and 95% dioxane was investigated spectroscopically (UV) and conductometrically by Popov and Humphrey (92). There was no evidence for ion-pairing in water or acetonitrile, while the other three solvents exhibited slight ion-pairing. This behavior can probably be extended to the case of tetraphenylborate salt in water and acetonitrile, with no ion-pairing expected.

The assumption was tested both theoretically and experimentally by Kim et al. (93-95). The electrostatic contribution was calculated for interactions between ions and multipoles of solvent molecules. The neutral term is derived from experimental  $\Delta\bar{G}_{tr}$  for the neutral analogs of the ions: tetraphenylgermanium for tetraphenylarsonium and tetraphenylmethane for tetraphenylborate. The sum of these contributions was then compared to experimentally determined  $\Delta\bar{G}_{tr}$  for complete electrolytes, with substantial agreement between the values within experimental error. An important conclusion reached was that the  $\Delta\bar{G}_{tr}$  should not be apportioned equally between cation and anion, rather that the cation should have a slightly greater portion.

The assumption was theoretically tested by Treiner (96)

using the scaled-particle theory (97). The scaled-particle theory estimates the free energy required to form a cavity the size of the reference ion, assuming equivalent solvent-ion interactions in all solvents. He concluded the assumption was not valid for the transfer of tetraphenylarsonium tetraphenylborate from water to dimethylformamide (DMF), dimethylsulfoxide (DMSO), sulpholane, propylene carbonate (PC), and N-methyl-pyrrolidone (NMP). These conclusions were later refuted by Abraham and Nasehzadeh (98).

The reference electrolyte assumption was critically compared to the ferrocene-ferricinium assumption by Kolthoff and Chantooni (99,100). The conclusion, based upon experimental data, was that the reference electrolyte is preferred, since the values derived are chemically significant. Some data based upon the ferrocene-ferricinium assumption leads to conclusions which are contrary to generally accepted theories of solvation (i.e., the medium effect for a proton transferred from water to methanol is approximately zero, while all other evidence indicates that water is a stronger base).

The general consensus of these studies was that the standard reference electrolyte assumption (particularly the tetraphenylarsonium tetraphenylborate assumption) is a valid hypothesis for the determination of single ion activity coefficients. Many studies then ensued (101-106, etc.) which measured single ion activity coefficients using this assumption.

#### 1.4. A Nuclear Magnetic Resonance Study

It was of interest to study the tetraphenylarsonium tetraphenylborate single ion assumption using nuclear magnetic resonance. The NMR technique is very sensitive to the immediate chemical environment around the probe nucleus, which should yield valuable information about the solvation and any interactions of these ions with the solvent or one another. The only previous NMR study (88) investigated primarily the solvent, whereas this study focused directly on the ion. The nuclei  $^{75}\text{As}$ ,  $^{31}\text{P}$ ,  $^{11}\text{B}$ ,  $^{13}\text{C}$  and  $^1\text{H}$  of the tetraphenylphosphonium, tetraphenylarsonium and tetraphenylborate ions were studied as a function of salt concentration, counter-ion, and solvent.

##### 1.4.1. Arsenic-75 NMR

Despite the fact that  $^{75}\text{As}$  has a 100% natural abundance and a relative sensitivity of 0.025 compared to the proton (overall sensitivity of 2.5, see Table I), this nucleus has been little studied by NMR. This lack of interest is probably due to the high quadrupole moment (0.3 dB), which produces a broad signal. Nonetheless, chemical shift and linewidth data should provide some information on the electronic environment around the nucleus.

The  $^{75}\text{As}$  resonance in liquid  $\text{AsF}_6$  was observed by Jones and Vehling (107) using a Knight high-level

spectrometer. The linewidth was found to be  $\sim 15$  gauss at a frequency of 8.8 MHz, with no evidence of structure. The magnetic moment and linewidth in aqueous solution were found to be  $+1.4347$  nuclear magnetons and  $\sim 8$  gauss by Dharmatti and Weaver (108) in 1951. However, the first and only aqueous study of various alkyl-arsonium compounds using Fourier transform NMR was done in 1977 by Baliman and Pregosin (109,110). These authors obtained linewidth and chemical shift data for a variety of compounds, including several tetraphenylarsonium salts. The linewidth of the tetraphenylarsonium salts was found to be on the order of 1300 Hz, which renders the chemical shift data accurate to no better than  $\pm 7$  ppm. It is no wonder that interest has been lacking when such large errors (due to the high quadrupole moment) are evident.

#### 1.4.2. Phosphorous-31 NMR

Phosphorous-31 NMR has been studied to a much larger extent than arsenic-75 NMR, due to its  $1/2$  spin (no quadrupole moment) and overall sensitivity of 6.6 (relative sensitivity of 0.06% and 100% natural abundance), as well as its large biological significance. Indeed, several volumes have been written on this subject (111-113) as well as extensive compilation of coupling constant data (114).

The tetraphenylphosphonium ion, however, has not been



well studied. The first study of this ion was in 1966 by Grim, et al. (115), with the observed resonance appearing 23.2 ppm downfield from the 85%  $\text{H}_3\text{PO}_4$  reference in deuterated chloroform. The behavior of phenyl-phosphorous compounds of penta-coordinated phosphorous were then studied by Latscha (116). An attempt was made to derive an empirical relation between the substituents and the observed chemical shift. This line of inquiry was also pursued by Schmidpeter and Brecht (117). A relationship between the chemical shifts of substituted trioxyphosphorous and substituted triphenylphosphorous compounds based on empirical data was developed. The spin-lattice relaxation time  $T_1$  of organophosphorous compounds was studied by Koole et al. (118) and Wilke (119). In the former study it was concluded that dipole-dipole contributions to the relaxation rate were the dominant factor at normal temperatures (25-60°C). The latter study reached the same conclusions using both  $^{31}\text{P}$  and  $^{13}\text{C}$  data.

#### 1.4.3. Boron-11 NMR

There are two isotopes of boron, boron-11 and boron-10, which have an odd spin nucleus rendering them suitable for NMR study. Boron-10 has a relative NMR sensitivity of  $1.99 \times 10^{-2}$  with respect to the proton and a natural abundance of 19.58%. Boron-11 has a relative NMR sensitivity of 0.165

and a natural abundance of 80.42%. The overall sensitivity of  $^{11}\text{B}$  is 34 times that of  $^{10}\text{B}$ , which led to the choice of  $^{11}\text{B}$  as the nucleus to study.

Boron-11 studies of sodium tetrphenylborate were first conducted by Onak, et al (130) in 1959. The authors studied a number of alkyl and aryl boron compounds and published a large compilation of chemical shift values. Later studies by Noeth, et al (131), Thompson and Davies (132), and Gragg, et al. (126) were concerned with a correlation between the observed  $^{11}\text{B}$  chemical shifts and the substituent electronegativity for a series of ions with the structure  $\text{B}(\text{X})_4^-$ .

#### 1.4.4. Carbon-13 and Proton

Carbon-13 NMR studies of tetraphenylarsonium and tetraphenylphosphonium salts have been few. The aforementioned study by Wilke (119) was used for the assignment of the  $^{13}\text{C}$  resonance peaks in tetraphenylphosphonium salts, while the work of Baliman, et al. (109,110) was used to assign the  $^{13}\text{C}$  resonance peaks of tetraphenylarsonium salts. Contrary to an apparent lack of interest in the cations, sodium tetrphenylborate has been studied rather extensively using  $^{13}\text{C}$  NMR. All of the authors, however, were interested primarily in  $^{11}\text{B}$ - $^{13}\text{C}$  coupling constants, although they did study the ion in a few nonaqueous solvents.

Weigert and Roberts (122) were the first to study the  $^{11}\text{B}$ - $^{13}\text{C}$  coupling constants for this anion in  $\text{D}_2\text{O}$  solution. Their work was later followed by Axelson, et al. (123), Hall, et al (124), and Odom, et al. (125), who obtained essentially the same results as did the original investigators. The chemical shifts of the boron and  $\text{C}_1$  carbon as a function of the substituent group (including tetraphenylborate) were studied by Gragg, et al. (126). Finally, the effect of simultaneous decoupling of  $^{11}\text{B}$  and  $^1\text{H}$  from the  $^{13}\text{C}$  spectra of tetraphenylborate was studied by Mazurek, et al. (127).

The proton NMR behavior of tetraphenylarsonium, tetraphenylphosphonium, and tetraphenylborate ion has not been studied in any detail. The proton NMR spectra of tetraphenylarsonium chloride, tetraphenylphosphonium chloride, and sodium tetraphenylborate were observed by Coetzee and Sharpe (88), but the authors were unable to distinguish separate peaks for the different protons. The Sadtler spectra (121) of tetraphenylphosphonium iodide and sodium tetraphenylborate are also lacking in resolution, with the signals appearing only as a complex multiplet.

### 1.5. Conclusions

Very little work has been done on the  $^{75}\text{As}$ ,  $^{31}\text{P}$ ,  $^{11}\text{B}$ ,  $^{13}\text{C}$ , and proton NMR behavior of tetraphenylarsonium, tetraphenylphosphonium, and tetraphenylborate salts. Such

studies should yield useful information about the solvation and solution interactions of these ions. This information, in turn, will help assay the validity of the reference electrolyte assumption for the calculation of medium effects.

CHAPTER II

RESULTS AND DISCUSSION

## 2.1. Introduction

The ions chosen as reference electrolytes (tetraphenylphosphonium and tetraphenylarsonium as the cations, and tetraphenylborate as the anion) have nearly equivalent molecular structures (Figure 9). All have a central atom, where the preponderance of charge is presumed to reside, surrounded by bulky phenyl rings. These phenyl rings serve two purposes: to "shield" the central charge from the solvent environment and to constitute the bulk of the volume associated with the ion. Because of the extensive shielding, a minimal surface charge can be assumed. This would tend to imply that the ion is solvated equivalently regardless of the charge on the central atom. The large volume of the rings assures that both the cation and anion have approximately the same size. Together, these assumptions imply that, in the absence of ion-ion interactions, the cation and anion should be equivalently solvated.

Multinuclear NMR is a suitable technique for testing the validity of the above assumptions. The sensitivity of this method to the immediate environment of a nucleus (both electrons and nearest neighboring atoms or molecules) renders it a powerful tool for probing ion-ion and ion-solvent interactions. The assumption of a central

atom shielded from the solvent and other ions was tested by observing the  $^{75}\text{As}$ ,  $^{31}\text{P}$ , and  $^{11}\text{B}$  resonance signal as a function of the solvent, concentration, and counter-ion. The amount of surface charge was qualitatively estimated by observing the  $^{13}\text{C}$  and proton chemical shift differences between the cation and anion. The relative position of the  $^{13}\text{C}$  and proton chemical shifts of the cation with respect to the anion can be related to the relative electron density at that carbon or proton. The extent and nature of the ion-ion and ion-solvent interactions were investigated by the observation of the relative positions of the  $^{13}\text{C}$  and proton resonances, as well as their behavior as a function of solvent, concentration, and counter-ion.

## 2.2. Phosphorous-31 NMR Results

The phosphorous-31 NMR results of the study of tetraphenylphosphonium salts in water, methanol, DMSO, DMF, nitromethane, acetonitrile, propylene carbonate, and pyridine solutions are presented in Table V. The values are close to the chemical shift value obtained by Grim, et al. (115) in deuterated chloroform. A comparison of the results for different halide counter-ions (at the same salt concentration), using a student t test (128), led to the conclusion that there was no dependence of the observed chemical shift on the counter-ion. Due to the low solubility of tetraphenylarsonium (or tetraphenylphosphonium)

Table V. The  $^{31}\text{P}$  Chemical Shifts in ppm for Tetraphenylphosphonium Salts as a Function of Counterion, Solvent, and Concentration.

Conc. in Molarity	Counterion Iodide	Bromide	Chloride	Tetraphenylborate	Mean Chemical Shift for a Solvent
<u>Methanol</u>					
0.05	22.9	23.1	22.9		22.9±0.1
0.10	22.9	23.1	22.9		
0.25	22.8	23.0	22.8		
1.00		22.3	22.3		
<u>DMSO</u>					
0.05	22.5	22.8	22.5	22.5*	22.5±0.1
0.10	22.5	22.7	22.5		
0.25	22.4	22.5	22.4		
0.50			22.2		
<u>DMF</u>					
0.05	22.7	22.7	22.6		22.61±0.06
0.10	22.6	22.6	22.6		
0.25	22.5	22.6	22.6		
0.50			22.3		
<u>Nitromethane</u>					
0.05	22.9	23.3	23.0		23.0±0.1
0.10	23.0	23.2	23.0		
0.25	22.9	23.1	22.9		
saturated			22.5		



Table V. Continued.

Conc. in Molarity	Counterion Iodide	Bromide	Chloride	Tetraphenylborate	Mean Chemical Shift for a Solvent
<u>Acetonitrile</u>					
0.05	23.1	23.2	23.0		23.07±0.08
0.10	23.0*	23.1	23.0		
0.25		23.0	22.9		
saturated			22.7		
<u>Propylene Carbonate</u>					
0.05	22.8	22.9	22.8		22.8±0.1
0.10	22.8	22.9	22.7		
0.25	22.7	22.7	22.6		
<u>Pyridine</u>					
0.05	22.2	22.4	22.4		22.3±0.1
0.10	22.2*	22.3	22.2		
0.25		22.3*	22.1		
<u>H<sub>2</sub>O</u>					
0.05			22.8		22.7±0.2
0.10			22.7		
0.25			22.5		

\* saturated solutions.

Mean for a given counter-ion  
 22.7±0.3      22.8±0.3      22.7±0.2

tetraphenylborate, which fall below the NMR limits of detection in most cases, halide salts of the cations were studied. As such, any ion-ion interactions detected would be of a "worst case" sort, since the bulky, shielded tetraphenylborate anion would be expected to interact to a lesser extent than a halide ion with the tetraphenylarsonium (or tetraphenylphosphonium) cation.

The fact that there is no apparent counter-ion dependence for the series chloride, bromide, and iodide indicates that the ion-ion interactions have not penetrated to the central atom. If such interactions were significant, the effect of the higher surface charge density of the chloride ion on the observed  $^{31}\text{P}$  chemical shift would be the most pronounced, while that of the iodide ion would be the least. This reasoning can be extended to the tetraphenylborate salt, with the lack of ion-ion interactions between the cation and halide ions leading to the conclusion that ion-ion interactions are not significant for most salts of tetraphenylphosphonium ion.

There is a small concentration dependence to the observed chemical shift which is probably due to changes in the bulk magnetic susceptibility of the solution (see Section 2.5.) with concentration, with its subsequent effect on the observed chemical shift. The average observed chemical shift varies with the solvent. The variation

is 0.8 ppm (pyridine to acetonitrile) compared to a typical standard deviation within a given solvent of 0.1 ppm. The solvent dependence is significant, but not large enough to attempt to correlate the average chemical shift for a solvent with such solvent properties as the Gutmann donor number or the solvent dielectric constant. It is concluded that the phenyl rings do shield the cation from the ion-ion interactions, but do not shield the central atom (and hence the charge) entirely from the solvent, although the effects of the solvent on the central atom are minor.

### 2.3. Arsenic-75 NMR Results

The results of an  $^{75}\text{As}$  NMR study of tetraphenylarsonium salts in water, methanol, DMSO, DMF, acetonitrile, nitromethane, propylene carbonate, and pyridine solution are given in Tables VI and VII. Due to a very broad linewidth, the accuracy of the chemical shifts are estimated at  $\pm 7$  ppm. Within this error range, our values are equivalent to those obtained by Baliman and Pregcsin (109,110). There is no apparent dependence of the observed chemical shift on the concentration, counter-ion, or solvent. The average chemical shift is  $225 \pm 1$  ppm downfield from the reference with all values occurring within  $\pm 2$  ppm of this average.

If the tetraphenylarsonium salts exhibit an NMR behavior similar to the tetraphenylphosphonium salts, the

Table VI. The  $^{75}\text{As}$  Chemical Shift in ppm ( $\pm 7$  ppm) for Tetraphenylarsonium Ion as a Function of Concentration, Counterion, and Solvent.

Conc. in Molarity	Chloride	Iodide	Conc. in Molarity	Chloride	Iodide
<u>Water</u>			<u>Acetonitrile</u>		
0.305	227				
0.100	225				
0.050	225		0.010	224	225
<u>Methanol</u>			<u>Nitromethane</u>		
0.276	224				
0.100	224				
0.050	225	224	0.010	226	226
0.010	225	224			
<u>DMSO</u>			<u>Propylene Carbonate</u>		
0.000	224		0.101	226	
0.050	226		0.050	224	
0.010	224	224	0.010	225	224
<u>DMF</u>			<u>Pyridine</u>		
0.102	224		0.100	225	
0.050	224		0.050	225	
0.010	224	223	0.010	224	

Table VII. Some Representative  $^{75}\text{As}$  Linewidths for Tetraphenylarsonium Chloride in Various Solvents ( $\pm 80$  Hz).

Solvent	Conc. in molarity	$\Delta\nu_{1/2}$ in Hz
$\text{H}_2\text{O}$	0.3	3830
	0.1	1860
	0.05	990
Methanol	0.3	740
	0.01	450
DMSO	0.1	1670
	0.01	1300
DMF	0.01	800
Pyridine	0.1	2100
	0.01	1360
Propylene Carbonate	0.1	1850
	0.01	1150

total ex

ppm. Th

the lan

measur

appropri

chemica

tetraph

can be

The

height

viscosi

tion

change

tion,

toward

centra

linea

tion,

have b

2.4.

Th

borate

propyl

Sasak

sligh

total extent of change in the chemical shift would be 0.8 ppm. These changes would not be apparent when considering the large error associated with any given chemical shift measurement. The conclusion is that  $^{75}\text{As}$  NMR is not an appropriate technique for such precise measurements of chemical shifts. No conclusions on the validity of the tetraphenylarsonium tetraphenylborate single ion assumption can be drawn from  $^{75}\text{As}$  NMR measurements.

The trend in linewidths (full width at half peak height), shown in Table VII, generally follows solution viscosity trends. As per the discussion in Part I, Section 3.5.2., the increase in viscosity, whether due to a change in solvent or an increase in the solute concentration, will lead to an increase in linewidth. The trend towards increasing linewidth with increasing solute concentration is evident in all solvents. A comparison of the linewidths between solvents, at the same solute concentration, shows that the more viscous solvents will tend to have broader linewidths.

#### 2.4. Boron-11 NMR Results

The results of the  $^{11}\text{B}$  NMR study of sodium tetraphenylborate in water, DMSO, DMF, acetonitrile, nitromethane, propylene carbonate, and pyridine, conducted by Dr. Yukuo Sasaki, are presented in Tables VIII and IX. There is a slight concentration dependence of the observed chemical

---

---

Conc. in  
Molarity

---

H<sub>2</sub>O

0.7

0.5

0.25

0.1

DMSC

0.7

0.5

0.25

0.1

Nitrom

0.4

0.25

0.1

0.05

Aceton

0.7

0.5

0.2

0.1

Pyrid

0.4

0.2

0.1

0.05



Table VIII. The  $^{11}\text{B}$  Chemical Shifts of Sodium Tetraphenylborate as a Function of Concentration and Solvent in Various Solvents.

Conc. in Molarity	$\delta$ in ppm	Conc. in Molarity	$\delta$ in ppm	Conc. in Molarity	$\delta$ in ppm
<u>H<sub>2</sub>O</u>					
0.7	-26.26	0.05	-26.18	0.0025	-26.29
0.5	-26.16	0.025	-26.21	0.001	-26.29
0.25	-26.19	0.01	-26.23	$5 \times 10^{-4}$	-26.34
0.1	-26.20	0.005	-26.24		
<u>DMSO</u>					
0.7	-25.72	0.05	-25.70	0.0025	-25.70
0.5	-25.70	0.025	-25.70	0.001	-25.76
0.25	-25.68	0.01	-25.68	$5 \times 10^{-4}$	-25.65
0.1	-25.65	0.005	-25.70		
<u>Nitromethane</u>					
0.4	-25.00	0.025	-24.94	0.001	-24.89
0.25	-24.98	0.01	-24.94	$5 \times 10^{-4}$	-24.85
0.1	-24.96	0.005	-24.98		
0.05	-24.94	0.0025	-24.91		
<u>Acetonitrile</u>					
0.7	-25.40	0.05	-25.34	0.0025	-25.36
0.5	-25.40	0.025	-25.33	0.001	-25.37
0.25	-25.38	0.01	-25.35		
0.1	-25.38	0.005	-25.36		
<u>Pyridine</u>					
0.4	-25.38	0.025	-25.29	0.001	-25.26
0.25	-25.36	0.01	-25.27	$5 \times 10^{-4}$	-25.27
0.1	-25.29	0.005	-25.27		
0.05	-25.31	0.0025	-25.21		

Table W

---

---

Conc. of  
Molarities

---

Property

0.7

0.5

0.25

0.1

0.7

0.5

0.25

0.1

---

Table VIII. Continued.

Conc. in Molarity	$\delta$ in ppm	Conc. in Molarity	$\delta$ in ppm	Conc. in Molarity	$\delta$ in ppm
<u>Propylene Carbonate</u>					
0.7	-25.87	0.05	-25.89	0.0025	-25.86
0.5	-25.89	0.025	-25.84	0.001	-25.89
0.25	-25.84	0.01	-25.88	$5 \times 10^{-4}$	-25.76
<u>DMF</u>					
0.7	-25.64	0.05	-25.57	0.0025	-25.57
0.5	-25.63	0.025	-25.55	0.001	-25.55
0.25	-25.59	0.01	-25.55	$5 \times 10^{-4}$	-25.51
0.1	-25.59	0.005	-25.56		

Table 1

---

---

Solvent
H <sub>2</sub> O
DMSO
Hexane
Acetone

---

---

Table IX. The Infinite Dilution  $^{11}\text{B}$  Chemical Shifts, Corrected for Bulk Magnetic Susceptibilities, as a Function of Solvent.

Solvent	$\delta_\infty$ in ppm	Solvent	$\delta_\infty$ in ppm
$\text{H}_2\text{O}$	$-26.23 \pm 0.06$	Pyridine	$-25.72 \pm 0.06$
DMSO	$-26.18 \pm 0.05$	Propylene Carbonate	$-26.23 \pm 0.09$
Nitromethane	$-26.31 \pm 0.04$	DMF	$-26.17 \pm 0.04$
Acetonitrile	$-26.13 \pm 0.07$		

shift

netic

salt o

Table

finite

the ab

tempt o

shift o

or butr

the phs

the phs

solute

2.5. 2

The

MSO, 2

and pyr

ME dat

Table 3

Figure

bromide

the exp

of the

absence

solvent

actions

shift which may be attributed to changes in the bulk magnetic susceptibilities of the solution with changes in salt concentration (see Section 2.5.). As can be seen in Table IX, there is a slight solvent dependency of the infinite dilution chemical shift. As in the case of the  $^{31}\text{P}$  chemical shift data, the trend is too slight to attempt a correlation between the infinite dilution chemical shift and such solvent properties as the dielectric constant or Gutmann donor number. The conclusion reached is that the phenyl rings do not shield the central atom (and hence the charge on the central atom) entirely from solvent-solute interactions.

## 2.5. Carbon-13 NMR Results

The results of the  $^{13}\text{C}$  NMR studies in water, methanol, DMSO, DMF, acetonitrile, nitromethane, propylene carbonate, and pyridine are presented in Tables X - XVII. The  $^{13}\text{C}$  NMR data on sodium tetraphenylborate were provided by Dr. Yukuo Sasaki. A sample spectra of each ion is shown in Figure 10. Studies of tetraphenylphosphonium chloride, bromide, iodide, and thiocyanate salts show that, within the experimental error of  $\pm 0.03$  ppm, there is no effect of the counter-ion on the observed chemical shift. This absence of counter-ion dependency indicates that in the solvents studied, the anion-tetraphenylphosphonium interactions tend to be minimal.

Table X. Carbon-13 Chemical Shift Changes with Concentration for Tetraphenylarsonium ( $\text{As}(\text{Ph})_4^+$ ) and Tetraphenylphosphonium ( $\text{P}(\text{Ph})_4^+$ ) Salts in  $\text{H}_2\text{O}$ .

Conc. in Mol.	$\text{C}_1$	meta	ortho	para
<u><math>\text{As}(\text{Ph})_4\text{Cl}</math></u>				
0.750	122.81	133.33	135.19	137.04
0.498	122.94	133.36	135.36	137.04
0.252	123.13	133.33	135.52	137.04
0.098	123.32	133.26	135.69	137.01
0.047	123.45	133.27	135.79	136.92
<u><math>\text{P}(\text{Ph})_4\text{Cl}</math></u>				
0.400	120.05±0.04	132.73±0.03	136.91±0.03	137.84±0.05
0.301	120.1 ±0.1	132.66±0.03	136.94±0.03	137.88±0.03
0.207	120.19±0.02	132.63±0.04	136.97±0.03	137.85±0.07
0.100	120.30±0.03	132.62±0.04	137.1 ±0.7	137.76±0.05
0.050	120.37±0.02	132.60±0.04	137.21±0.04	137.8 ±0.1
<u>0.1M <math>\text{As}(\text{Ph})_4\text{Cl}</math> with Variable NaCl Concentration</u>				
0.101	123.27±0.02	133.26±0.01	135.65±0.02	136.97±0.02
0.196	123.25±0.03	133.27±0.04	135.62±0.02	136.98±0.03
0.299	123.22±0.02	133.26±0.04	135.59±0.02	136.96±0.01
0.405	123.20±0.01	133.29±0.02	135.60±0.02	136.98±0.03
0.489	123.20±0.03	133.29±0.04	135.60±0.02	136.94±0.03



Table XI. Carbon-13 Chemical Shift Changes with Concentration for Tetraphenylarsonium ( $\text{As}(\text{Ph})_4^+$ ) and Tetraphenylphosphonium ( $\text{P}(\text{Ph})_4^+$ ) Salts in MeOH.

Conc. in Molarity	$C_1$	meta	ortho	para
<u><math>\text{As}(\text{Ph})_4\text{Cl}</math></u>				
0.399	124.17	134.01	136.14	137.48
0.321	124.16	133.98	136.16	137.48
0.250	124.18	134.10	136.24	137.54
0.160	124.19	133.98	136.19	137.51
0.100	124.22	134.01	136.13	137.55
<u><math>\text{P}(\text{Ph})_4\text{Cl}</math></u>				
0.400	121.07±0.01	133.39±0.02	137.60±0.03	138.30±0.03
0.300	121.13±0.04	133.43±0.04	137.65±0.01	138.4 ±0.1
0.201	121.18±0.01	133.42±0.01	137.71±0.05	138.42±0.02
0.102	121.22±0.02	133.45±0.01	137.70±0.03	138.45±0.03
0.049	121.26±0.02	133.43±0.02	137.7 ±0.1	138.47±0.02
<u><math>\text{P}(\text{Ph})_4\text{Br}</math></u>				
0.398	121.06±0.03	133.40±0.04	137.54±0.03	138.34±0.01
0.302	121.14±0.01	133.43±0.03	137.65±0.02	138.42±0.01
0.100	121.24±0.01	133.50±0.02	137.69±0.07	138.47±0.02
0.052	121.26±0.02	133.47±0.04	137.75±0.03	138.48±0.04
<u><math>\text{P}(\text{Ph})_4\text{I}</math></u>				
0.152	121.15±0.0	133.43±0.05	137.64±0.03	138.30±0.05
0.114	121.18±0.02	133.44±0.05	137.69±0.03	138.41±0.05
0.099	121.20±0.03	133.44±0.01	137.69±0.01	138.5 ±0.1
0.053	121.26±0.02	133.48±0.01	137.77±0.03	138.48±0.02

Table XIII. Carbon-13 Chemical Shift Changes with Concentration for Tetraphenylarsonium and Tetraphenylphosphonium Salts in DMSO.

Conc. in Mol.	C <sub>1</sub>	meta	ortho	para
<u>As(Ph)<sub>4</sub>Cl</u>				
0.401	124.42	134.45	136.66	137.80
0.299	124.51	134.46	136.70	137.86
0.176	124.53	134.41	136.64	137.73
0.100	124.60	134.54	136.74	137.92
0.050	124.54	134.45	136.89	137.77
0.040	124.66	134.57	136.84	138.04
0.030	124.55	134.60	136.66	137.90
0.026	124.54	134.42	136.80	137.77
<u>P(Ph)<sub>4</sub>Cl</u>				
0.400	121.07±0.02	133.97±0.04	138.00±0.05	138.78±0.02
0.299	121.13±0.03	133.97±0.04	138.00±0.02	138.76±0.04
0.201	121.15±0.02	134.00±0.05	138.1 ±0.1	138.8 ±0.1
0.102	121.22±0.01	134.08±0.03	138.15±0.06	138.80±0.04
0.054	121.26±0.02	134.04±0.06	138.2 ±0.1	138.87±0.03
<u>P(Ph)<sub>4</sub>Br</u>				
0.400	121.12±0.03	134.1 ±0.1	138.05±0.06	138.72±0.01
0.302	121.13±0.01	134.07±0.02	138.15±0.01	138.77±0.02
0.200	121.17±0.02	133.98±0.03	138.11±0.05	138.83±0.04
0.101	121.25±0.02	134.0 ±0.1	138.08±0.02	138.74±0.01
0.050	121.25±0.03	134.04±0.05	138.14±0.03	138.8 ±0.1

Table XII. Continued.

Conc. in Mol.	$C_1$	meta	ortho	para
<u><math>P(Ph)_4I</math></u>				
sat.	121.1 ± 0.1	133.98 ± 0.06	137.96 ± 0.06	138.75 ± 0.04
0.200	121.14 ± 0.02	134.04 ± 0.0	138.04 ± 0.02	138.73 ± 0.01
0.102	121.2 ± 0.1	134.1 ± 0.1	138.11 ± 0.02	138.8 ± 0.1
0.051	121.2 ± 0.1	134.0 ± 0.1	138.20 ± 0.05	138.86 ± 0.06
<u><math>P(Ph)_4SCN</math></u>				
0.106	121.22 ± 0.01	134.00 ± 0.02	138.16 ± 0.03	138.88 ± 0.01
0.052	121.24 ± 0.02	134.01 ± 0.01	138.14 ± 0.02	138.9 ± 0.1
0.026	121.24 ± 0.01	134.00 ± 0.03	138.15 ± 0.04	138.88 ± 0.01
<u><math>As(Ph)_4B(Ph)_4</math></u> $As(Ph)_4^+$ $\delta$ in ppm				
sat				
(~0.02M)	124.61	134.58	136.74	137.86
<u><math>B(Ph)_4^-</math></u>				
		ortho	meta	para
		139.08	128.85	125.07

Table XIII. Carbon-13 Chemical Shift Changes with Concentration for Tetraphenylarsonium and Tetraphenylphosphonium Salts in DMF.

Conc. in Mol.	$\delta$ in ppm			
	$C_1$	Meta	Ortho	Para
<u>As(Ph)<sub>4</sub>Cl</u>				
0.402	124.51	134.29	136.66	137.64
0.301	124.60	134.30	136.69	137.66
0.249	124.42	134.13	136.70	137.61
0.201	124.53	134.20	136.64	137.55
0.150	124.67	134.27	136.73	137.63
0.100	124.54	134.16	136.66	137.51
0.052	124.54	134.13	136.66	137.57
0.040	124.57	134.10	136.60	137.63
0.024	124.54	134.13	136.72	137.54
<u>P(Ph)<sub>4</sub>Cl</u>				
0.402	121.07±0.02	133.60±0.01	137.79±0.06	138.40±0.03
0.298	121.15±0.02	133.63±0.03	137.87±0.02	138.36±0.05
0.204	121.21±0.02	133.62±0.02	137.97±0.06	138.57±0.03
0.097	121.26±0.01	133.61±0.01	138.05±0.05	138.65±0.02
0.052	121.30±0.02	133.63±0.04	138.02±0.04	138.50±0.04
<u>P(Ph)<sub>4</sub>Br</u>				
0.398	121.07±0.02	133.56±0.01	137.81±0.02	138.48±0.03
0.199	121.20±0.02	133.59±0.02	137.91±0.02	138.50±0.02
0.051	121.28±0.03	133.59±0.03	137.97±0.03	138.48±0.08
<u>P(Ph)<sub>4</sub>I</u>				
0.201	121.20±0.01	133.59±0.02	137.94±0.01	138.47±0.01
0.098	121.26±0.01	133.61±0.01	138.10±0.06	138.51±0.04
0.047	121.29±0.01	133.58±0.04	137.99±0.03	138.6 ±0.1

Table XIII. Continued.

Conc. in Mol.	$C_1$	meta	ortho	para
$As(Ph)_4B(Ph)_4$				
	$As(Ph)_4^+$			in ppm
$B(Ph)_4^-$	134.11	136.64	137.52	
saturated	128.32	139.11	124.58	

Table XIV. Carbon-13 Chemical Shift Changes with Concentration for Tetraphenylarsonium and Tetraphenylphosphonium Salts in Nitromethane.

Conc. in Mol.	$\delta$ in ppm			
	$C_1$	meta	ortho	para
<u>As(Ph)<sub>4</sub>Cl</u>				
0.399	124.72	134.67	136.89	138.24
0.299	124.65	134.65	136.83	138.18
0.200	124.66	134.57	136.98	138.24
0.151	124.76	134.70	137.00	138.29
0.026	124.70	134.60	136.92	138.24
<u>P(Ph)<sub>4</sub>Cl</u>				
0.399	121.53±0.03	133.91±0.02	138.19±0.01	138.93±0.03
0.300	121.59±0.01	133.94±0.04	138.28±0.01	138.96±0.01
0.200	121.65±0.01	133.92±0.04	138.29±0.02	139.00±0.05
0.099	121.73±0.01	134.01±0.03	138.39±0.05	139.10±0.04
0.052	121.76±0.01	134.05±0.05	138.41±0.01	139.1 ±0.1
<u>P(Ph)<sub>4</sub>Br</u>				
0.299	121.58±0.01	133.96±0.01	138.28±0.01	139.00±0.02
0.201	121.64±0.01	133.97±0.02	138.31±0.01	139.03±0.01
0.149	121.66±0.01	133.98±0.04	138.32±0.02	139.03±0.03
0.099	121.66±0.01	133.96±0.05	138.33±0.03	139.05±0.03
0.051	121.75±0.01	133.99±0.01	138.41±0.02	139.12±0.02
<u>P(Ph)<sub>4</sub>I</u>				
0.124	121.70±0.01	133.99±0.03	138.32±0.01	139.03±0.05
0.094	121.69±0.02	134.00±0.02	138.36±0.02	139.06±0.02
0.050	121.71±0.01	133.98±0.05	138.33±0.03	139.13±0.04

Table XV. Carbon-13 Chemical Shift Changes with Concentration for Tetraphenylarsonium and Tetraphenylphosphonium Salts in Propylene Carbonate.

Conc. in Mol.	$\delta$ in ppm			
	$C_1$	meta	ortho	para
<u>As(Ph)<sub>4</sub>Cl</u>				
0.3625	123.67±0.01	133.75±0.02	135.92±0.02	137.23±0.01
0.1812	123.74±0.02	133.74±0.02	135.97±0.02	137.25±0.03
0.0906	123.77±0.02	133.76±0.01	135.99±0.01	137.28±0.02
0.0493	123.76±0.01	133.76±0.01	136.00±0.02	137.26±0.03
0.0227	123.81±0.02	133.78±0.02	136.02±0.01	137.27±0.02
<u>P(Ph)<sub>4</sub>Cl</u>				
0.3879	120.61±0.02	133.17±0.02	137.34±0.02	138.16±0.02
0.3020	120.65±0.02	133.17±0.02	137.37±0.02	138.17±0.01
0.2019	120.71±0.02	133.15±0.03	137.38±0.03	138.18±0.02
0.0998	120.73±0.02	133.16±0.02	137.43±0.01	138.18±0.02
0.0528	120.74±0.02	133.16±0.02	137.43±0.03	138.19±0.03
<u>P(Ph)<sub>4</sub>Br</u>				
0.2999	120.62±0.02	133.16±0.02	137.36±0.02	138.15±0.02
0.0990	120.70±0.01	133.17±0.01	137.42±0.02	138.18±0.02
0.0800	120.72±0.02	133.18±0.02	137.43±0.01	138.18±0.02
0.0501	120.73±0.02	133.16±0.02	137.43±0.01	138.18±0.02
<u>P(Ph)<sub>4</sub>I</u>				
0.0986	120.69±0.02	133.16±0.02	137.40±0.01	138.15±0.02
0.0498	120.73±0.01	133.17±0.01	137.42±0.02	138.18±0.02

Table XVI. Carbon-13 Chemical Shift Changes with Concentration for Tetraphenylarsonium and Tetraphenylphosphonium Salts in Acetonitrile.

Conc. in Mol.	$C_1$	$\delta$ in ppm		
		meta	ortho	para
<u>As(Ph)<sub>4</sub>Cl</u>				
0.412	124.16	134.25	136.54	137.77
0.299	124.14	134.20	136.55	137.74
0.198	124.23	134.29	136.67	137.91
0.149	124.36	134.30	136.69	137.86
0.100	124.34	134.25	136.60	137.68
0.048	124.28	134.25	136.60	137.83
0.024	-----	134.22	136.57	137.80
<u>P(Ph)<sub>4</sub>Cl</u>				
0.300	121.13±0.07	133.66±0.03	137.95±0.04	138.68±0.01
0.201	121.18±0.01	133.66±0.03	137.95±0.01	138.68±0.01
0.100	121.22±0.01	133.65±0.03	137.97±0.02	138.61±0.08
0.051	121.28±0.02	133.72±0.04	138.10±0.01	138.70±0.01
<u>P(Ph)<sub>4</sub>Br</u>				
0.303	121.1 ±0.1	133.66±0.05	137.92±0.05	138.63±0.01
0.250	121.19±0.03	133.72±0.05	138.00±0.02	138.7 ±0.1
0.200	121.18±0.02	133.64±0.03	138.01±0.05	138.73±0.01
0.100	121.16±0.01	133.68±0.05	138.03±0.01	138.75±0.03
0.051	121.23±0.01	133.71±0.02	138.10±0.02	138.73±0.03
<u>P(Ph)<sub>4</sub>I</u>				
0.099	121.25±0.0	133.73±0.03	138.04±0.02	138.68±0.01
0.051	121.27±0.0	133.65±0.06	138.10±0.03	138.67±0.01



Table XVII. Carbon-13 Chemical Shift Changes for Sodium Tetraphenylborate in Various Solvents as a Function of Concentration.

Solvent	Conc. in		$\delta$ in ppm			$\delta$ in ppm			meta
	Molarity	meta	ortho	para	meta	ortho	para		
H <sub>2</sub> O	0.7	138.59	122.67	125.90	0.1	138.51	122.71	126.11	
	0.5	138.59	122.70	125.99	0.05	138.50	122.82	126.21	
	0.25	138.49	122.70	125.99	0.025	138.53	122.76	126.19	
DMSO	0.7	138.95	128.69	124.90	0.1	138.81	128.68	124.82	
	0.5	138.95	128.69	124.92	0.05	138.84	-----	-----	
	0.25	138.98	128.69	124.91	-----	-----	-----	-----	
DMF	0.7	138.68	127.95	124.20	0.1	138.64	127.88	124.13	
	0.5	138.72	127.94	124.22	0.05	138.63	127.94	124.10	
	0.25	138.58	127.88	124.12	0.025	138.65	127.89	-----	
Nitromethane	0.4	138.14	128.09	124.28	0.05	138.07	127.91	124.04	
	0.25	138.07	127.92	124.11	0.025	138.03	128.10	124.01	
	0.1	138.02	127.89	124.03	-----	-----	-----	-----	
Acetonitrile	0.7	138.39	128.39	124.50	0.1	138.35	128.24	124.38	
	0.5	138.41	128.31	124.51	0.05	138.37	128.16	124.49	
	0.25	138.33	128.18	124.43	0.025	138.34	128.11	124.36	
Propylene Carbonate	0.7	138.80	128.49	124.88	0.1	138.75	128.41	124.75	
	0.5	138.80	128.49	124.83	0.05	138.78	128.44	124.77	
	0.25	138.74	128.38	124.78	0.025	138.80	-----	-----	
Pyridine	0.4	139.22	128.23	124.38	0.05	139.29	127.98	124.33	
	0.25	139.27	128.11	124.39	0.025	139.30	127.90	124.49	
	0.1	139.29	128.02	124.39	-----	-----	-----	-----	

or

p:



o

p:



Figure 10.

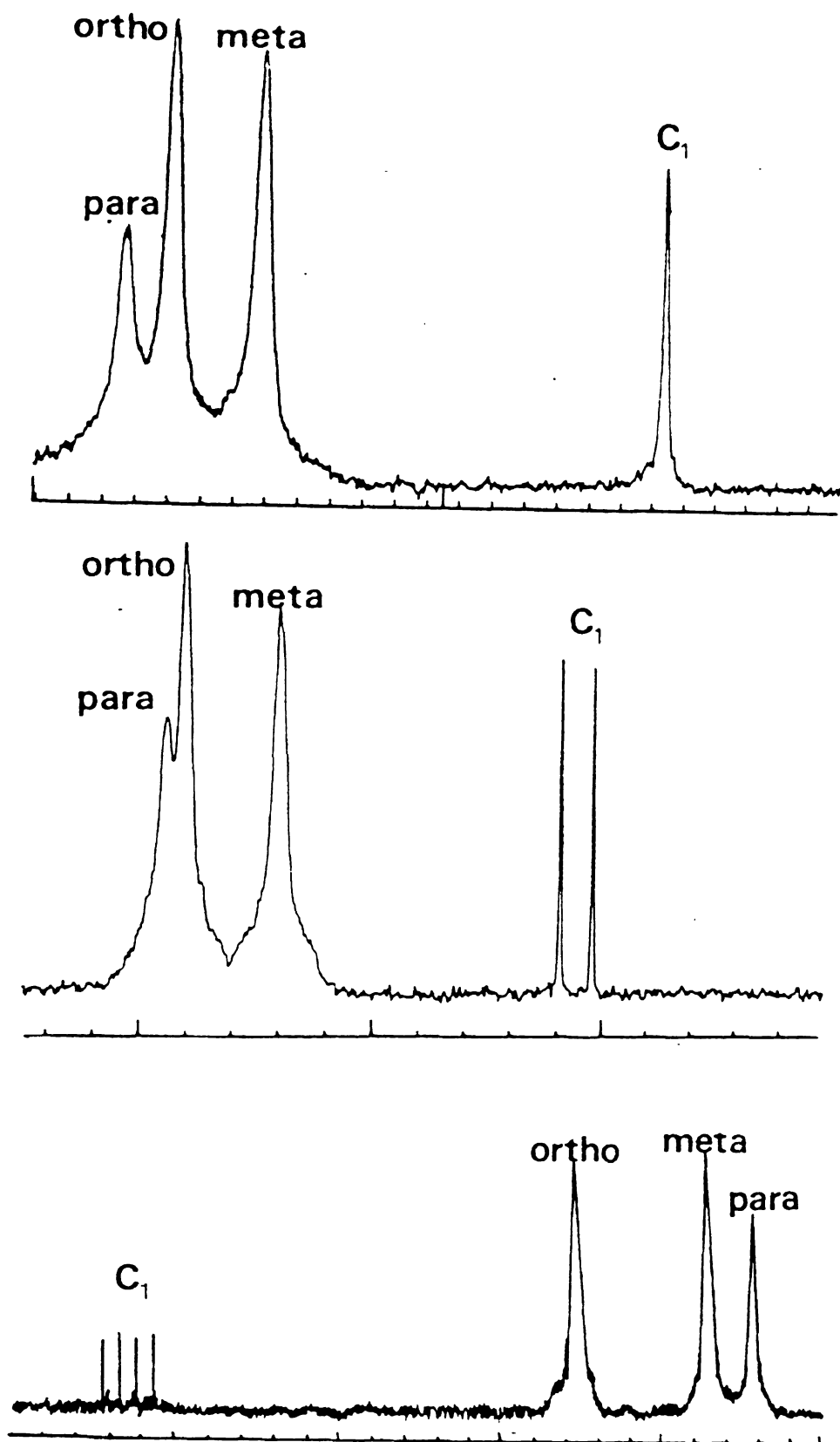


Figure 10. The  $^{13}\text{C}$  NMR spectra of: Upper - tetraphenylarsonium chloride, Middle - tetraphenylphosphonium chloride, and Lower - sodium tetraphenylborate in DMSO.

As a t  
chloride i  
the tetrap  
constant)  
resulting  
smaller th  
arsonium c  
shifts are  
ment, with  
ability of  
A further  
phenylars  
Figure 11  
tetrapheny  
studies of  
together a  
those for  
the cation  
our system  
or have n  
There  
of 0.3 ppm  
phenylpho  
A portion  
change in  
the solut

As a test of this hypothesis, the concentration of chloride ion was increased in the aqueous solution (while the tetraphenylarsonium chloride concentration was kept constant) by the addition of potassium chloride. The resulting changes in chemical shift (see Table X) are smaller than when the total concentration of tetraphenylarsonium chloride is increased. The changes in chemical shifts are within the experimental error of a given measurement, with minor corrections for bulk magnetic susceptibility changes with concentration (see next paragraph). A further test was to measure the chemical shifts of tetraphenylarsonium tetraphenylborate in the DMSO and DMF (Figure 11). The low solubility of tetraphenylarsonium tetraphenylborate in most solvents precludes further NMR studies of this salt. The chemical shifts of the ions together are the same, within the experimental error, as those for the sodium salt of the anion and the chloride of the cation. These data lead to the conclusion that, in our systems, the ion-ion interactions are either absent, or have no effect on the  $^{13}\text{C}$  chemical shift.

There is a slight concentration dependence (a maximum of 0.3 ppm) of the observed tetraphenylarsonium, tetraphenylphosphonium, and tetraphenylborate chemical shift. A portion of this change in chemical shift is due to the change in bulk magnetic susceptibility of the solutions as the solute concentration is increased. This change in

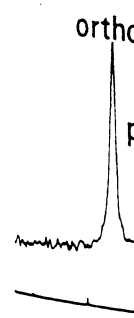
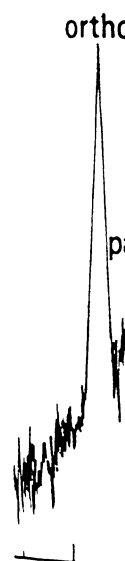


Figure 11.

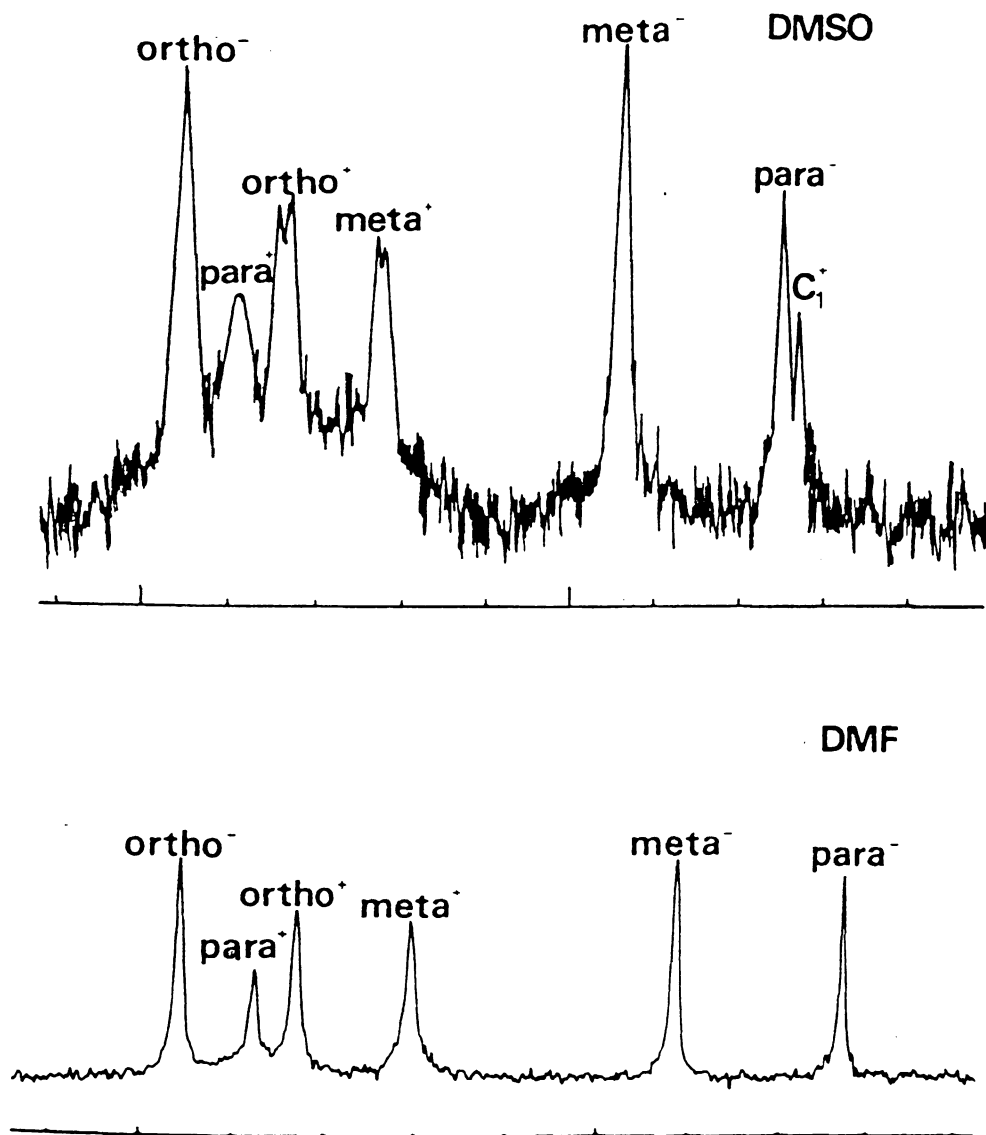


Figure 11. The  $^{13}\text{C}$  NMR spectra of tetraphenylarsonium tetraphenylborate in DMSO and DMF.

the bulk m  
change in v  
relationships

where the  
2.5.4. The  
magnetic s

The same s  
super-cond  
chemical s

from which  
Using Equa  
cal shift  
are presen  
correction  
in the obs  
range from  
cal shift



the bulk magnetic susceptibility manifests itself as a change in chemical shift through the Live and Chan (37) relationship for a superconducting magnet:

$$\delta_{\text{corr}} = \delta_{\text{obs}}^{\text{S}} + 2\pi/3 (\chi_{\text{ref}} - \chi_{\text{sample}}) \quad (11)$$

where the symbols have been defined in Part I, Section 2.5.4. The chemical shift correction due to the bulk magnetic susceptibility for an iron-core magnet is

$$\delta_{\text{corr}} = \delta_{\text{obs}}^{\text{I}} - 4\pi/3 (\chi_{\text{ref}} - \chi_{\text{sample}}) \quad (12)$$

The same sample was studied using both an iron-core and a super-conducting magnet. The resulting difference in chemical shifts is

$$\delta_{\text{obs}}^{\text{I}} - \delta_{\text{obs}}^{\text{S}} = 2\pi(\chi_{\text{ref}} - \chi_{\text{sample}}) \quad (13)$$

from which the quantity  $(\chi_{\text{ref}} - \chi_{\text{sample}})$  was determined. Using Equation (2), the correction to the observed chemical shift was then calculated. The results of such a study are presented in Table XVIII. Bulk magnetic susceptibility corrections account for an approximately 0.06 ppm change in the observed chemical shift with concentration in the range from 0.4 to 0.05 M. The remaining change in chemical shift (0.09 ppm in DMSO) is probably due to solute-

Table XVIII. Bulk Magnetic Susceptibility Corrections as a Function of Tetraphenyl-  
phosphonium Chloride Concentration in DMF.

---

---

Magnetic Susc.

Table XVIII. Bulk Magnetic Susceptibility Corrections as a Function of Tetraphenylphosphonium Chloride Concentration in DMSO.

Conc. in Molarity	$\delta$ in ppm on the DA-60	$\delta$ in ppm on the WM-250	$(\delta_I - \delta_S)_{av}$	Magnetic Susc. Corr. for the WM-250
0.5006	138.27 137.37 133.40 120.50 138.29 137.42 133.44 120.56 138.28 137.42 133.41 120.56 138.21 137.38 133.34 120.52	138.81 137.94 133.95 121.03 138.81 137.93 133.96 121.06 138.83 137.99 133.98 121.10 138.82 137.99 133.94 121.10	-0.55±0.02  -0.52±0.02  -0.56±0.02  -0.60±0.02	-0.36±0.01  -0.34±0.01  -0.37±0.01  -0.40±0.01
Infinite Dilution				-0.482 (Ref. 158)

solvent int

A change

observed pr

a changing

planation.

indicating

chemical s

tion is th

tion. Thi

while bein

in the phe

center. I

solvent in

shown pre

invariant

will shif

The in

arsenium,

tions in d

is a defi

chemical

vated dif

sistent w

authors (

solvation

energy of

solvent interactions.

A change in the chemical shift upon dilution has been observed previously for some aromatic systems (129), with a changing solvation shell upon dilution used as an explanation. However, the chemical shift change is slight, indicating that the forces responsible for the change in chemical shift are weak. Consistent with this explanation is the shift of the para carbon resonance upon dilution. This position is the most sensitive to the solvent, while being the least sensitive to electron density shifts in the phenyl rings, since it is furthest from the charge center. There is a small shift, indicating some solute-solvent interaction, although it is slight. As has been shown previously (129), the meta position is relatively invariant with concentration, while the ortho position will shift similar to the para.

The infinite dilution chemical shifts of tetraphenylarsonium, tetraphenylphosphonium, and tetraphenylborate ions in different solvents are shown in Table XIX. There is a definite solvent dependency of the infinite dilution chemical shifts, which implies that a given ion is solvated differently in each solvent. These data are consistent with the non-zero  $\Delta\bar{G}_{tr}^{\circ}$  determinations of several authors (33,40,42-46) for these ions, since an equivalent solvation in two different solvents implies a transfer free energy of zero. However, the infinite dilution chemical

Table XIX.

Solvent

 $F(Ph)_4^+$ H<sub>2</sub>O

Methanol

DMSO

DMF

Nitrometha

Acetonitr

Propylene  
Carbonate $As(Ph)_4^+$ H<sub>2</sub>O

Methanol

DMSO

DMF

Nitrometha

Acetonitr

Propylene  
Carbonate $B(Ph)_4^-$ H<sub>2</sub>O

DMSO

DMF

Nitrometh

Acetonitr

Propylene

Pyridine

\* Correcte

Table XIX. The Infinite Dilution  $^{13}\text{C}$  Chemical Shifts\* for Tetraphenylborate, Tetraphenylphosphonium, and Tetraphenylarsonium Ions as a Function of Solvent.

Solvent	Infinite Dilution $\delta$ in ppm			
	$\text{C}_1$	meta	ortho	para
<u><math>\text{P}(\text{Ph})_4^+</math></u>				
$\text{H}_2\text{O}$	120.40	132.58	137.20	137.75
Methanol	120.41	132.61	136.89	137.62
DMSO	120.78	133.54	137.69	138.37
DMF	120.71	132.99	137.45	137.94
Nitromethane	120.38	132.64	137.02	137.74
Acetonitrile	120.49	132.92	137.30	137.92
Propylene Carbonate	120.41	132.80	137.09	137.83
<u><math>\text{As}(\text{Ph})_4^+</math></u>				
$\text{H}_2\text{O}$	123.42	133.27	135.78	136.98
Methanol	123.36	133.16	135.32	136.70
DMSO	124.12	134.04	136.32	137.40
DMF	123.95	133.49	136.05	136.93
Nitromethane	123.37	133.27	135.64	136.86
Acetonitrile	123.68	133.54	135.91	137.12
Propylene Carbonate	123.44	133.41	135.66	136.92
<u><math>\text{B}(\text{Ph})_4^-</math></u>				
		ortho	meta	para
$\text{H}_2\text{O}$		137.95	129.22	125.63
DMSO		138.54	128.38	124.54
DMF		138.39	127.65	123.86
Nitromethane		138.16	128.00	124.12
Acetonitrile		138.19	127.98	124.21
Propylene Carbonate		138.40	128.04	124.38
Pyridine		138.98	127.59	124.08

\* Corrected for the bulk magnetic susceptibility of the solvent.

shifts of  
property s  
mann donor

The cr  
tetrapheny  
vion of th  
density at  
for the an  
cation sur  
change on  
ments, equ  
anion reso  
a given pa  
tion  $^{13}\text{C}$   
shown in  
 $^{13}\text{C}$  spectr  
DMF and DM  
differenc  
meta, and  
positions  
the diffe  
The negat  
density a  
around th  
does not  
(86).



shifts of these ions do not correlate with such solvent property scales as the dielectric constant and the Gutmann donor number.

The crux of the tetraphenylarsonium (or -phosphonium) tetraphenylborate assumption is the equivalency of solvation of the cation and anion which implies that the charge density at any given carbon on the ring should be the same for the anion and cation, since a positive charge on the cation surface would be solvated differently than a negative charge on the anion surface. In terms of  $^{13}\text{C}$  NMR measurements, equivalent solvation would result in the cation and anion resonance peaks occurring at the same frequency for a given carbon. The difference between the infinite dilution  $^{13}\text{C}$  chemical shifts as a function of the solvent are shown in Table XX. This difference may also be seen in the  $^{13}\text{C}$  spectrum of tetraphenylarsonium tetraphenylborate in DMF and DMSO, as shown in Figure 11. There is a significant difference in the chemical shifts of corresponding ortho, meta, and para carbons. The difference between the ortho positions between the cation and anion are attributable to the different charges on the central atom in each case. The negative charge on the boron imparts a higher electron density around the ortho carbon of the anion than that around the cation. This model is incomplete, since it does not consider electron density shifts within the ring (86).

Table XI.

Solvent
H <sub>2</sub> O
DMSO
DME
Nitromethane
Acetonitrile
Propylene

H <sub>2</sub> O
DMSO
DME
Nitromethane
Acetonitrile
Propylene

Table XX. The Difference in  $^{13}\text{C}$  Infinite Dilution Chemical of Tetraphenylarsonium (and Tetraphenylphosphonium) vs Tetraphenylborate Ion as a Function of Solvent.

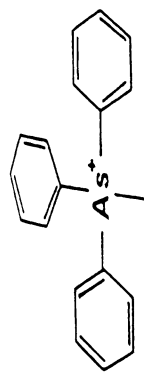
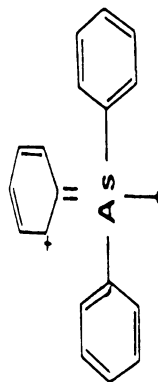
Solvent	$\Delta\delta$ ( $\delta\text{As}(\text{Ph})_4^+$ - $\delta\text{B}(\text{Ph})_4^-$ ) in ppm		
	ortho	meta	para
$\text{H}_2\text{O}$	-2.2	4.1	11.4
DMSO	-2.2	5.7	12.9
DMF	-2.3	5.8	13.1
Nitromethane	-2.5	5.3	12.7
Acetonitrile	-2.3	5.6	12.9
Propylene Carbonate	-2.7	5.4	12.5

Solvent	$\Delta\delta$ ( $\delta\text{P}(\text{Ph})_4^+$ - $\delta\text{B}(\text{Ph})_4^-$ ) in ppm		
	ortho	meta	para
$\text{H}_2\text{O}$	-0.8	3.4	12.1
DMSO	-0.9	5.2	13.8
DMF	-0.9	5.3	14.1
Nitromethane	-1.1	4.6	13.6
Acetonitrile	-0.9	4.9	13.7
Propylene Carbonate	-1.3	4.8	13.5

The te  
ion may be  
Figure 12.  
phenylbora  
electrons  
case, sinc  
electrons.  
carbon on  
density) c  
The para o  
shifts, du  
while bein  
This carbo  
ference be  
clusion is  
resonance  
tion of th  
the cation  
it is reas  
tive dipol  
electron o  
respect to  
the reson  
anion sign  
electron  
tion of t

The tetraphenylarsonium (and tetraphenylphosphonium) ion may be represented by the resonance structures in Figure 12. The electrons on the phenyl rings of tetraphenylborate would not be expected to resonate with the electrons on the boron atom, as opposed to the arsenic case, since all the electrons on the boron are bonding electrons. Hence, the resonance frequency of the ortho carbon on the anion is further downfield (higher electron density) than that of the ortho carbon on the cation. The para carbons are the least sensitive to such electron shifts, due to their distance from the charge center, while being the most sensitive to the solvent environment. This carbon also exhibits the largest chemical shift difference between the cation and anion (13 ppm). The conclusion is that solvation is a dominant factor in the resonance frequency of the para carbon, and that the solvation of the cation and anion are somewhat different. Since the cation para position has a partial positive character, it is reasonable to assume that it would attract the negative dipole of the solvent which would lead to a higher electron density at the para carbon of the cation (with respect to the para position on the anion), resulting in the resonance signal occurring further downfield than the anion signal. The meta position would be subject to both electron shift and solvation forces, with the interpretation of the relative chemical shift rendered less definite.



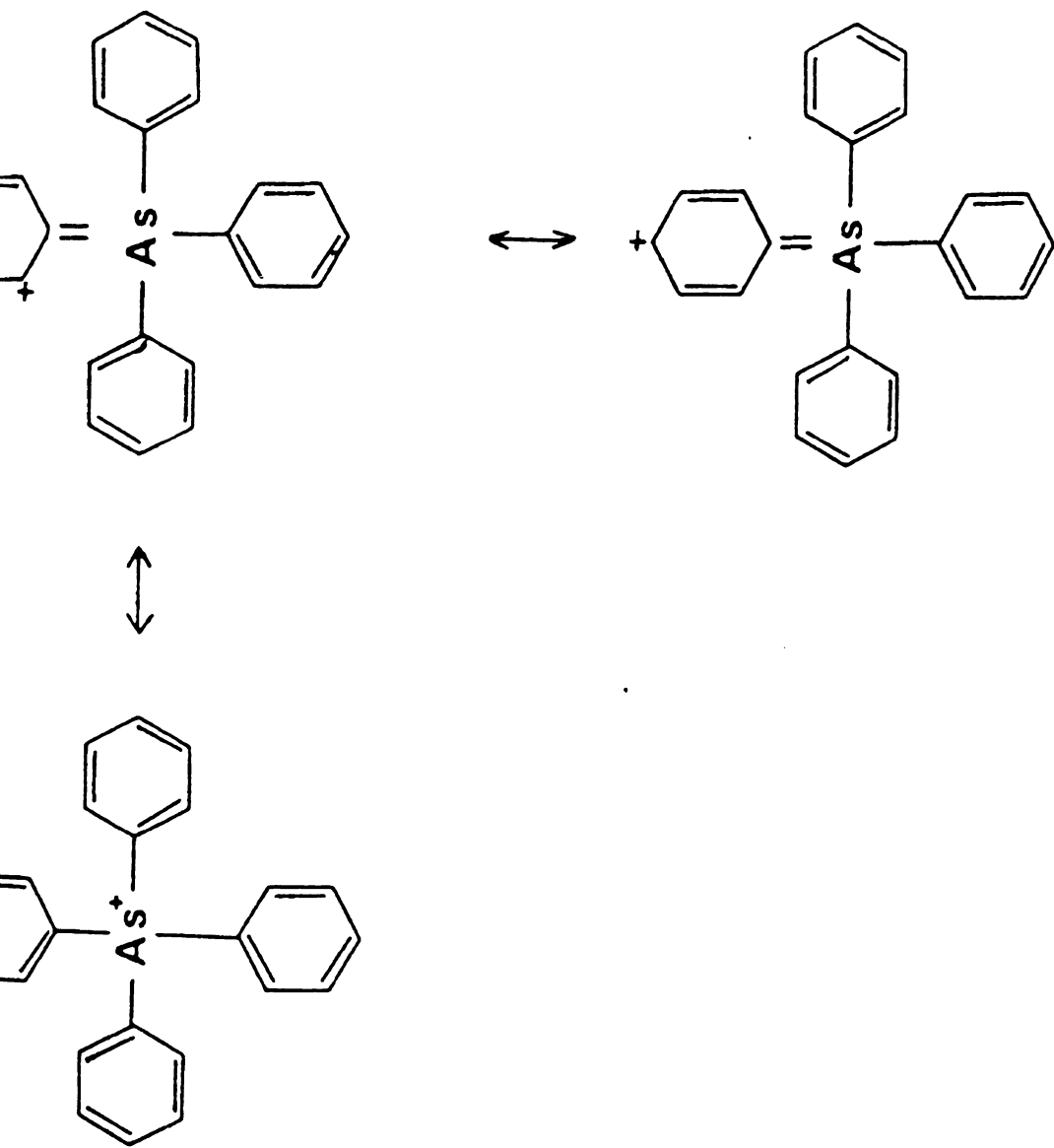


Figure 12. Some resonance structures of tetraphenylarsonium ion.

The C<sub>1</sub> can  
by the ef  
chemical  
the other  
upfield.

The di  
shifts of  
approxima  
ortho carb  
As mention  
bon chemi  
the metal  
hold for  
discussed  
the cation  
tetrapheny  
tetrapheny  
is too sma  
cation ove  
the dielec  
in the -3-

It was  
shifts of  
phenylars  
used as th

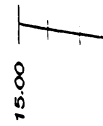


The  $C_1$  carbon chemical shifts (not shown) are dominated by the effects of the charge on the central atom; the anion chemical shift occurred the furthest downfield of any of the other positions, while the cation occurred furthest upfield.

The difference between the meta carbon chemical shifts of the cation and anion were solvent dependent to approximately the same extent as the para carbon, while the ortho carbon exhibited a much smaller solvent dependence. As mentioned previously, the interpretation of the para carbon chemical shifts are more straight forward than for the meta carbon, therefore, although similar arguments hold for the meta carbon, only the para position will be discussed. The range of chemical shift differences between the cation and anion was 1.72 ppm for tetraphenylarsonium tetraphenylborate and 1.96 ppm for tetraphenylphosphonium tetraphenylborate. The difference between the two salts is too small to make a statement on the preference of one cation over the other. There is a relationship between the dielectric constant of the solvent and the difference in the  $^{13}C$  chemical shifts for the para carbon (Figure 13), although the correlation is slight.

It was also of interest to compare the  $^{13}C$  chemical shifts of tetraphenylgermanium with those of the tetraphenylarsonium ion, since tetraphenylgermanium is often used as the neutral analog of the cation (93-95).

15.00



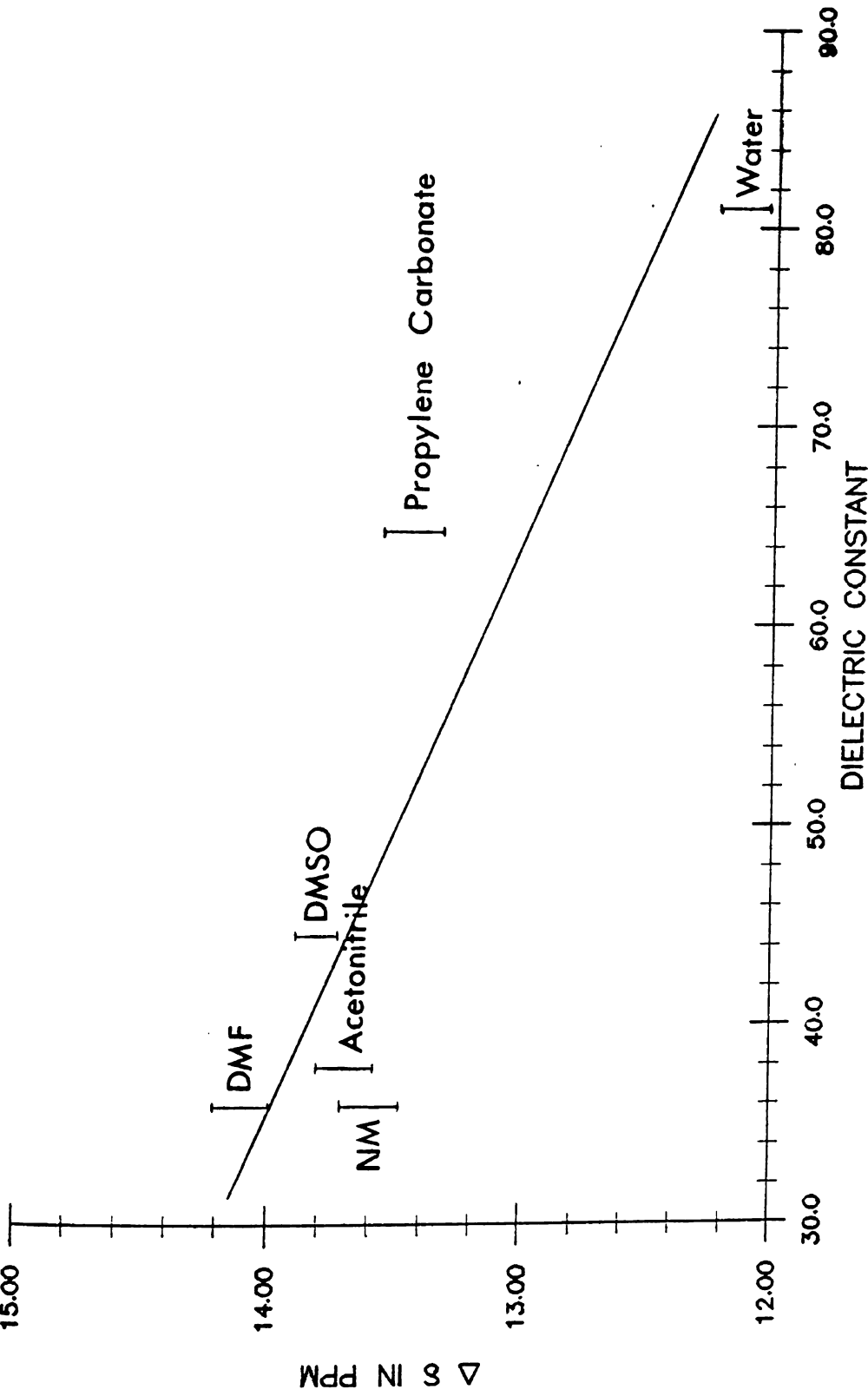


Figure 13. A plot of the difference in chemical shifts between the cation and anion vs the dielectric constant.

Table XVI

chlorometh

two molec

the peaks

coincide.

The c

phenylars

borate si

tions stu

that tetr

phenylger

equivalen

## 2.6. Proc

The p

arsenium,

ion in wa

methane,

presente

sodium t

The stud

arsonium

graphica

of the c

ium ion

XXII-XXI

Table XXI shows the results of such a comparison in dichloromethane and deuterated chloroform solutions. The two molecules are clearly not solvated equivalently, as the peaks for the ortho, meta, and para carbon do not coincide.

The conclusions of the carbon-13 study of the tetraphenylarsonium (or tetraphenylphosphonium) tetraphenylborate single ion assumption are as follows: in the solutions studied the ion-ion interactions are negligible, and that tetraphenylarsonium (or tetraphenylphosphonium), tetraphenylgermanium, and tetraphenylborate are not solvated equivalently.

## 2.6. Proton NMR Results

The proton NMR results from a study of tetraphenylarsonium, tetraphenylphosphonium, and tetraphenylborate in water, methanol, DMSO, DMF, acetonitrile, nitromethane, propylene carbonate, and pyridine solution are presented in Tables XXII-XXIX. The proton NMR data on sodium tetraphenylborate was furnished by Dr. Yukuo Sasaki. The studies of sodium tetraphenylborate and tetraphenylarsonium chloride in a variety of solvents are presented graphically in Figures 14-19. The concentration dependence of the observed chemical shift of the tetraphenylphosphonium ion as a function of the counter-ion is shown in Tables XXII-XXIX. No apparent dependence of the chemical shift



Solvent	Molecule	C <sub>1</sub>	δ in ppm		
			ortho	meta	para
Dichloromethane	Ge(Ph) <sub>4</sub>	138.51±0.01	137.74±0.01	130.72±0.01	131.57±0.01
	As(Ph) <sub>4</sub> Cl	122.95±0.01	133.77±0.01	135.44±0.01	137.36±0.02
Deuterated Chloroform	Ge(Ph) <sub>4</sub>	138.58±0.0	137.86±0.02	131.55±0.0	130.73±0.0
	As(Ph) <sub>4</sub> Cl	122.94±0.0	134.19±0.0	135.54±0.0	137.66±0.0

Table XXII. Proton Chemical Shift Data for Tetraphenylarsonium Chloride, Tetraphenylphosphonium Chloride and Tetraphenylborate in Water.

---

$\delta$  in ppm

---



Conc. in Molarity	δ in ppm			Conc. in Molarity	δ in ppm		
	ortho	meta	para		ortho	meta	para
<u>As(Ph)<sub>4</sub>Cl</u>							
0.751	7.236	7.364	7.525	0.0502	7.644	7.661	7.797
0.500	7.324	7.434	7.598	0.0251	7.720	7.699	7.849
0.253	7.450	7.526	7.688	0.0103	7.748	7.723	-----
0.101	7.598	7.626	7.778				
<u>NaB(Ph)<sub>4</sub></u>							
0.7	7.389	7.031	6.884	0.1	7.435	7.177	7.034
0.5	7.404	7.072	6.928	0.05	7.446	7.194	7.051
0.25	7.427	7.133	6.991	0.025	7.439	7.197	7.053
<u>P(Ph)<sub>4</sub>Cl</u>							
0.400	7.414	7.502	7.719	0.100	7.619	7.648	7.856
0.301	7.469	7.543	7.758	0.0502	7.674	7.700	7.888
0.202	7.556	7.579	7.795				

Table XXIII. Proton Chemical Shifts of Tetraphenylarsonium Chloride as a Function of the Total Chloride Ion Concentration.

---

---

the Total Chloride Ion Concentration.

Conc. in Molarity	Conc. of KCl in Molarity	Total Chloride Ion Conc.	$\delta$ in ppm		
			ortho	meta	para
0.101	0	0.101	7.617	7.644	7.797
0.101	0.0952	0.196	7.597	7.625	7.780
0.0987	0.200	0.299	7.580	7.610	7.766
0.101	0.304	0.405	7.553	7.596	7.753
0.0964	0.392	0.488	7.542	7.589	7.747



Conc. in Molarity	$\delta$ in ppm			Conc. in Molarity	$\delta$ in ppm		
	ortho	meta	para		ortho	meta	para
<u>As(Ph)<sub>4</sub>Cl</u>							
0.399	8.319	8.344	8.42	0.100	8.486	8.493	8.57
0.321	8.363	8.389	8.47	0.0506	8.486.	8.512	8.61
0.250	8.392	8.420	8.51	0.0262	8.508	8.534	8.61
0.160	8.439	8.465	8.55				
<u>P(Ph)<sub>4</sub>Cl</u>							
0.400	8.304	8.348	8.469	0.102	8.446	8.496	8.651
0.300	8.352	8.396	8.524	0.049	8.469	8.509	8.676
0.201	8.399	8.445	8.604				
<u>P(Ph)<sub>4</sub>Br</u>							
0.398	8.302	8.344	8.493	0.0996	8.450	8.492	8.656
0.302	8.349	8.393	8.546	0.0519	8.471	8.515	8.679
<u>P(Ph)<sub>4</sub>I</u>							
0.152	8.418	8.461	8.618	0.0992	8.443	8.487	8.648
0.114	8.438	8.479	8.638	0.0528	8.468	8.510	8.672



Conc. in Molarity	δ in ppm			Conc. in Molarity	δ in ppm		
	ortho	meta	para		ortho	meta	para
<u>As(Ph)<sub>4</sub>Cl</u>							
0.500	8.151	8.176	8.25	0.0497	8.314	8.339	8.43
0.299	8.252	8.277	8.35	0.0401	8.340	8.367	8.44
0.251	8.234	8.270	8.35	0.302	8.336	8.361	8.45
0.176	8.296	8.321	8.40	0.0258	8.317	8.342	8.43
0.100	8.283	8.310	8.41				
<u>NaB(Ph)<sub>4</sub></u>							
0.7	7.633	7.335	7.189	0.1	7.719	7.461	7.323
0.5	7.665	7.379	7.235	0.05	7.724	7.468	7.330
0.25	7.698	7.649	7.300	0.025	7.731	7.471	7.334
<u>P(Ph)<sub>4</sub>Cl</u>							
0.501	8.145	8.234	8.364	0.251	8.226	8.310	8.459
0.447	8.160	8.248	8.390	0.201	8.243	8.327	8.477
0.400	8.174	8.261	8.405	0.102	8.270	8.354	8.507
0.349	8.192	8.279	8.423	0.0535	8.288	8.369	8.526
0.299	8.208	8.295	8.542				
<u>P(Ph)<sub>4</sub>Br</u>							
0.400	8.163	8.248	8.395	0.101	8.269	8.353	8.513
0.302	8.202	8.284	8.437	0.0495	8.288	8.385	8.526
0.200	8.238	8.321	8.480				

Table XXV. Continued.

$\delta$  in ppm

$\delta$  in ppm



Conc. in Molarity	$\delta$ in ppm			Conc. in Molarity	$\delta$ in ppm		
	ortho	meta	para		ortho	meta	para
<u>P(Ph)<sub>4</sub>I</u>							
saturated	8.216	8.299	8.451	0.102	8.266	8.347	8.511
0.200	8.229	8.310	8.463	0.0508	8.284	8.365	8.522
<u>P(Ph)<sub>4</sub>SCN</u>							
0.106	8.270	8.349	8.503	0.0257	8.294	8.374	8.537
0.0523	8.286	8.367	8.523				



Conc. in Molarity	δ in ppm			Conc. in Molarity	δ in ppm		
	ortho	meta	para		ortho	meta	para
<u>As(Ph)<sub>4</sub>Cl</u>							
0.402	8.279			0.0997	8.398		
0.301	8.317			0.0517	8.463		
0.249	8.343			0.0395	8.463		
0.201	8.361			0.0241	8.473		
0.150	8.380						
<u>NaB(Ph)<sub>4</sub></u>							
0.7	7.673	7.280	7.128	0.1	7.796	7.433	7.286
0.5	7.721	7.336	7.188	0.05	7.812	7.450	7.305
0.25	7.765	7.396	7.250	0.025	7.821	7.452	7.305
<u>P(Ph)<sub>4</sub>Cl</u>							
0.402	8.240	8.284		0.097	8.362	8.412	
0.298	8.296	8.323		0.052	8.374	8.424	
0.204	8.325	8.355					
<u>P(Ph)<sub>4</sub>Br</u>							
0.398	8.235	8.284					
0.199	8.321	8.350					
0.051	8.371	8.422					



Conc. in Molarity	$\delta$ in ppm			Conc. in Molarity	$\delta$ in ppm		
	ortho	meta	para		ortho	meta	para
<u>P(Ph)<sub>4</sub>I</u>							
0.201	8.318	8.349					
0.098	8.355	8.398					
0.047	8.374	8.424					

Table XXVII. Proton Chemical Shift Data for Tetraphenylarsonium Chloride, Some Tetraphenylphosphonium Salts, and Sodium Tetraphenylborate in Acetonitrile.

Conc. in Molarity	δ in ppm			Conc. in Molarity	δ in ppm		
	ortho	meta	para		ortho	meta	para
<u>As(Ph)<sub>4</sub>Cl</u>							
0.412	8.382	8.412	8.53	0.0998	8.520	8.549	8.65
0.299	8.431	8.460	8.58	0.0484	8.546	8.576	8.71
0.198	8.473	8.502	8.62	0.0244	8.557	8.586	8.72
0.149	8.502	8.533	8.64				
<u>NaB(Ph)<sub>4</sub></u>							
0.7	7.905	7.595	7.429	0.1	8.070	7.795	7.639
0.5	7.959	7.662	7.500	0.05	8.095	7.816	7.661
0.25	8.029	7.746	7.589	0.025	8.099	7.821	7.669
<u>P(Ph)<sub>4</sub>Cl</u>							
0.300	8.396	8.467	8.637	0.0996	8.487	8.533	8.733
0.201	8.446	8.513	8.690	0.0514	8.500	8.551	8.748
<u>P(Ph)<sub>4</sub>Br</u>							
0.303	8.387	8.455	8.630	0.100	8.484	8.538	8.735
0.250	8.412	8.482	8.659	0.051	8.492	8.550	8.747
0.200	8.440	8.507	8.681				
<u>P(Ph)<sub>4</sub>I</u>							
0.0991	8.493	8.539	8.737				
0.0508	8.507	8.552	8.450				

Table XXVIII. Proton Chemical Shift Data for Tetraphenylammonium Chloride, Some Tetraphenylphosphonium Salts, and Sodium Tetraphenylborate in Nitromethane.



Tetraphenylphosphonium Salts, and Sodium Tetraphenylborate in Nitro-methane.

Conc. in Molarity	δ in ppm			Conc. in Molarity	δ in ppm		
	ortho	meta	para		ortho	meta	para
<u>As(Ph)<sub>4</sub>Cl</u>							
0.399	8.796	8.814	8.899	0.151	8.948	8.965	9.058
0.299	8.852	8.870	8.958	0.0257	9.027	9.046	9.143
0.200	8.924	8.942	9.033				
<u>NaB(Ph)<sub>4</sub></u>							
0.4	8.410	8.051	7.885	0.05	8.554	8.215	8.051
0.25	8.478	8.125	7.961	0.025	8.566	8.227	8.064
0.1	8.532	8.086	8.022				
<u>P(Ph)<sub>4</sub>Cl</u>							
0.399	8.792	8.822	8.975	0.0991	9.001	9.020	9.160
0.300	8.850	8.879	9.034	0.052	9.027	9.045	9.186
0.200	8.911	8.945	9.102				
<u>P(Ph)<sub>4</sub>Br</u>							
0.299	8.848	8.878	9.033	0.0987	8.970	8.988	9.128
0.149	8.936	8.954	9.094	0.0510	9.028	9.046	9.186
<u>P(Ph)<sub>4</sub>I</u>							
0.124	8.980	8.997	9.136	0.0502	9.025	9.045	9.188
0.0937	8.994	9.011	9.152				



Conc. in Molarity	$\delta$ in ppm			Conc. in Molarity	$\delta$ in ppm		
	ortho	meta	para		ortho	meta	para
<u>As(Ph)<sub>4</sub>Cl</u>							
0.363	7.913	7.939	8.018	0.0453	8.002	8.028	8.116
0.181	7.968	7.995	8.079	0.0227	8.002	8.027	8.115
0.0906	7.990	8.018	8.103				
<u>NaB(Ph)<sub>4</sub></u>							
0.7	7.439	7.107	6.961	0.1	7.496	7.200	7.058
0.5	7.450	7.134	6.990	0.05	7.494	7.203	7.063
0.25	7.482	7.175	7.034	0.025	7.504	7.208	7.068
<u>P(Ph)<sub>4</sub>Cl</u>							
0.388	7.874	7.927	8.092	0.0998	7.957	8.003	8.174
0.302	7.902	7.953	8.121	0.053	7.965	8.013	8.186
0.202	7.932	7.982	8.154				
<u>P(Ph)<sub>4</sub>Br</u>							
0.300	7.895	7.944	8.113	0.0800	7.958	8.005	8.176
0.0990	7.952	7.999	8.171	0.0501	7.965	8.013	8.186
<u>P(Ph)<sub>4</sub>I</u>							
0.0986	7.951	7.996	8.175				
0.0498	7.965	8.011	8.188				



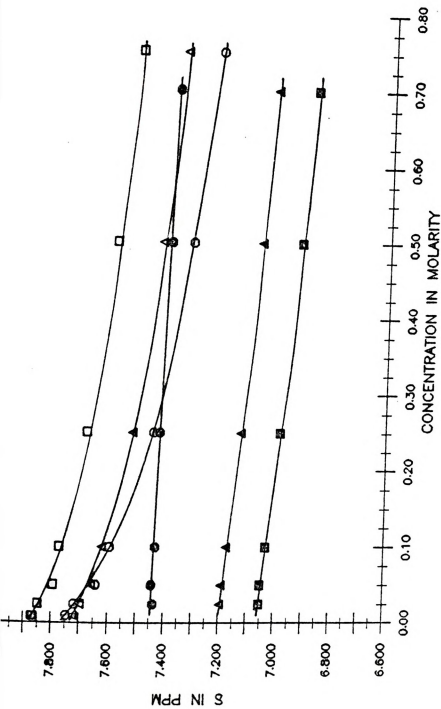


Figure 14. A plot of the proton chemical shift vs total salt concentration in water. (Squares - para protons, triangles - meta protons, circles - ortho protons, open symbols - tetraphenylarsonium chloride, closed symbols - sodium tetraphenylborate).

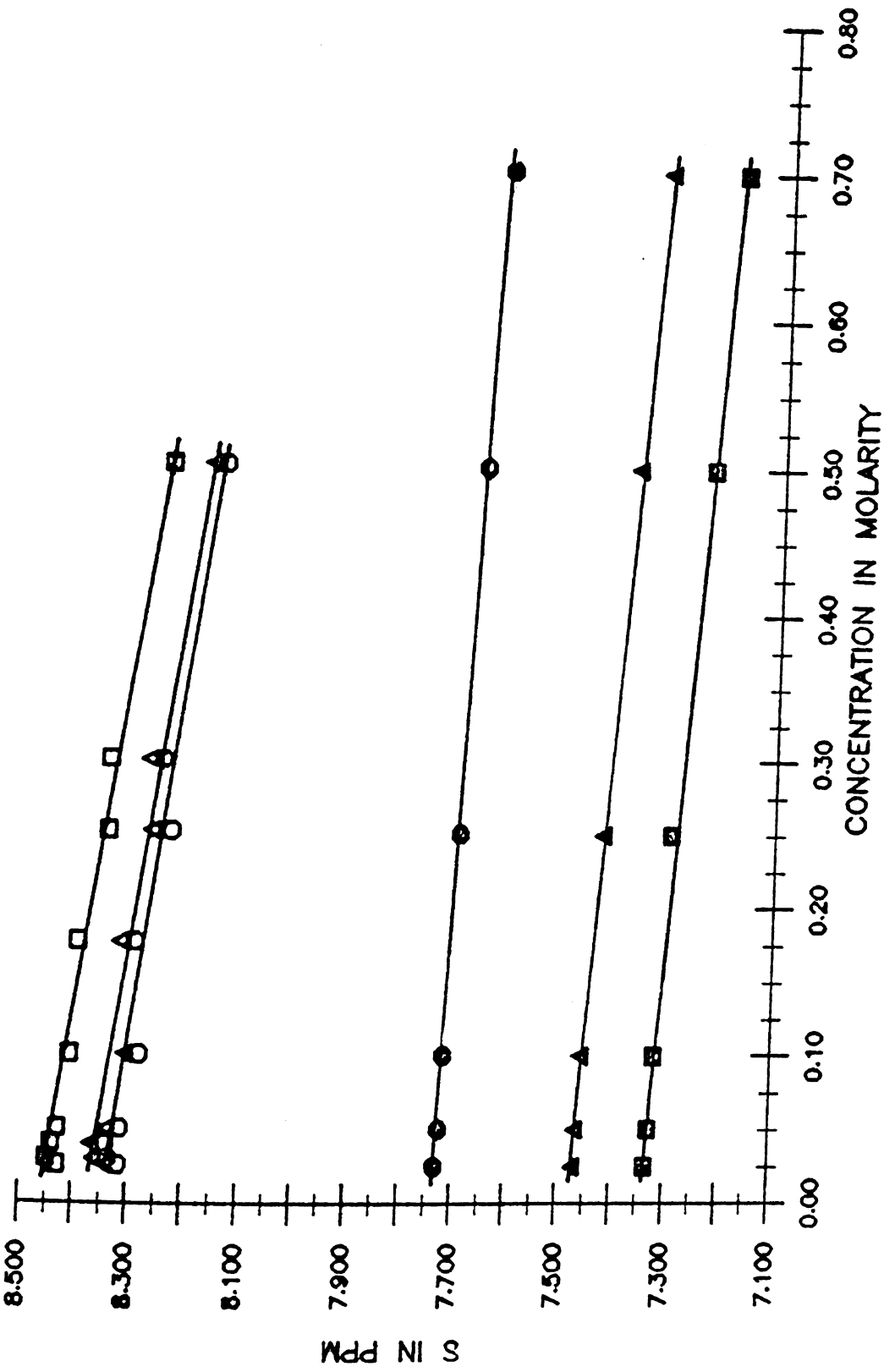


Figure 15. A plot of the proton chemical shift vs total salt concentration in DMSO.

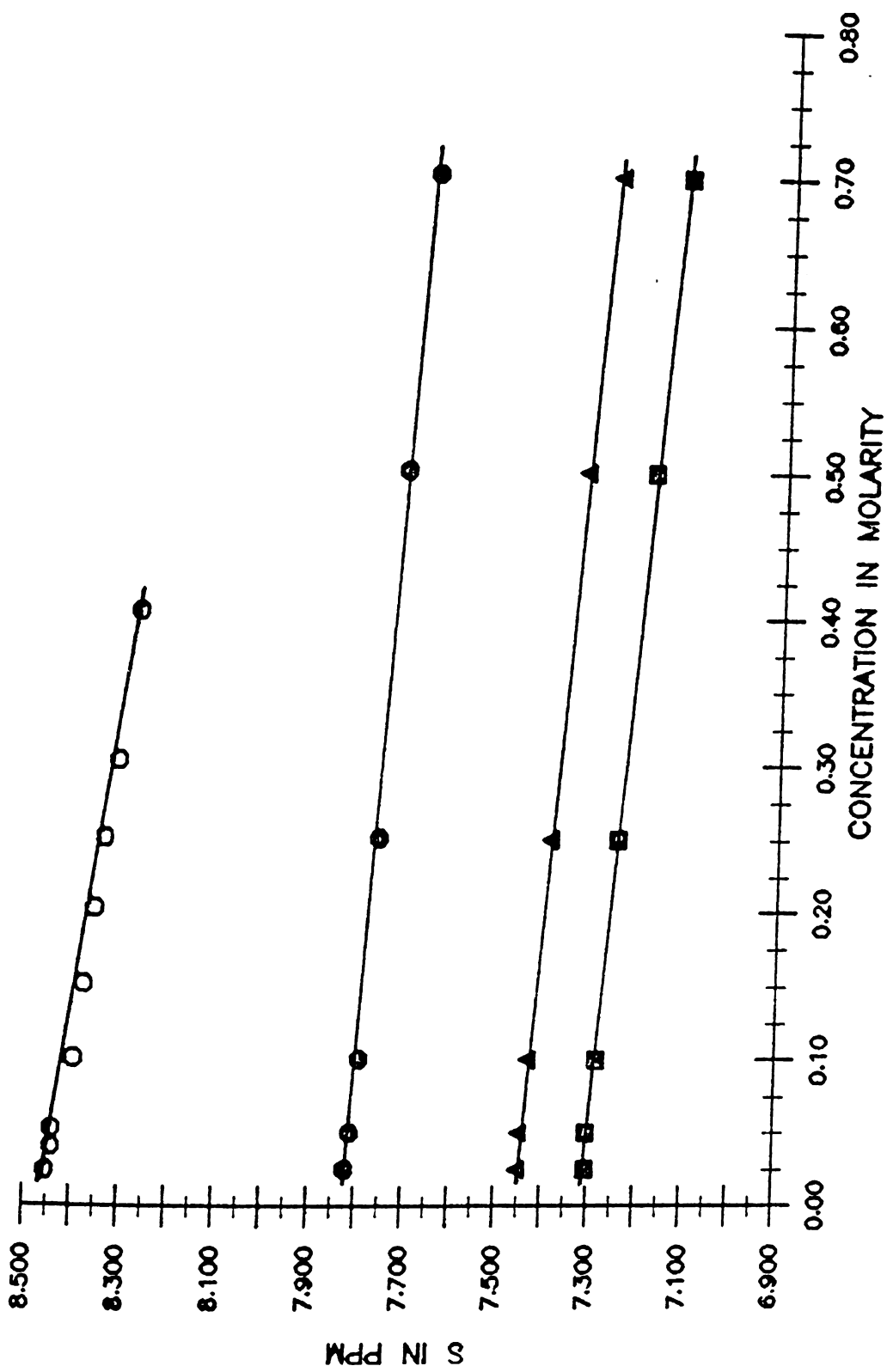


Figure 16. A plot of the proton chemical shift vs total salt concentration in DMF.





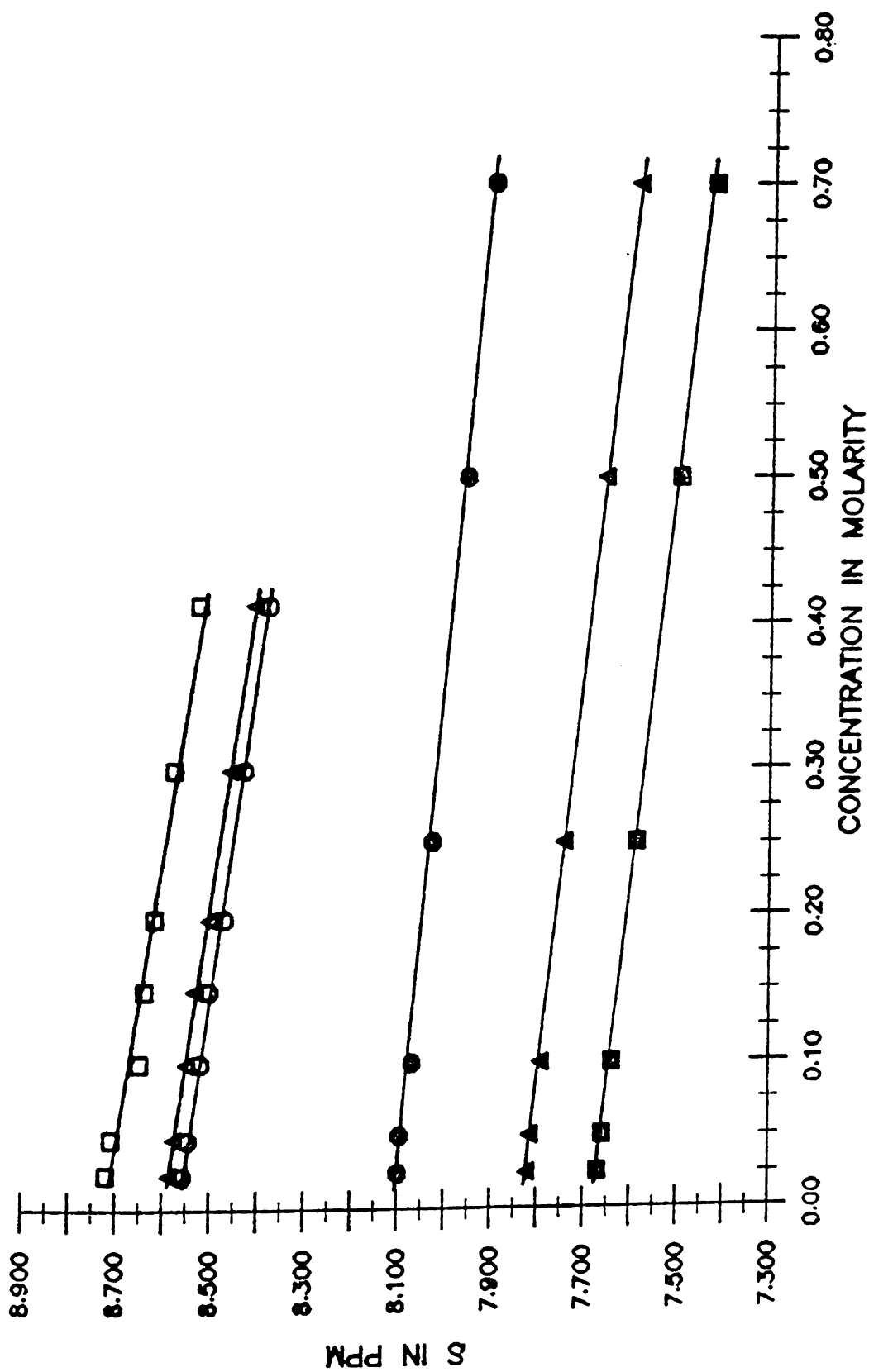


Figure 17. A plot of the proton chemical shift vs total salt concentration in acetonitrile.

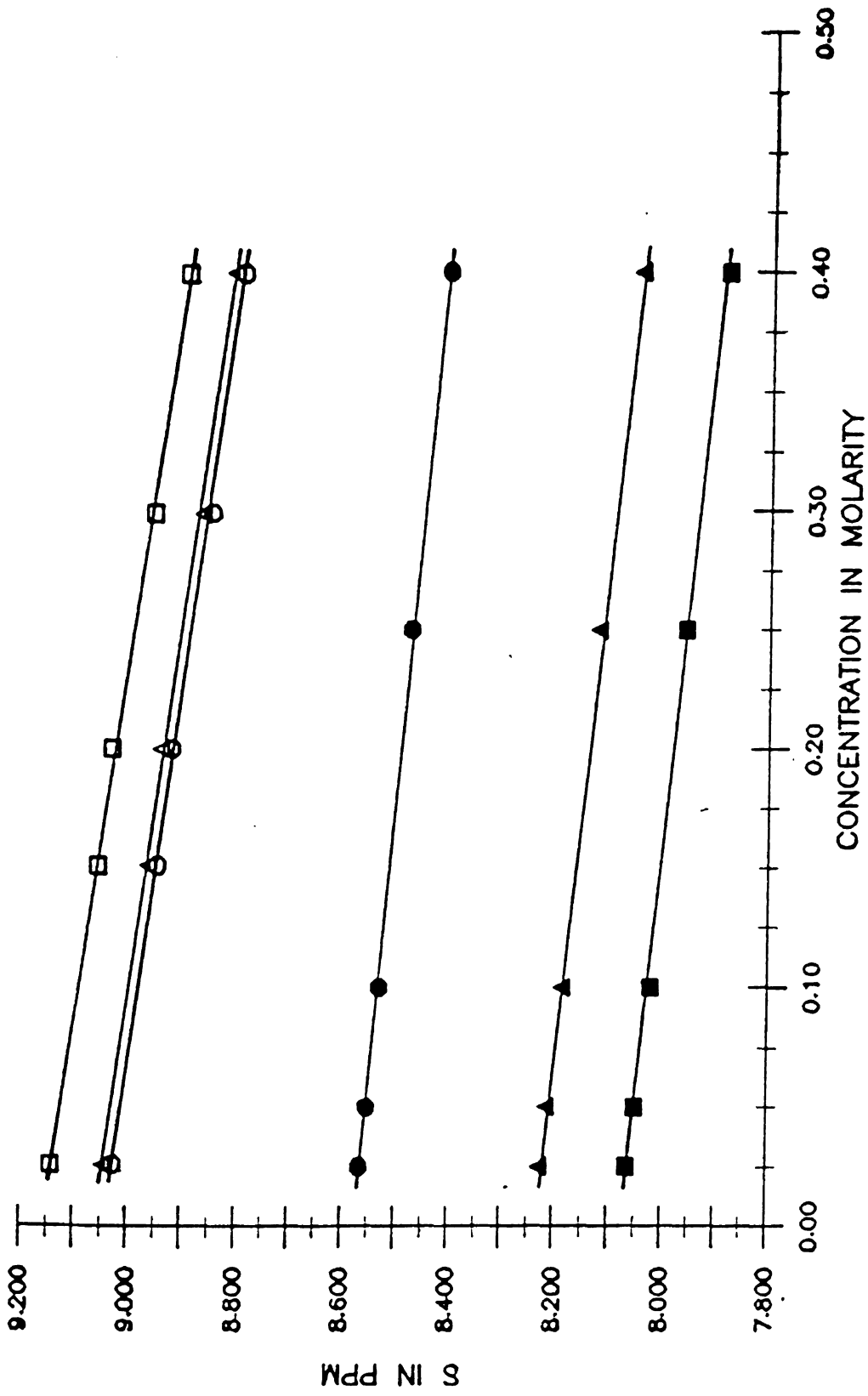


Figure 18. A plot of the proton chemical shift vs total salt concentration in nitromethane.

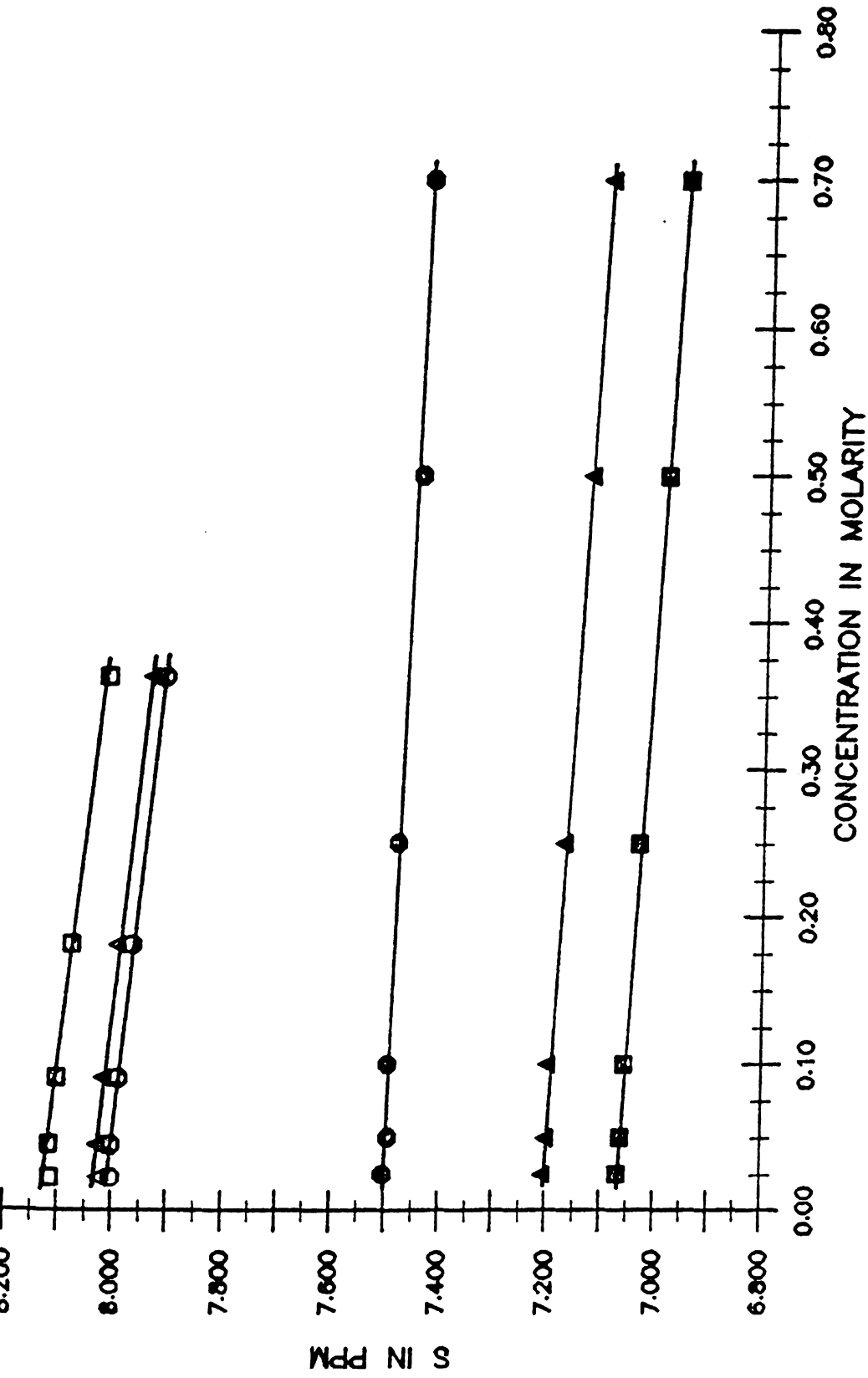


Figure 19. A plot of the proton chemical shift vs total salt concentration in propylene carbonate.

(within

chloric

Fig

of tet.

the to

The co

total

chemic

ibilit

Te

DMSO a

the ob

borate

served

salt o

indica

in the

S

shifts

tion s

of the

arson

corre

shift

with

T

(within the experimental error) was observed for the chloride, bromide, iodide, and thiocyanate counterions.

Figure 20 shows a plot of the observed chemical shift of tetraphenylarsonium chloride in water as a function of the total chloride ion concentration (adjusted with KCl). The concentration dependence is much less than when the total salt concentration was varied. The variation in chemical shift is due predominantly to magnetic susceptibility changes (see Section 2.5.) with concentration.

Tetraphenylarsonium tetraphenylborate was studied in DMSO and DMF, with no significant difference seen between the observed chemical shift of the chloride and tetraphenylborate salt of tetraphenylarsonium, or between the observed chemical shift of the sodium and tetraphenylarsonium salt of tetraphenylborate (see Figure 21). These data indicate that cation-anion interactions are negligible within the experimental error of the proton NMR measurements.

Similarly to the  $^{13}\text{C}$  data, the observed proton chemical shifts exhibit a concentration dependence. In DMSO solution a large portion of this chemical shift change ( $\sim 50\%$  of the chemical shift from 0.05 to 0.5 M) for tetraphenylarsonium chloride was due to bulk magnetic susceptibility corrections (see Section 2.6). The rest of the chemical shift change may be attributed to a change in solvation with the concentration of the solute.

The behavior in water (Figure 14) was anomalous in

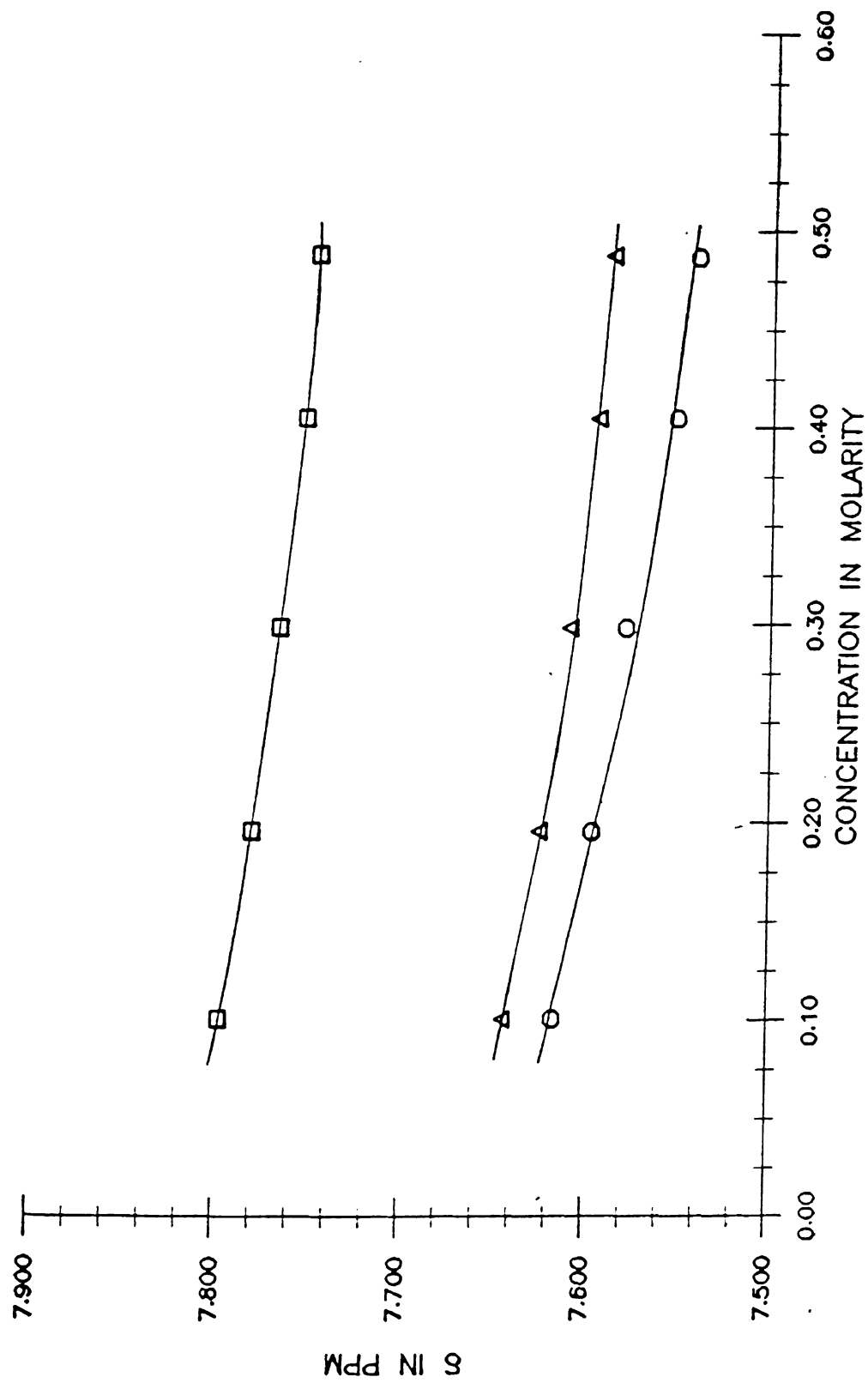


Figure 20. A plot of the proton chemical shift vs total chloride ion concentration for tetraphenylarsonium chloride in water.

Tetraph

Tetraph



Figure

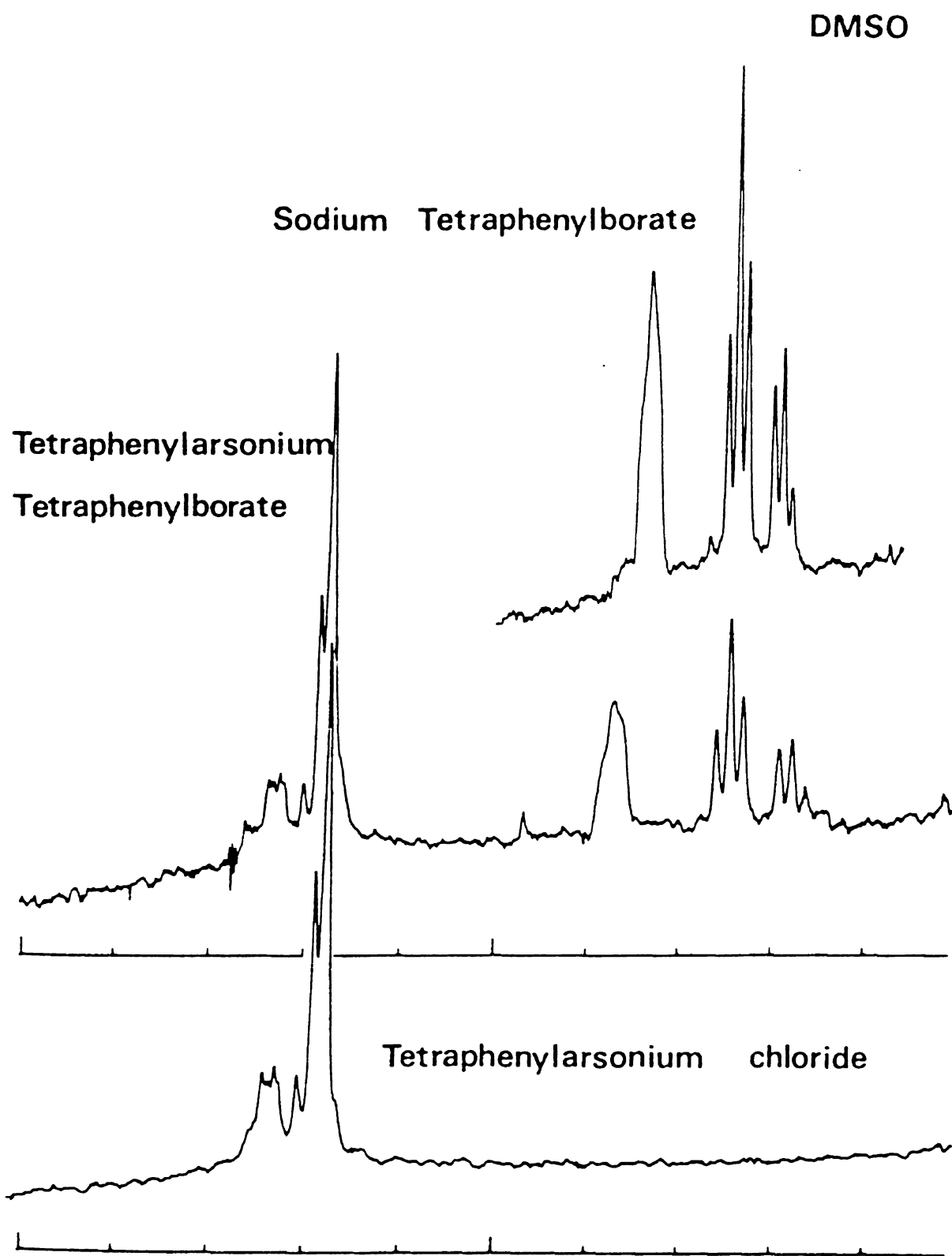


Figure 21. The proton NMR spectra of sodium tetrphenylborate, tetraphenylarsonium chloride, and tetraphenylphosphonium chloride in DMSO.



that of  
below a  
phospho  
the cur  
an inf  
chlorid  
the cr  
furthe  
chemic  
tween  
an int  
bond,  
and or  
chemic  
follow  
ceptib

Th  
meta,  
phosph  
XXX.  
vent o  
as sho  
spectr  
shape  
This  
the s

that there was a pronounced curvature in the chemical shift below a concentration of 0.5 M (the behavior of tetraphenylphosphonium and tetraphenylborate ion were similar, although the curvature was less pronounced). The extrapolation of an infinite dilution chemical shift for tetraphenylarsonium chloride was subject to a large error, but the shifts of the ortho, meta, and para proton were generally among the furthest downfield of all the solvents. The downfield chemical shifts tend to indicate a strong interaction between the negative dipole of the water and the ion. Such an interaction might cause a rotation about the As - C bond, leading to steric hinderance effects for the meta and ortho position (greater for the ortho proton). The chemical shift of the ortho proton then shifts the greatest, followed by the meta, with the para proton the least susceptible to such effects.

The infinite dilution chemical shifts of the ortho, meta, and para proton of tetraphenylarsonium, tetraphenylphosphonium, and tetraphenylborate ions are shown in Table XXX. As with the  $^{13}\text{C}$  chemical shift data, there is a solvent dependence of the observed chemical shift. However, as shown by a comparison of the tetraphenylarsonium chloride spectra in a number of solvents (Figure 22), the actual shapes of the peaks do not vary much from solvent to solvent. This behavior implies that solvation forces are similar in the solvents studied. The ortho position shows the least

---

---

So

P(Ph)<sub>3</sub><sup>+</sup>

H<sub>2</sub>O

Methan

DMSO

DMF

Aceton

Nitrom

Propyl

As(Ph)<sub>3</sub>

H<sub>2</sub>O

Methan

DMSO

DMF

Aceton

Nitrom

Propyl

B(Ph)<sub>3</sub>

H<sub>2</sub>O

DMSO

DMF

Aceton

Nitrom

Propy

Pyrid

---

---

\*  
Corr

Table XXX. The Infinite Dilution Proton Chemical Shifts\* for Tetraphenylarsonium, Tetraphenylphosphonium, and Tetraphenylborate Ion as a Function of the Solvent.

Solvent	$\delta$ in ppm		
	Ortho	Meta	Para
<u><math>P(Ph)_4^+</math></u>			
H <sub>2</sub> O	7.78	7.76	7.96
Methanol	7.635	7.679	7.848
DMSO	7.822	7.904	8.061
DMF	7.779	7.825	-----
Acetonitrile	7.747	7.800	7.991
Nitromethane	7.684	7.699	7.836
Propylene Carbonate	7.623	7.669	7.843
<u><math>As(Ph)_4^+</math></u>			
H <sub>2</sub> O	7.79	7.75	7.88
Methanol	7.663	7.684	7.770
DMSO	7.857	7.883	7.970
DMF	7.858	-----	-----
Acetonitrile	7.787	7.816	7.939
Nitromethane	7.664	7.682	7.780
Propylene Carbonate	7.653	7.679	7.768
<u><math>B(Ph)_4^-</math></u>			
H <sub>2</sub> O	7.45	7.20	7.07
DMSO	7.251	7.036	6.862
DMF	7.206	6.844	6.699
Acetonitrile	7.324	7.050	6.897
Nitromethane	7.195	6.857	6.694
Propylene Carbonate	7.144	6.852	6.712
Pyridine	7.634	-----	-----

\* Corrected for the bulk magnetic susceptibility of the solvent.

Figur

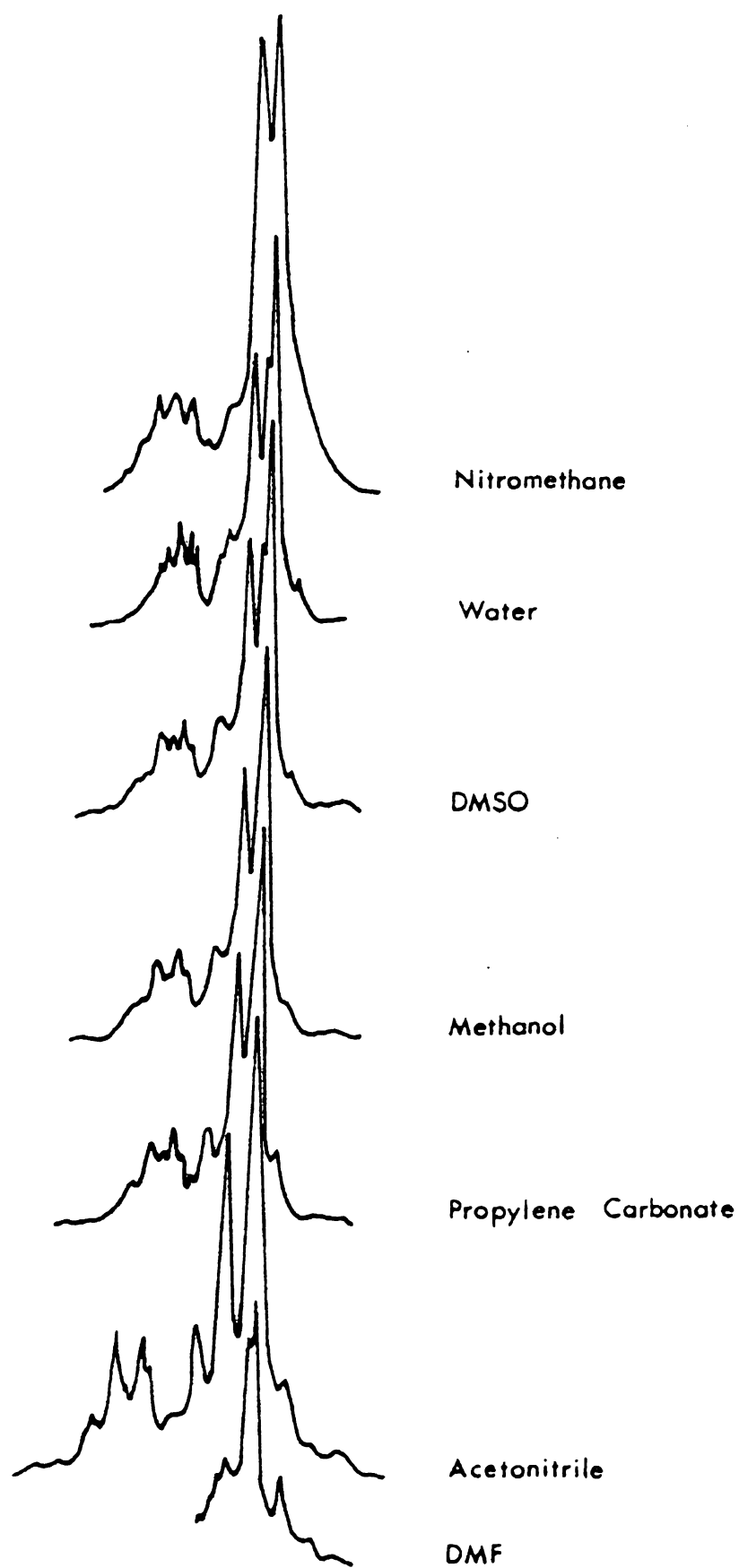


Figure 22. The proton NMR spectra of tetraphenylarsonium chloride in different solvents.

solvent

exhibi

is no a

cal shi

donor r

The

shifts

The di

spectru

is show

para p

by sol-

current

the ne

of the

electr

has th

neares

respec

positi

dipole

The re

the ca

althou

betwee

Th

solvent dependency, while the meta and para position exhibit approximately the same shift with solvent. There is no apparent correlation of the infinite dilution chemical shifts with the dielectric constant or the Gutmann donor number of the solvent.

The difference between the infinite dilution chemical shifts of the cations and anion are shown in Table XXXI. The difference may also be seen in Figure 21, where a spectrum of tetraphenylarsonium tetraphenylborate in DMSO is shown. The relative position of the ortho, meta, and para proton shifts of the cations and anion are dominated by solvation forces, as opposed to the carbons where ring current effects were also significant. The proximity of the negative dipole of the solvent causes the chemical shift of the cation protons to occur further downfield (higher electron density) than those of the anion. The para proton has the highest electron density, as it is the proton nearest the solvent, followed by the meta and ortho protons respectively. A similar rationale was used to explain the position of the anion protons, except that the positive dipole of the solvent is oriented towards the protons. The relative chemical shift of the anion with respect to the cation has been observed by Coetzee and Sharp (28), although their resolution did not allow them to distinguish between the ortho, meta, and para protons.

The difference between the infinite dilution proton



Table

---

S

---

H<sub>2</sub>O  
DMSO  
DMF  
Aceton  
Nitron  
Propyl

---

H<sub>2</sub>O  
DMSO  
DMF  
Aceton  
Nitron  
Propyl

---

Table XXXI. The Difference in Proton Infinite Dilution Chemical Shifts of Tetraphenylarsonium vs Tetraphenylborate Ion as a Function of Solvent.

Solvent	$\Delta\delta (\delta\text{As}(\text{Ph})_4^+ - \delta\text{B}(\text{Ph})_4^-)$ in ppm		
	$\Delta$ ortho	$\Delta$ meta	$\Delta$ para
H <sub>2</sub> O	0.33	0.56	0.9
DMSO	0.57	0.87	1.20
DMF	0.57	0.98	-----
Acetonitrile	0.42	0.75	1.09
Nitromethane	0.49	0.84	1.14
Propylene Carbonate	0.48	0.82	1.13

Solvent	$\Delta\delta (\delta\text{P}(\text{Ph})_4^+ - \delta\text{B}(\text{Ph})_4^-)$ in ppm		
	$\Delta$ ortho	$\Delta$ meta	$\Delta$ para
H <sub>2</sub> O	0.34	0.55	0.81
DMSO	0.61	0.85	1.11
DMF	0.65	-----	-----
Acetonitrile	0.46	0.77	1.04
Nitromethane	0.47	0.83	1.09
Propylene Carbonate	0.51	0.83	1.06

chemic

solvent

ortho

meta l

probab

- O<sub>2</sub> b

for su

solvent

in the

hibit

nounce

the p

the p

a dir

phenom

the p

ortho

protol

tion

A

the p

compa

in Ta

vated

by an

T

chemical shift of the cation and anion exhibits a definite solvent dependence. However, contrary to the  $^{13}\text{C}$  case, the ortho proton exhibited the largest solvent dependency, meta less, and para the least. This relative order is probably due to rotational changes about the central atom -  $\text{C}_1$  bond. Solvent-solute interactions are probable causes for such rotational changes; the extent of change is then solvent dependent. This rotation was manifested in a change in the solute chemical shift, with the ortho proton exhibiting the greatest change. This effect was less pronounced for the meta proton and probably negligible for the para proton. The difference in the chemical shifts of the protons with solvent is then a composite of two effects; a direct solvent dipole - ion interaction and a rotational phenomena caused by solvation. The former is dominant at the para position, while the latter is dominant at the ortho position. The major conclusion derived from this proton NMR study is that there is a difference in solvation of the cation and anion which is solvent dependent.

As in the  $^{13}\text{C}$  study, it was of interest to determine the proton NMR chemical shifts of tetraphenylgermanium as compared to tetraphenylarsonium ion. The results are shown in Table XXXII. Clearly, the two molecules are not solvated equivalently, since the corresponding peaks differ by an average of 0.24 ppm.

The conclusion from the proton NMR study of the

Table 1

---

---

So

---

Dichlo

Deuter

Chloro

---

---

Table XXXII. The Proton Chemical Shifts of Tetraphenylgermanium and Tetraphenylarsonium Chloride in Dichloromethane and Deuterated Chloroform.

Solvent	Molecule	$\delta$ in ppm		
		ortho	meta	para
Dichloromethane	$\text{Ge}(\text{Ph})_4$	7.387	7.508	7.533
	$\text{As}(\text{Ph})_4\text{Cl}$	7.639	7.770	7.868
Deuterated Chloroform	$\text{Ge}(\text{Ph})_4$	4.681	4.824	4.848
	$\text{As}(\text{Ph})_4\text{Cl}$	4.856	5.033	5.082

tetrapl

phenyl

study:

phenyl

and te

lently

2.7.

The

conclu

action

phonic

likewi

also e

and l

shiel

that

withi

the e

state

insul

impor

indio

valer

pheny

vate

tetraphenylarsonium (or tetraphenylphosphonium) tetraphenylborate system are the same as that from the  $^{13}\text{C}$  study: ion-ion interactions are negligible and that tetraphenylarsonium, tetraphenylphosphonium, tetraphenylgermanium, and tetraphenylborate molecules are not solvated equivalently.

## 2.7. Summary and Conclusions

The  $^{31}\text{P}$ ,  $^{11}\text{B}$ ,  $^{13}\text{C}$ , and proton NMR data all lead to the conclusion that, in the solvents studied, ion-ion interactions between tetraphenylarsonium or tetraphenylphosphonium cation and tetraphenylborate anion are negligible. Likewise, all halide or alkali salts of these ions will also exhibit negligible ion-ion interactions. The  $^{31}\text{P}$  and  $^{11}\text{B}$  data indicate that the central atom is not shielded completely from the solvent, while  $^{13}\text{C}$  data indicate that the phenyl groups undergo electron density shifts within the rings so that the charge is distributed over the entire molecule. Contrary to the original assumption stated in Section 2.1, the phenyl rings do not effectively insulate the central atom from the solvent. The most important consideration is that the  $^{13}\text{C}$  and proton data indicate that the cation and anion are not solvated equivalently. Also, the  $^1\text{H}$  and  $^{13}\text{C}$  data indicate that tetraphenylgermanium and tetraphenylarsonium ion are not solvated equivalently.



This study indicates that caution is advised when using the tetraphenylarsonium tetraphenylborate reference electrolyte single ion assumption. Several key assumptions in this hypothesis have been shown to be questionable. It should be emphasized, though, that NMR data provides only qualitative information on the assumption, i.e., the NMR data do not indicate to what extent (in terms of kilocalories) it is in error. The difference in solvation evidenced by NMR measurements may be negligible in the measurements of  $\Delta\bar{G}_{tr}^{\circ}$  within the estimated experimental error,  $\pm 0.3$  kcal (93), of such determinations.

PART III

PHOSPHONOACETIC ACID STUDIES

CHAPTER I

HISTORICAL REVIEW

1.1.

D

ture

(Figur

Herpe

an in

agent

Herpe

group

cell

disea

ing o

herpe

(the

Epste

and o

monor

cons:

spec:

Amer:

its

bodi

Herp

## 1.1. Introduction

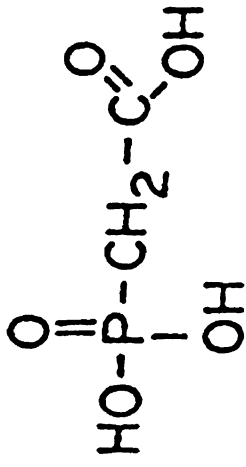
During a random testing of compounds with a cell culture screen, it was found that phosphonoacetic acid (PAA) (Figure 23) was an effective inhibitor of some forms of Herpes simplex viruses (133,134). This discovery led to an interest in this compound as a possible therapeutic agent for the treatment of other forms of Herpes virus. Herpes is the genus of a deoxyribonucleic acid core virus group which replicates itself in the nucleus of the host cell (135). Some common forms of this virus which cause disease in man are: herpes simplex (which causes blistering of the lips, external nares, glans, prepuce, and vulva), herpes labialis (commonly called cold sores), herpes-zoster (the cause of shingles), varicella-zoster (chicken pox), Epstein-Barr virus (responsible for infectious mononucleosis), and cytomegalovirus (causes pneumonitis, cytomegalovirus mononucleosis). The list is far from complete when it is considered that there are many more forms of Herpes virus specific to animals. It is estimated that 10% of all Americans suffer recurrent herpes infections, usually in its milder forms of cold sores, while fully 70% have antibodies which would indicate a past exposure to Herpes.

The therapeutic value of PAA in the treatment of Herpes viruses was of interest because few drugs exist

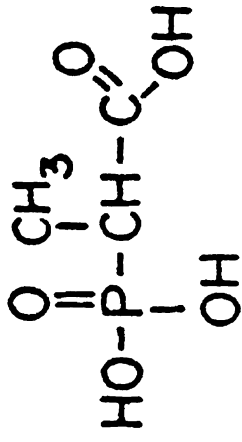
PHOSPHONO ACETIC ACID (PAA)

2-PHOSPHONOPROPIONIC ACID

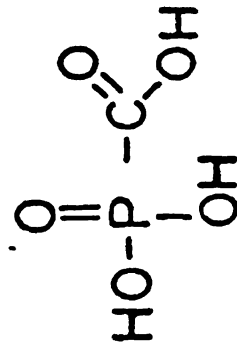
## PHOSPHONO ACETIC ACID (PAA)



## 2-PHOSPHONOPROPIONIC ACID



## PHOSPHONOFORMIC ACID (PFA)



## 3-PHOSPHONOPROPIONIC ACID

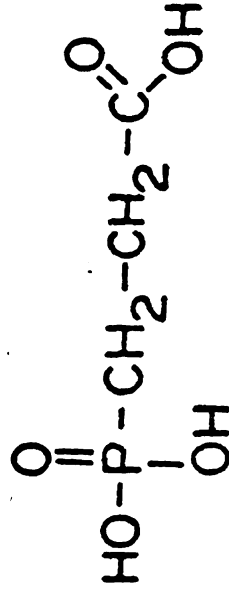


Figure 23. The structures of phosphonoacetic acid (PAA), phosphonoformic acid (PFA), 2-phosphonopropionic acid, and 3-phosphonopropionic acid.

which

these

a pote

such,

or thr

these

fects

A) was

Simple

effect

The ti

fibron

fects

Kerat.

fect

tilon

Herpe

(144)

prese

it do

in bi

1

T

stran

will



which have an antiviral action against Herpes. Most of these drugs are nucleoside analogs (136,137), which hold a potential for teratogenic or carcinogenic behavior. As such, only one is commercially used in the U.S., while two or three are available elsewhere in the world. Some of these have been compared to PAA in their inhibitory effects. The compound 9-B-D-arabinofuranosyl adenosine (Ara-A) was found to be as effective as PAA against Herpes Simplex virus type 1 (138), while showing no therapeutic effect in clinical trials for Herpes Genitalis (139,140). The therapeutic effects of Ara-A and PAA against Shope fibroma in rabbits were the same (141), as were the effects of idoxuridine and PAA in the treatment of Herpes Keratitis (142,143). There was a greater therapeutic effect by PAA than Ara-A against cytomegalovirus. The drug tilorone hydrochloride had no inhibitory effect against Herpes Simplex virus type 1, as compared to PAA, in mice (144). Hence, PAA is as effective as any of the drugs presently available for the treatment of Herpes virus, and it does not exhibit a teratogenic or carcinogenic behavior in biological studies.

#### 1.1.1. Viral Replication

The Herpes virus are capsid protein enclosed DNA strands. When the capsid encounters a cell membrane it will merge with the cell until the naked DNA is released.

The D

self t

factur

and p

This i

where

repea

cell i

the c

1

T

virus

polym

separ

Decoxy

site

that

the t

the p

rever

meras

The w

DNA h

T

The DNA then migrates to the nucleus where it attaches itself to the DNA of the cell. The virus DNA will then manufacture ribonucleic acid ( $RHA_{HV}$ ) which leaves the nucleus and produces a DNA polymerase enzyme in the cytoplasm. This DNA polymerase then migrates back into the nucleus where it replicates the viral DNA ( $DNA_{HV}$ ). The entire cycle repeats itself, increasing the amount of  $DNA_{HV}$  until the cell begins to lyse. The encapsulated  $DNA_{HV}$  then leaves the cell to propagate the disease further in other cells.

#### 1.1.2. Inhibition of the Viral Replication Path by

##### PAA

The basic pathway involved in the replication of Herpes virus specific DNA is shown in Figure 24. The enzyme DNA polymerase reversibly binds to the  $DNA_{HV}$ , which is separated, one nucleic acid at a time, into two strands. Deoxynucleoside triphosphate (dNTP) then binds to another site on the enzyme. An internal reorientation occurs such that the dNTP binds to the complementary nucleic acid on the template  $DNA_{HV}$ , forming an inorganic pyrophosphate in the process (145). The inorganic pyrophosphate is then reversibly released, followed by the movement of the polymerase to the next nucleic acid link in the DNA chain. The whole process is repeated until the entire strand of DNA has been replicated into two identical daughter strands. There have been two mechanisms postulated (see Figure

$F_{DNA}$

$\rightarrow$

$\kappa_1 DNA$

$\left[ \right.$

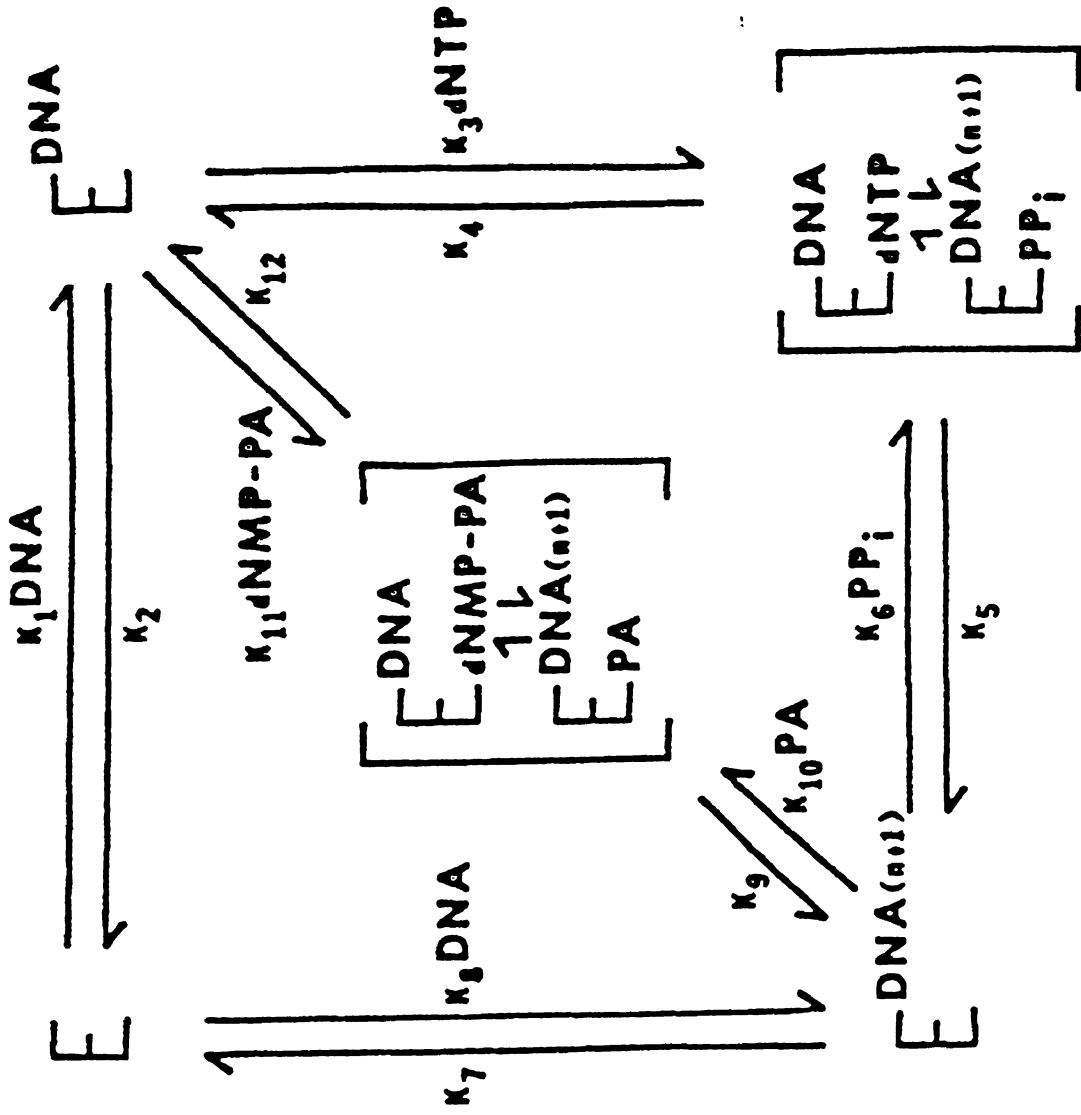


Figure 24. DNA synthesis and the proposed PAA inhibition mechanism.

24) f

DNA r

to th

late

comp

exch

soci

go a

of t

side

(145

mech

the

are

lat

so :

phos

tio

con

(14

Was

the

men

wit

PAF

24) for the inhibition of Herpes virus of turkey induced DNA polymerase by PAA (146). The phosphonoacetate binds to the polymerase at the inorganic pyrophosphate site (postulated via a complexation with magnesium ion) and acts as a competitive inhibitor of inorganic pyrophosphate in the exchange reaction. The PAA can then act either to dissociate from the enzyme complex  $E_{PA}^{DNA(N+1)}$ , or it may undergo a reorientation with the nucleotide at the 3' position of the DNA template to form the nucleotide deoxynucleoside monophosphate-phosphono acetate (dNMP-PA) and  $E^{DNA}$ .

A kinetic study of the system by Leinbach, et al. (145), yielded results which were not consistent with the mechanism in which the PAA only binds and dissociates from the  $E^{DNA(N+1)}$  complex (a deadend inhibitor). The results are consistent with the second mechanism, although the isolation of dNMP-PA, which would confirm this hypothesis, has so far eluded investigators.

From the proposed mechanism it is evident that pyrophosphate and PAA act similarly to inhibit DNA<sub>HV</sub> replication. That is, an increase in the PAA or pyrophosphate concentration should inhibit viral replication. Studies (145) have shown this to be the case, although the PAA was two or three orders of magnitude more effective than the pyrophosphate. This is seen from the dosage requirements necessary to produce similar inhibitory effects, with 100 to 1000 times more pyrophosphate required than PAA.

1.2.

W  
the t  
effec  
intra  
in ra  
altho  
mice  
:  
admin  
keys  
in t  
redu  
dose  
to t  
peut  
50 m  
230  
have  
rat:  
four  
rat  
mg/  
on  
dru



## 1.2. Toxicity of PAA

While it is evident that PAA shows great promise in the treatment of Herpes viruses, it is not free from side effects. Studies by Meyer et al. (143) indicate that intravenous injections of PAA, at the level of 300 mg/kg, in rabbits often produced fatal tetanic muscular spasms, although the same dose given orally or intraperitoneally to mice was tolerated (133,138).

It was found by Roboz et al. (146) that subcutaneously administered doses of 500 mg/kg PAA were lethal to monkeys within two days. The resultant concentration of PAA in the blood was 0.5 - 3 mg/ml. If the total dosage is reduced to 100 mg/kg (subcutaneously injected in 25 mg/kg doses every two hours), the blood level of PAA is reduced to the 1 mg/ml range, which is easily tolerated. For therapeutic trials the recommended blood level is a continuous 50 mg/ml, which results from a dosage of approximately 230 mg/kg.

Carbon-14 studies of labeled PAA by Bopp et al. (147) have shown significant bone deposition of this drug in rats, rabbits, monkeys, and dogs. The concentrations found in dry femur after seven days were: 55 mg/g in rats, 62 mg/g in rabbits, 24 mg/g in monkeys, 4 and 57 mg/g in adult dogs and puppies, respectively. Studies on rabbits indicated that the drug, or a metabolite of the drug, was retained in the bone for over two hundred days.

These

with

postu

cause

1.3.

were

and t

by H

subs

phos

inhi

test

show

form

the

acid

phos

agai

trol

PAA

whic

fect

simp

These studies tend to implicate a secondary complexation with calcium (aside from the primary inhibitory effect postulated to occur via magnesium complexation), which causes the observed side effects.

### 1.3. Analogs of Phosphonoacetic Acid

The antiviral properties of structural analogs of PAA were investigated to understand the drug mode of action and to attempt to minimize the toxic side effects. Studies by Herrin et al. (148) and Lee et al. (149), indicate that substitution of functional groups for the carboxylic or phosphono-moiety drastically reduces or eliminates the inhibitory effect. The only two analogs among the many tested which exhibit an inhibitory effect of the magnitude shown by PAA are 2-phosphonopropionic acid and phosphonoformic acid (150). The phosphonoformic acid (PFA) had the same inhibitory effect as PAA, while 2-phosphonopropionic acid was 50 times less effective than PAA. The analog 3-phosphonopropionic acid (3-PAA) has no therapeutic effect against Herpes virus (150) and hence it is used as a control for comparison with the physicochemical properties of PAA and PFA.

The PFA analog decomposes at low pH values (151,152), which would tend to recommend it over PAA. It is as effective as PAA against Herpes virus of turkey and Herpes simplex virus, but not effective against mutant strains

resis

of ac

prope

to fa

1.4.

these

(34)

Orig:

for r

by E

cium

by E

and

Mao

obta

with

was

phys

to t

0.15

of t

use

and

resistant to PAA (150). This implies that it has a mode of action similar to PAA as well as similar biochemical properties; its physiological decomposition properties tend to favor its use.

#### 1.4. Chemical Properties of PAA and its Analogs

The compounds PAA and PFA, as well as various salts of these ligands, were first synthesized by Nylén in 1924 (34); the 3-PPA molecule was synthesized in 1926 (35). Originally, PAA was used primarily as an extracting agent for rare earth ions (153), with particular interest shown by Elesin (154,155) in its complexing ability with americium, curium, and promethium ions.

The  $pK_a$  values for this triprotic acid were determined by Elesin (155), Mao et al. (156), Heubel and Popov (51), and Stunzi and Perrin (157). The values of Elesin and Mao have been criticized by Heubel (158), while the values obtained by Stunzi et al., were reported simultaneously with the article by Heubel (51). The study by Stunzi was conducted at 37°C and  $I = 0.15$  (in order to approximate physiological conditions) and was therefore not applicable to this work (25°C and varying ionic strengths less than 0.15). Heubel and Popov determined the  $pK_a$ 's as a function of both temperature and ionic strength, which led to the use of those values in the present investigation. Stunzi and Perron studied PAA complexation with  $Mg^{+2}$ ,  $Ca^{+2}$ ,  $Cu^{+2}$

and

con

mar

and

1.5

ISE

suc

wit

a

bei

ti

th

de

hy

co

te

ma

te

si

g

(1

and  $Zn^{+2}$ , although, again, at  $37^{\circ}C$  and  $I = 0.15$ . Heubel conducted investigations of the complexation of PAA primarily with  $Mg^{2+}$ , while complexations with  $Ca^{2+}$ ,  $Sr^{2+}$ ,  $Ba^{2+}$ , and  $Cd^{2+}$  were briefly studied.

## 1.5. Experimental Techniques

### 1.5.1. Calcium Ion Selective Electrodes

The prototype of the commercially available calcium ISE was developed by Ross (159) in 1967. The composition of such electrodes (Figure 25) are similar to glass electrodes with the exception that the potential is developed across a liquid ion exchanger rather than a glass membrane. The behavior of the electrode, i.e., the sensitivity, selectivity, stability, lifetime, etc., is highly dependent upon the specific liquid ion exchanger used (160-163).

The calcium ion selective electrode has been used to determine the dissociation constant of calcium sulfate dihydrate (164) as well as the formation constants for  $Ca^{2+}$  complexes with the following ligands: ethylenediamine tetracetate (EDTA) and nitrilotriacetate (NTA) (165), malate, citrate, and trans-1,2-d,aminocyclohexane-N,N,N',N'-tetracetate (166), tri and tetrametaphosphate (167), adenosine triphosphate (ATP) (168), ATP, EDTA, and ethylene glycol-bis(2-aminoethylether)-N,N,N',N'-tetraacetate (EGTA) (169), and citrate, malate, malonate, oxalate, EDTA, NTA,

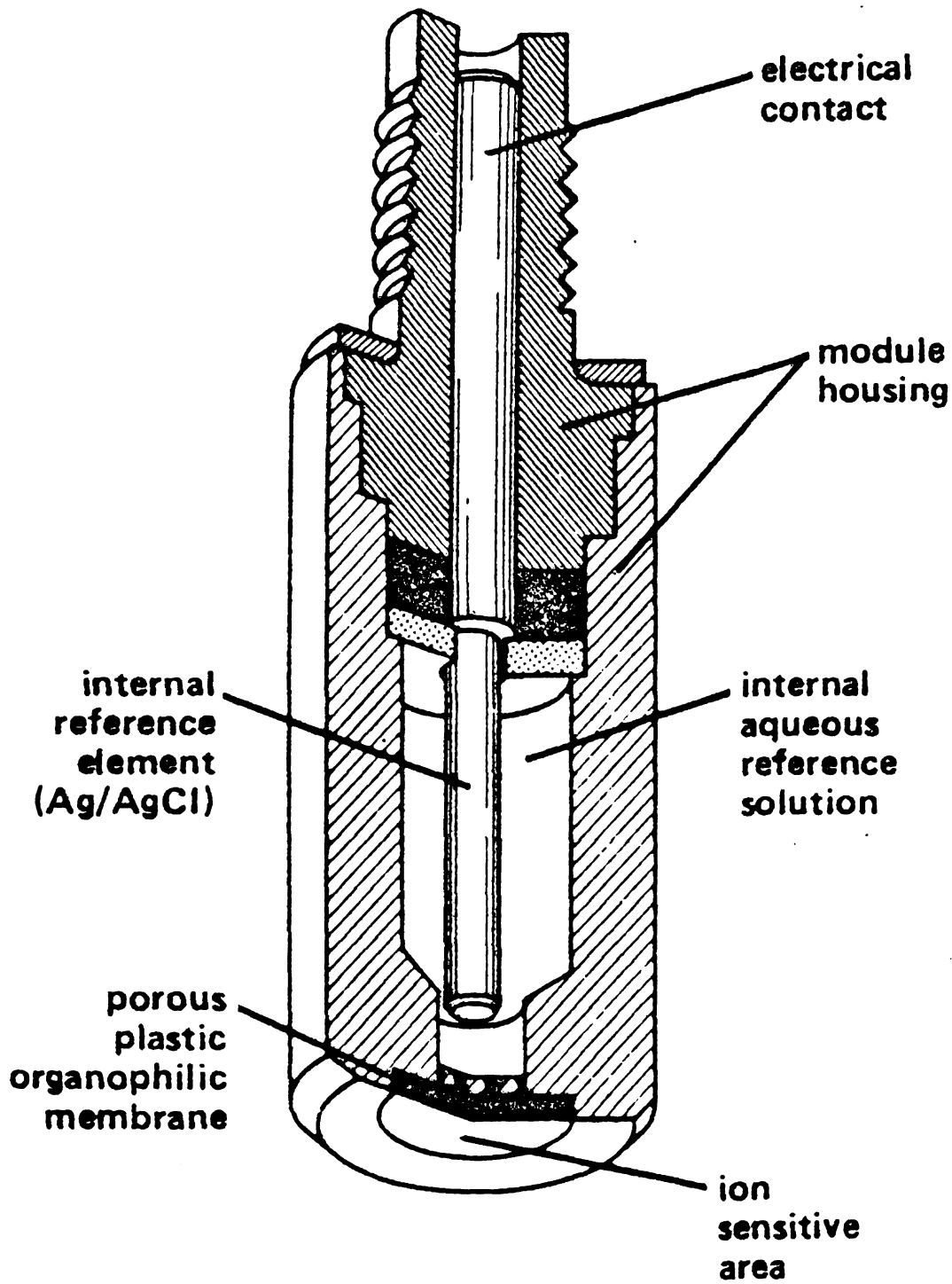
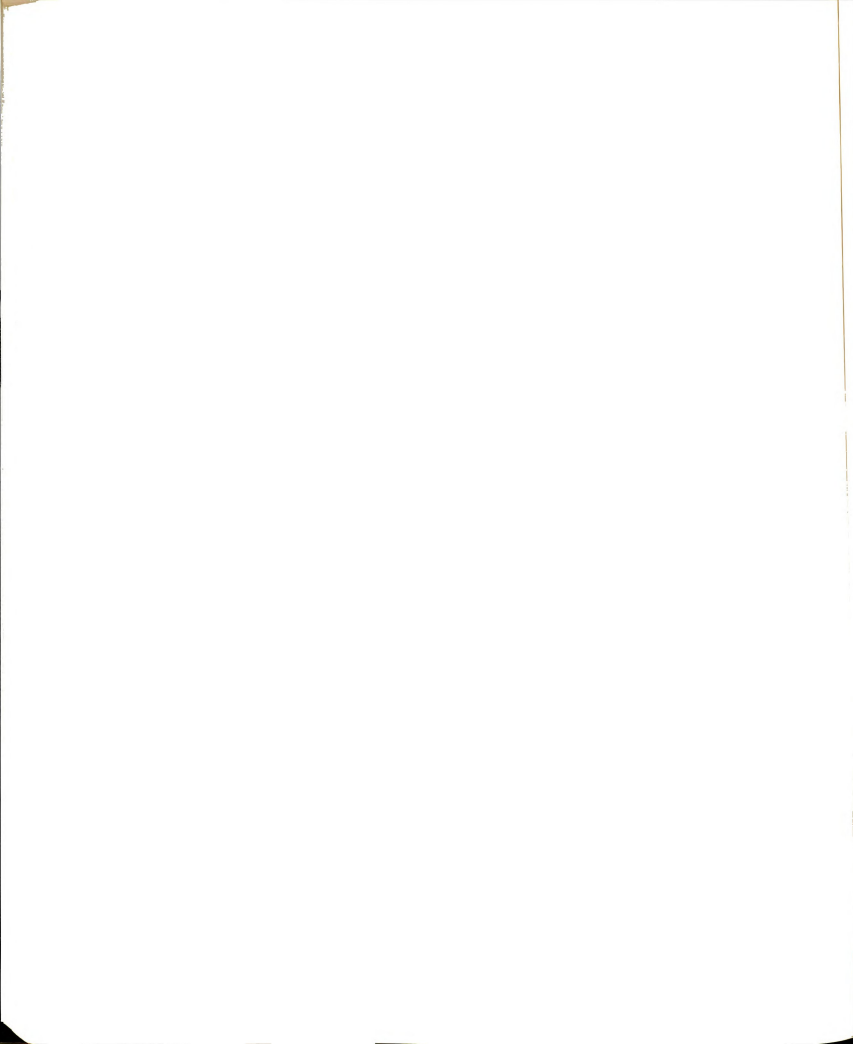


Figure 25. A schematic representation of the Orion 90-20 calcium ion selective electrode.

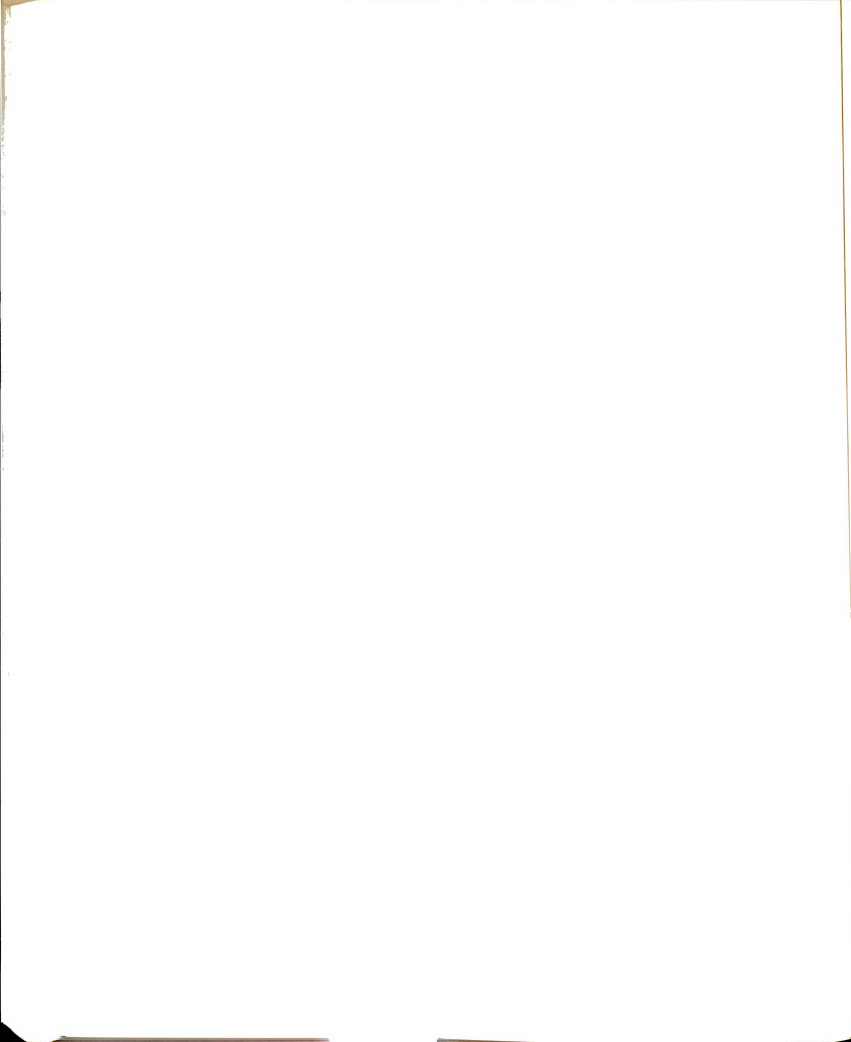




sulfate, orthophosphate, tripolyphosphate, and pyrophosphate (170). In all cases the authors compared the values obtained using a calcium selective electrode to literature values obtained using other techniques (primarily potentiometry using a pH electrode). The general consensus was that the calcium ion-selective electrode was a valid analytical tool for the determination of calcium(II) ion aqueous complexation constants.

#### 1.5.2. Manganese Electron Spin Resonance

Although manganese(II) ion is of biological and chemical interest, its complexation solution chemistry has not been investigated too thoroughly due to technical difficulties of studying this ion in solution. Direct electrochemical observation of this ion is difficult due to the very negative electrochemical potential of the  $\text{Mn}^{2+}/0$  couple and its generally irreversible behavior in aqueous solutions. The difficulty in obtaining an organic ion exchanger that is highly selective for manganese, yet suitable for a membrane, has hindered the development of an ion selective electrode for potentiometric studies. Spectroscopic studies in the UV and visible region are only plausible in cases where highly colored  $\text{Mn}^{2+}$  complexes are formed, and hence, are not universally applicable. Most other common techniques are either difficult, destructive, not applicable, and/or time-consuming.



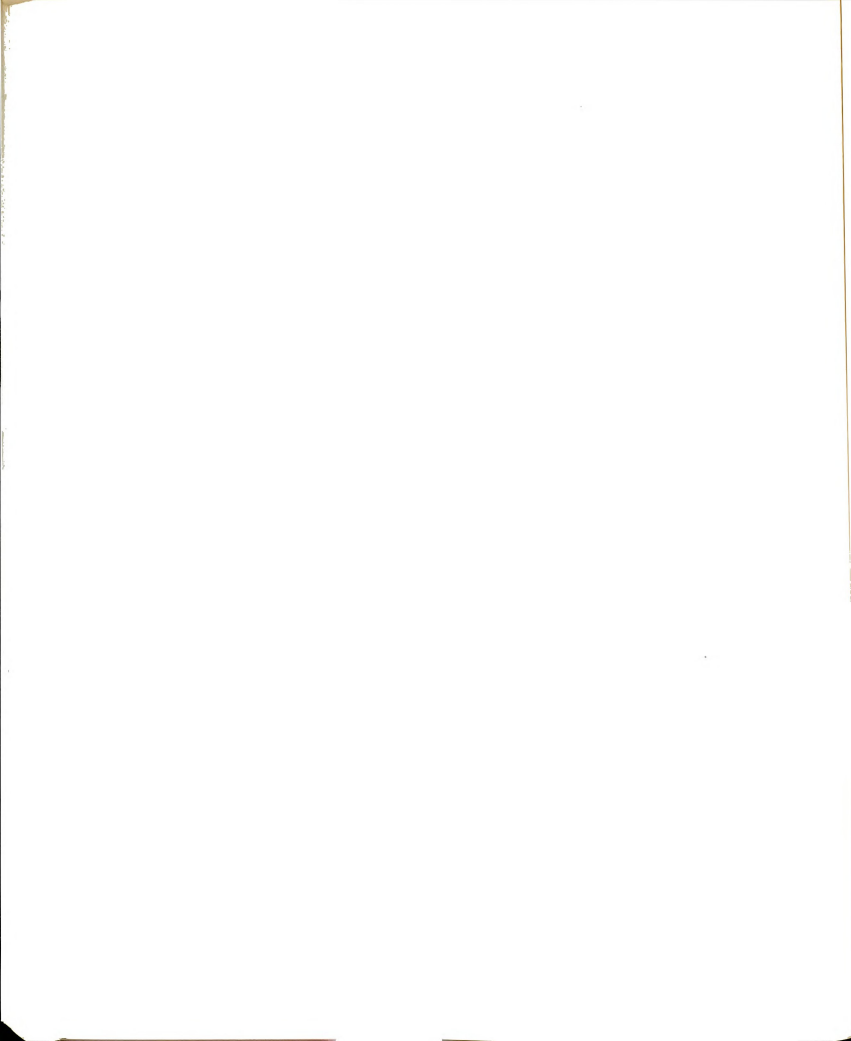
One technique which shows great promise in the study of manganese(II) ion solution chemistry is electron spin resonance (ESR). Similar to NMR spectroscopy, ESR responds to species with an odd spin, except in this case it is the odd spin of an unpaired electron. With five unpaired electrons in a  $\text{Mn}(\text{H}_2\text{O})_6^{2+}$  complex, the manganese ion is ideal for observation with ESR. The similarity to NMR spectroscopy also extends to the wealth of information available from linewidth, intensity, and chemical shift data on an observed manganese resonance.

The application of manganese ESR to the study of aqueous solution chemistry was pioneered by Townsend (171) in 1954. The complexation formation constants of manganese with malonic acid, glycylglycine, glucose, and histidine were determined. The behavior of manganese salts in aqueous solutions was then investigated by Hayes et al. (172) and Flato (173), while the mixed solvent behavior of salt solutions was studied by Bard et al. (174), Vishnevskay et al. (175), and Burlamacchi (176). The linewidth and chemical shift of the observed manganese resonance were found to be independent of the chloride and perchlorate ion concentration below 0.05M, while the sulfate ion led to a decrease in intensity and an increase in the linewidth even at low concentrations. The conclusion is that, in order to minimize effects due to the counterion, a chloride or, preferably, a perchlorate salt of the manganese(II)

ion should be used.

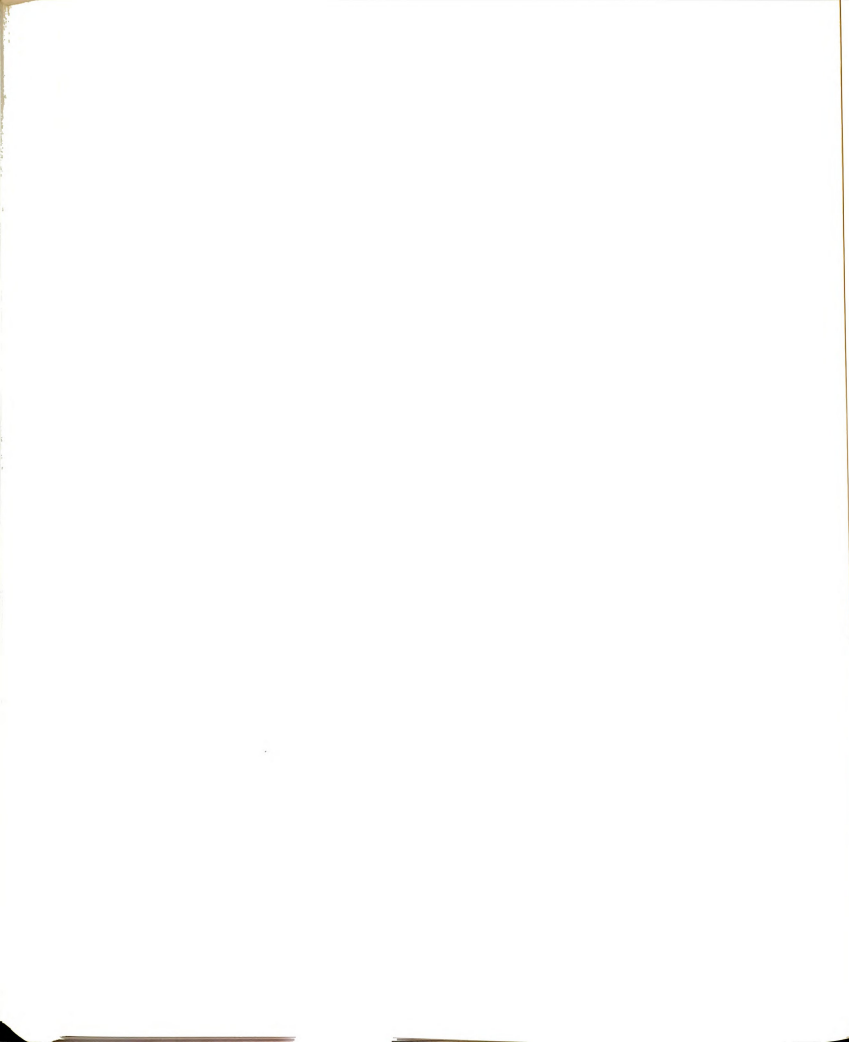
Complexation studies since Townsend's have dealt primarily with biomacromolecules. Blankenship and Saver (177) studied the environment of chloroplasts washed in a tris buffer and estimated the dissociation constants for the binding sites to be  $1.2 \times 10^{-4}$  M. Complexes of manganese with nucleobases, nucleotides, nucleosides, and DNA were studied by Basosi et al. (178,179), to obtain structural information on these systems. The effects of substrates, cofactors and substrate analogs on the complexation of manganese(II) isocitrate dehydrogenase was qualitatively investigated by Levy and Villafranca (180). Correlations between the appearance of fine structure and the binding of individual substrates were found. Nicotinamide adenine dinucleotide complexes with manganese were studied by Green and Kotowycz (181), who found two metal binding sites with formation constants of  $640 \pm 90$  and  $88 \pm 13$ . Armstrong et al. (182) investigated the kinetics and formation constants of manganese binding to adenosine-3',5'-monophosphate dependent protein kinase from bovine heart. A rapid equilibrium was found with the manganese(II) ion binding to a nucleotide site and a protein site.

While most studies have been restricted to biomacromolecules, there is no a priori reason why this method should not be applicable to the study of smaller ligand complexation reactions with manganese ion.



### 1.6. Conclusions

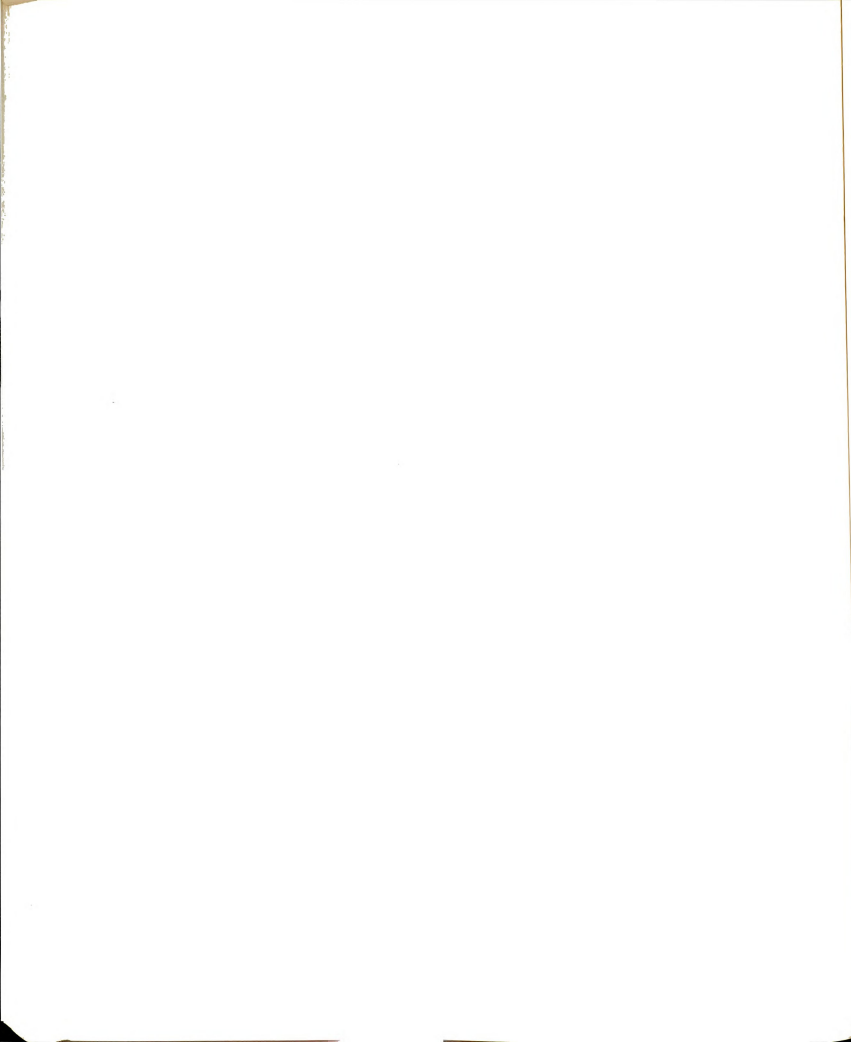
The biological side effects attributed to the use of PAA as a therapeutic agent would tend to implicate a complexation reaction with calcium. It is then of interest to investigate the solution chemistry of the calcium-PAA system to determine the validity of this hypothesis, as well as to elucidate thermodynamic information about the complexation process. Since this drug is of therapeutic value, it is also of interest to study its complexation properties with other biologically important ions, especially manganese(II) ion. Together with the information derived from a study of analogs of PAA it is hoped that the in vivo behavior of this drug may be better understood from the derived in vitro models.





CHAPTER II

MATERIALS AND METHODS



## 2.1. Reagents

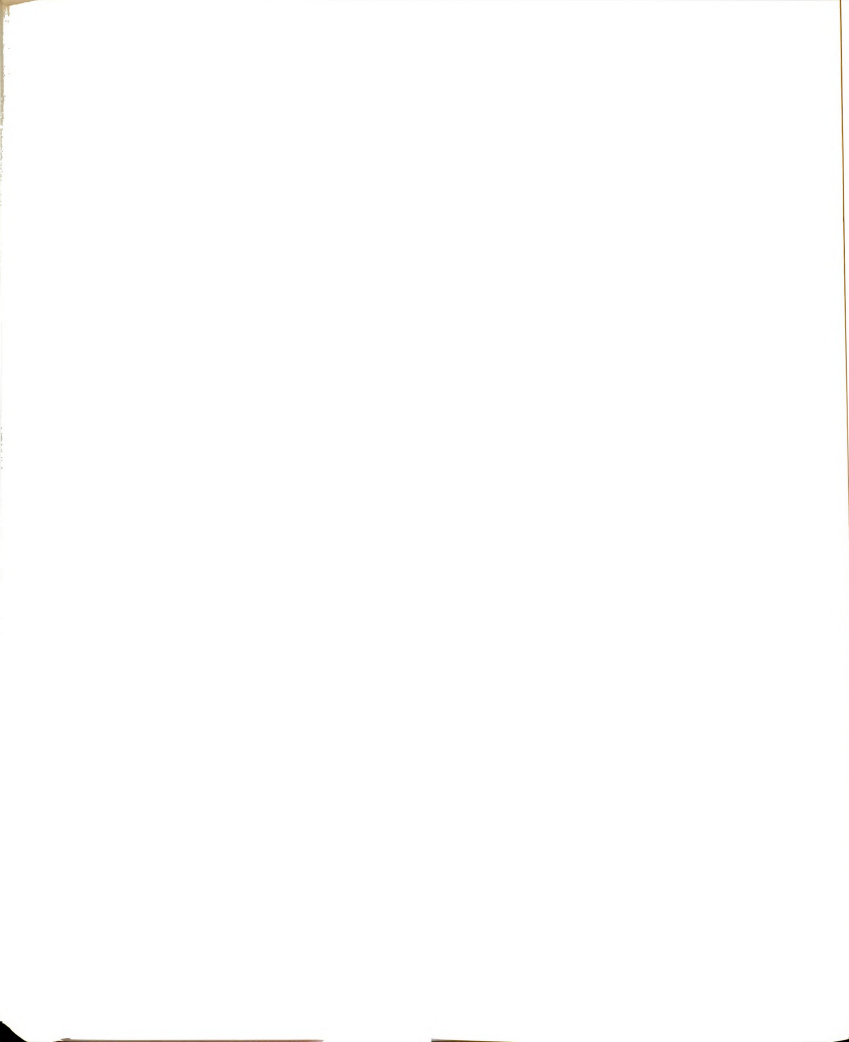
All reagents and purification schemes are as given in Section 1.2.1.

## 2.2. Experimental Methods

### 2.2.1. Electron Spin Resonance Spectroscopy

The aqueous solution chemistry of manganese(II) ion was studied using a Varian E-4 Electron Paramagnetic Resonance Spectrometer at a resonance frequency of 9.407 Gigahertz. The modulation frequency was 100 kHz with a peak-to-peak amplitude of 12.5 gauss. A sweep width of 1000 gauss was used with the midpoint of the range set at 3550 gauss. Ten decibels of power were output to the sample at a detector current of 300 mA, while the first derivative time constant was set at one second. The total sweep time of this continuous wave instrument was 8 minutes. These parameters were the optimized conditions for the maximum sensitivity with a minimal loss due to saturation of the resonance signal.

A Wilmad aqueous EPR cell (catalog No. WG-812) was used for all measurements. The cell is made of quartz, with a small path length to minimize dipole absorption



from the solvent. Ten solutions were studied to yield one formation constant.

### 2.2.2. Cyclic Voltammetry

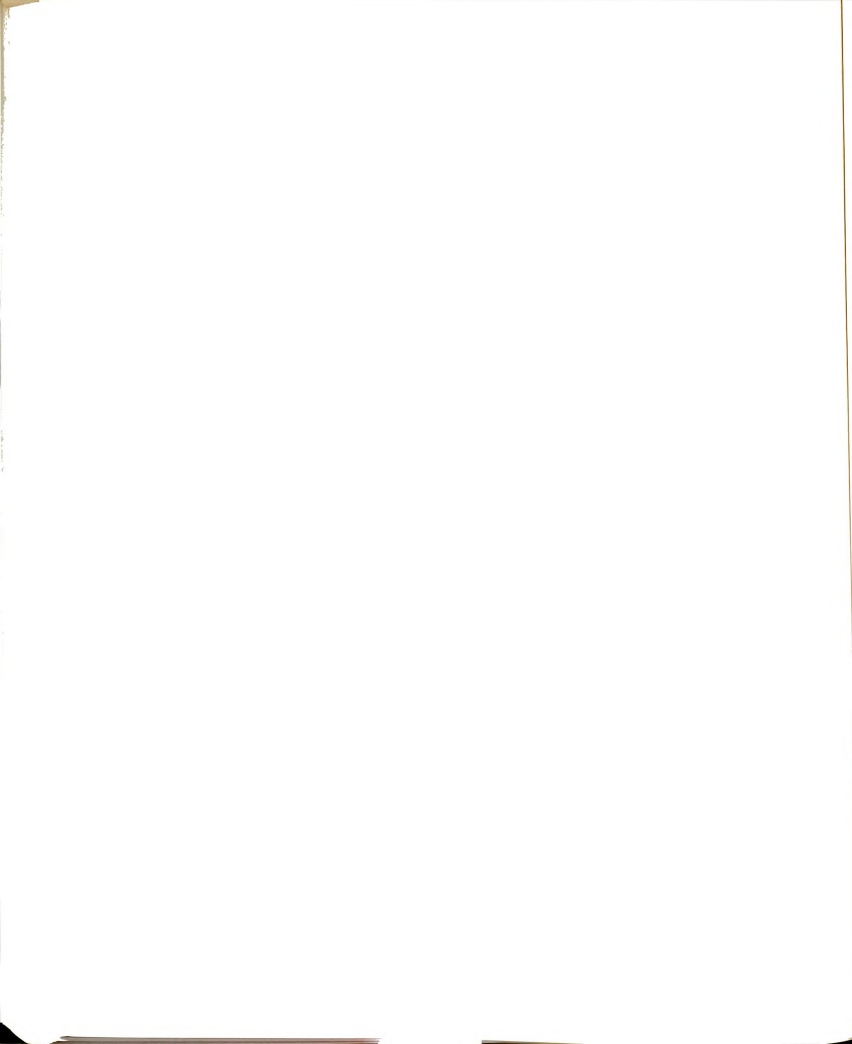
Cyclic voltammetric studies were conducted with a PAR Model 174-A polarographic analyzer and recorded on a Hewlett-Packard x-y recorder. The cell used is shown in Figure 26. The main compartment of the water-jacketed cell was thermostated at  $25.0 \pm 0.1^\circ\text{C}$ , while the reference side-arm was allowed to equilibrate with the atmosphere. All solutions were degassed for 20 minutes with deoxygenated nitrogen. The nitrogen was deoxygenated by passage through two solutions of ammonium vanadate in HCl (183), which is oxidized in the presence of oxygen. The vanadate was regenerated by reaction with a Zn-Hg amalgam in the solution. The nitrogen was then washed by passage through water.

The working electrode was a hanging mercury drop electrode (HMDE), the counter electrode, a platinum wire, and a standard calomel electrode (SCE) was used as a reference. The sweep rate was 100 mV/s. The half-wave potential of a metal ion for a given solution was obtained by averaging the maximum current for the anodic and cathodic waves. Five such determinations were conducted on each solution and the results averaged to yield the reported half-wave potentials. Five solutions were required to obtain a formation constant.

### 2.2.3. Potentiometry

Potentiometric measurements were conducted with a line-powered Analogic (#AN2546) voltmeter with a range of  $\pm 2$  volts and a stability of  $\pm 0.1$  mV. The voltmeter was connected to the sensing electrode via a high impedance buffer built locally in the Chemistry Department electronics shop. The sensing electrode was an Orion (93-20) calcium ion-selective electrode with an Orion (90-01) single junction reference electrode. The normal lifetime of the calcium ion-selective electrode (ISE) is approximately 6 months due to the deterioration of the membrane ion-exchanger. Normal symptoms of a deteriorating electrode were unstable readings and a decreasing calibration slope. It was also necessary to monitor the pH of all solutions, which led to the use of a Beckman Expanded Scale pH meter and an Orion (91-05) combination electrode.

Silver complexation studies were conducted using a silver wire electrode. This electrode was pretreated in nitric acid to roughen the surface. A calibration curve yielded a slope of  $63.3 \pm 0.6$  mV per decade change in the concentration of  $\text{AgNO}_3$ , which is close to the theoretical slope of 59.2 mV expected for a reversible system. It was then concluded that this silver wire electrode exhibited Nernstian behavior and was suitable as a specific ion electrode. The counter-electrode was the single

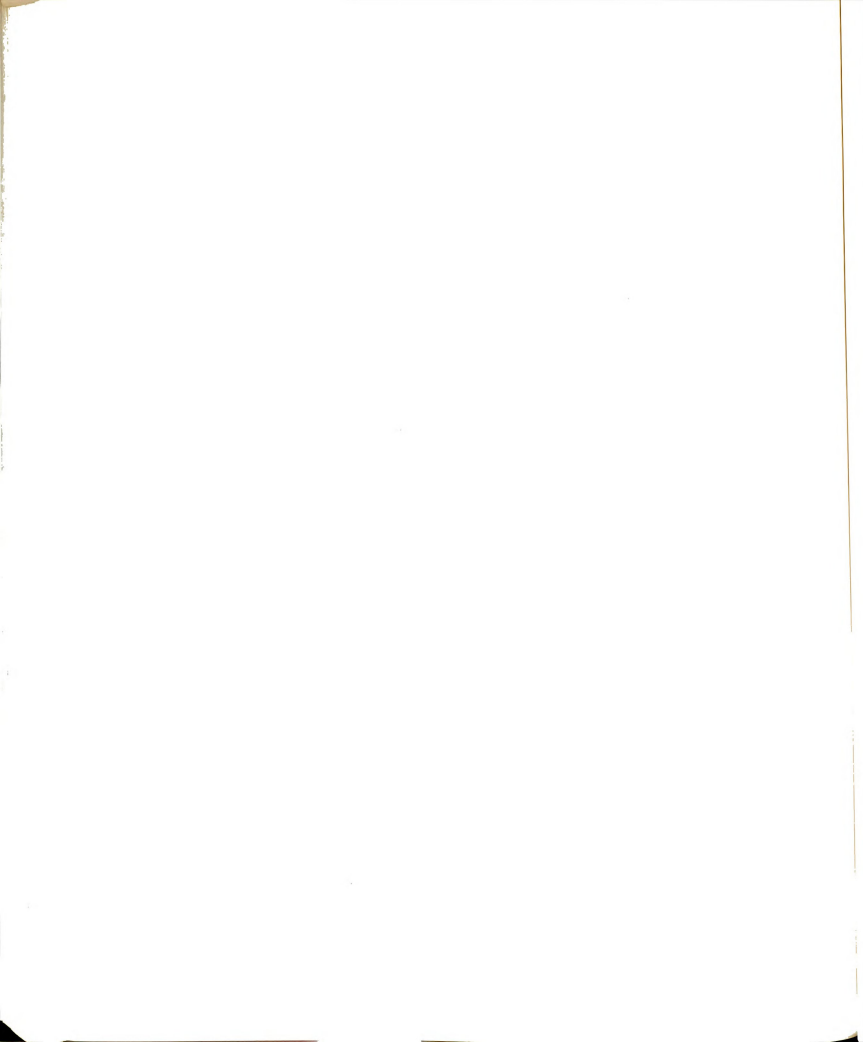


junction reference mentioned above.

Titrations were carried out using the cell shown in Figure 26. The temperature was maintained by circulating water through the outer jacket, with a degassing of the solution also possible through the inlet arm. A Teflon cap was used to enclose the cell, cutting down the solution evaporation. Stirring was accomplished with an air-driven magnetic stirrer. The entire apparatus was enclosed in a Faraday cage to reduce the "noise" detected by the voltmeter. The "noise" is random fluctuations in the observed potential due to static charges built up on the equipment (and operator) and 60 cycle line noise from house voltage sources. The fluctuations were on the order of 80 mV outside the cage and  $\pm 0.1$  mV in the Faraday cage. The use of the coulometric equipment (described in the next section) in a pH stat mode caused major fluctuations in the voltage readings from the pH and Ca ISE when a current was passed through solution. The coulometric cables themselves (due to leakage from the current source) were also a source of noise, even though the current was not switched on. Hence, whenever voltage readings were made (pH and calcium ISE) the coulometric cables were isolated by grounding them.

Thermal equilibrium was established initially by waiting 20 minutes prior to the first measurement. Upon additions of titrant, the solution pH was coulometrically





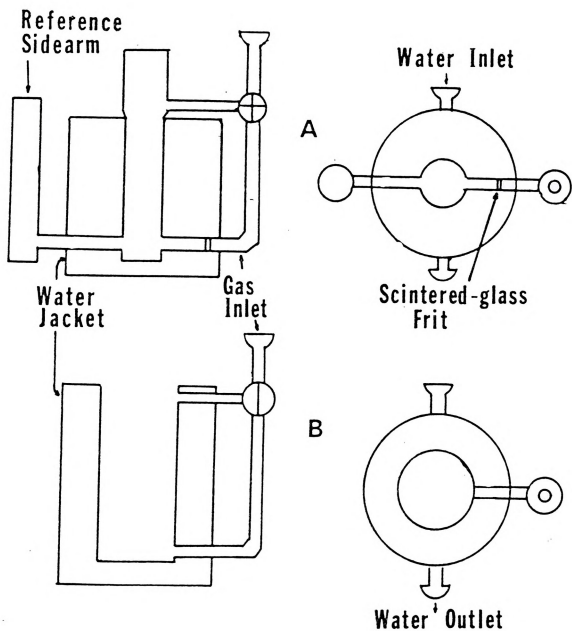
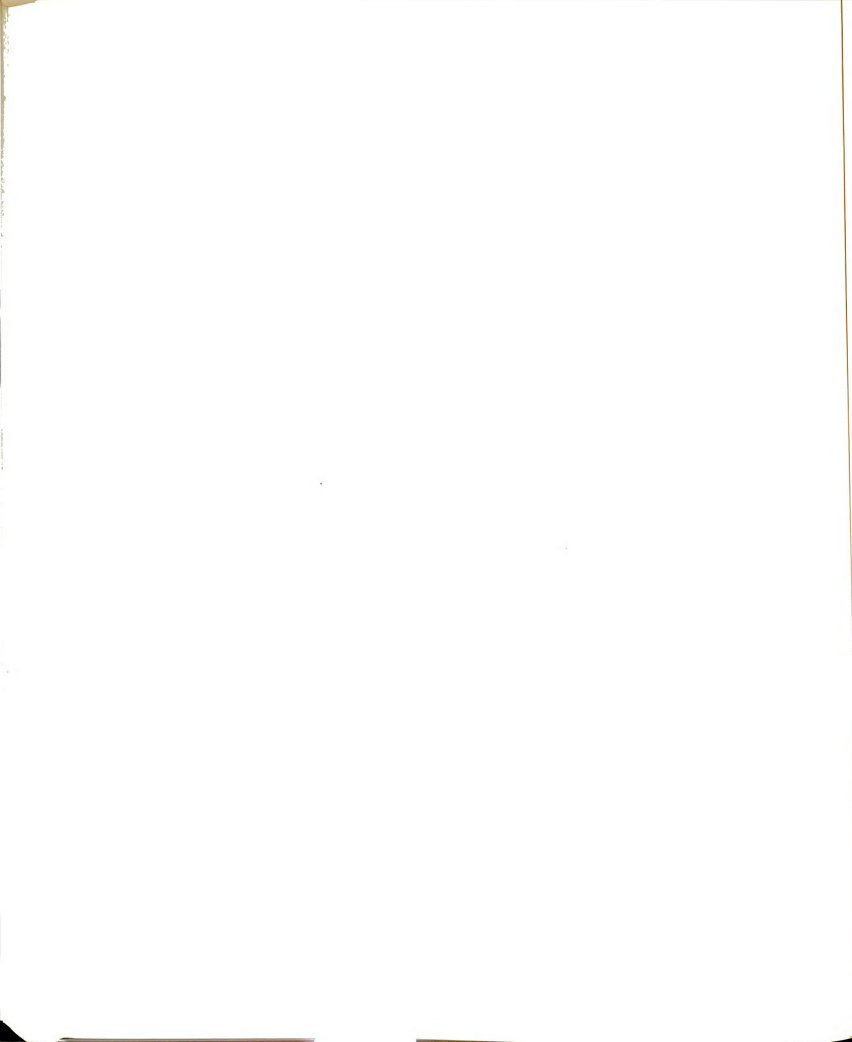


Figure 26. A schematic representation of the pyrex glass cells used for A - cyclic voltammetric studies, and B - potentiometric studies.

adjusted/maintained (approximately two minutes), the solution allowed to mix and equilibrate (two minutes), and the emf was observed and averaged over 30 seconds. The total time associated with one titration point was then approximately five minutes. At least 30 points were taken to form a calibration curve, and 30 points for the titration curve.

#### 2.2.4. Coulometer

The pH of the solution was recorded at the same time the calcium ISE emf was recorded. The pH was maintained at a constant value by the coulometric generation of protons or hydroxide ions. The coulometric electrodes consisted of a platinum rectangle ( $\sqrt{17 \times 10}$  mm) anode and a platinum grid ( $\sqrt{30}$  mm in length, 32 mm in diameter) as the cathode. A 12 mm OD glass tube, 15 cm in length, acted as the anodic compartment. The end of the tube in contact with the solution was closed off by an anion transfer membrane which was held in place with an "O" ring and Teflon cap (158). The anion transfer membrane was impermeable to the solvent, but allowed the passage of the supporting electrolyte. The electrodes were cleaned prior to usage by immersion in 6 M  $\text{HNO}_3$  with a current passed through the electrodes for 60 seconds using first one, then the other electrode, as the cathode.



The electronics of the coulometer have been mentioned previously (158) and will not be dealt with here. The use of this equipment by Heubel (158) was for the generation of hydroxide ions as a titrant for determinations of the  $pK_a$ 's of PAA. The use of the equipment to adjust and maintain the pH at a constant value required less stringent demands in performance, with the conclusion that this equipment is more than adequate for this study.

### 2.3. Sample Preparation

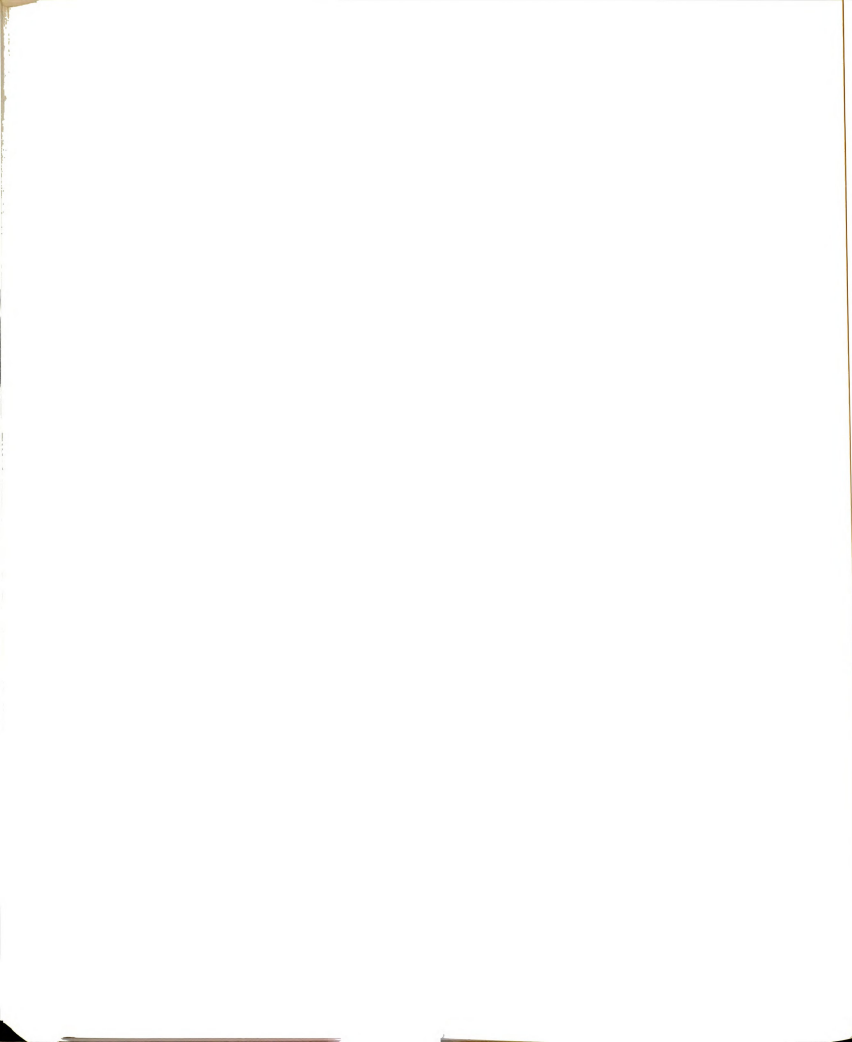
#### 2.3.1. Manganese Electron Spin Resonance

A calibration curve of resonance line intensity vs concentration in the range of  $10^{-3}$  -  $10^{-6}$  M was prepared by dilution of stock solutions of  $MnCl_2$  and measuring the intensity of the resonance lines. The effect of a tris buffer at a pH of 8 and the supporting electrolyte tetraethylammonium perchlorate on the manganese resonance were then tested, with no change in linewidth or decrease in the intensity of the manganese signal resulting. Complexation studies were then performed at a pH of 8 and 4.5 (adjusted with tetramethylammonium hydroxide) at various ionic strengths. The manganese chloride concentration was approximately  $10^{-3}$  M; the ligand concentration was varied. In the case of strong complexation ( $\log K_f > 4$ ) the mole ratio of ligand-to-manganese varied from 0 to 1.

With weak complexes ( $\log K_f < 4$ ), the mole ratio was increased to a maximum of 5:1 and when no complexation was evident, the mole ratio covered the range from 0 to 10.

Since the manganese ion can be oxidized in basic solutions by dissolved oxygen (184) (although the rate is slow), the solutions were degassed prior to the measurements of the ESR intensity. A comparison of these results to those obtained when solutions were not degassed showed no significant difference in the data sets within the experimental error. The conclusion is that over the course of a single experiment, approximately 3 hours, the oxidation of manganese proceeds at a negligible rate.

The intensity of an ESR resonance due to the aquo manganese complex was obtained by measuring the peak-to-peak (minimum to maximum) height of the fourth peak from the low field for a first derivative plot of magnetic field vs absorption and dividing by the receiver gain of the instrument. The error associated with one measurement, which is composed of solution preparation errors, sample placement errors, sample fill factor errors, the change in the cavity resonance with a change in sample, instrumental errors, etc., is estimated by repetitive measurement to be 4% of the intensity.



### 2.3.2. Cyclic Voltammetry

Stock solutions of the metal ion and the ligand were used to prepare solutions of varying concentration. The metal ion concentration was on the order of 0.1 - 0.05 mM, and the ligand concentrations was held in excess by a factor of 2 to 50 times the metal ion concentration to satisfy the restrictions of the Lingane and Buck equations. The ionic strength was maintained with TEAP, while the pH was monitored and adjusted with either tetramethylammonium hydroxide or perchloric acid. The alkylammonium cation tends to adsorb on the mercury surface of the HMDE. This creates a positive sheath in the double layer of the electrode which tends to repel the positive metal ions. The net effect of this adsorption is to slow electrode kinetics such that some reactions appear irreversible. For those reactions where this is not a problem, TEAP was used because of its lack of complexation properties. When the TEAP was found to cause irreversible behavior, the supporting electrolyte chosen was then  $\text{LiClO}_4$ . It is doubtful that the lithium ion would form a complex with the ligand, as it is very small and highly solvated.

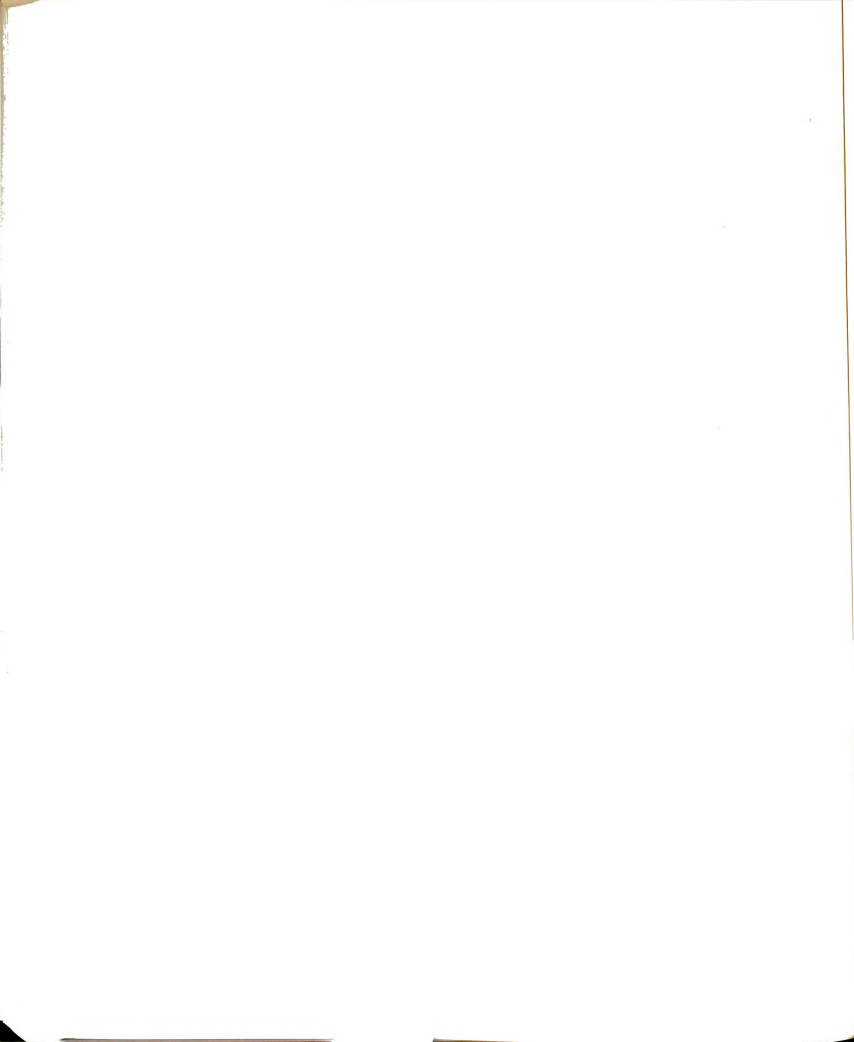
In cases where metal ions exhibited irreversible behavior even in  $\text{LiClO}_4$  solutions, the double layer was altered using para-toluene sulfonate (185). The para-toluene sulfonate (PTS) adsorbs on the mercury surface much as the alkyl ammonium ion does, except that in this



case the ion is negatively charged. The double layer is then negatively charged, with the positive metal ions attracted to it. This increases the rate of charge transfer to produce reversible behavior. In all cases, with TEAP, PTS,  $\text{LiClO}_4$ , tetramethyl ammonium hydroxide, and perchloric acid, there was no shift in the half-wave potential of the metal ion upon addition of these species. This implies that these species are inert with respect to complexation with the metal ion, as well as implying no alteration in the charge transfer kinetics of the electrode reaction.

### 2.3.3. Potentiometry

The potentiometric cell initially contained 25 ml of supporting electrolyte solution, to which was added 0.05 ml of 0.01 M  $\text{CaCl}_2$  from a precision buret. Thermal equilibrium was established, the emf recorded, and the next increment of the calcium solution was added as described in Section 2.2.3. The procedure was continued a total of 4 ml of calcium solution was added. The calibration range of emf vs calcium ion concentration was approximately  $10^{-5}$  to  $10^{-3}$  M. The metal ion was then titrated with the ligand (approximately 0.005 M) following the procedure of Section 2.2.3. The titration was stopped when the ligand to metal ion ratio was approximately two. In

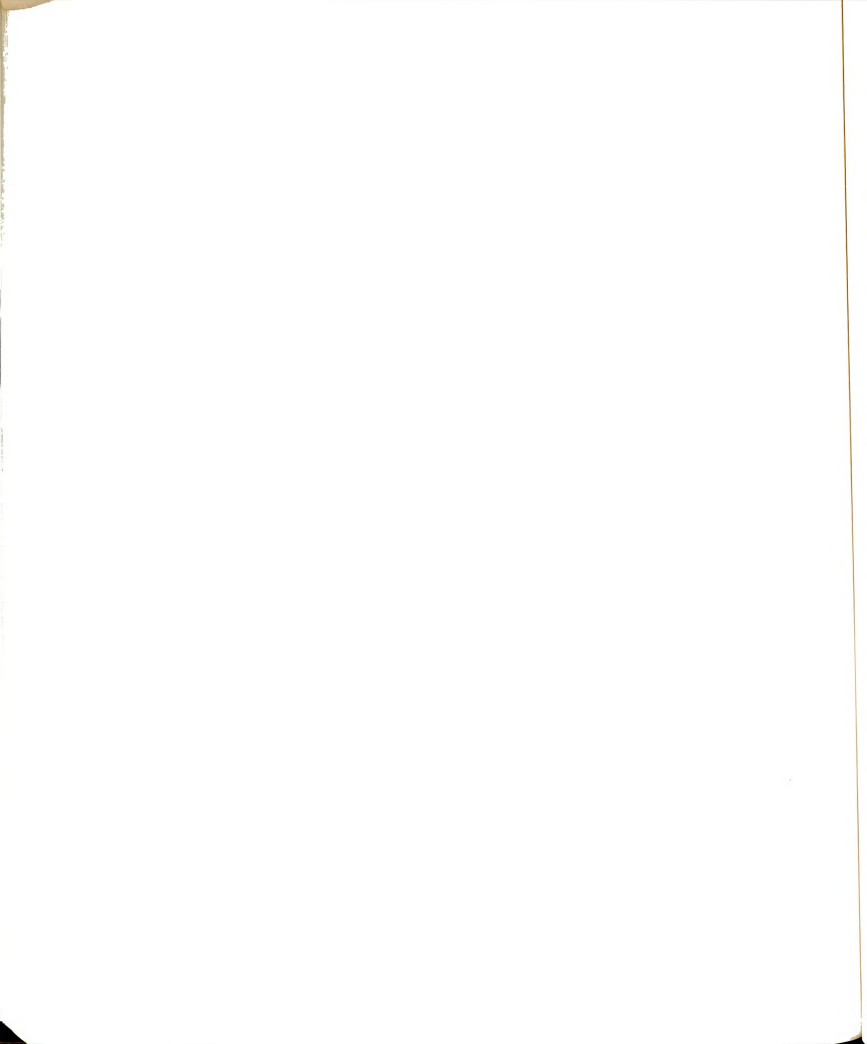


this manner, changes in the liquid junction potential were minimized.

The volume correction for solution expansion or contraction (186) when the system was studied at temperatures other than 25°C was found to have a negligible effect on the calculated free calcium ion concentration.

The supporting electrolyte chosen was KCl. Tetraalkyl ammonium ions tended to interfere with the measured emf due to interactions with the organic membrane of the calcium ISE, leading to somewhat large errors in the calculated formation constant. Perchlorate ions also interfere due to their penetration into the organic membrane. Potassium chloride is the recommended supporting electrolyte for use with a calcium ISE (187), even though it may potentially compete with the calcium ion for the ligand. A comparison of the results using tetramethylammonium chloride and KCl, however, showed that these values agreed within the experimental error of the KCl data. These results suggest that a competition between calcium and potassium ions for the ligand is small or negligible.

Conductance water obtained from the laboratory of Dr. Weaver was used in most cases. Some experiments were conducted using water distilled from  $2 \times 10^{-2}$  M  $\text{KMnO}_4$  and  $2 \times 10^{-2}$  M KOH. When calibration curve results using conductance water and permanganate distilled water were compared to house distilled water, the house distilled



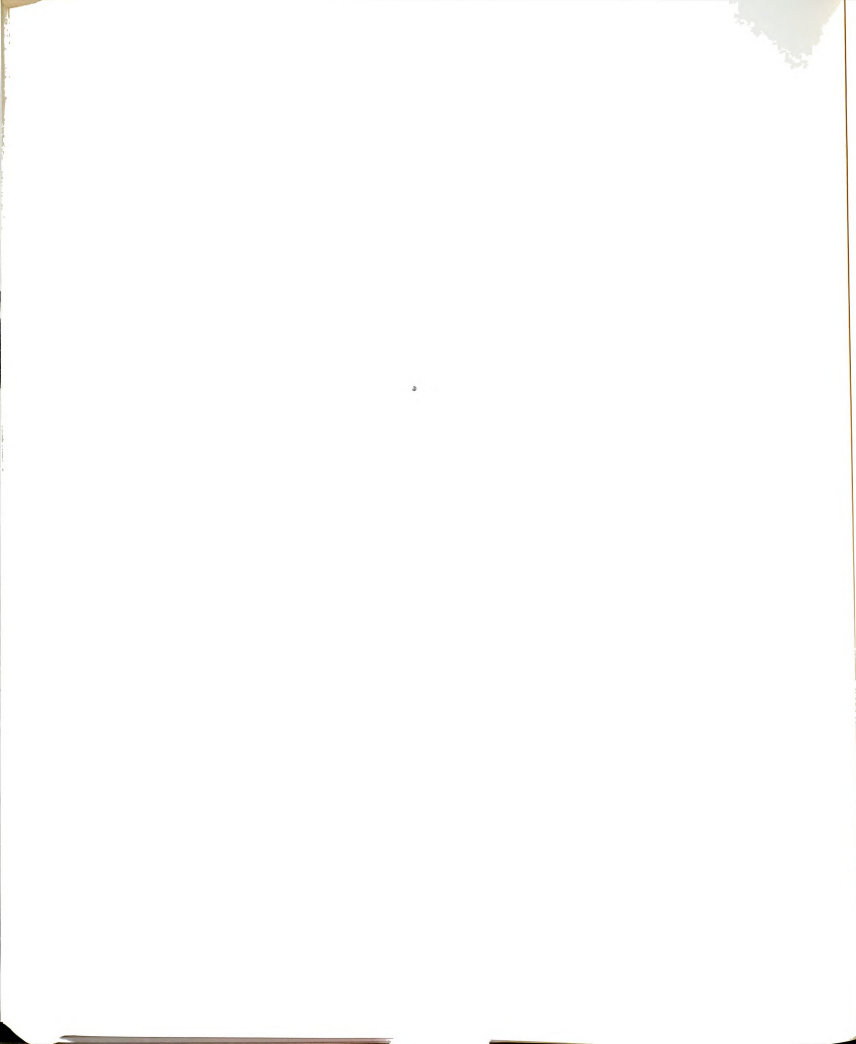
water was found to contain residual calcium on the order of  $10^{-6}$  -  $10^{-7}$  M. Since the typical free calcium concentration in complexation studies ranges from  $10^{-3}$  to  $10^{-4}$  M, this represents at worst an error of 1%. The use of conductance water is recommended to minimize this source of error.

The contribution to the ionic strength from ions other than the supporting electrolyte will cause an error of 5% (worst case with  $I_{KCl} = 0.02$ ) in the total ionic strength. During the course of a single experiment, however, the ionic strength will vary as the concentration of ions in solution changes by less than 1%. The total ionic strength may then be corrected for the complexation reaction by summing the ionic strength due to the supporting electrolyte and the average ionic strength due to all other species in solution (as measured over the course of the experiment).

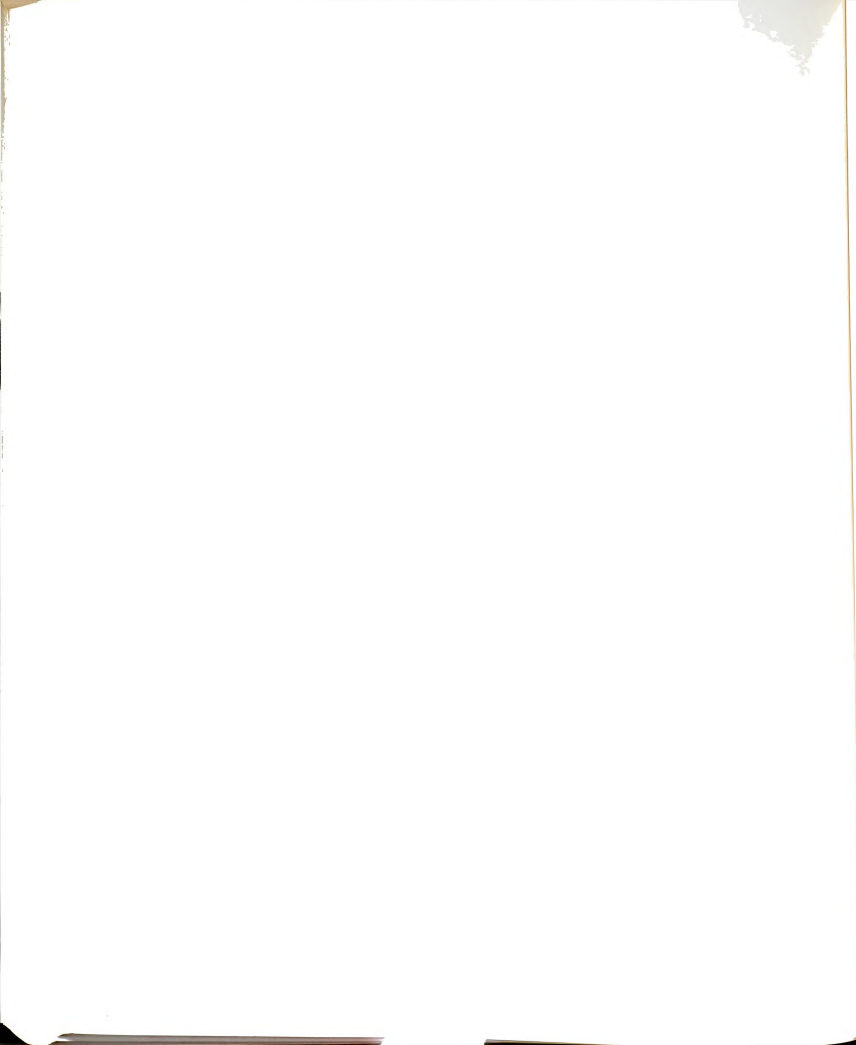
The use of the term "constant ionic strength", then, while not strictly valid, is a good approximation.

#### 2.4. Data Handling

The computer program KINFIT4 (38) was used to fit the calcium ISE calibration curve data. This is a general purpose non-linear curve fitting routine. The calibration data were then fed to the program MINIQAD (188) which calculated the complexation formation constants for the



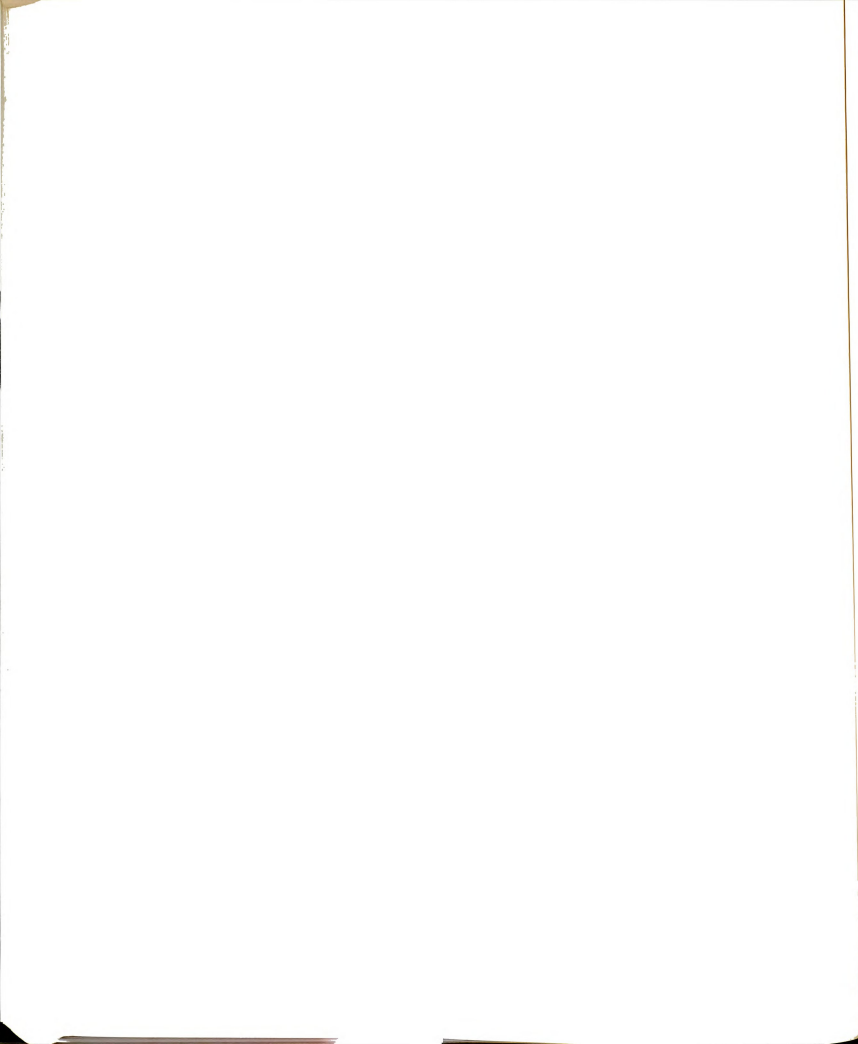
deprotonated ligands with the calcium ion. When mono-protonated ligands were studied, the calibration data were given to the computer program shown in Appendix C, which then calculated the formation constants for these complexes with the calcium ion. Cyclic voltammetry,  $\Delta G_{25^\circ\text{C}}^\circ$ ,  $\Delta H^\circ$ , and  $\Delta S^\circ$  data were processed using KINFIT4.





CHAPTER III

RESULTS AND DISCUSSION

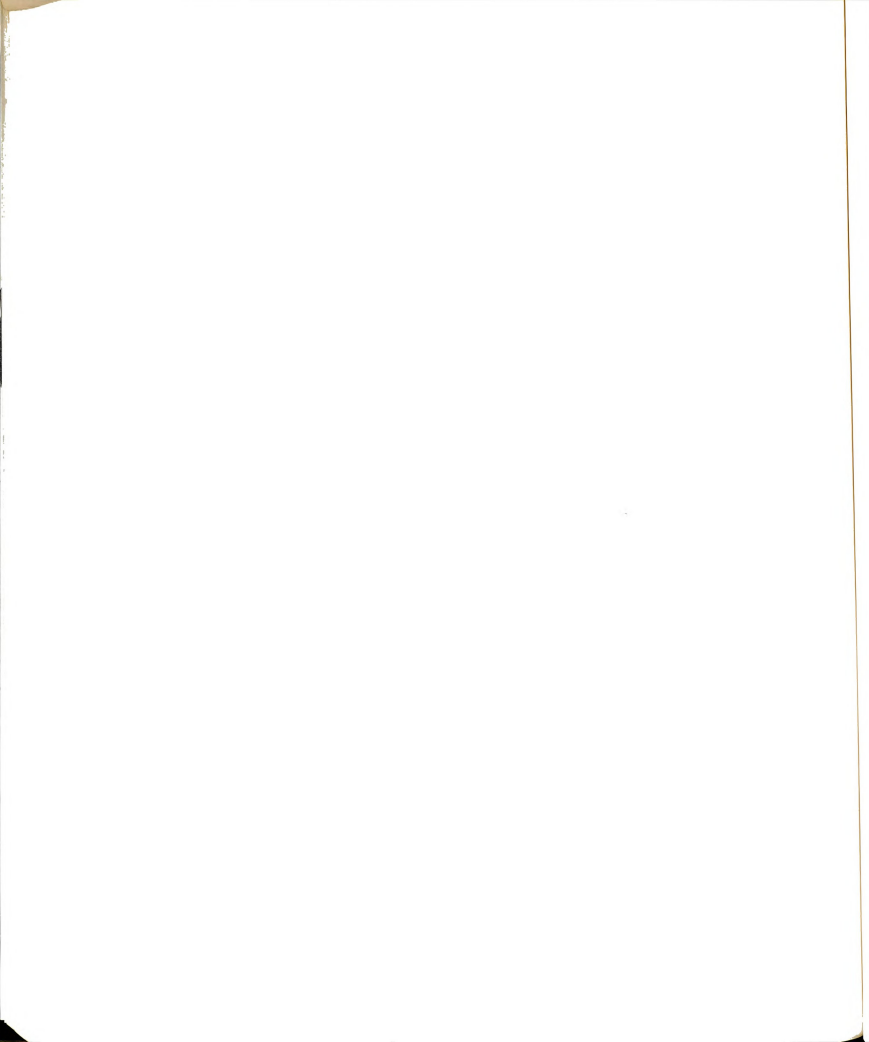


### 3.1. Complexation Studies of PAA

#### 3.1.1. Manganese Electron Spin Resonance

A calibration curve of the ESR resonance intensity vs  $Mn^{2+}$  concentration, resulting from 67 measurements, is shown in Figure 27. The data were computer fitted to obtain a slope of  $3.04 \pm 0.02 \times 10^6$  and an intercept of  $0.53 \pm 0.03$ . These values were used to determine the concentration of free manganese(II) ions upon the addition of PAA. No effect of the supporting electrolyte or the tris buffer on the intensity of the observed manganese ion resonance was found.

Prior to studies of the manganese-PAA system, the general applicability of this technique to the investigation of aqueous solution complexation was tested. It was desired to determine the formation constant of a manganese complex with a ligand that was both similar to PAA and well studied. The manganese citrate complex fulfilled these objectives very well. Citric acid is a triprotic acid (as is PAA) with successive  $pK$ 's (negative log of the protonation constant) of  $pK_3 = 5.78$ ,  $pK_2 = 4.32$ , and  $pK_1 = 2.89$  (63). The low value of  $pK_3$  allows the study of the deprotonated citrate at a pH of  $\sim 8$ . However, the



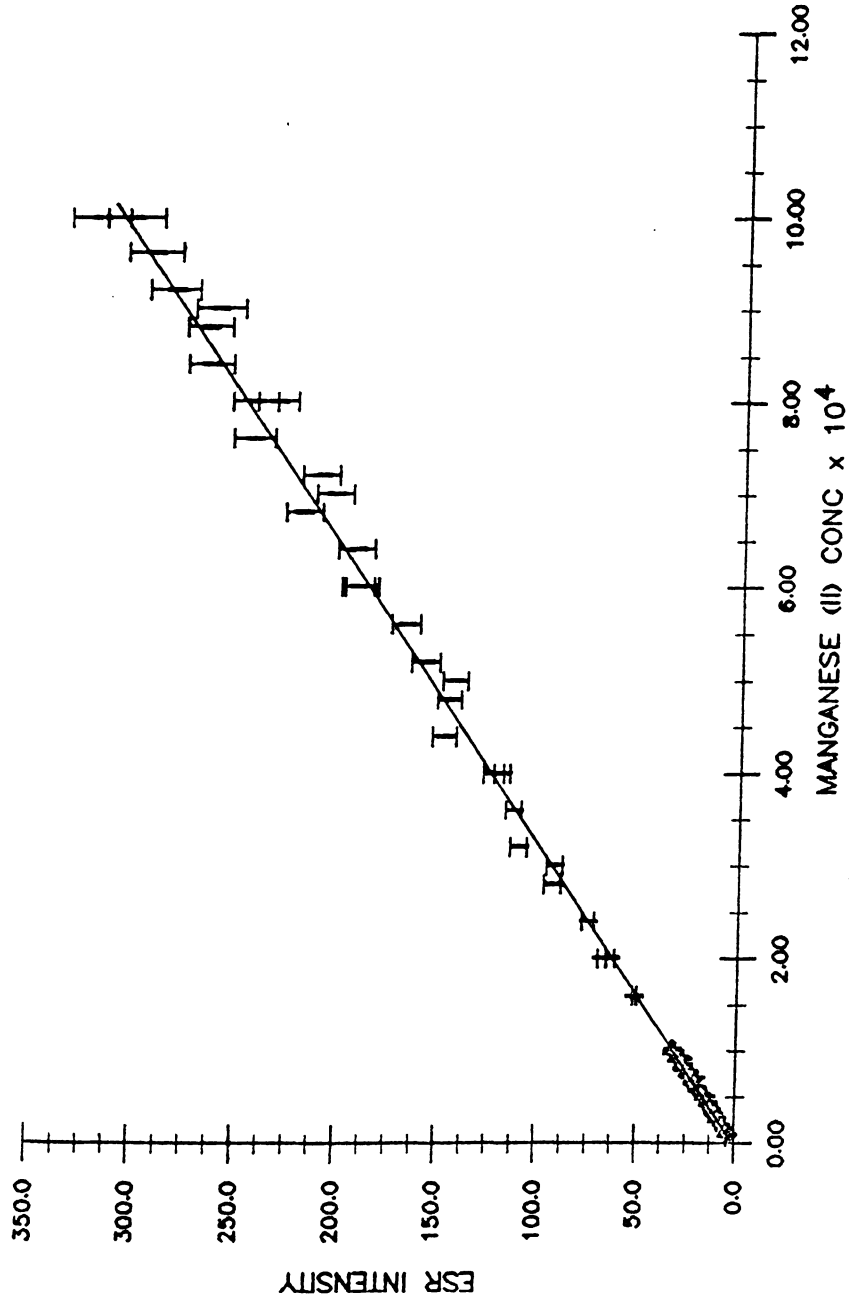
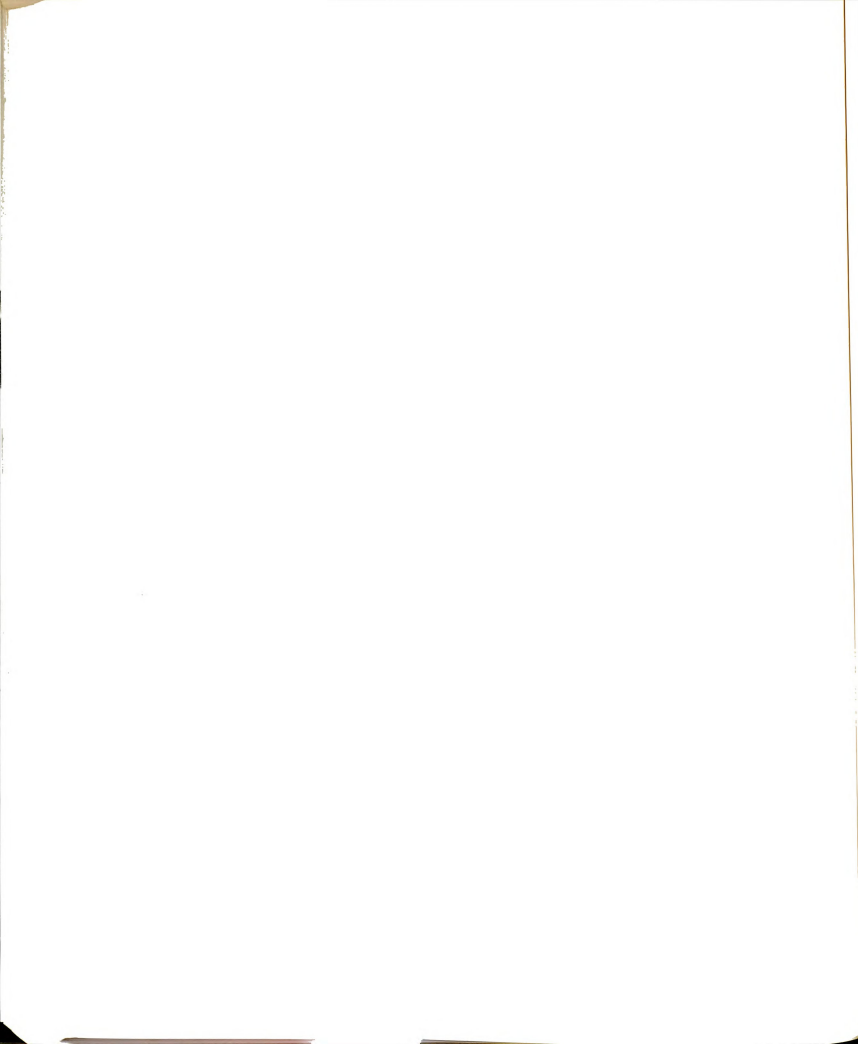


Figure 27. A calibration plot of the observed ESR intensity as a function of  $\text{MnCl}_2$  concentration.



similarity in  $pK_3$  and  $pK_2$  render the determination of a monoprotinated complex with manganese subject to a large degree of error. Therefore, only the deprotonated complex with manganese was studied.

The results, along with values obtained from the literature, are shown in Table XXXIII. The manganese-citrate formation constant was determined using both TEAP and tetramethylammonium chloride (TMAC). The ion-pair formation constant for manganese chloride was found to be 3.7 from pH studies by Grzybowski et al (189). With the exception of reference d, all previous citric acid-manganese (II) ion studies were conducted using chlorides as the supporting electrolyte. A formation constant was determined with TMAC as the "inert" electrolyte so as to compare our results with the above values, while a formation constant using TEAP was compared to the data of Grzybowski et al. (189). The values agree well when the difference in ionic strength of the two solutions are taken into account. The data of Grzybowski et al (189) are considered to be the most accurate, since ion-pairing and manganese hydroxide formation were considered. Our work agrees with that of Grzybowski et al. (189) to 0.09 log K units when corrected to an ionic strength of 0.1 using the Debye-Hückel equation.

The value obtained using TMAC is within the range (a rather broad range) of the other literature values. As

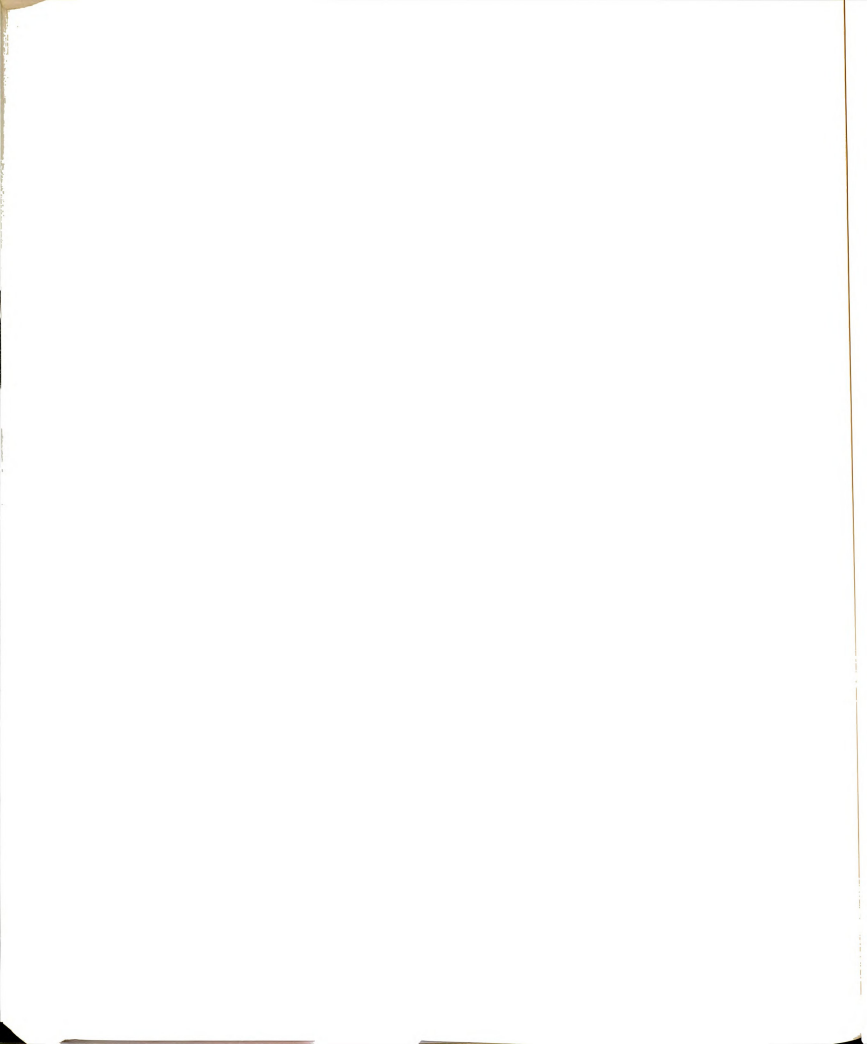




Table XXXIII. Formation Constants of a Deprotonated Manganese-Citrate Complex.

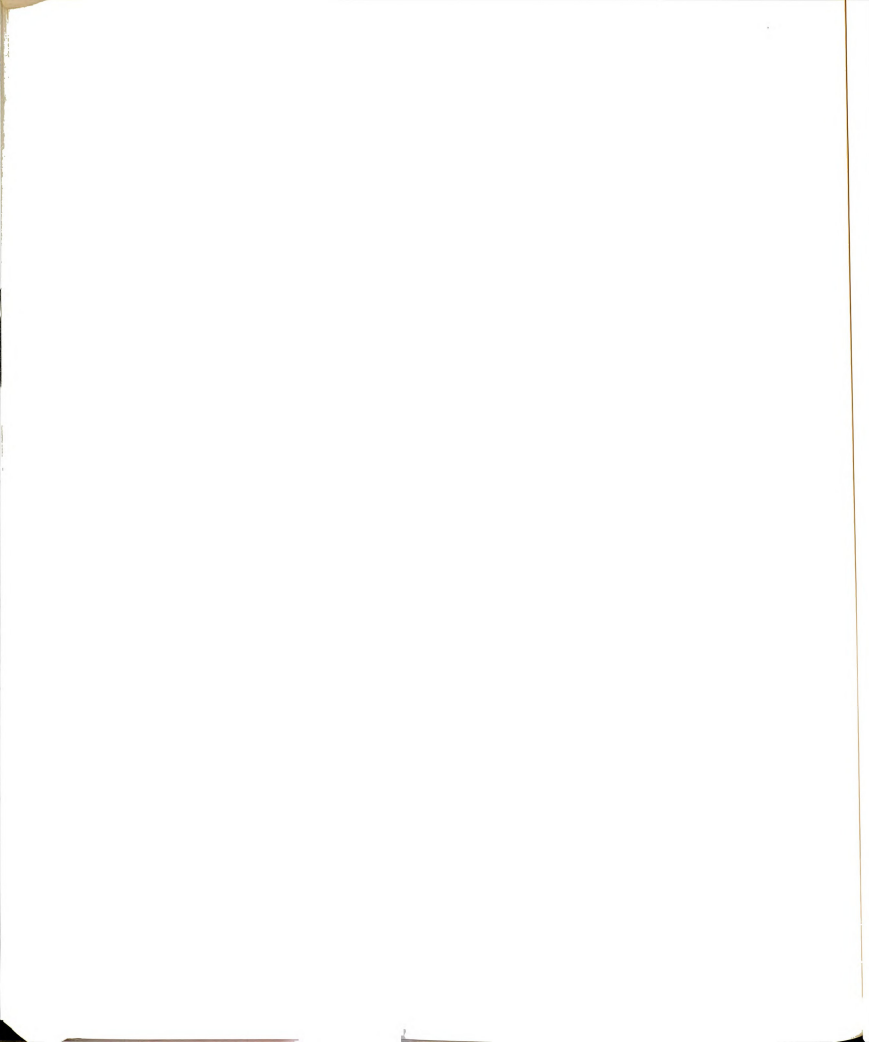
log K	Supporting Electrolyte	Method	Ref.
3.6	KCl	Potentiometry (pH) and visible spectroscopy (competition)	a
3.69	NaCl	Radio isotope ion-exchange	b
3.83	NaCl	Radio isotope ion-exchange	c
3.74±0.03	(Me) <sub>4</sub> NCl	Mn ESR	this work
4.28±0.04	(Me) <sub>4</sub> NClO <sub>4</sub>	Mn ESR	this work
4.15±0.02	(Me) <sub>4</sub> NCl	Potentiometry (pH)	d

<sup>a</sup>I. E. Kalinichenko, Ukrain. khim. Zhur., 36, 92 (1970).

<sup>b</sup>N. C. Li, A. Lindenbaum, J. M. White, J. Inorg. Nucl. Chem., 12, 122 (1959).

<sup>c</sup>J. S. Wiberg, Arch. Biochem. Biophys., 73, 337 (1958).

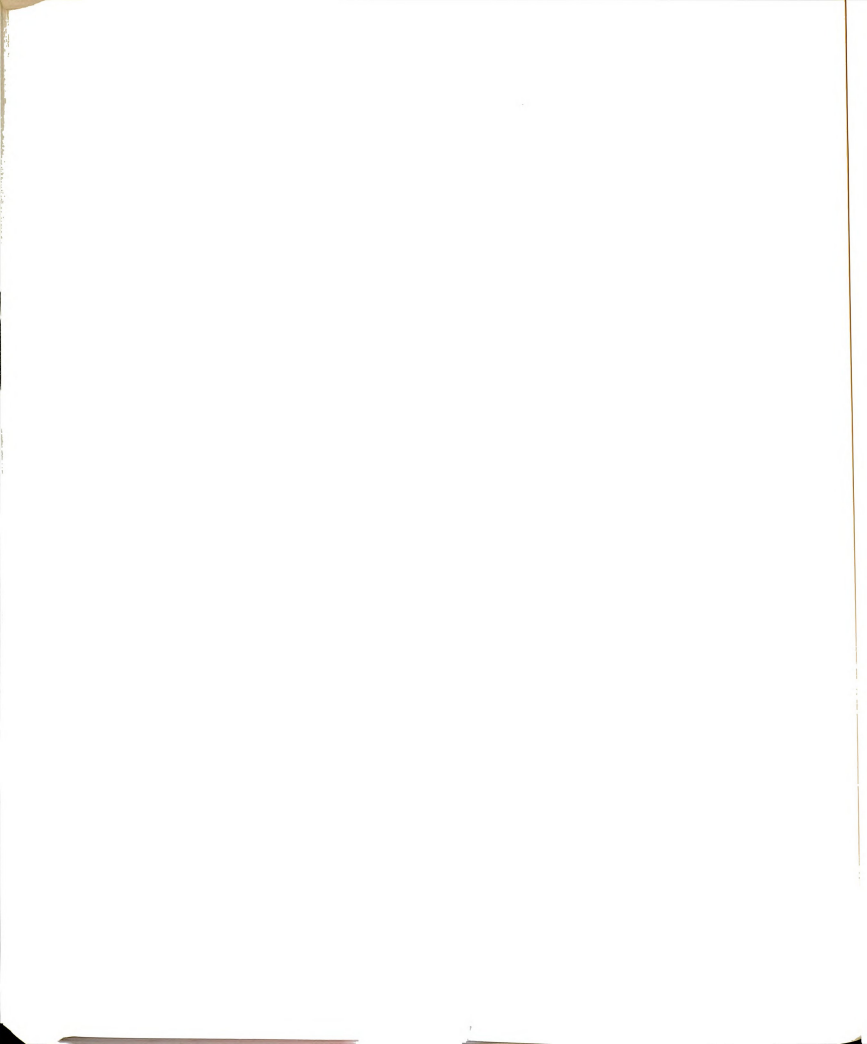
<sup>d</sup>A. K. Grzybowski, S. S. Tate, S. P. Data, J. Chem. Soc. (A), 241 (1970).

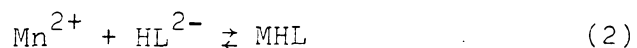
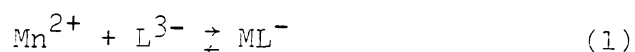


a test of self-consistency, the formation constant of the manganese citrate complex using TMAC as a supporting electrolyte was corrected for the formation of the  $\text{MnCl}^+$  ion-pair using the ion-pair formation constant of Grzybowski *et al.* (189). This calculated formation constant agrees with the value obtained using TEAP as a supporting electrolyte to within 0.04 log K units. Therefore, the technique is at least self-consistent under different experimental conditions. This self consistency, together with the agreement between literature values and those obtained in this study, was considered sufficient evidence to indicate the validity of this technique in determining manganese formation constants.

In all of the complexation studies it was important to establish that the signal intensity is due only to the free manganese(II) ion. That is, there is no contribution to the observed intensity from the complex. When an excess of ligand was added so that manganese is almost entirely complexed, the resulting intensity was due only to the residual free manganese(II) ion. There was no evidence for a contribution from the complexed manganese ion resonance to the observed free manganese ion resonance.

The manganese(II) ion can complex with both the deprotonated and monoprotinated forms of PAA (as shown by Heubel (29)) according to the equilibria

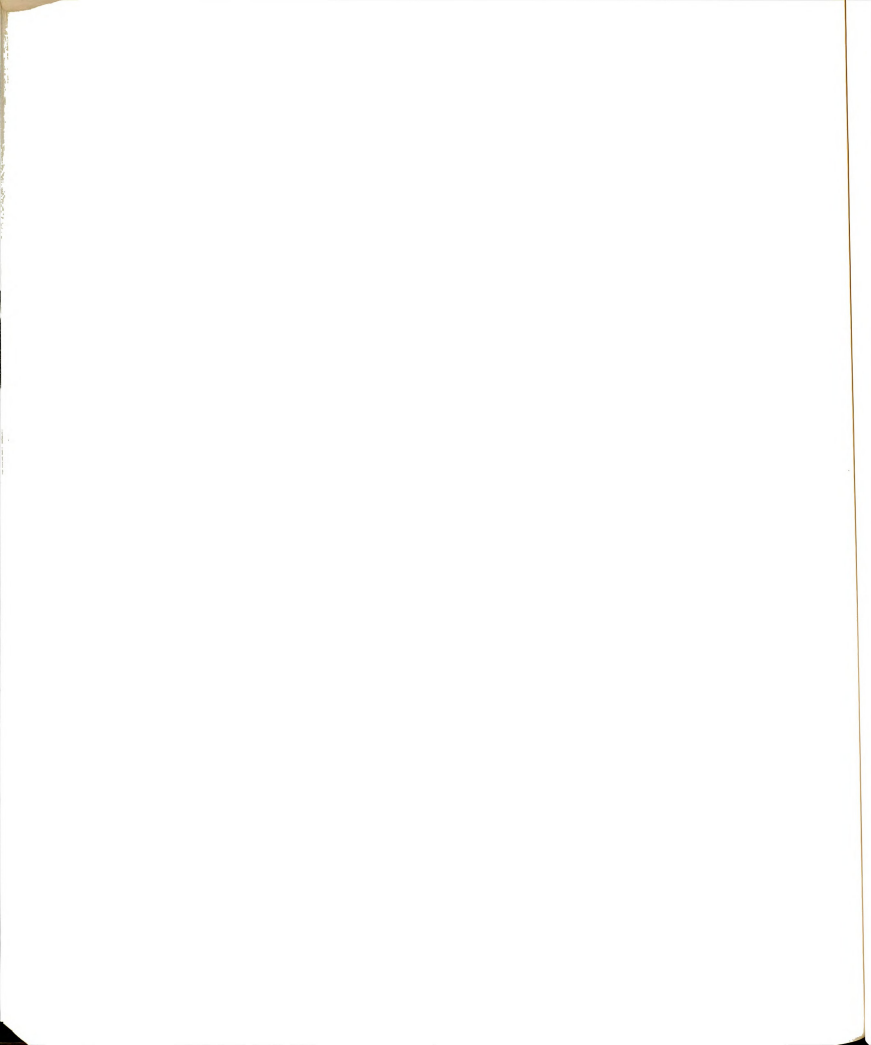




where  $\text{L}^{3-}$  and  $\text{HL}^{2-}$  represent the deprotonated and mono-protonated forms of PAA. The ligand is a triprotic acid and undergoes the following equilibria



The thermodynamic values for the negative log of the acidity constants are:  $\text{pK}_3 = 8.69 \pm 0.05$ ,  $\text{pK}_2 = 5.11 \pm 0.04$ ,  $\text{pK}_1 = 2.0$  (158). The values at a given ionic strength were calculated using the Guntelburg (128) equation. Clearly, the complexation of  $\text{Mn}^{2+}$  ion with PAA is pH dependent, with equilibrium (1) dominating at high pH and equilibrium (2) dominating in a pH range of 3.5 - 4.5. The contribution of equilibrium (2) to the overall complexation is small (<1%) at the experimental pH of  $\sim 8$ . From the pH and manganese ESR intensity data (which was used to calculate the free  $\text{Mn}^{2+}$  concentration) at pH of  $\sim 8$ , the formation constant for equilibrium (1) was calculated. Equilibrium (2) was



then studied at a pH of 4.0, where equilibrium (1) had a small but still significant contribution. The formation constant was calculated for equilibrium (2) from pH and ESR data, correcting for equilibrium (1) using the previously determined formation constant.

The constant for the deprotonated complex can then be refined by incorporating the value for the monoprotated ligand. The cycle is iterative, although convergence is attained in one or two iterations, since the monoprotated equilibria is almost negligible at higher pH's. There is no evidence for other complexation equilibria occurring in solution.

The concentration formation constant for equilibrium (1) is given by

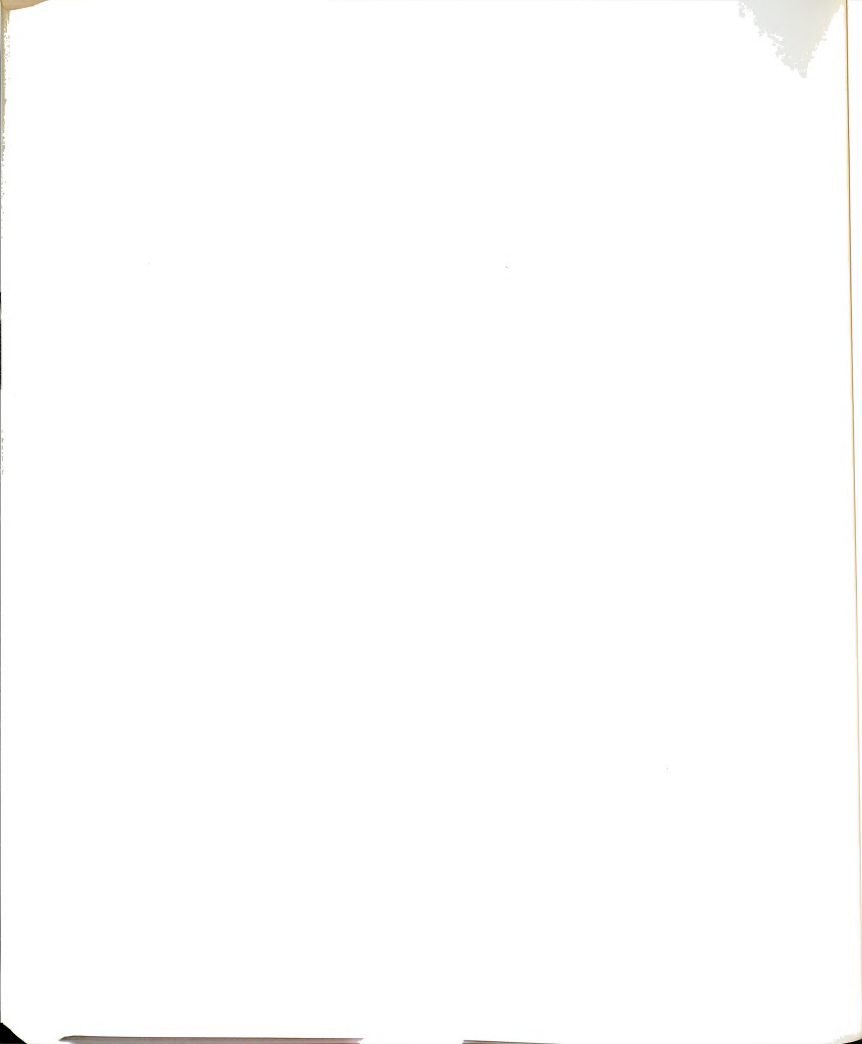
$$K_{cd} = [\text{MnL}^-] / [\text{Mn}^{2+}][\text{L}^{3-}] \quad (6)$$

while the relationship between the concentration formation constant,  $K_c$ , and the thermodynamic formation constant,  $K_t$ , is

$$K_{td} = K_{cd} \gamma_{\text{ML}^-} / \gamma_{\text{Mn}^{2+}} \gamma_{\text{L}^{3-}} \quad (7)$$

Using the Debye-Hückel equation

$$\log \gamma_i = - A z_i^2 \sqrt{I} / (1 + B a_i \sqrt{I}) \quad (8)$$





where

$$A = 1.823 \times 10^6 / (\epsilon T)^{3/2} \quad (9)$$

and

$$B = 50.3(\epsilon T)^{-1/2}$$

Equation (7) may be rewritten as

$$\log K_{cd} = \log K_{td} + (Z_{MnL}^2 - Z_{Mn2+}^2 - Z_{PAA3-}^2)\sqrt{I}/(1+B\alpha\sqrt{I}) \quad (10)$$

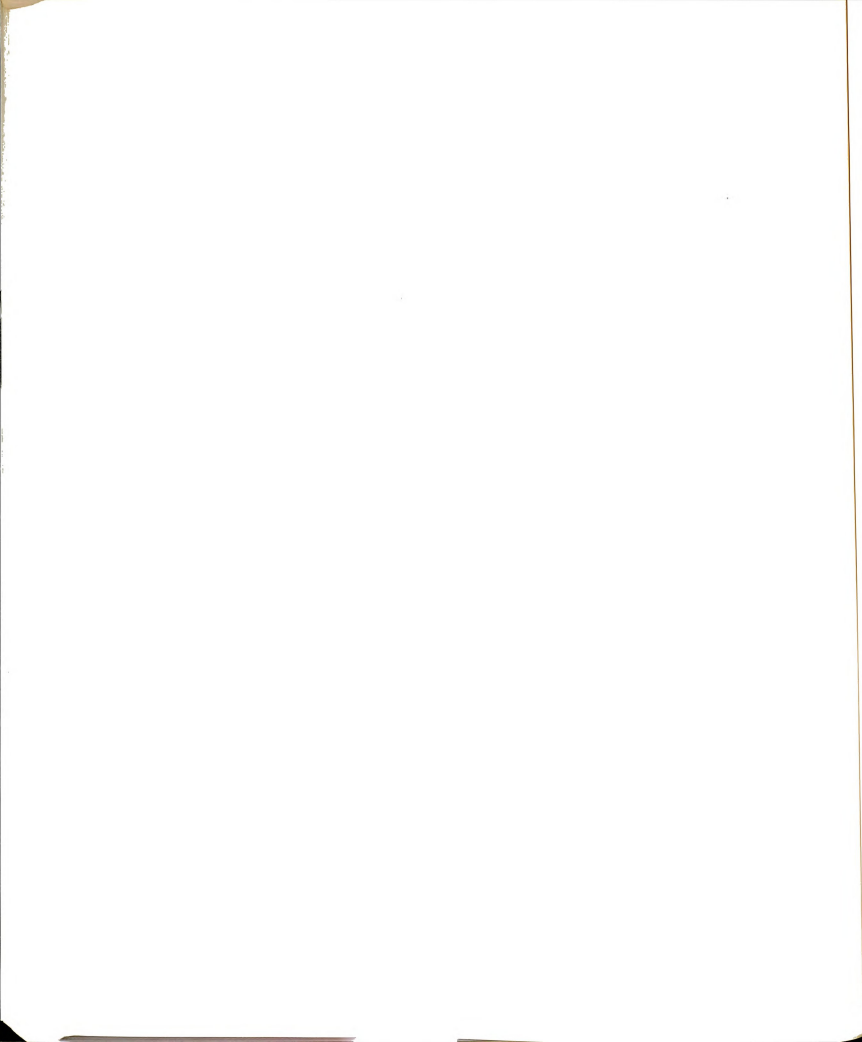
or

$$\log K_{cd} = \log K_{td} - 12A\sqrt{I}/(1+B\alpha\sqrt{I}) \quad (11)$$

where at 25° in aqueous solution,  $B = 0.328 \times 10^7 \text{ M}^{-1}$ ,  $A = 0.510$ , and  $\alpha$  is an adjustable parameter which is considered to be the solvated radius of the metal ion (190, 191). Similarly, the thermodynamic formation constant for equilibrium (2) is,

$$\log K_{cm} = \log K_{tm} = 8A\sqrt{I}/(1+B\alpha\sqrt{I}) \quad (12)$$

The Debye-Hückel equation is generally considered to be valid to approximately 0.1  $M$  ionic strength, which led to



the use of ionic strengths equal to or lower than this value. The presence of other ions in solution, e.g.,  $Mn^{2+}$ ,  $MnL^-$ ,  $L^{3-}$ , contributed to the ionic strength to the extent of about a 7% error at  $I = 0.03$ . During the course of a single experiment, the change in ionic strength with a change in ligand concentration was approximately 3%. The former may be corrected for, while the latter is inherent to the method. These considerations set a lower limit of 0.03 for the ionic strength.

The formation constants for the manganese-PAA complex were determined at seven different ionic strengths. The data are listed in Table XXXIV while the plot of  $\log K$  as a function of the ionic strength is shown in Figure 28. The theoretical slopes for the deprotonated and monoprotated complexes at 25°C are -6.11 and -4.07, respectively. The data were fitted to Equations (11) and (12) using these slopes, with  $K_t$  and  $\underline{a}$  as the unknowns. This resulted in the average  $\underline{a}$  of  $6 \pm 2 \text{ \AA}$  for the complexes. While the error is large, this value for  $\underline{a}$  is comparable to the values of  $6 \text{ \AA}$  estimated by Kielland (191) and  $4.7 \text{ \AA}$  determined by Stokes (190). The  $\log K_t$  values for the mono- and deprotonated complexes were found to be  $3.5 \pm 0.2$  and  $6.3 \pm 0.1$ , respectively.

The errors of 0.1 and 0.2 pK units are larger than those normally attained from potentiometric measurements, although they are on the order of the experimental error

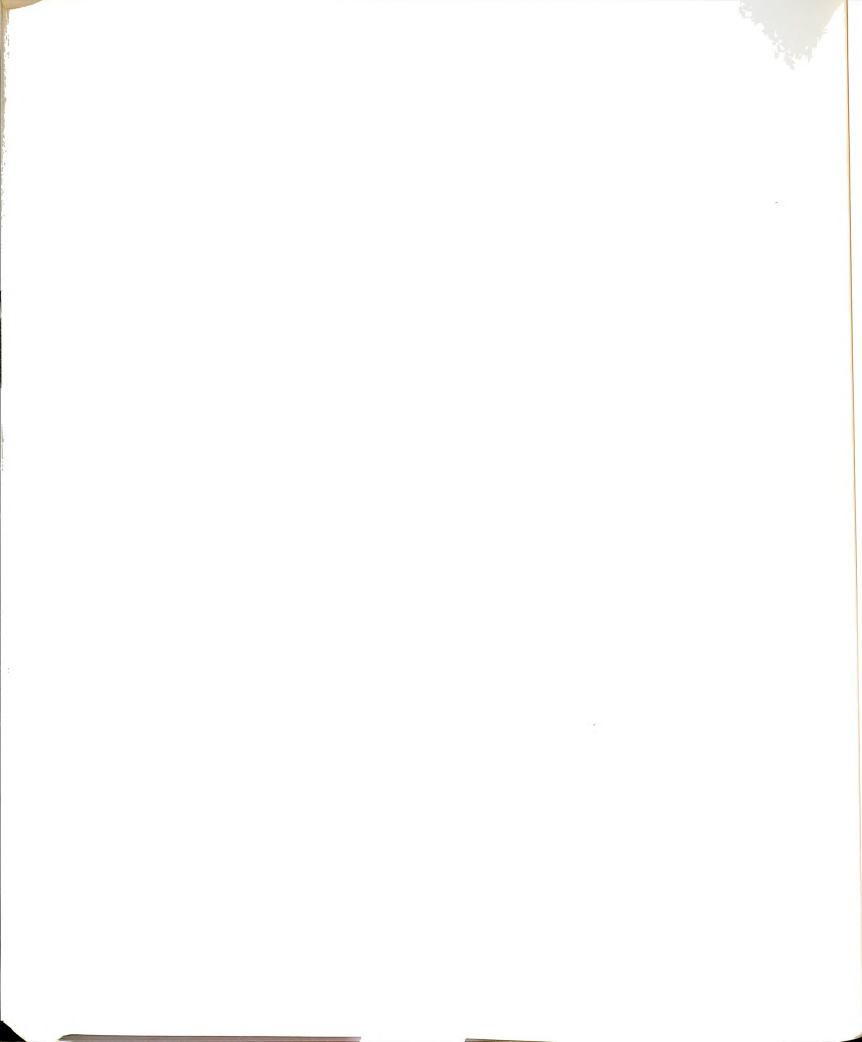
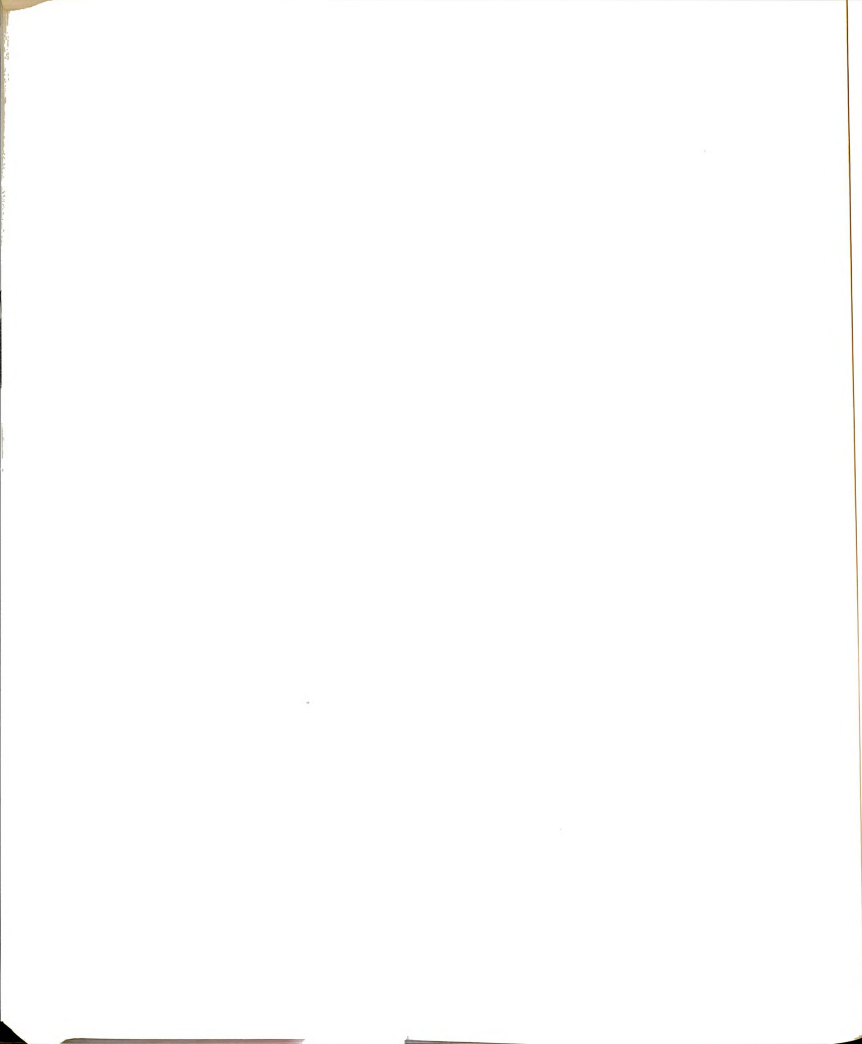


Table XXXIV. Formation Constants of Manganese(II) Ion-PAA Complexes at Different Ionic Strengths and 25°C.

Ionic Strength	$\log K_f^{ML}$	$\log K_f^{MHL}$
0.03	5.5±0.1	3.11±0.08
0.04	5.39±0.07	3.04±0.06
0.05	5.25±0.06	3.0±0.1
0.06	5.0±0.1	2.79±0.08
0.07	5.00±0.07	2.9±0.1
0.08	4.99±0.08	3.07±0.06
0.09	-----	2.80±0.08
0.10	4.96±0.05	-----



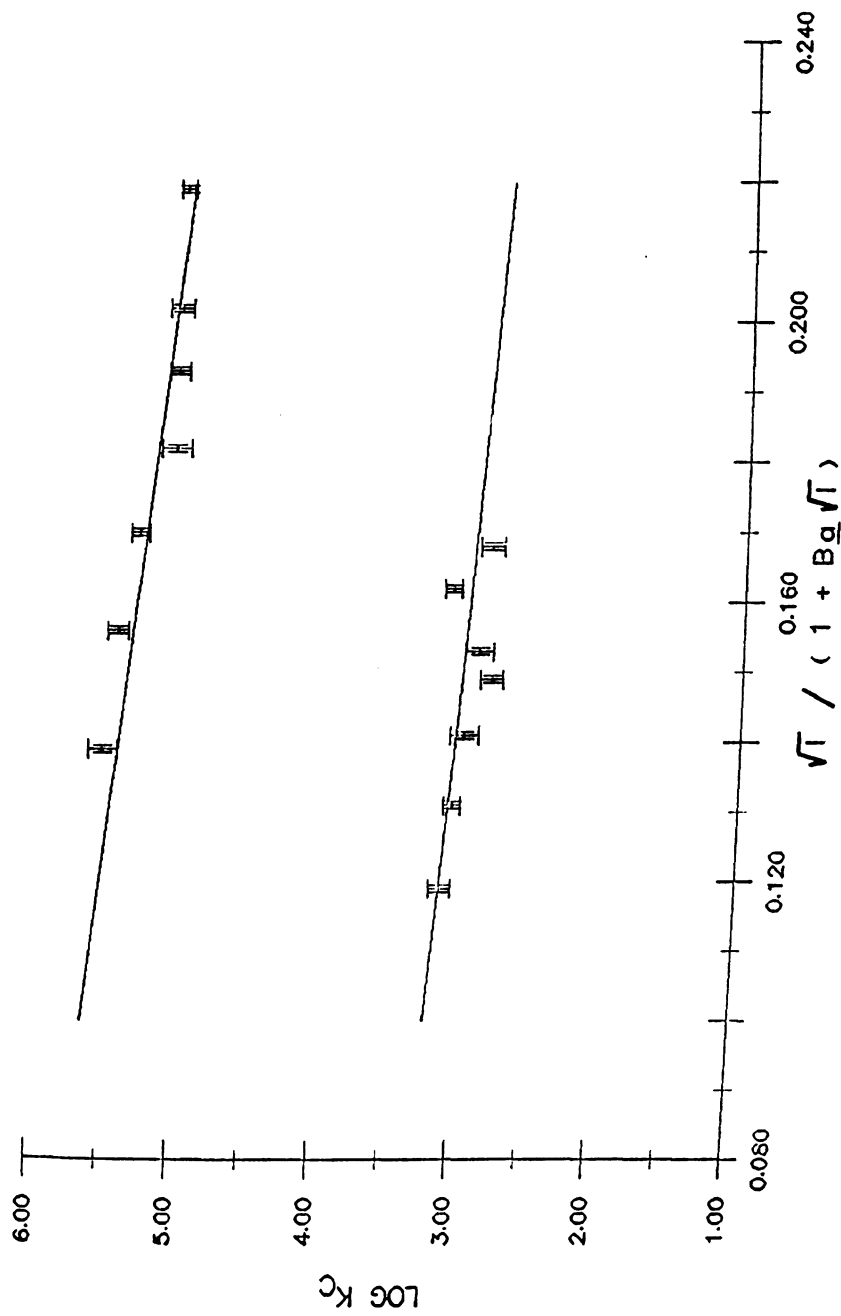
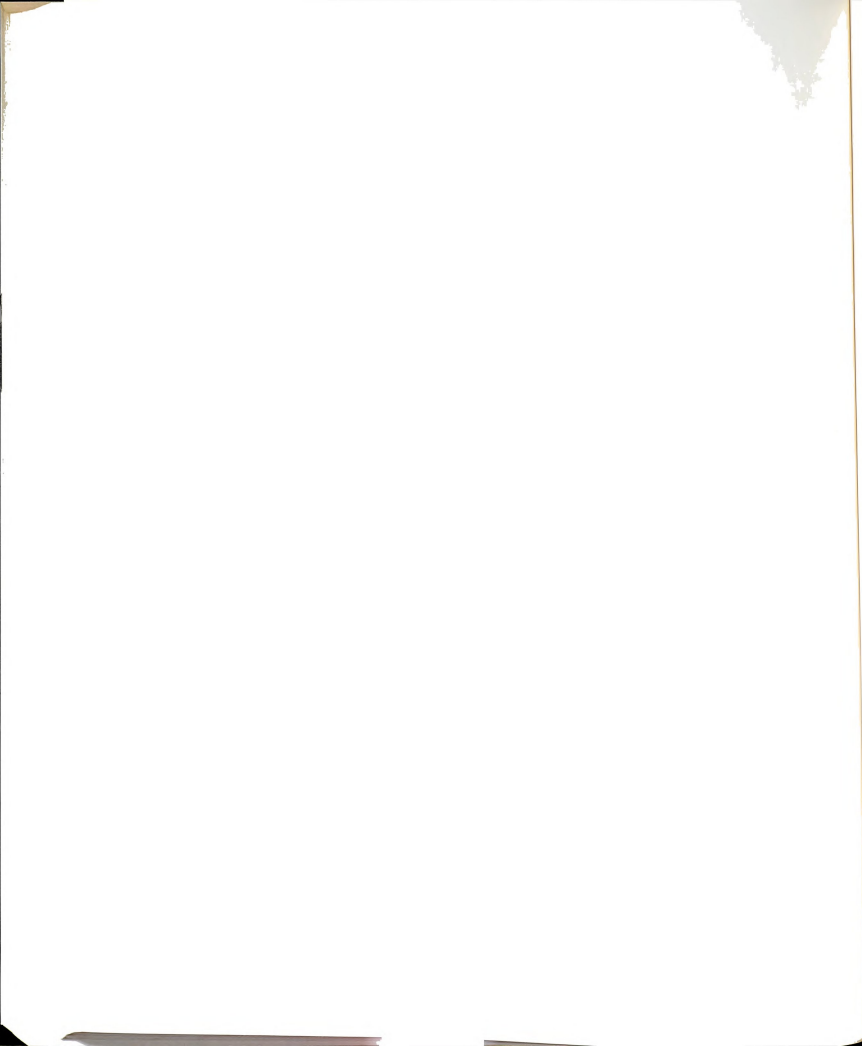


Figure 28. A plot of the log formation constant of Mn-PAA as a function of the ionic strength (upper curve - deprotonated PAA, lower curve - monoprotonated PAA).

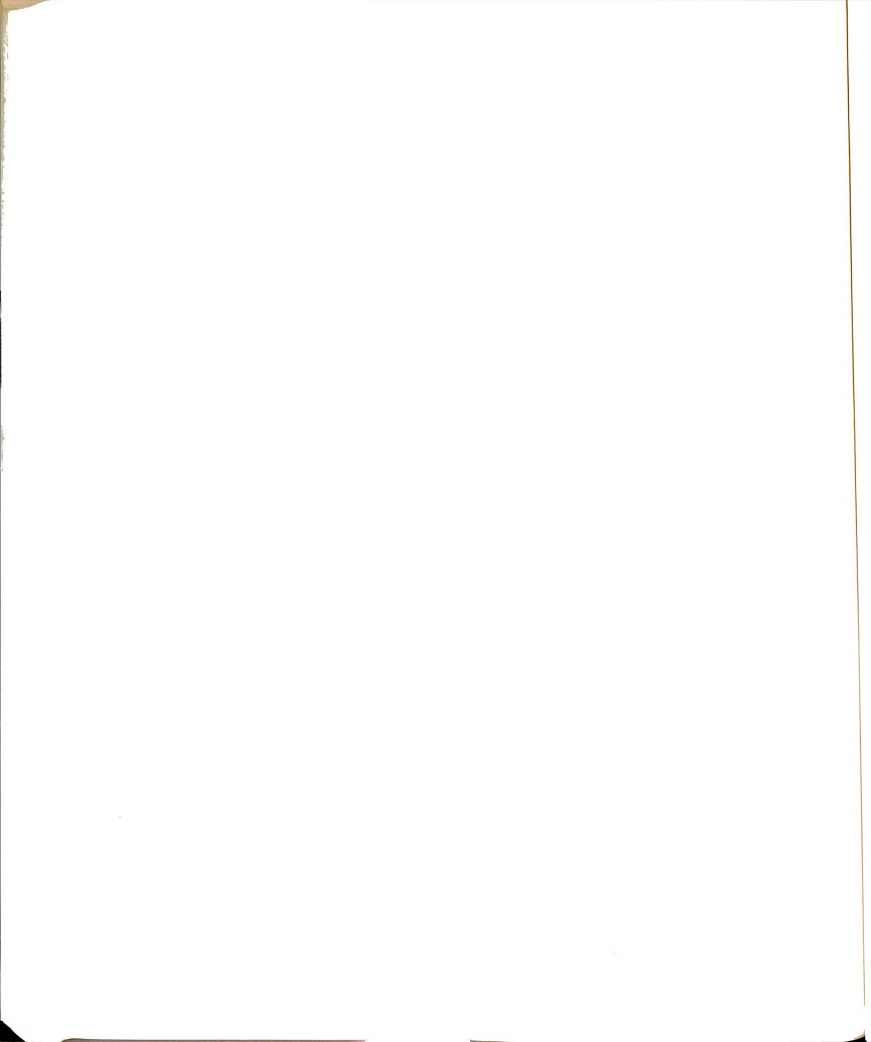




associated with cyclic voltammetric determinations. The technique of manganese electron spin resonance for the determination of formation constants has been shown to be accurate, relatively precise, and suitable for these studies when compared to other techniques. This method should prove to be a powerful tool in the study of both aqueous and nonaqueous solution chemistry, especially as newer instrumentation with greater computer capabilities further enhances the precision of measurements.

### 3.1.2. Cyclic Voltammetry

Cyclic voltammetry was used to study the complexation of PAA with  $Zn^{2+}$ ,  $Cu^{2+}$ ,  $Ni^{2+}$ ,  $Co^{2+}$ ,  $Fe^{2+}$ ,  $Mn^{2+}$ ,  $Pb^{2+}$ , and  $Tl^+$  ions. The above transition metal ions have similar sizes, of  $\sim 0.8 \text{ \AA}$  radius (192) while the  $Pb^{2+}$  ion and  $Tl^+$  ion have radii of  $1.32 \text{ \AA}$  and  $1.49 \text{ \AA}$ , respectively. The sizes of these ions are intermediate between that of magnesium(II) ( $0.78 \text{ \AA}$  radius) and calcium(II) ( $1.06 \text{ \AA}$  radius) with the exception of lead and thallium, which are larger. If size alone were the criterium for predicting the extent of complexation with PAA, the transition metals would have a formation constant value between those obtained for  $Mg^{2+}$  and  $Ca^{2+}$ , whereas lead and thallium would have a much lower  $K_f$ . It was also possible that, if the formation constant of a Tl-PAA complex was large enough, competition studies would lead to the determination of a formation constant with other



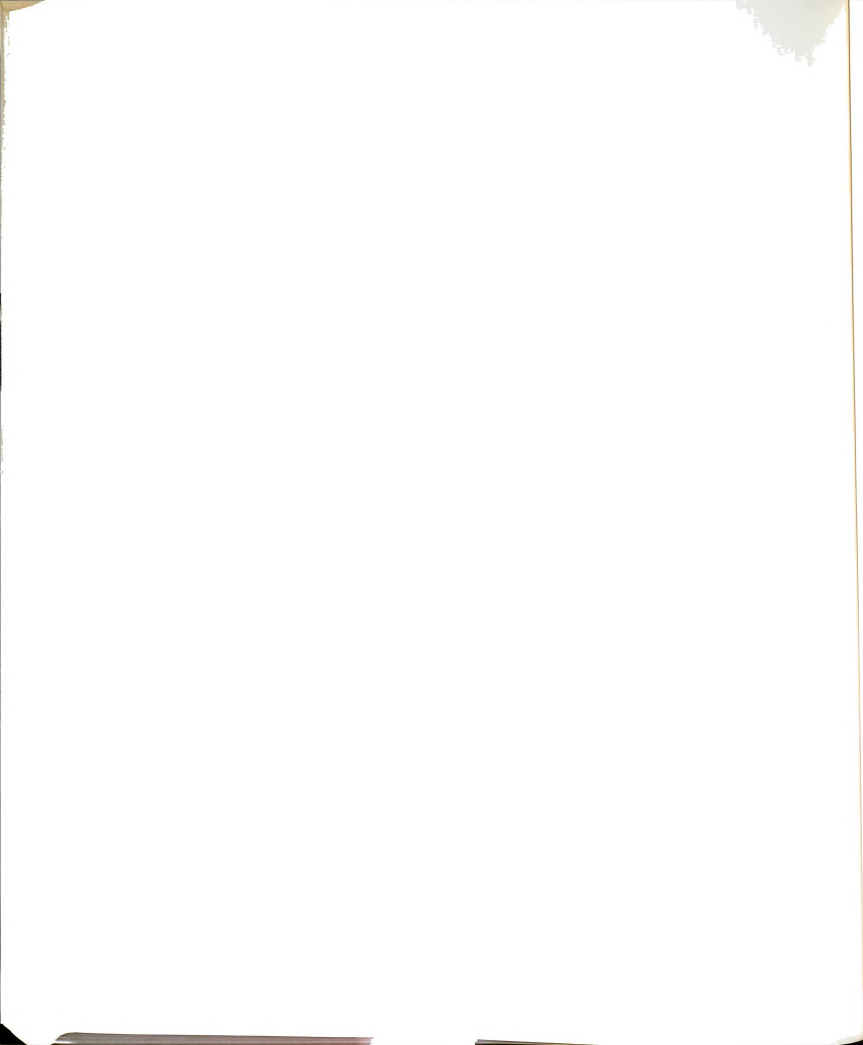
metals (as has been done with the thallium-cryptate complexes by Weaver et al. (193)). A value obtained for the Mn-PAA system would also provide a cross-check with the electron spin resonance determinations in Section 3.1.1.

Unfortunately,  $\text{Ni}^{2+}$ ,  $\text{Co}^{2+}$ , and  $\text{Mn}^{2+}$  exhibit irreversible behavior at the hanging mercury drop electrode (HMDE). That is, no anodic wave was observed after cathodic reduction. In the case of iron(II), quasi-reversible behavior was observed, which became irreversible upon addition of the ligand. Quasi-reversible in this sense means that an anodic peak was observed, but the separation between the cathodic and anodic peaks was much greater than the theoretical 29.5 mV. Zinc was found to be reversible, but the electron transfer kinetics became irreversible upon the addition of PAA. Hence, formation constants were only determined for  $\text{Cu}^{2+}$ ,  $\text{Pb}^{2+}$ , and  $\text{Tl}^+$ .

The well-known Lingane (194) equation was used to fit the data for strong complexes;

$$E_{1/2}^c - E_{1/2}^f = - RT/nF (\ln K_f + p \ln[\text{PAA}]) \quad (13)$$

where  $E_{1/2}^c$  and  $E_{1/2}^f$  are the half-wave potentials of the free and complexed metal ion,  $K_f$  is the formation constant of the complex,  $p$  is the stoichiometric coefficient of PAA and  $[\text{PAA}]$  is the total concentration of PAA. The other symbols have their usual meaning. Where weak complexation

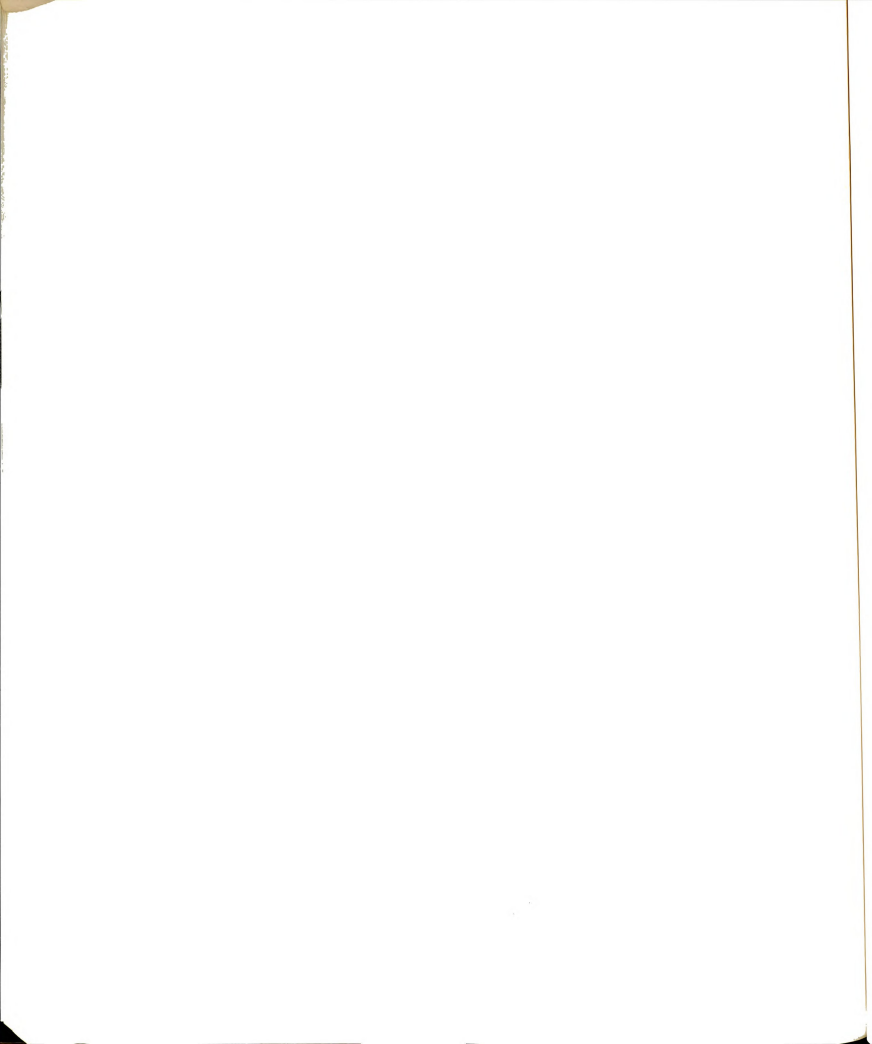


was found, the modification of this equation formulated by Buck (195) was used;

$$E_{1/2}^c = E_{1/2}^f = -RT/nF(\ln K_f + p \ln [\text{PAA}] + \ln(1 + 1/K_f[\text{PAA}])) \quad (14)$$

with the symbolism the same as in Equation (13). The Buck equation differs from the Lingane equation in the last term on the right, which is negligible when  $K_f$  is large.

The use of the Lingane and Buck equations requires that several experimental conditions be met. The electrode kinetics must be reversible, which is experimentally seen as a difference in the anodic and cathodic peaks of 29.5 mV for a two electron transfer and 59 mV for a one electron transfer reaction. The thallium-PAA system exhibited a peak separation of  $59 \pm 2$  mV, while the lead and copper systems had a separation of  $30 \pm 4$  mV, indicating reversible behavior. The ligand-to-metal concentration ratio must be such that the concentration of free metal ion is small in comparison to total metal ion concentration. The diffusion coefficients for the free and complexed ions should be approximately equal and the transition state for the electron transfer should be approximately half-way between the two oxidation states. The former condition is assumed, while the latter may be checked for gross errors by observing the symmetry of the anodic and cathodic peaks (symmetry indicates that the condition is



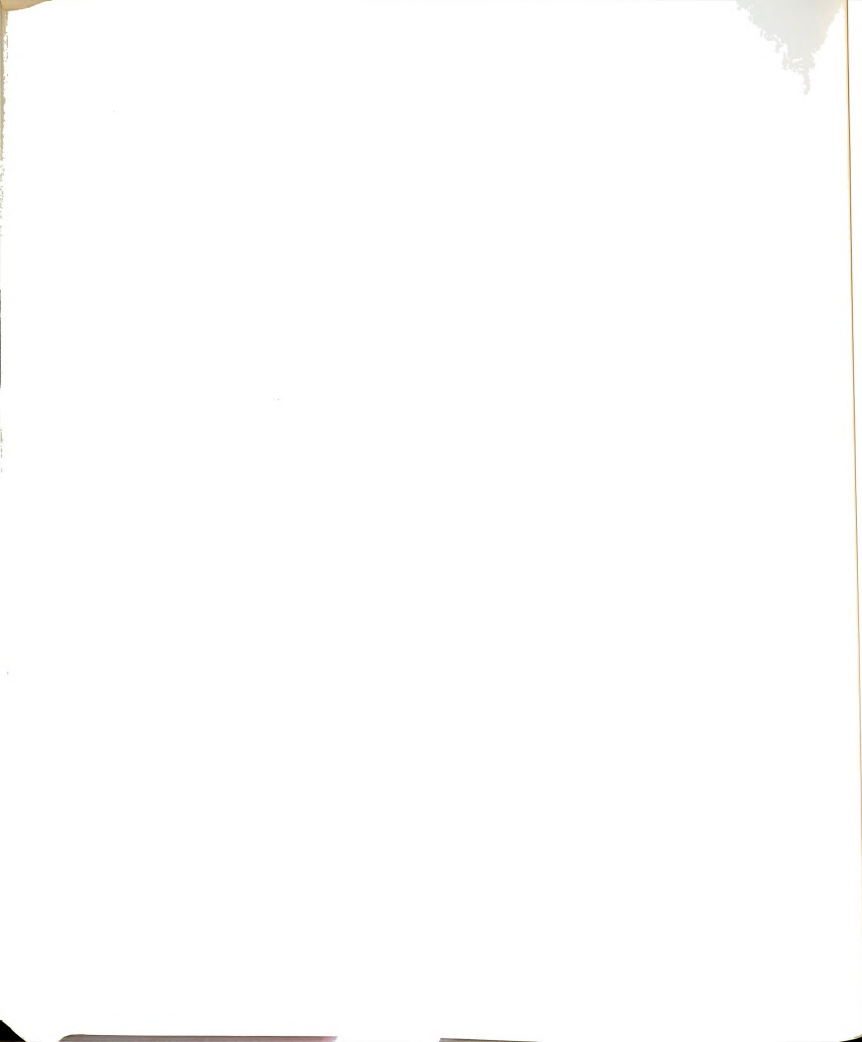
fulfilled).

The data for PAA complexes with  $Pb^{2+}$ ,  $Cu^{2+}$ , and a sample graph for  $Tl^{+}$  are plotted in Figures 29-31 and tabulated in Tables XXXV - XXXVII. The slopes of the lines are  $1 \pm 0.3$ , indicative of a stoichiometric ratio of one ligand to one metal ion for each of the complexes. The formation constants derived from such a treatment are:  $\log K_f^{CuI} = 8.0 \pm 0.1$ ,  $\log K_f^{CuHL} = 4.2 \pm 0.1$ ,  $\log K_f^{PbL} = 7.0 \pm 1$ ,  $\log K_f^{PbHL} = 4.1 \pm 0.1$ , and  $\log K_f^{TlL} = 2.3 \pm 0.1$  at  $25^\circ C$  and an ionic strength of 0.05. The monoprotonated thallium-PAA complex formation constant was too weak to measure using cyclic voltametry.

The thermodynamic formation constants was determined for the deprotonated thallium-PAA complex by using the Debye-Hückel equation

$$\log K_c = \log K_t - 6A\sqrt{I}/(1 + Ba\sqrt{I}) \quad (15)$$

where the symbols have been defined in Section 3.1.1. The results are given in Table XXXVIII and plotted in Figure 32. The theoretical slope of  $-3.05$  was attained when the ion size parameter  $a$  was 9.3, much larger than the value of 2.5 calculated by Kielland (191). This is probably due to a large contribution from the covalent character of thallium to the complexation with PAA, since





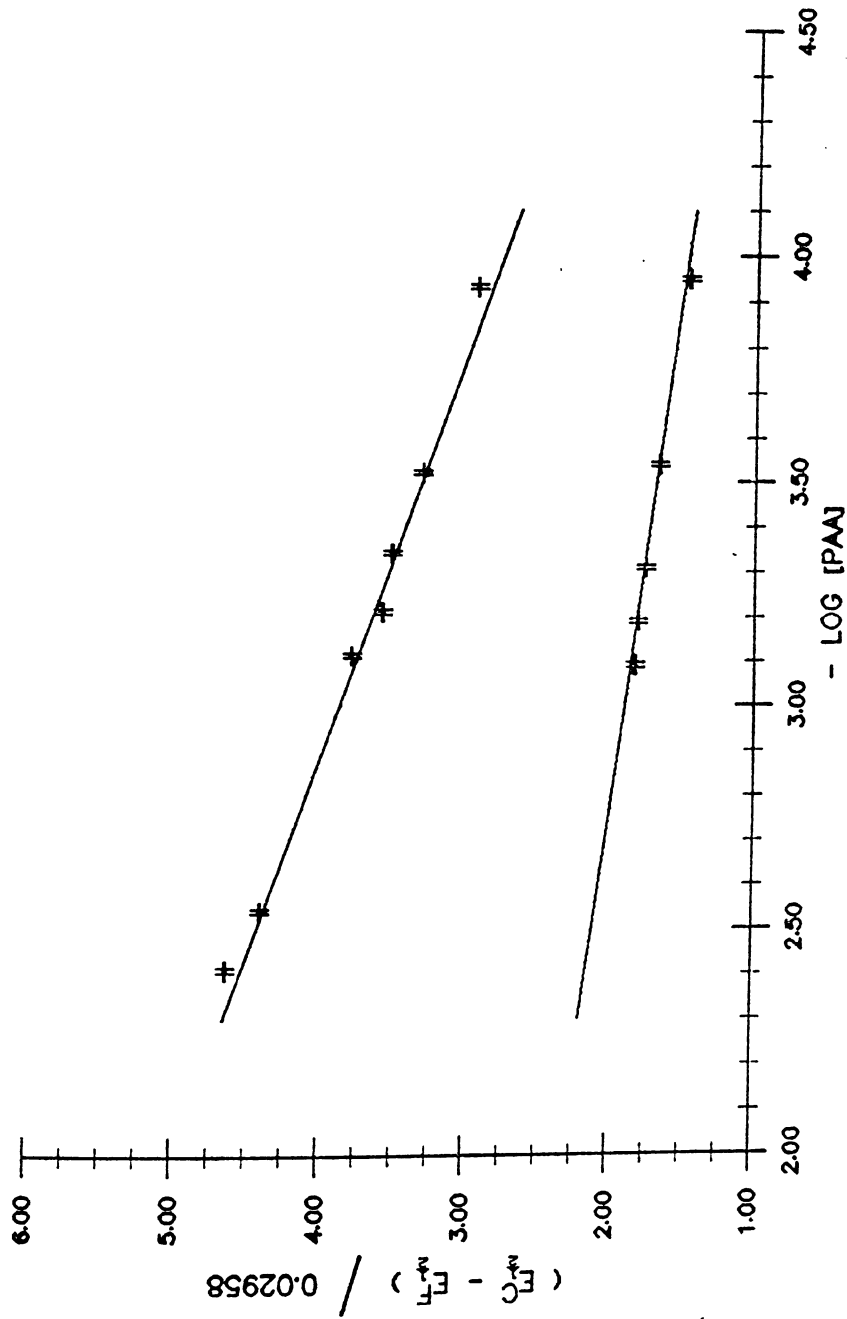
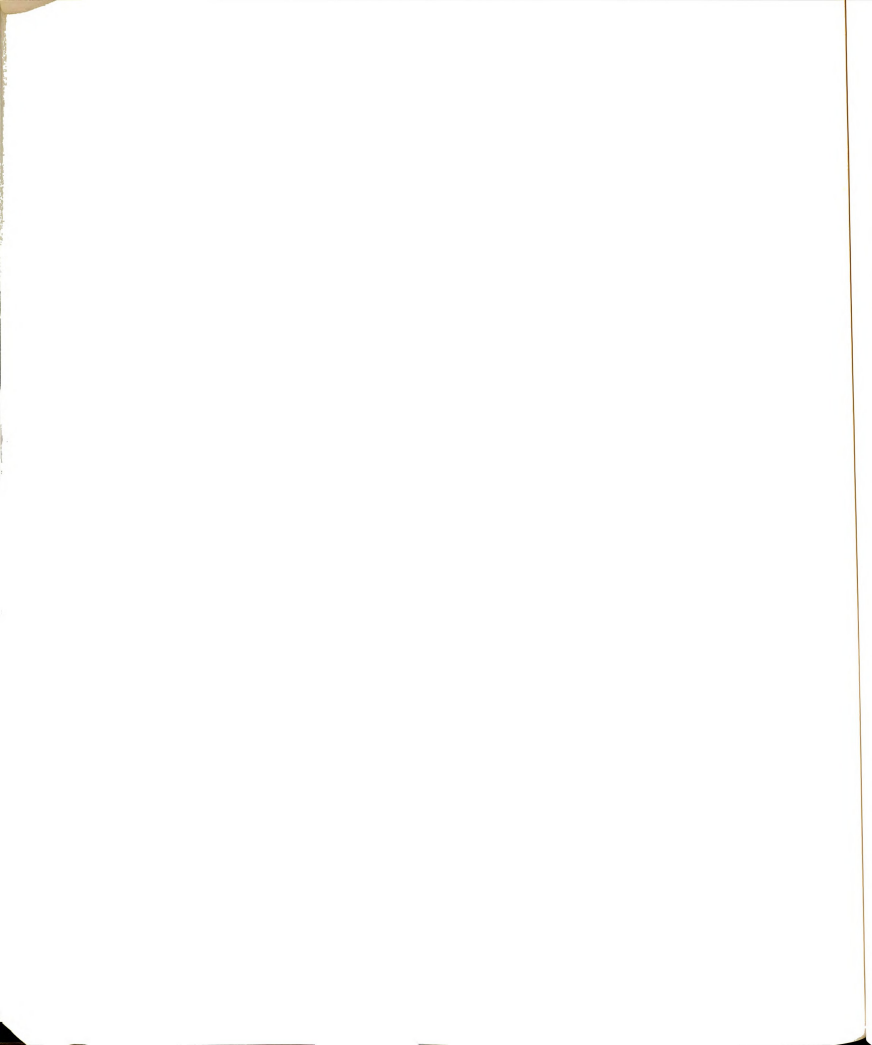


Figure 29. A plot of the change in Emf vs the negative log [PAA] to determine the formation constant of a Pb-PAA complex (upper curve - deprotonated PAA, lower curve - monoprotonated PAA).



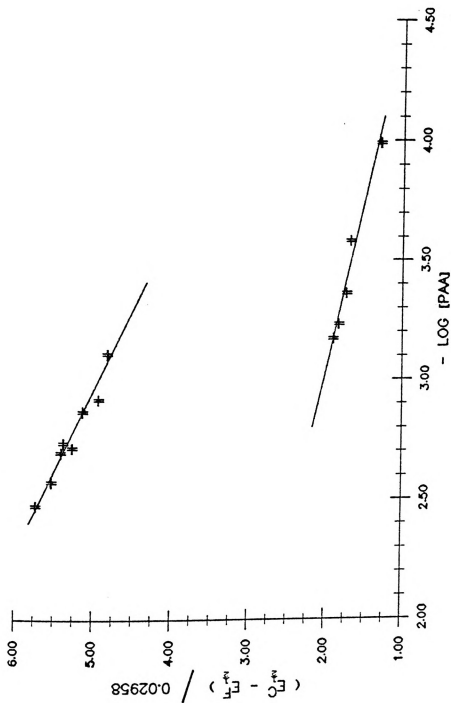
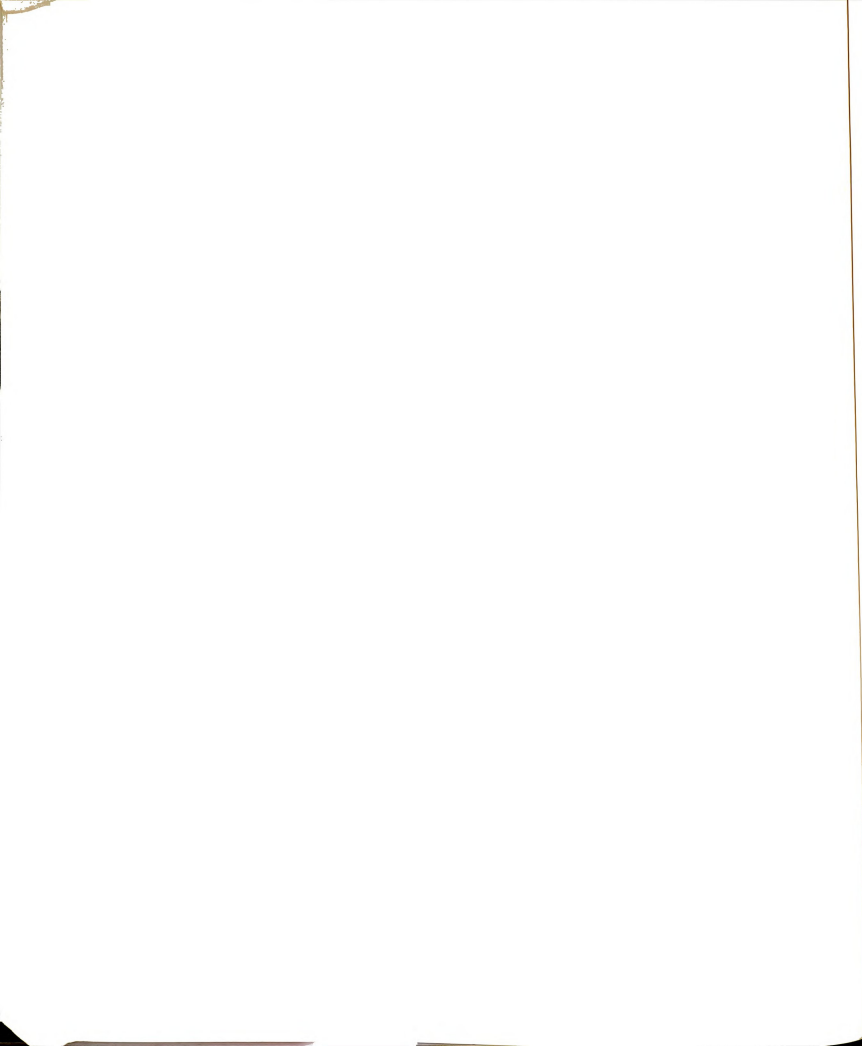


Figure 30. A plot of the change in Emf vs the negative log [PAA] to determine the formation constant of a Cu-PAA complex (upper curve - deprotonated PAA, lower curve - monoprotonated PAA).



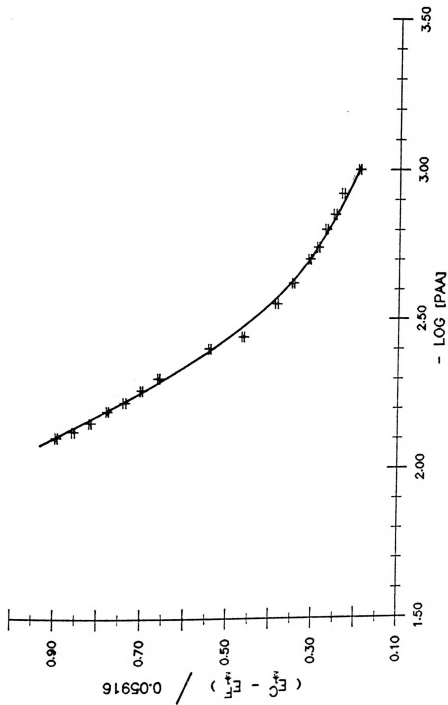


Figure 31. A plot of the change in Emf vs the negative log [PAA] to determine the formation constant of a monoprotonated PAA-Tl complex.

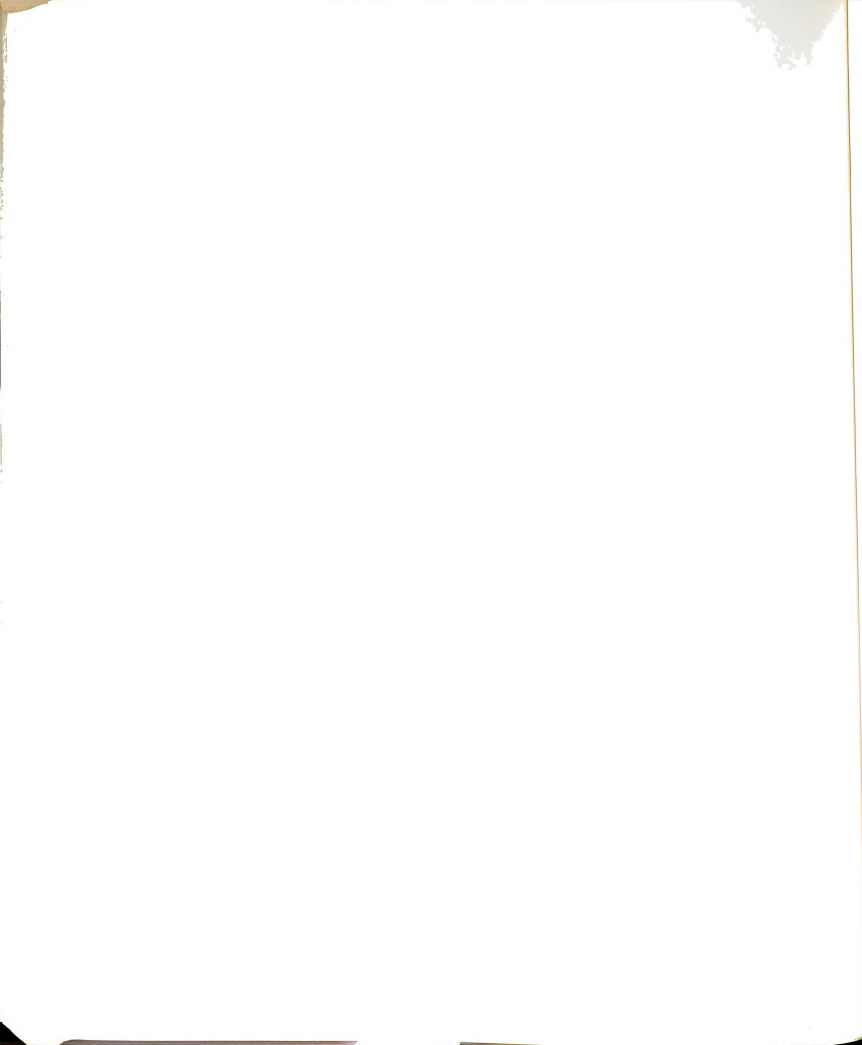


Table XXXV. The Change in the Emf of a Pb-PAA Complex as a Function of the Negative log [PAA] at 25°C, I = 0.05.

$\frac{(E_{1/2}^c - E_{1/2}^f)}{0.02958}$	ML	MHL	
	-log [PAA]	$\frac{(E_{1/2}^c - E_{1/2}^f)}{0.02958}$	-log [PAA]
4.63	2.41	1.83	3.09
4.40	2.54	1.81	3.19
3.79	3.11	1.76	3.31
3.58	3.21	1.67	3.54
3.52	3.34	1.47	3.95
3.31	3.52		
2.94	3.93		

Table XXXVI. The Change in the Emf of a Cu-PAA Complex as a Function of the Negative log [PAA] at 25°C, I = 0.05.

$\frac{(E_{1/2}^c - E_{1/2}^f)}{0.02958}$	ML	MHL	
	-log [PAA]	$\frac{(E_{1/2}^c - E_{1/2}^f)}{0.02958}$	-log [PAA]
5.73	2.47	1.91	3.17
5.53	2.57	1.84	3.23
5.41	2.69	1.74	3.36
5.38	2.73	1.69	3.58
5.27	2.71	1.30	3.94
5.14	2.86		
4.94	2.91		
4.83	3.10		





Table XXXVII. The Change in the Emf of a Tl-PAA Complex as a Function of the Negative log [PAA] at 25°C, I = 0.05.

$\frac{(E_{1/2}^c - E_{1/2}^f)}{0.05916}$	ML -log [PAA]	$\frac{(E_{1/2}^c - E_{1/2}^f)}{0.05916}$	ML -log [PAA]
0.20	3.00	0.55	2.40
0.23	2.92	0.66	2.30
0.25	2.85	0.70	2.26
0.27	2.80	0.74	2.22
0.29	2.74	0.78	2.19
0.31	2.70	0.82	2.15
0.35	2.62	0.86	2.12
0.39	2.55	0.90	2.10
0.47	2.44		

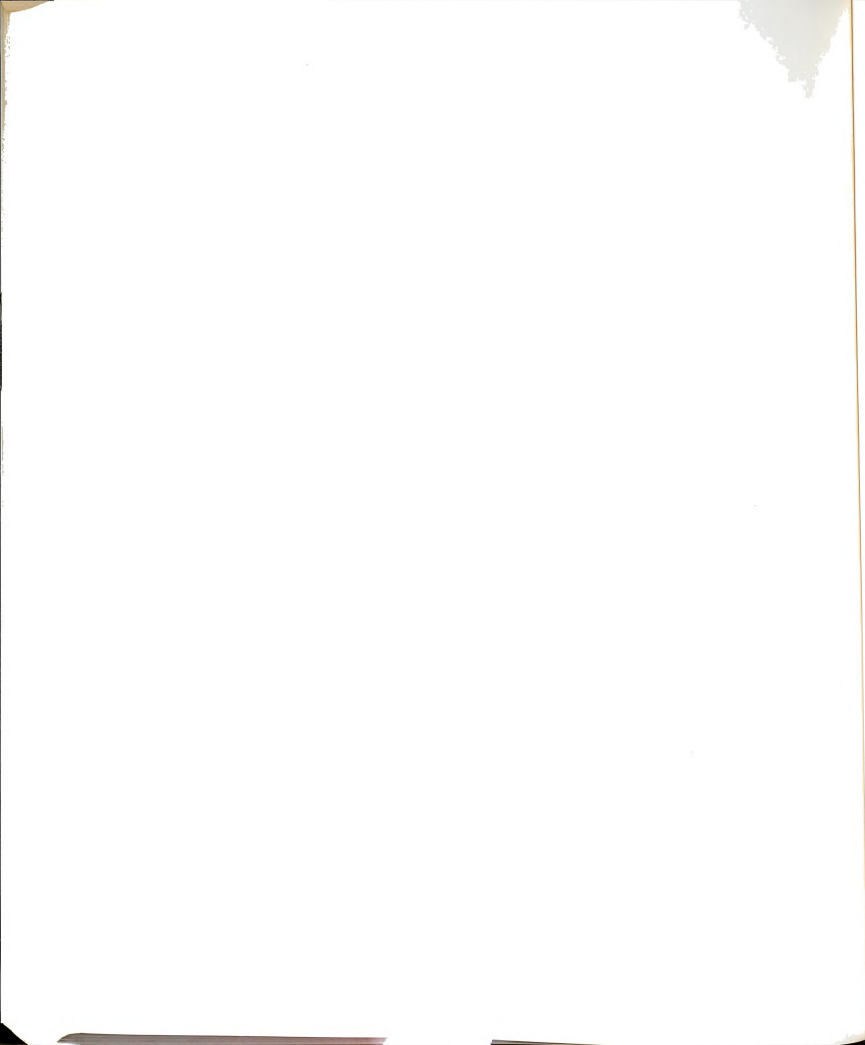
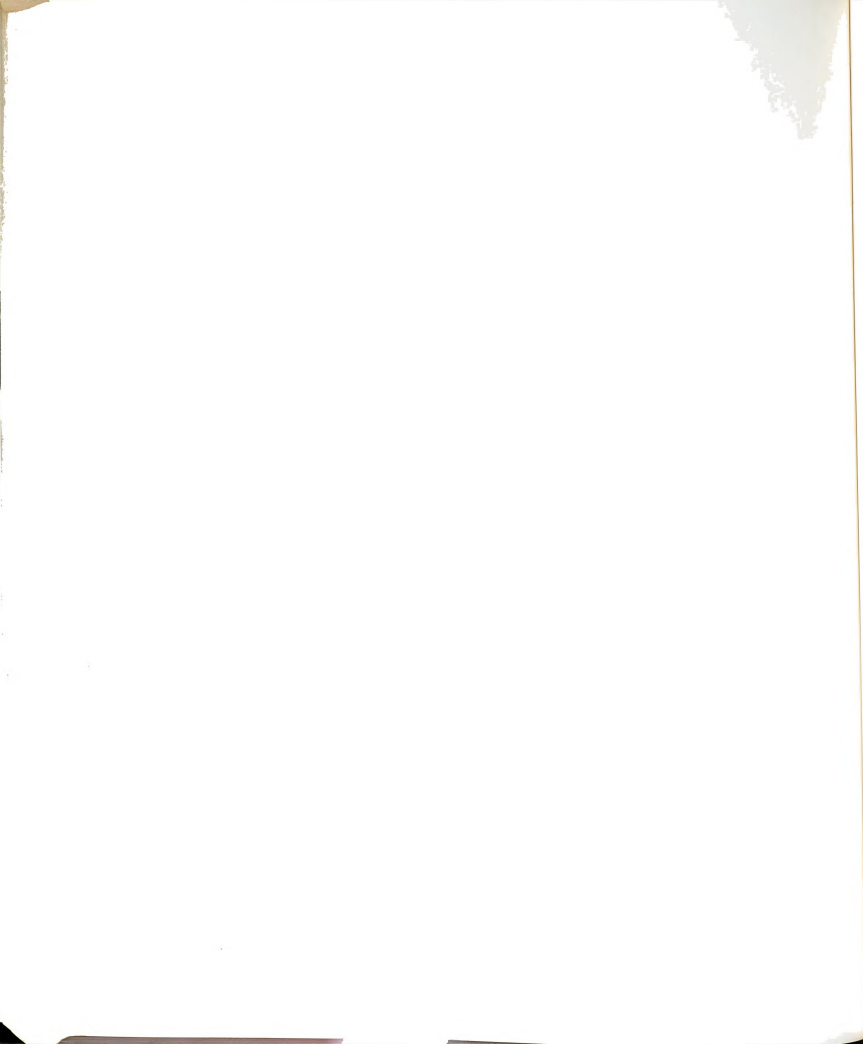


Table XXXVIII. Formation Constants of Thallium(I) - PAA Complexes at Different Ionic Strengths and 25°C.

Ionic Strength	$K_f^{ML}$
0.030	2.3 ± 0.1
0.040	2.31 ± 0.07
0.050	2.30 ± 0.07
0.060	2.25 ± 0.09
0.070	2.2 ± 0.1
0.090	2.2 ± 0.1
0.110	2.21 ± 0.08



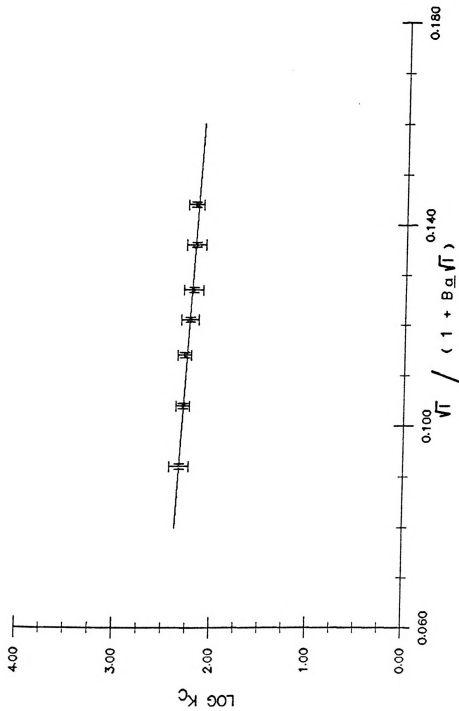
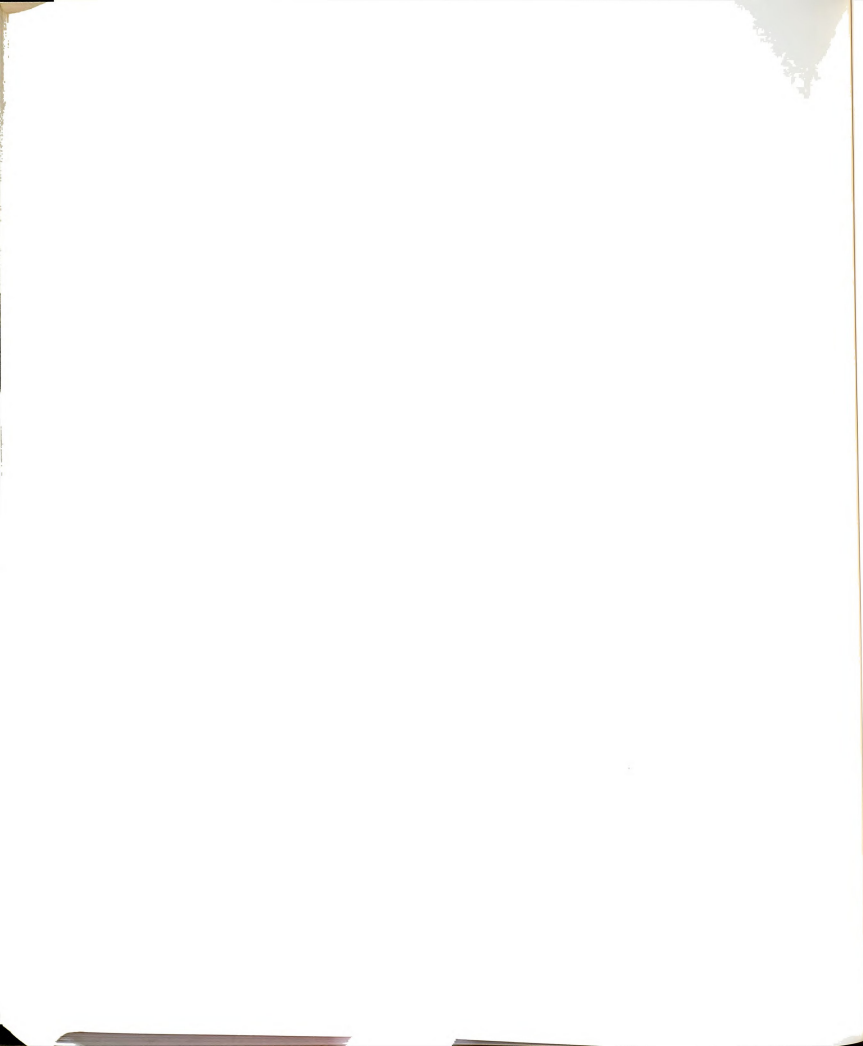


Figure 32. A plot of log formation constant of deprotonated PAA-TI complex as a function of the ionic strength.



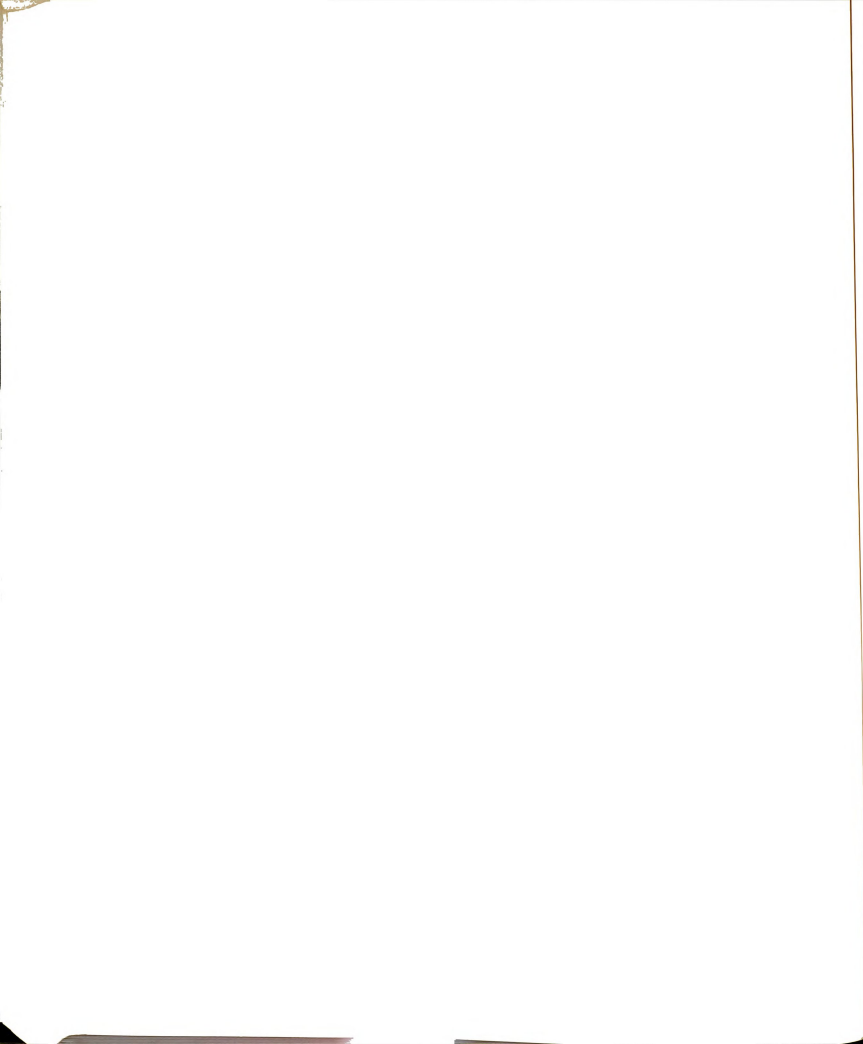
the Debye-Hückel equation considers only electrostatic interactions. The thermodynamic formation constant for the deprotonated complex was  $2.63 \pm 0.04$ . The low stability of the deprotonated PAA-thallium(I) complex does not lend itself to competition studies, which were subsequently abandoned.

The value obtained for the formation constant of the deprotonated and monoprotated Cu-PAA complexes agree fairly well with the values obtained by Stunzi and Perrin ( $\log K_f^{CuL} = 7.14$  and  $\log K_f^{CuHL} = 3.85$ ) when considering that they used an ionic strength of 0.15 and made the measurements at 37°C (157).

### 3.1.3. Potentiometric Studies

A silver specific ion electrode was used to determine the formation constants of  $Ag^+$  ion complex with the mono- and deprotonated forms of PAA. The calibration curve of the electrode, as well as the titration curve for the deprotonated complex, is shown in Figure 33. As can be seen, the calibration curve is relatively linear with a slope of  $63.3 \pm 0.6$  mV, close to the ideal Nernstian slope of 59.2 mV. The formation constants determined were:  $\log K_f^{AgL} = 3.11 \pm 0.05$  and  $\log K_f^{AgHL} = 2.7 \pm 0.1$  at 25°C and an ionic strength of 0.05.

The formation constants of the calcium ion with PAA were measured using a calcium ion selective electrode.





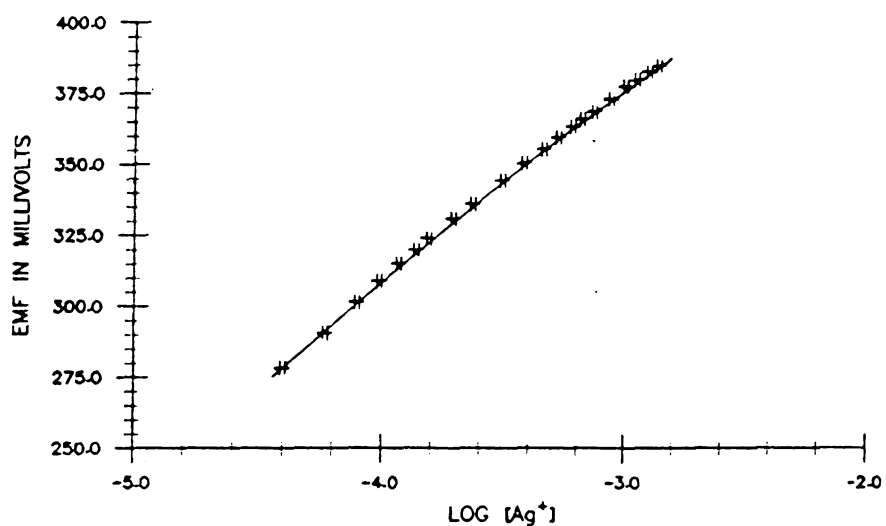
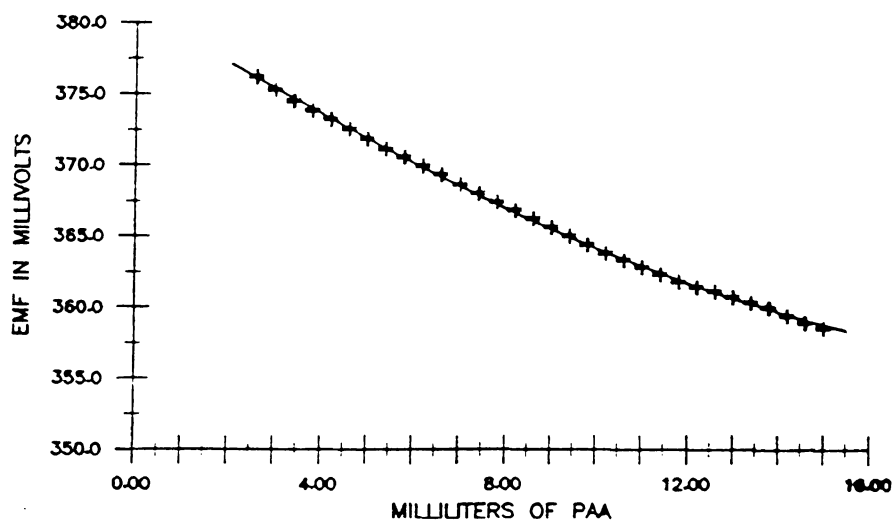
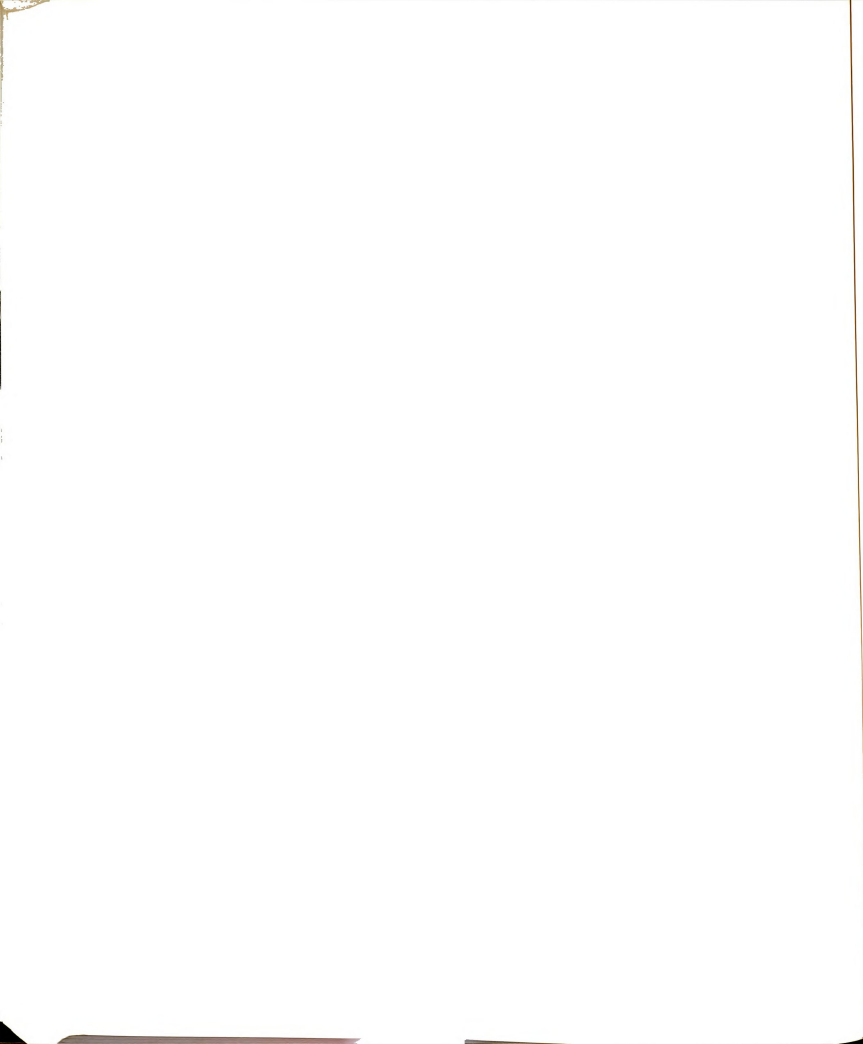
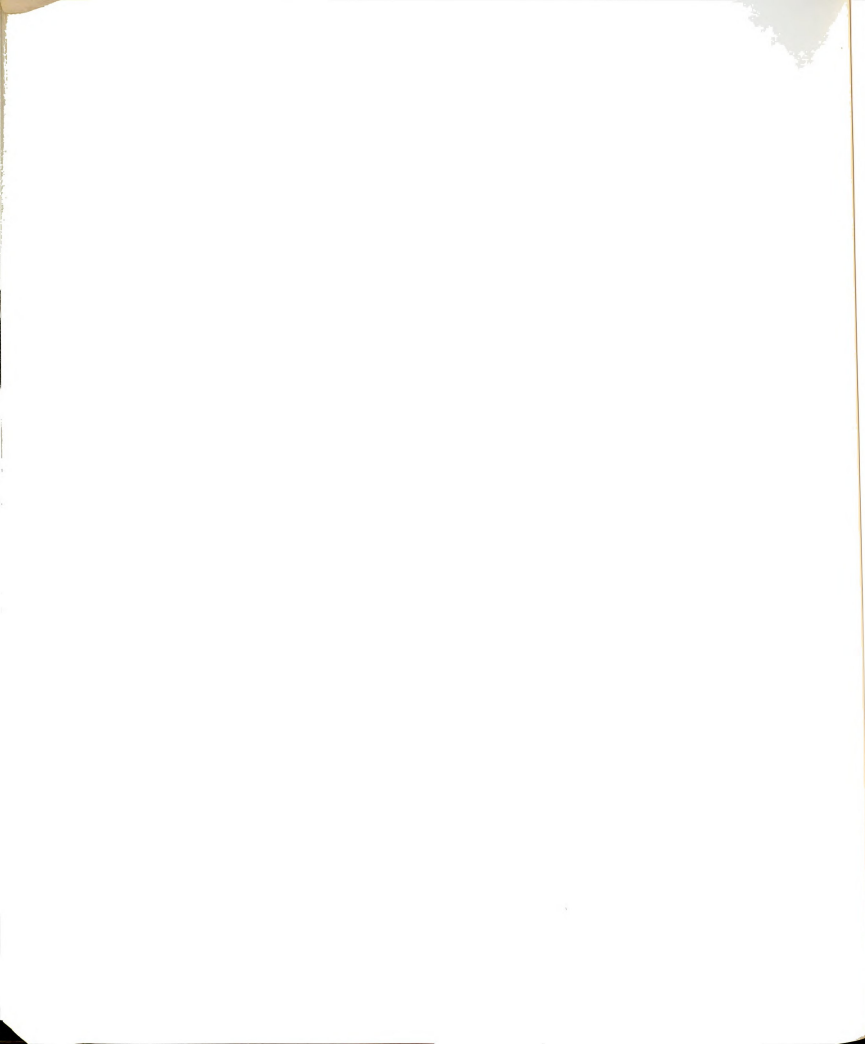
A CALIBRATION CURVE OF A  
SILVER ION SPECIFIC ELECTRODEA TITRATION CURVE OF Ag<sup>+</sup> WITH  
PAA AT 25°C AND I = 0.05

Figure 33. A sample calibration plot and titration curve of silver ion with deprotonated PAA using a silver ion specific electrode.



A typical calibration curve (25°C,  $I = 0.05$ ) is shown in Figure 34 along with the titration curve. The data were processed assuming the formation of a mono- and deprotonated complex. There is no evidence for the formation of other complexes in solution. Formation constants were determined at different ionic strengths and extrapolated to zero ionic strength to determine the thermodynamic formation constants using Equations (11) and (12). The formation constant and ion size parameter  $a$  were used as the fitted parameters. The resulting plots for the mono- and deprotonated complexes of PAA with calcium are shown in Figure 35 using the values given in Table XLIX. The logarithm of the thermodynamic formation constant of deprotonated PAA-Ca is  $4.68 \pm 0.03$ , with a value of  $2.68 \pm 0.08$  for the monoprotated formation constant. The ion size parameter was found to be  $5.2 \text{ \AA}$ , which compares to the Stokes determination of approximately  $5 \text{ \AA}$  (190) and that of Kielland  $6 \text{ \AA}$  (191).

The ionic strength was extended to 0.14 to more precisely compare the values obtained by this technique to those of Stunzi (157). The graph shows that linear behavior is exhibited even to this ionic strength when the Debye-Hückel equation is used. Thus, when enough data points are available to calculate an ion-size parameter, this equation is the preferred description of solution complexation behavior.



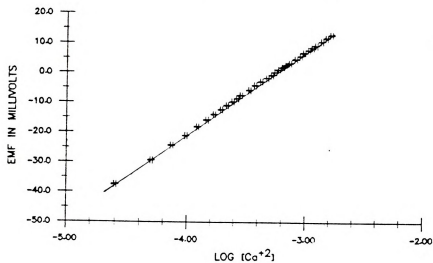
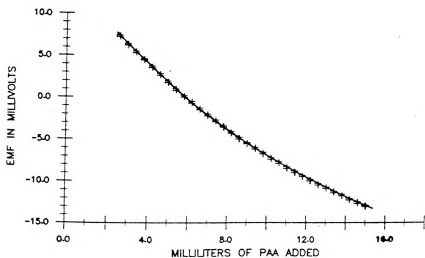
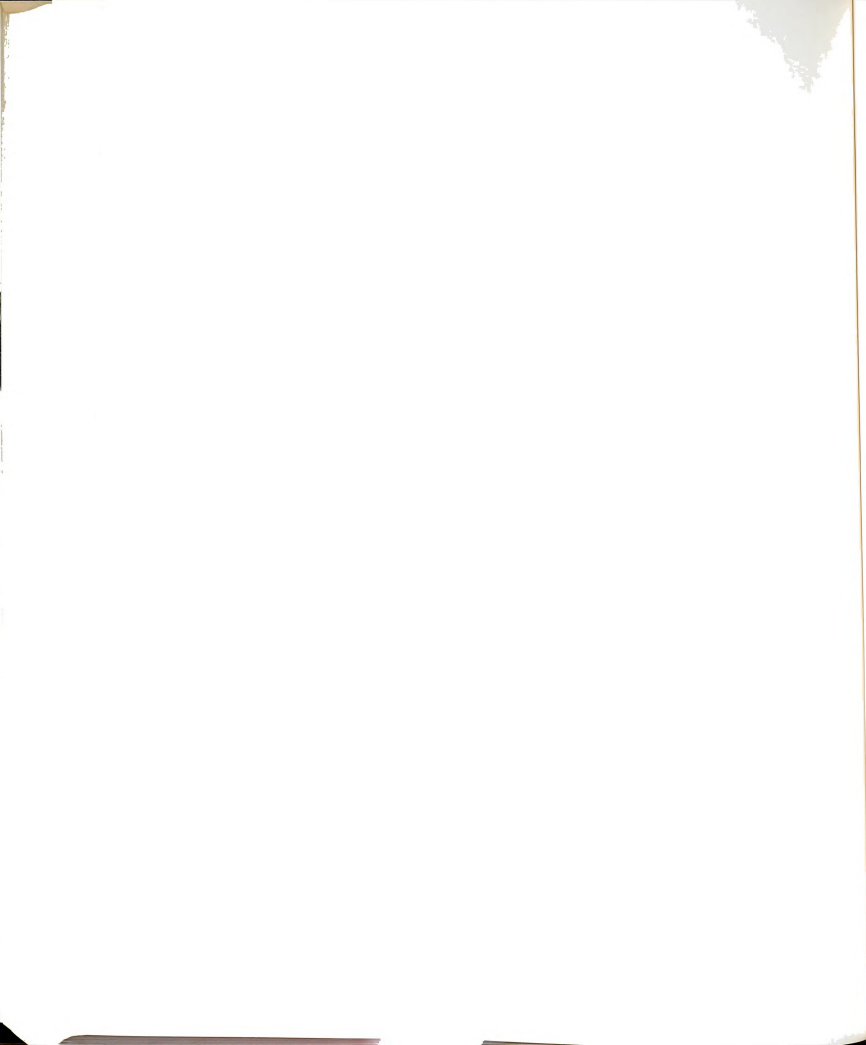
A CALIBRATION CURVE FOR A  
CALCIUM ION SELECTIVE ELECTRODEA TITRATION CURVE OF CALCIUM WITH  
PAA AT 25°C AND I = 0.01

Figure 34. A sample calibration plot and titration curve of calcium ion with deprotonated PAA using a calcium ion selective electrode.



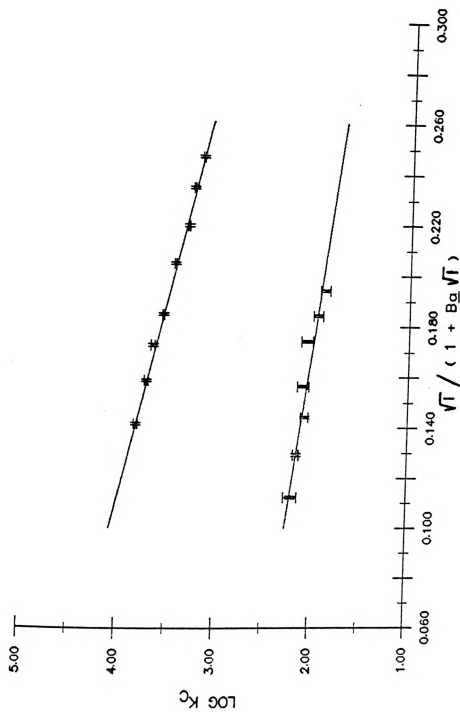


Figure 35. A plot of log formation constant of Ca-PAA as a function of the ionic strength (upper curve - deprotonated PAA, lower curve - monoprotonated PAA).

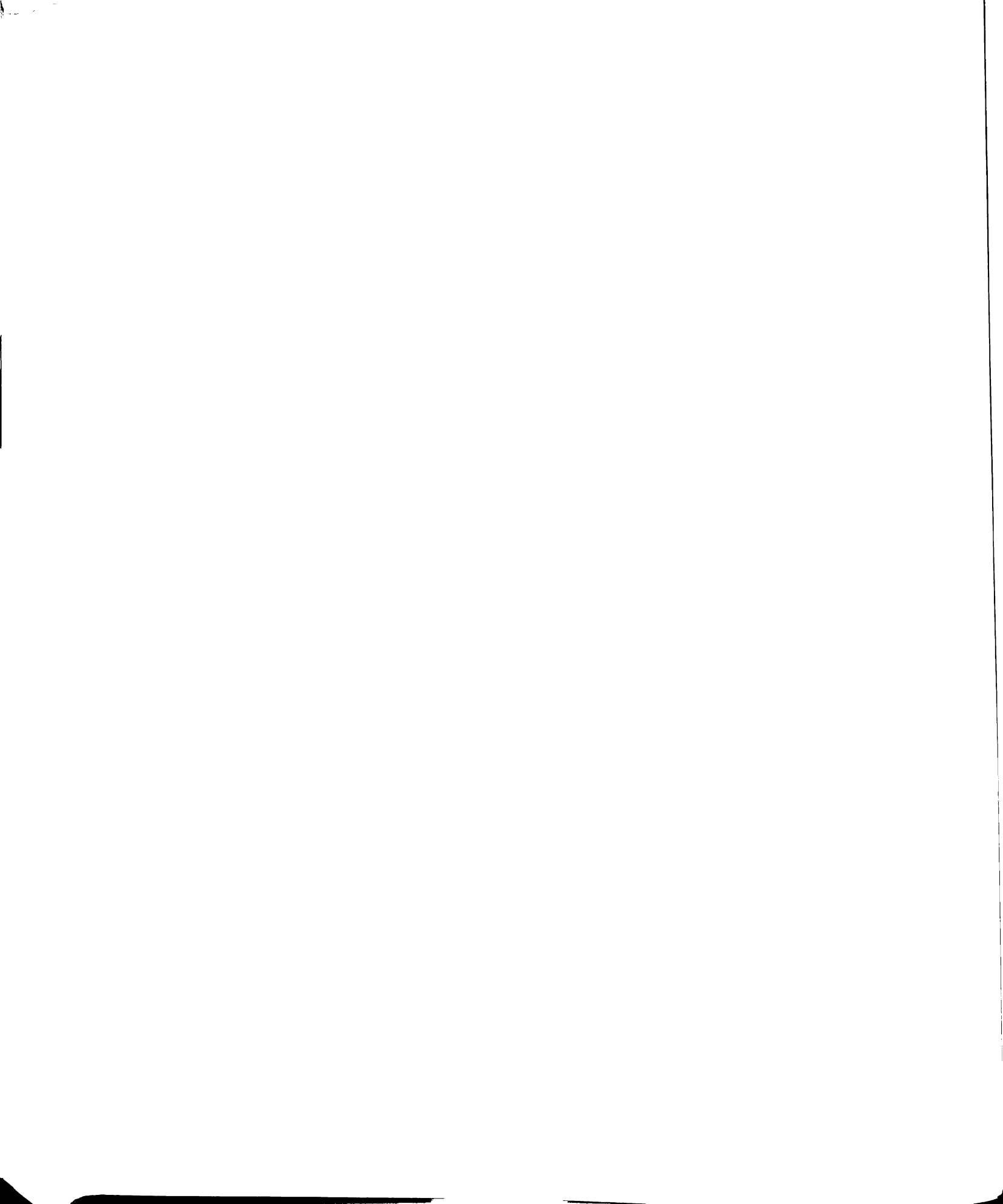




Table XXXIX. Formation Constants for Calcium(II) Ion-PAA Complexes as a Function of the Ionic Strength at 25°C.

Ionic Strength	$\log K_f^{ML}$	$\log K_f^{MHL}$
0.02	-----	2.21 ± 0.07
0.03	3.83 ± 0.02	2.16 ± 0.03
0.04	3.73 ± 0.02	2.08 ± 0.04
0.05	3.67 ± 0.02	2.10 ± 0.06
0.06	3.57 ± 0.01	2.07 ± 0.06
0.08	3.46 ± 0.01	1.96 ± 0.05
0.10	3.33 ± 0.01	1.89 ± 0.05
0.12	3.28 ± 0.01	-----
0.14	3.19 ± 0.01	-----



### 3.2. Thermodynamics of Calcium Complexation with PAA

The thermodynamic parameters  $\Delta H^\circ$  and  $\Delta S^\circ$  were determined from the relationship

$$-RT \ln K_t = \Delta G^\circ = \Delta H^\circ - T\Delta S^\circ \quad (16)$$

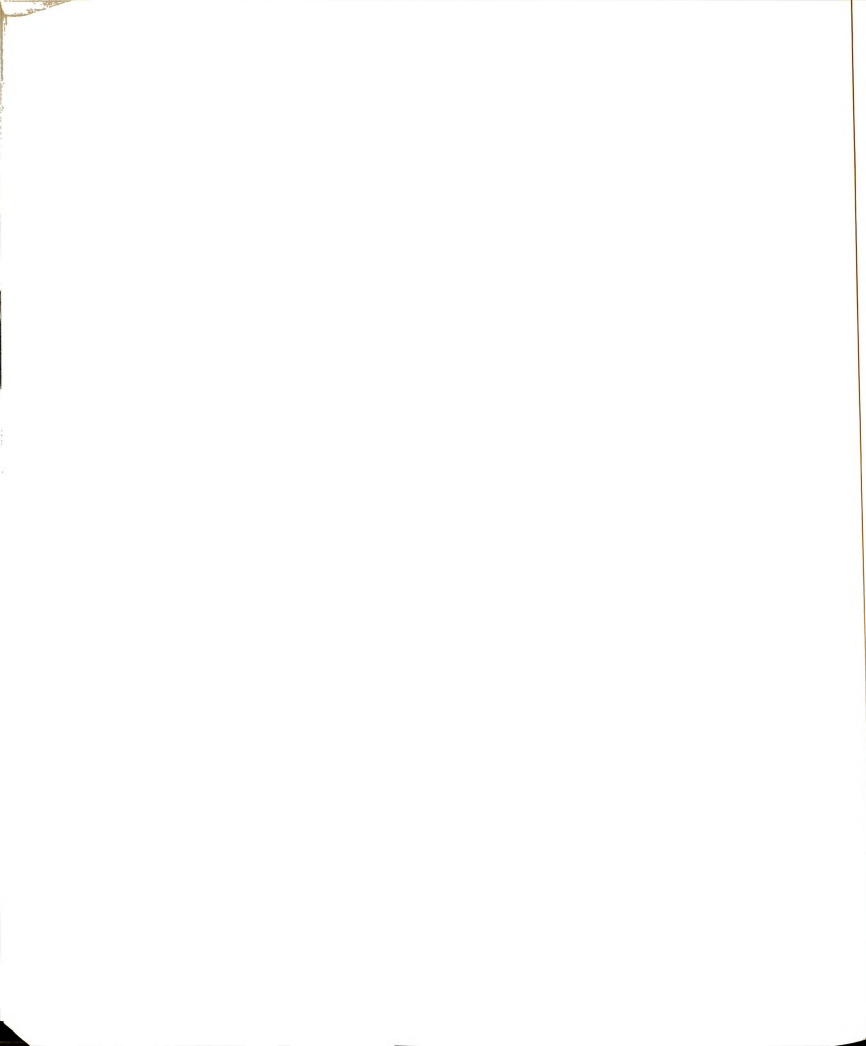
which can be rearranged to yield the van't Hoff relation

$$\ln K_t = -\Delta H^\circ/RT + \Delta S^\circ/R \quad (17)$$

Hence, a plot of  $\ln K_t$  vs  $1/T$  will have a slope of  $-\Delta H^\circ/R$  and an intercept of  $\Delta S^\circ/R$ .

The formation constants  $K_c$  were determined at an ionic strength of 0.05, with the  $K_t$  then calculated using the Debye-Hückel equation with an ion size parameter of 5.2 Å. As can be seen in Equations (8) and (9), the Debye-Hückel equation itself has the temperature dependent quantities A and B. Both are a function of the dielectric constant (a temperature dependent quantity) and the temperature. Values for these quantities were obtained at a given temperature by interpolating values given by Harned and Owen (196). The volume of the solution will also change with temperature (186), although the effect of such changes on the concentrations involved was negligible.

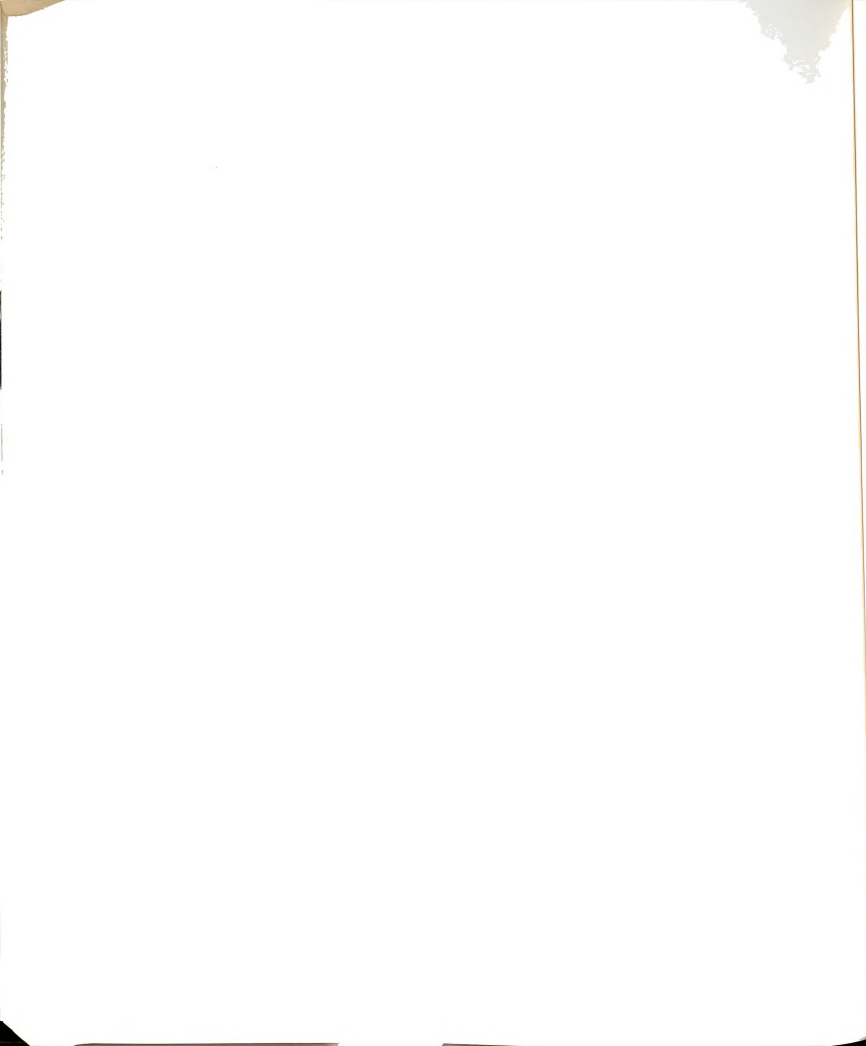
The  $\Delta H^\circ$  and  $\Delta S^\circ$  of complexation were not obtained for the monoprotonated complex, due to a large experimental



error. Generally, the error increases as weaker complexes are studied, because the relative error increases as the change in emf between two titration points decreases. The plots of  $\ln K_c$  vs  $1/T$  for the calcium-PAA complex and the calcium-3-PPA complex are shown in Figure 36. The computed thermodynamic quantities are given in Table XL along with values for the complexation of  $Mg^{2+}$  ion with PAA. The formation constants for  $Ca^{2+}$  and  $Mg^{2+}$  complexes with pyrophosphate are also shown for comparison in Table XL.

Complexes of calcium and magnesium ion with PAA and pyrophosphate anion are seen to be entropy stabilized and enthalpy destabilized. This behavior is attributable to the "chelate" effect, which will partially result from the release of solvent molecules upon complexation leading to an increase in the entropy of the system. The ligand PAA is more selective with respect to magnesium vs calcium complexation as the magnesium formation constant is approximately an order of magnitude greater than that of the calcium ion. This is different from the pyrophosphate case in which calcium and magnesium show approximately equivalent formation constants.

The effect of pyrophosphate on enzyme kinetics may be two-fold (200). The primary effect is an enhancement of activity via magnesium complexation (197), while a secondary effect is an inhibition due to calcium complexation (198). Hence, PAA would effect enzyme kinetics



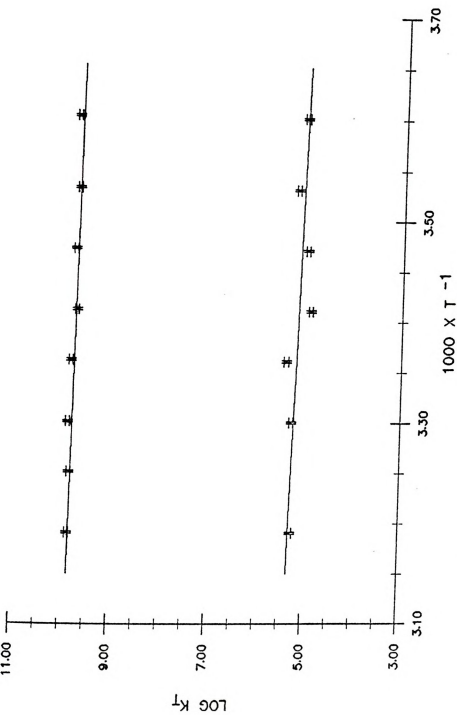


Figure 36. A plot of  $\log K_t$  vs  $1000 \times \text{temperature}^{-1}$  to determine the entropy and enthalpy of a deprotonated  $\text{Ca}^{2+}$  complex with deprotonated PAA (upper curve) and 3-PPA (lower curve).

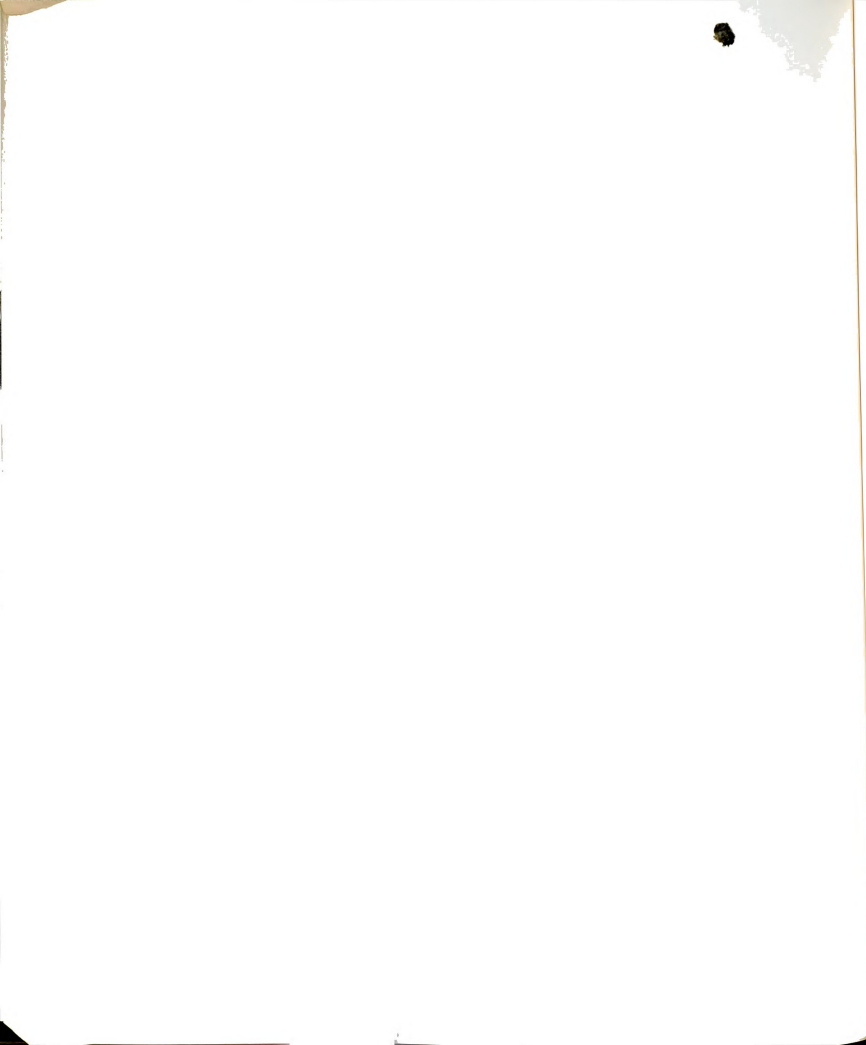




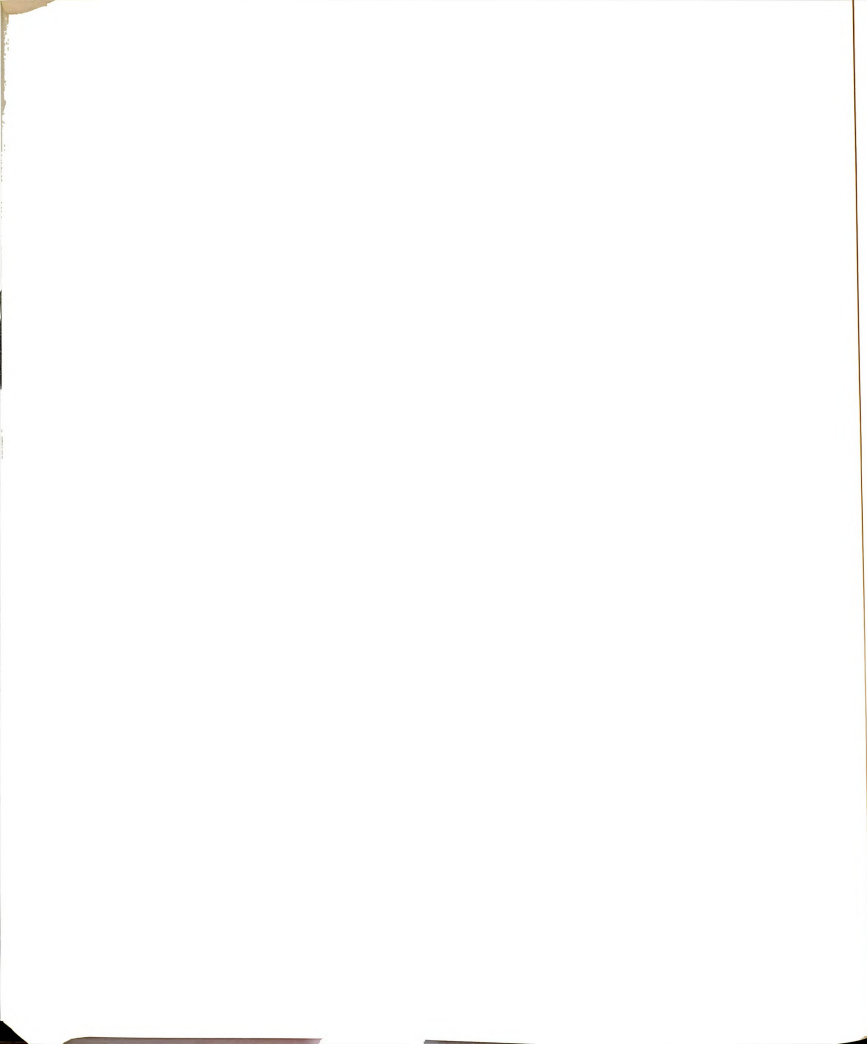
Table XL. Thermodynamic Quantities for Metal Ion Complexation with PAA.

	Log K <sub>f</sub>	$\Delta G^\circ$ (kcal/mole)	$\Delta H^\circ$ (kcal/mole)	$\Delta S^\circ$ (e.u.)	Reference
Ca <sup>2+</sup> ·PAA	4.68±0.03	-6.38±0.07	0.6±0.2	21.4±0.7	This work
Ca <sup>2+</sup> ·3-PPA	3.39±0.09	-4.6 ±0.2	1.1±0.9	14 ±3	This work
Mg <sup>2+</sup> ·PAA	5.58±0.09	-7.2±0.7	3 0.7	35 ±2	a
Ca <sup>2+</sup> ·P <sub>2</sub> O <sub>7</sub> <sup>4-</sup>	5.4	-7.3	4.6	46	b
Mg <sup>2+</sup> ·P <sub>2</sub> O <sub>7</sub> <sup>4-</sup>	5.45	-7.43	3	43	c

<sup>a</sup>P.-H. C. Heubel, Ph.D. Thesis, Michigan State University, (1978).

<sup>b</sup>L. G. Sillen, A. E. Martell, Stability Constants, London, Metcalf & Cooper Ltd., (1964).

<sup>c</sup>R. M. Smith, A. E. Martell, Critical Stability Constants, Vol. 4, Inorganic Ligands, New York, Plenum Press (1976).



more dramatically than pyrophosphate, for, although the magnesium complexation is approximately the same, the calcium complexation is weaker. This leads to an overall enhancement of enzyme kinetics of PAA vs pyrophosphate. The analogy is extended to the in vivo PAA case of replication inhibition, with PAA competing as effectively, and perhaps better, than pyrophosphate for the binding site in the scheme proposed in Section 1.2.2.

The extent of complexation of PAA with calcium would suggest that an in vivo calcium complex with this drug is a possible explanation for the observed side effects.

### 3.3. Summary and Discussion

The complexation formation constants for some metal ions with PAA at 25°C and an ionic strength of 0.05 are given in Table XLI, along with the  $\Delta S^\circ$  of solvation for each ion (196). The plot of the entropy of solvation vs the  $\log K_f^{ML}$  is shown in Figure 37. There appears to be two linear relationships between the solvation entropy and  $\log K_f^{ML}$ . For an entropy of solvation greater than ten e.u., a linear relationship is seen with the formation constant, although there are not enough points to reach a conclusion. Another linear relationship is seen for the remaining metal ions (correlation coefficient of 0.83) between the entropy of solvation and the formation constant. If it is considered that the calcium and magnesium

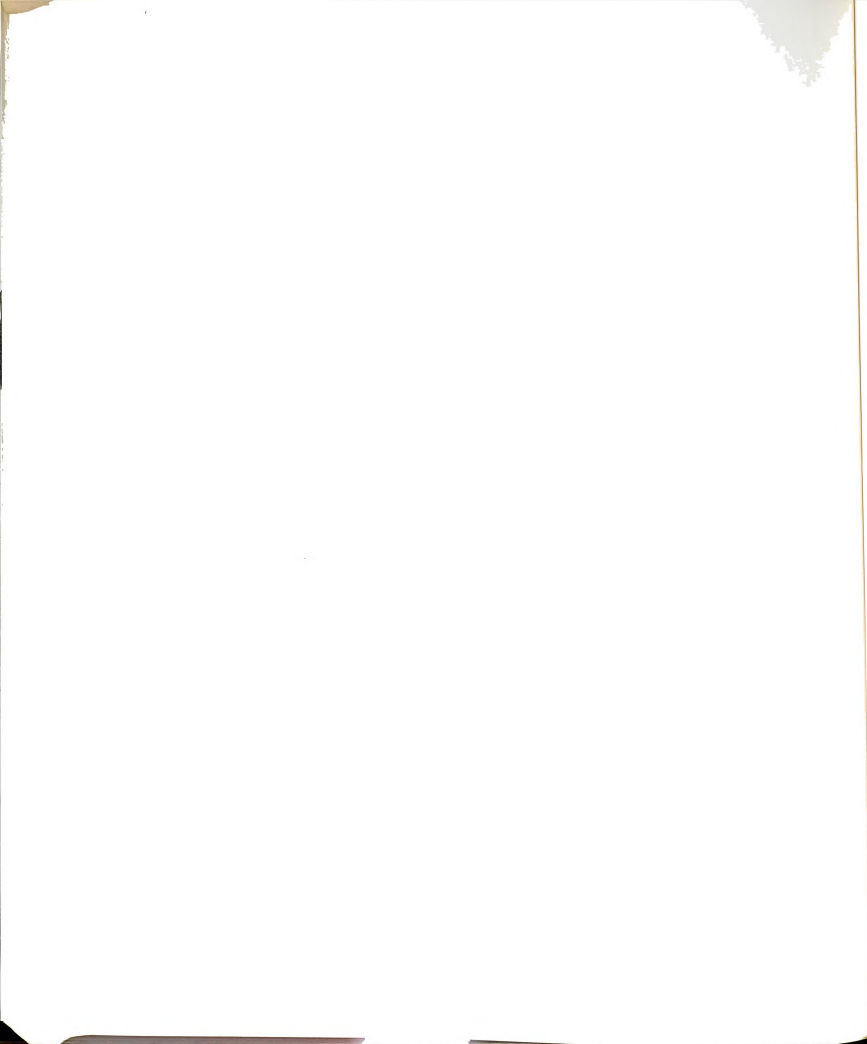


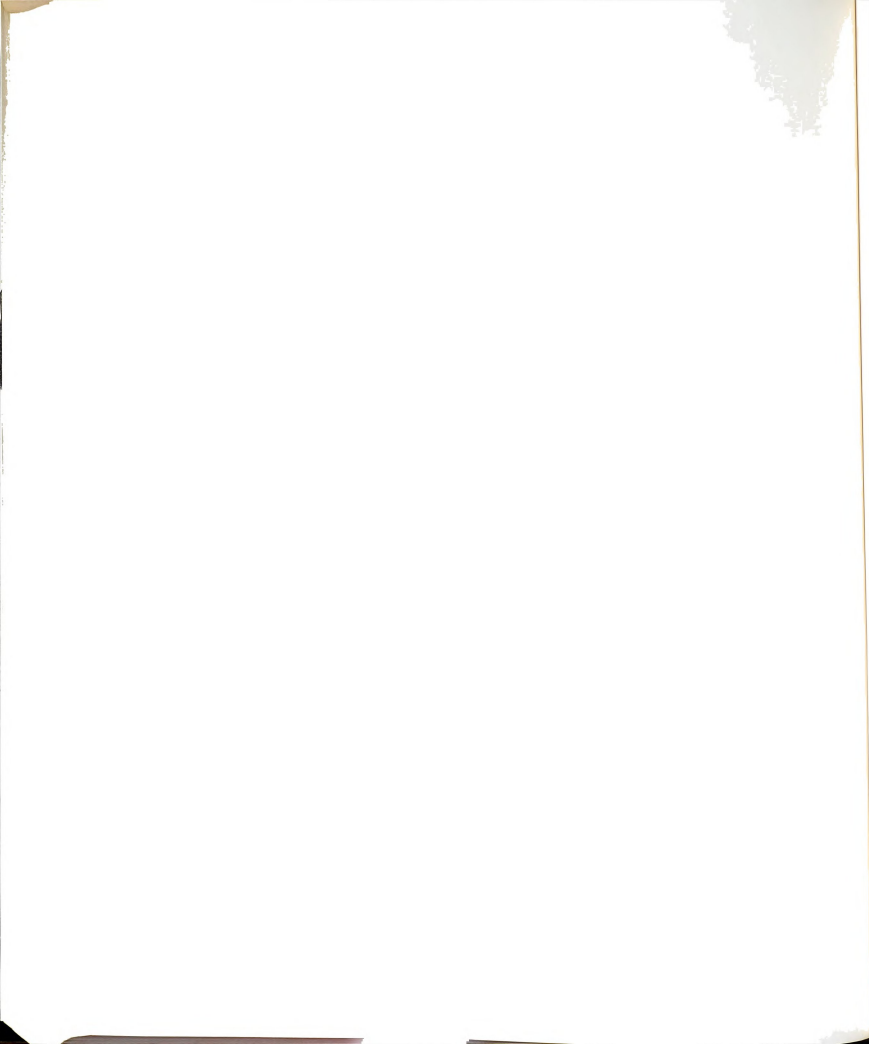
Table XLI. The Solvation Entropy, Radius, and Formation Constants of Some Metal Ions With PAA at 25°C and an Ionic Strength of 0.05.

	$R^{\circ}(\text{Å})$ (66)	$\Delta S^{\circ}_{\text{solv.}}$ in e.u.	$\log K^{\text{ML}}_f$	$\log K^{\text{MHL}}_f$	Source
$\text{Cu}^{2+}$	0.82	-14.5	$8.0 \pm 0.1$	$4.2 \pm 0.1$	This Work
$\text{Zn}^{2+ \text{a}}$	0.83	-11.9	$5.35 \pm 0.03$	$3.44 \pm 0.03$	(31)
$\text{Mg}^{2+}$	0.78	-11.7	$4.50 \pm 0.02$	$2.56 \pm 0.05$	(30)
$\text{Mn}^{2+}$	0.80	- 9.5	$5.25 \pm 0.06$	$3.0 \pm 0.1$	This work
$\text{Cd}^{2+ \text{b}}$	1.03	- 2.6	$3.9 \pm 0.1$		(30)
$\text{Ca}^{2+}$	1.06	1.8	$3.67 \pm 0.02$	$2.10 \pm 0.06$	This work
$\text{Sr}^{2+}$	1.27	3.4	$3.67 \pm 0.02$	$2.56 \pm 0.06$	(30)
$\text{Ag}^+$	1.13	3.7	$3.11 \pm 0.05$	$2.7 \pm 0.1$	This work
$\text{Na}^+ \text{c}$	0.98	5.1	$1.43 \pm 0.02$	$0.79 \pm 0.05$	(30)
$\text{Ba}^{2+}$	1.43	14.1	$3.67 \pm 0.02$	$2.50 \pm 0.06$	(30)
$\text{Tl}^+$	1.49	14.6	$2.51 \pm 0.03$	-----	This work
$\text{Pb}^{2+}$	1.32	15.2	$7.0 \pm 0.1$	$4.1 \pm 0.1$	This work

<sup>a</sup> $I = 0.15, 37^{\circ}\text{C}.$

<sup>b</sup> $I = 0.4.$

<sup>c</sup> $I = 0.078.$



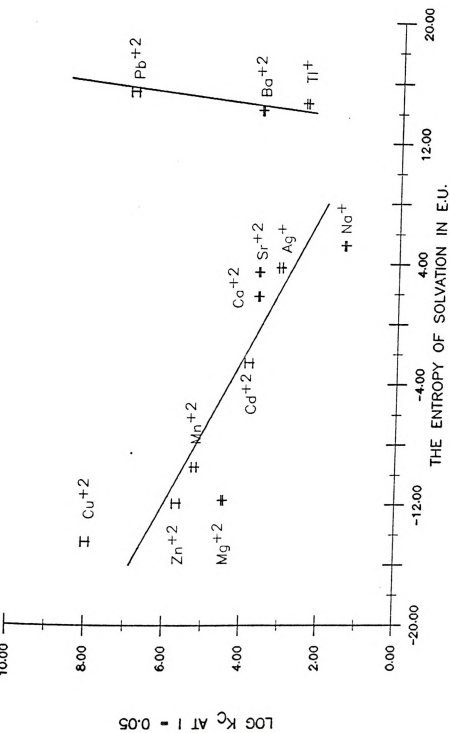
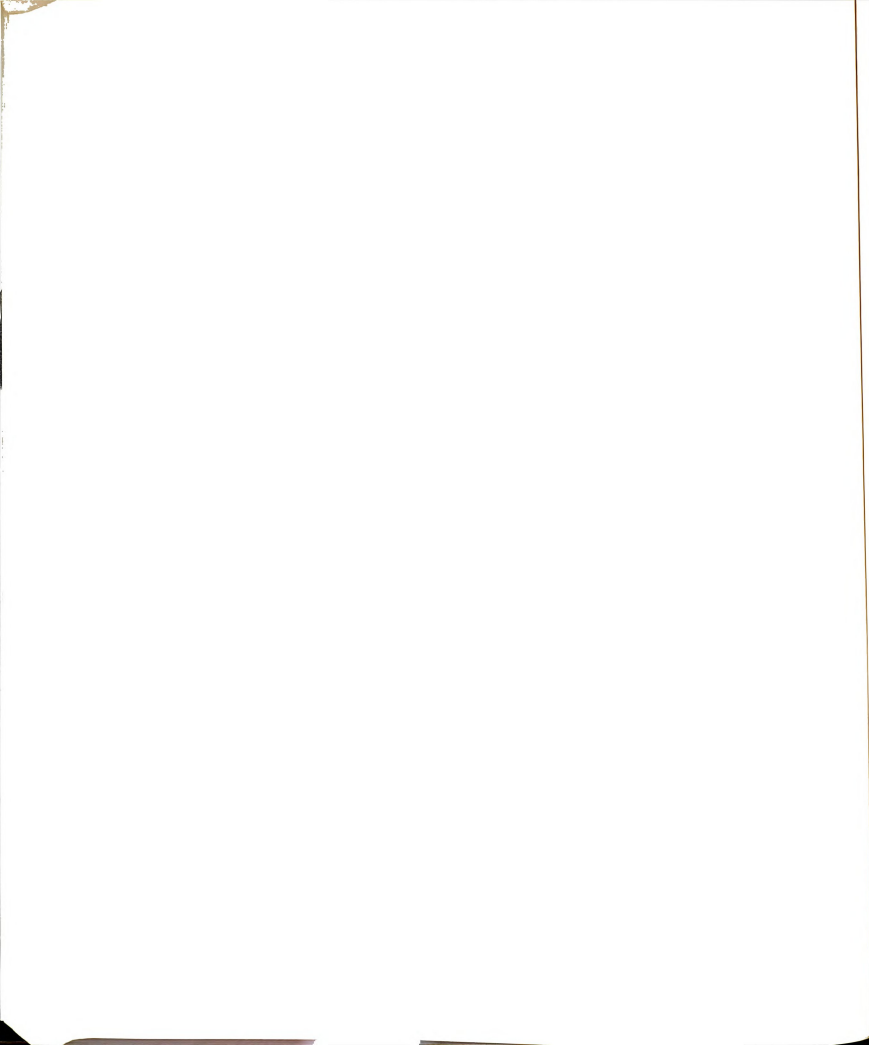


Figure 37. A plot of the entropy of solvation (e.u.) vs the log formation constant of some metal ion complexes with deprotonated PAA.

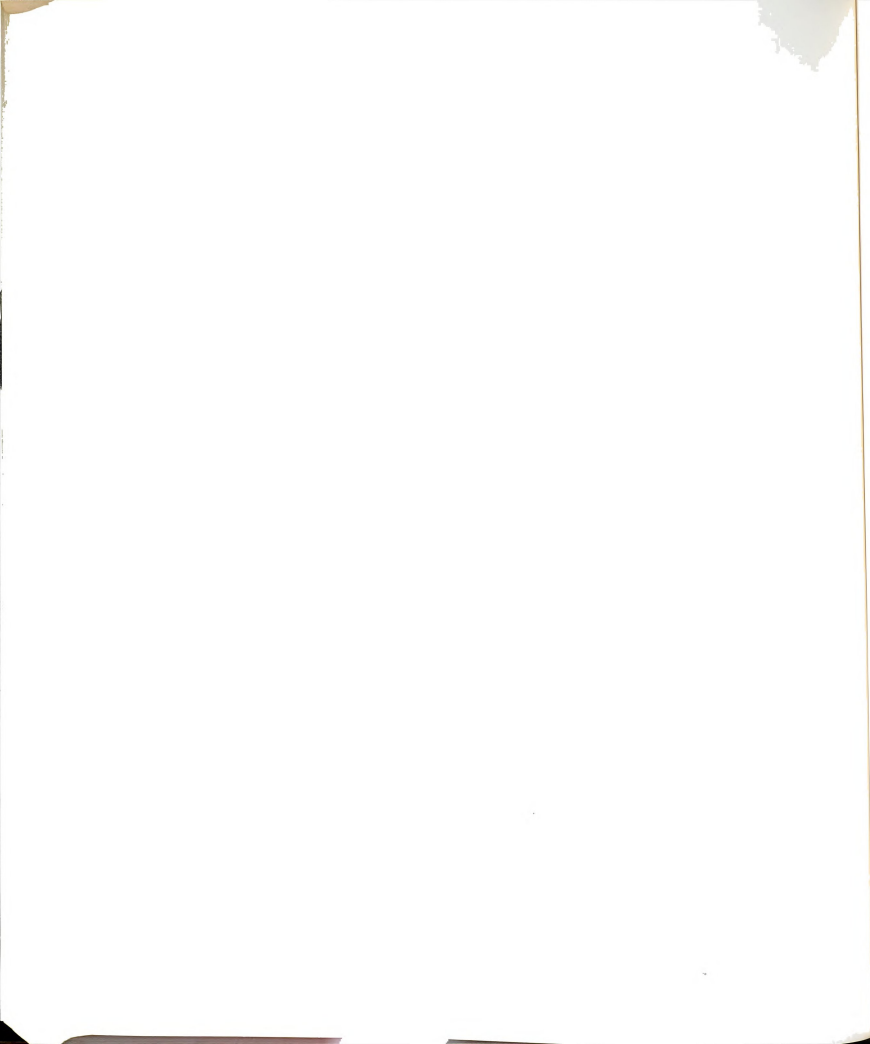




complexes are entropy stabilized, it may be generalized that these other cations might also exhibit an entropy stabilized complexation. (In the case of calcium and magnesium complexation, the enthalpy of complexation detracts less than 10% from the overall free energy of complexation. It is expected that the enthalpy will also play a minor role in all complexes with PAA.) This leads to the conclusion that stabilization of the complex is derived from the release of solvent molecules (thereby increasing the entropy) upon complexation. This phenomena is normally associated with the "chelate effect" (201).

#### 3.4. Phosphonoacetic Acid Analogs

Microbiological studies (150,199) of phosphonoformic acid (PFA) and 3-phosphonopropionic acid (3-PPA) indicate that the former inhibits the replication of some Herpes viruses while the latter does not. Complexation studies of PAA, PFA, and 3-PPA have shown that the biological inhibition trends of these ligands are paralleled by the extent of complexation with the magnesium(II) ion (158). To draw further analogies between the biological effects and complexation, the complexing ability of these drugs were tested with manganese(II), thallium(I), and calcium-(II) ions.

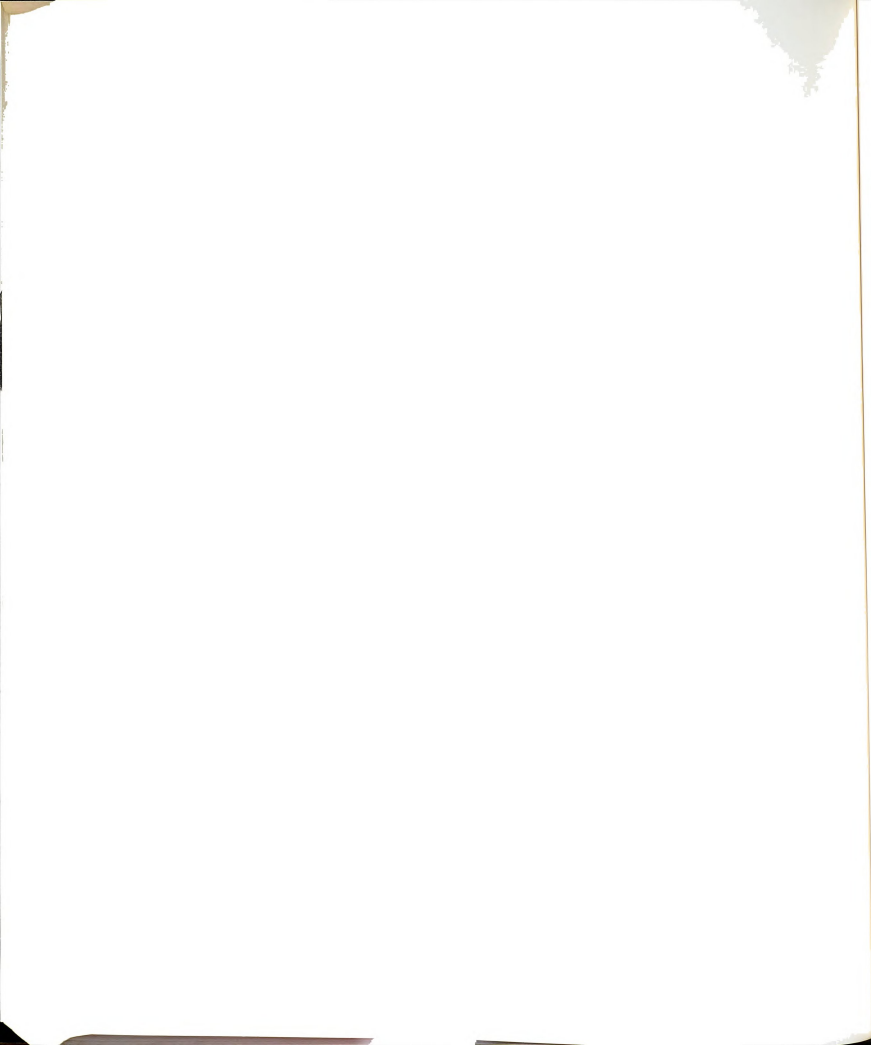


### 3.4.1. Manganese Electron Spin Resonance

Manganese electron spin resonance was used to study the complexation of manganese with PFA and 3-PPA at an ionic strength of 0.05. Both PFA and 3-PPA are triprotic acids which will protonate according to equilibria (3), (4) and (5). The protonation constants were determined at  $I = 0.05$  by Heubel (158) and are given in Table XLV, along with those of PAA at  $I = 0.05$ . The formation constants for complexes of manganese with these ligands were determined according to the procedures outlined in Sections 2.3.1 and 3.1.1. The resultant values were:  $\log K_f^{\text{MnPFA}} = 5.34 \pm 0.05$ ,  $\log K_f^{\text{MnHPFA}} = 2.57 \pm 0.05$ ,  $\log K_f^{\text{Mn-3-PPA}} = 3.15 \pm 0.04$ , and  $\log K_f^{\text{MnH-3-PAA}} = 1.6 \pm 0.2$ .

### 3.4.2. Cyclic Voltammetry

The  $pK_a$ 's of PFA and 3-PPA were calculated at a given ionic strength from the appropriate Guntelburg equation using the data of Heubel (158). Formation constants were then determined for a deprotonated thallium-PFA complex at different ionic strengths. There was no evidence of thallium complexation with 3-PPA or the protonated form of PFA. Equation (14) was then used to calculate the thermodynamic formation constant from a linear extrapolation to zero ionic strength, shown in Figure 38. The values of each point are given in Table XLII. The ion size parameter



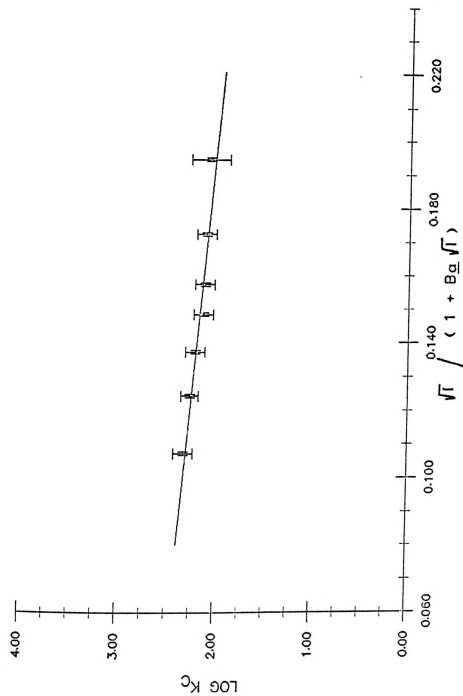
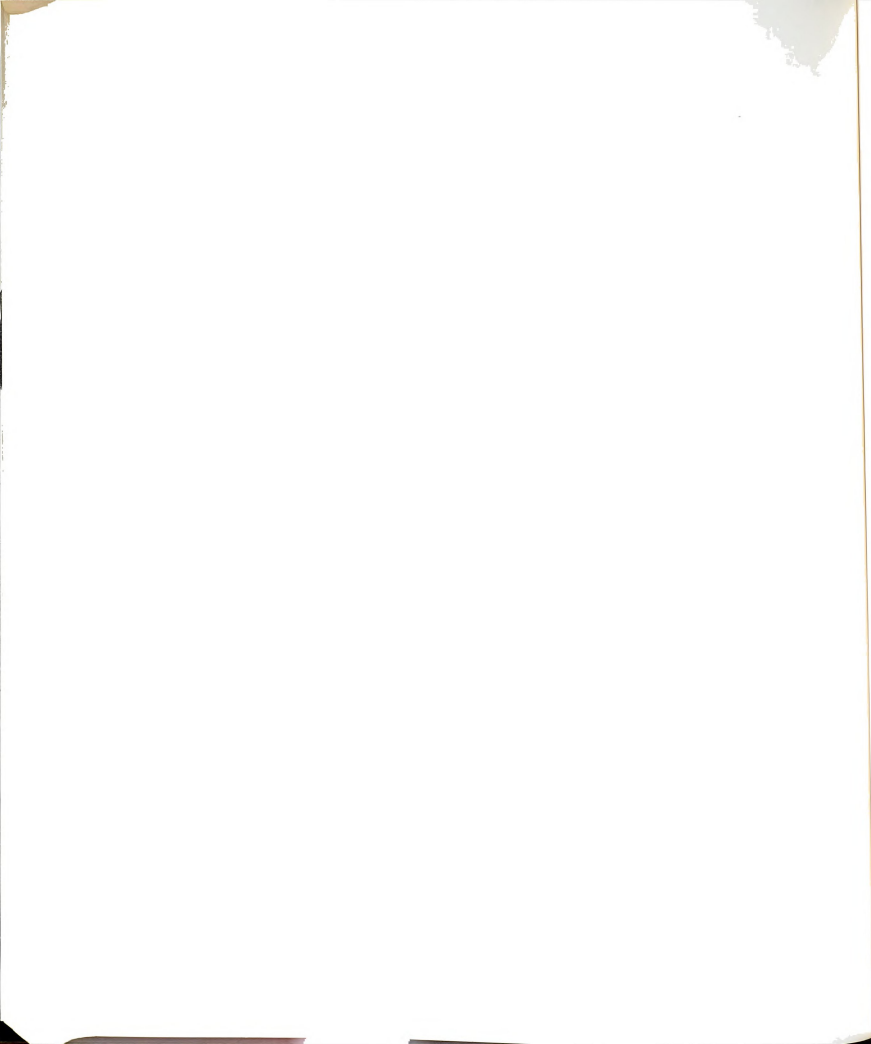


Figure 38. A plot of the log formation constant of a deprotonated PFA-Tl complex as a function of the ionic strength.



Table XLII. Formation Constants of Thallium (I)-PFA Complexes at Different Ionic Strengths and 25°C.

Ionic Strength	$\log K_f^{ML}$
0.030	2.3 ± 0.1
0.040	2.27 ± 0.09
0.050	2.2 ± 0.1
0.062	2.1 ± 0.1
0.070	2.1 ± 0.1
0.092	2.1 ± 0.1
0.131	2.0 ± 0.2





was found to be 9.0, again in poor agreement with other calculated values (190,191). The thermodynamic formation constant is  $2.65 \pm 0.07$ .

### 3.4.3. Potentiometry

Thermodynamic formation constants for Ca-PFA and Ca-3-PPA were calculated from potentiometric data using a calcium ion selective electrode. The formation constants were determined at different ionic strengths as in Section 3.1.3, then extrapolated to zero ionic strength using Equations (11) and (12). The data are plotted in Figures 39 and 40, with the values shown in Tables XLIII and XLIV. The resulting ion-size parameter of  $5 \pm 1 \text{ \AA}$  compares well with the values of Stokes (190) and Kielland (191), as well as with the value obtained from studies of the calcium-PAA system. The significance of the  $a$  parameter is seen in the self-consistency of its determination for a series of analogous ligands (PAA, PFA, and 3-PPA) and the agreement in values obtained by very different methods (190,191). While the interpretation of this parameter as the solvated radius may be debatable, these and other studies indicate that it does have a physical significance. The thermodynamic formation constants are:  $\log K_{ML}^{PFA} = 4.40 \pm 0.03$ ,  $\log K_{MHL}^{PFA} = 2.6 \pm 0.1$ ,  $\log K_{ML}^{3-PPA} = 3.39 \pm 0.09$ , and  $\log K_{MHL}^{3-PPA} = 2.3 \pm 0.1$ .



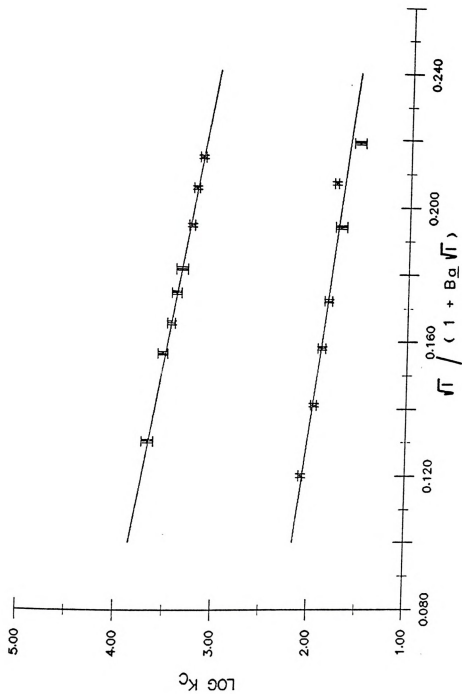
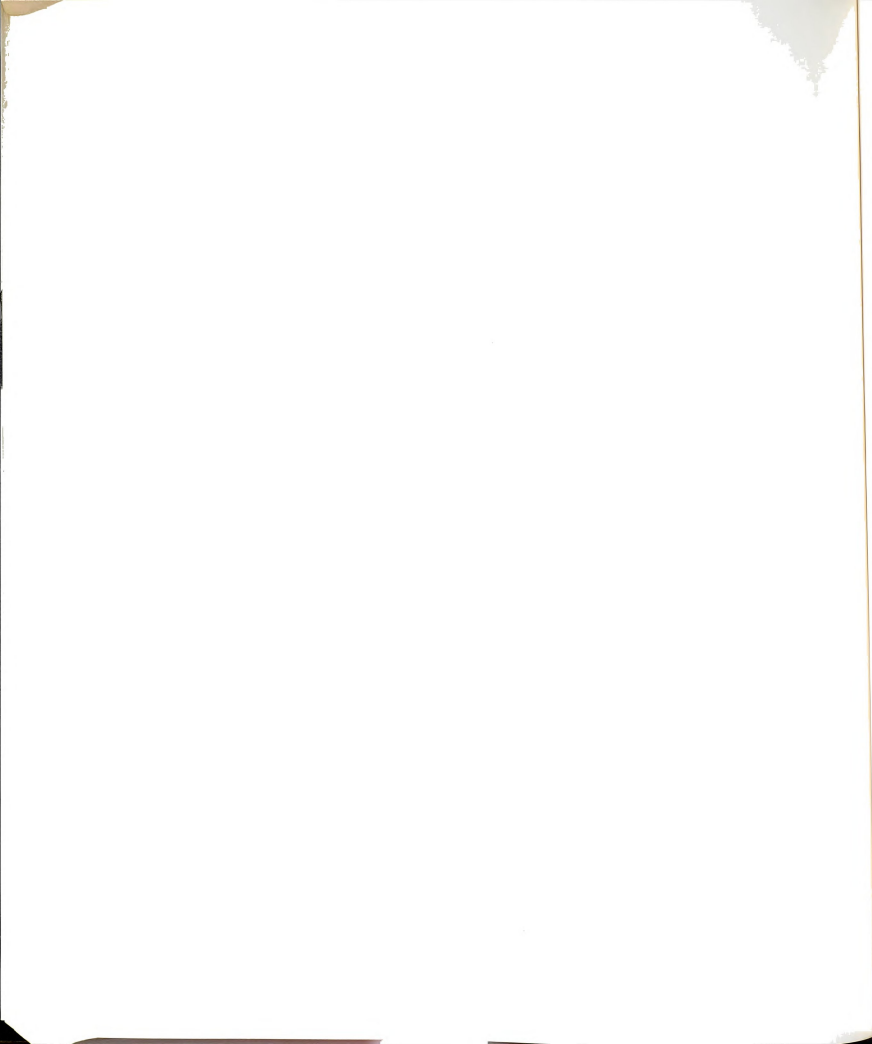


Figure 39. A plot of the log formation constant of Ca-PPA as a function of the ionic strength (upper curve - deprotonated PPA, lower curve - mono-protonated PPA).



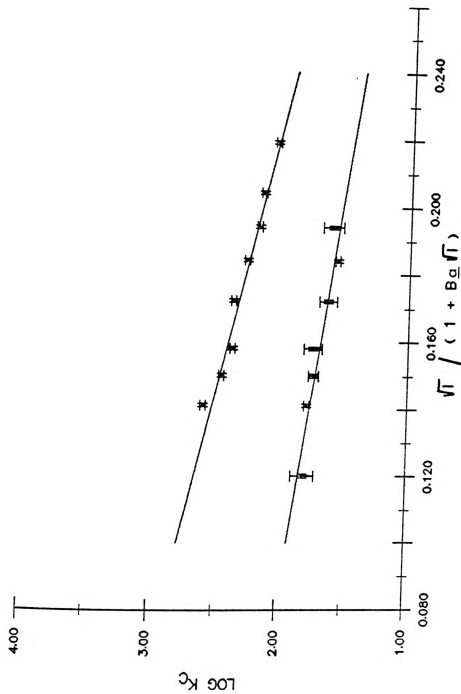


Figure 40. A plot of the log formation constant of Ca-3-PPA as a function of the ionic strength (upper curve - deprotonated PAA, lower curve - mono-protonated PAA).

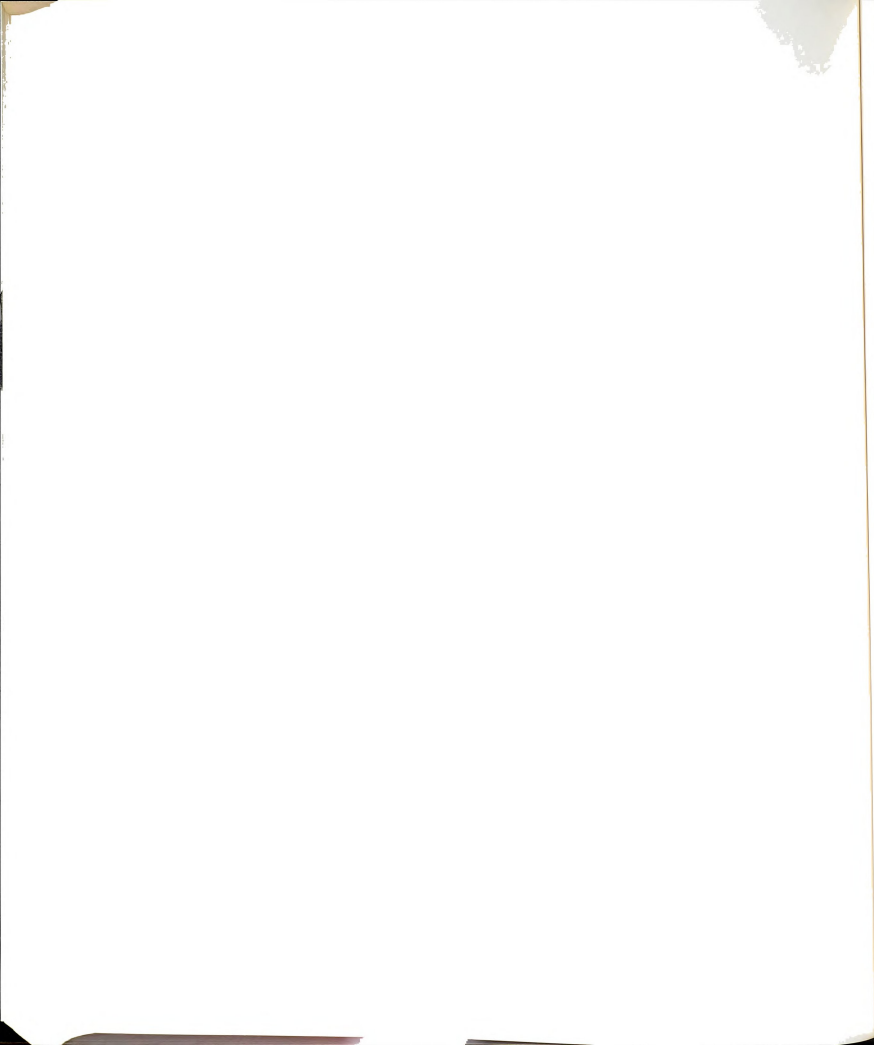


Table XLIII. Formation Constants of Calcium(II)-PFA Complexes as a Function of the Ionic Strength at 25°C.

Ionic Strength	$\log K_f^{ML}$	$\log K_f^{MHL}$
0.02	-----	2.09 ± 0.02
0.03	3.69 ± 0.06	1.97 ± 0.03
0.04	-----	1.90 ± 0.02
0.05	3.55 ± 0.05	1.84 ± 0.04
0.06	3.47 ± 0.04	-----
0.07	3.42 ± 0.05	1.72 ± 0.06
0.08	3.37 ± 0.06	1.78 ± 0.02
0.10	3.28 ± 0.03	1.54 ± 0.06
0.12	3.24 ± 0.03	-----
0.14	3.18 ± 0.03	-----

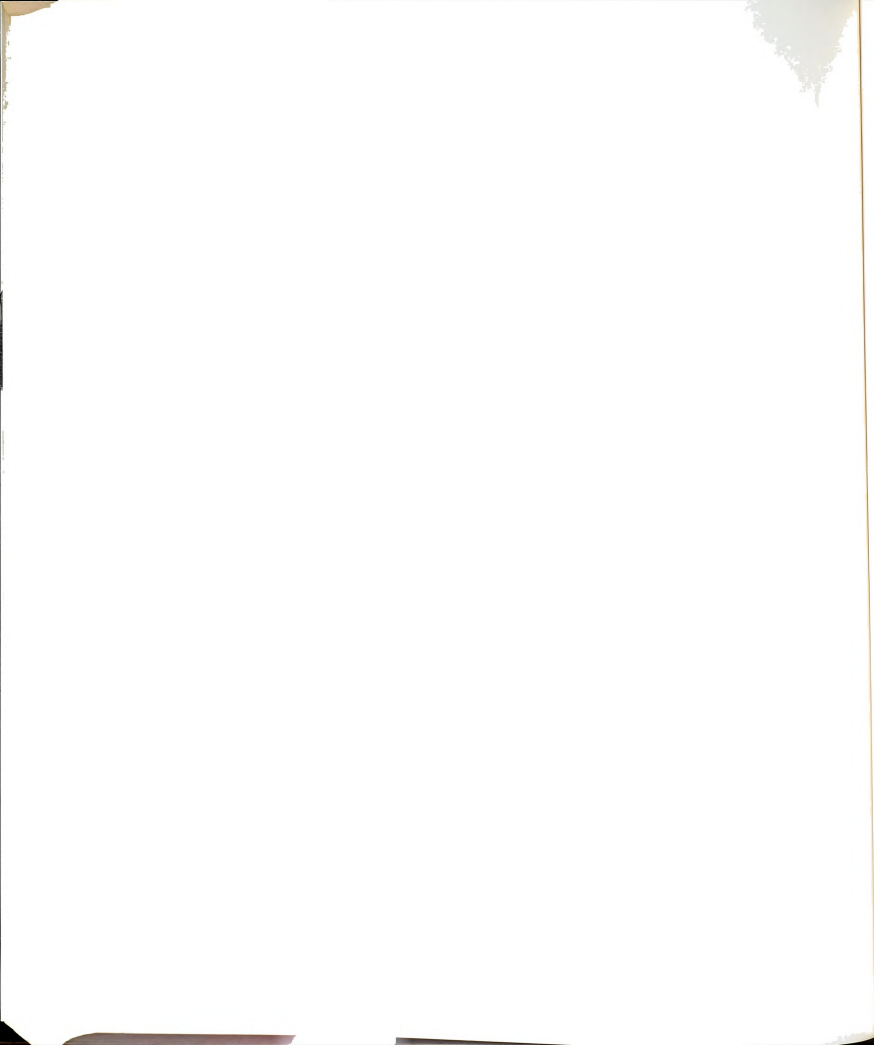




Table XLIV. Formation Constants of Calcium(II)-3-PPA Complexes as a Function of the Ionic Strength at 25°C.

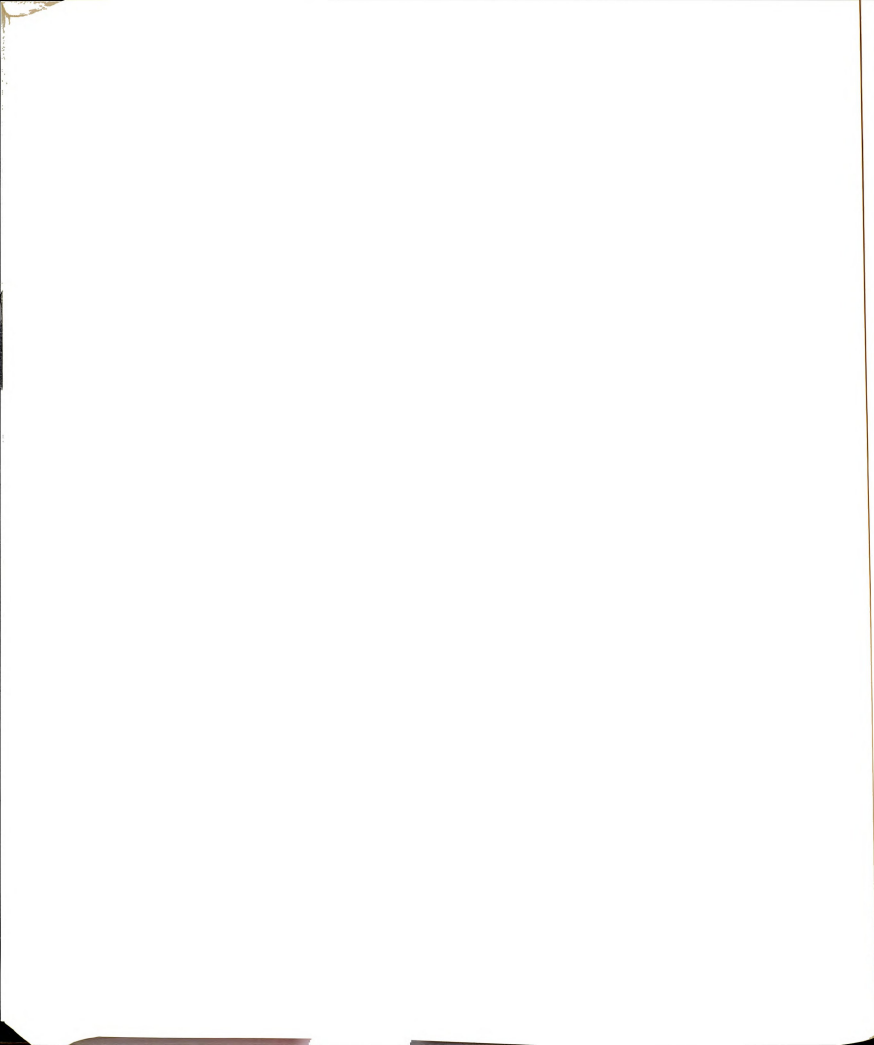
Ionic Strength	$\log K_f^{ML}$	$\log K_f^{MHL}$
0.02	-----	1.81 ± 0.09
0.03	2.60 ± 0.02	1.79 ± 0.02
0.035	2.46 ± 0.02	1.74 ± 0.04
0.04	2.38 ± 0.02	1.75 ± 0.07
0.05	2.38 ± 0.02	1.64 ± 0.07
0.06	2.28 ± 0.02	1.57 ± 0.02
0.07	2.19 ± 0.02	1.61 ± 0.08
0.08	2.16 ± 0.07	-----
0.10	2.06 ± 0.02	-----

1848

### 3.5. Thermodynamic Studies of 3-PPA Complexes

Since 3-PPA plays no role in inhibition of Herpes virus and exhibits a weak complex with calcium (as compared to PAA and PFA), it was of interest to contrast the enthalpy and entropy of complexation with that of PAA. The formation constant of a deprotonated calcium-3-PPA complex was determined for different temperatures at an ionic strength of 0.05. Again, due to the larger error, the mono-protonated complex was not studied. Using the Debye-Hückel equation with an  $a$  of  $5 \text{ \AA}$ , the thermodynamic formation constant was then calculated at a given temperature. Equation (17) was then used to calculate  $\Delta H^\circ$  and  $\Delta S^\circ$  of complexation, shown in Table XLV.

Similarly to the PAA case, the calcium-3-PPA complex is entropy stabilized and enthalpy destabilized. While the  $\Delta H^\circ$  values for PAA and 3-PPA calcium complexes are approximately equal, the  $\Delta S^\circ$  of complexation is much lower in the case of 3-PPA. The stability of these complexes with calcium is then a function of the entropy of complexation, with the enthalpy contributing only a small destabilizing effect. Hence, the chelate effect is likely the dominant mechanism in most complexes with PAA, PFA, and 3-PPA.



### 3.6. Summary and Discussion

The formation constants of some metal ions with PAA, PFA and 3-PPA are shown in Table XLV at 25°C and  $I = 0.05$ . The complexing ability of PAA and PFA are approximately equivalent for the deprotonated complexes, which will predominate at a biological pH of 7. The formation constants of PAA and PFA complexes with calcium and manganese ions agree well with each other, while that for the magnesium-PFA is closer to PAA than 3-PPA. Since the biological effects of PAA and PFA are also approximately equivalent, it seems that there may be a correlation between the biological effects of these drugs and their complexing ability. This conclusion is supported by the data from complexation studies of 3-PPA. This ligand has no biological inhibitory activity against Herpes Virus and shows a complexing ability that is at least an order of magnitude less than that for PAA or PFA when considering a deprotonated complex.

### 3.7. Conclusion

Complexation studies of PAA with  $Mn^{2+}$ ,  $Tl^{+}$ ,  $Cu^{2+}$ ,  $Pb^{2+}$ ,  $Ag^{+}$ , and  $Ca^{2+}$ , together with data from other sources (51,157) seem to indicate that there is a general relationship between the entropy of solvation and the strength of complexation. Temperature dependence studies of the calcium-PAA and 3-PPA systems have shown that complexation

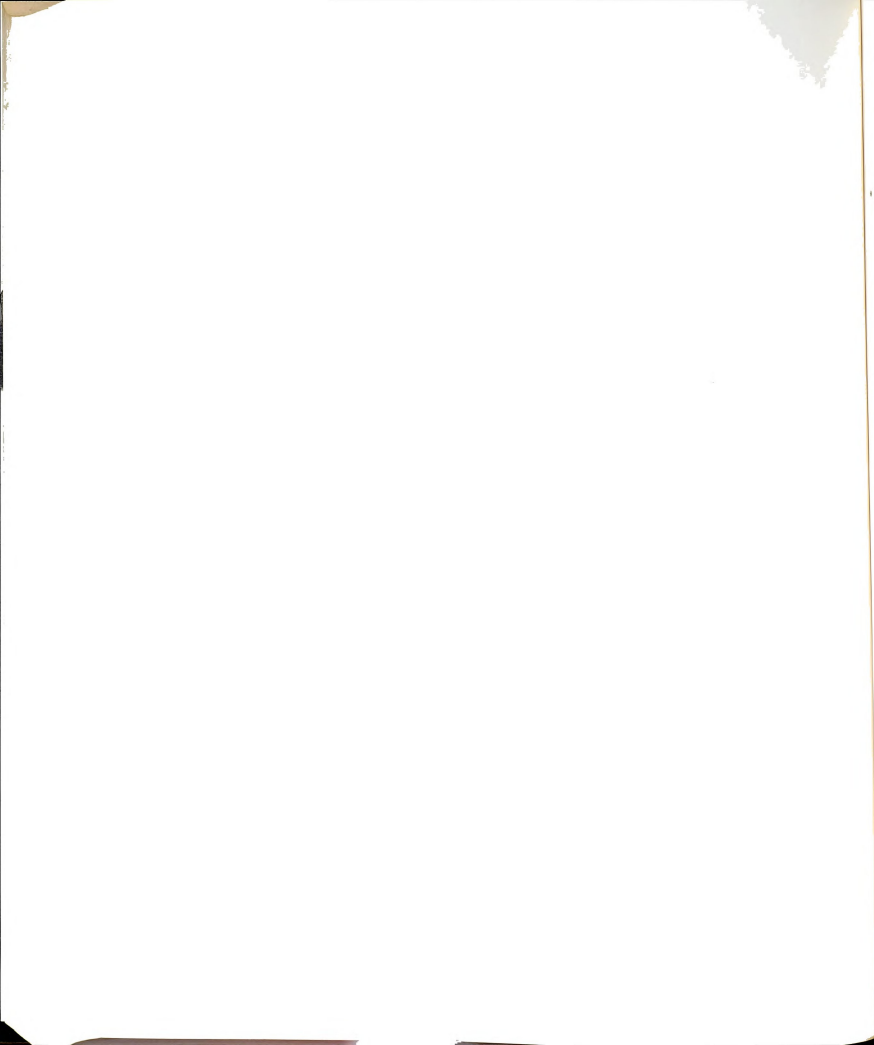
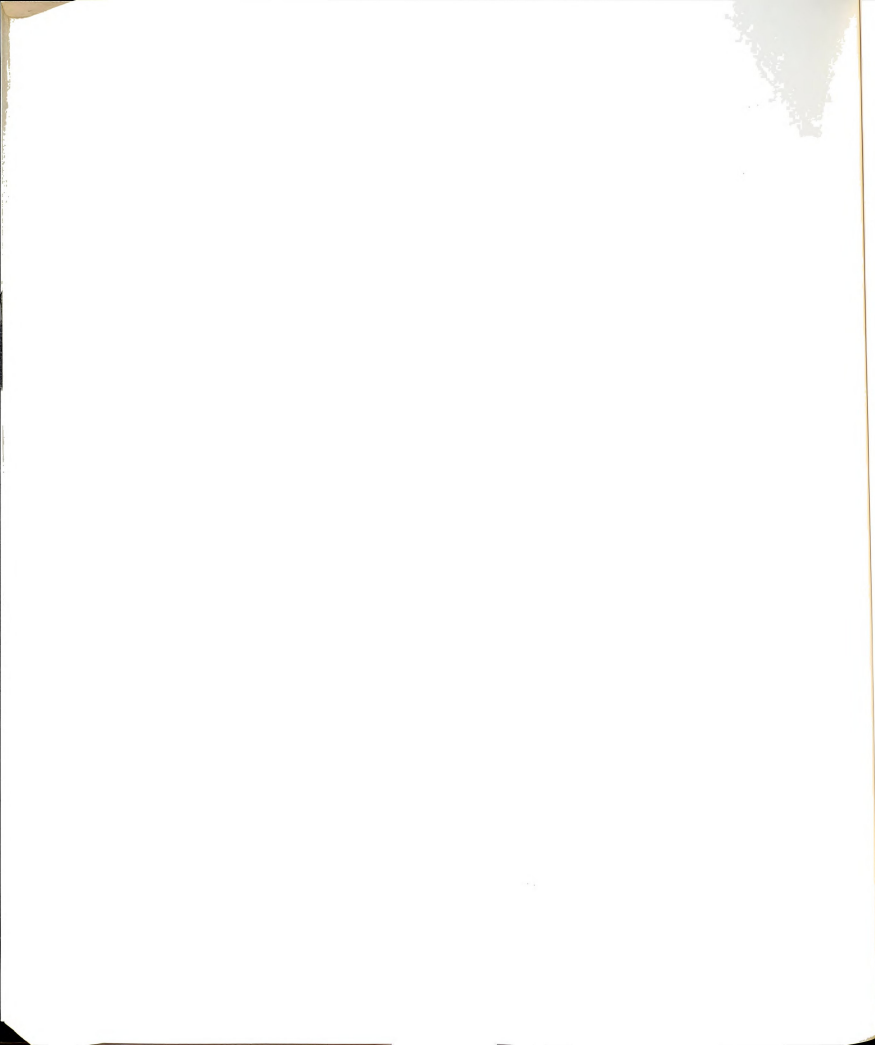


Table XLV. Formation Constants for Some Metal Ions with PAA, PFA, and 3-PPA at 25°C and I = 0.05.

	PFA	PAA	3-PPA
$\log K_f^{\text{MgL}} (30)$	3.59±0.05	4.50±0.05	2.28±0.05
$\log K_f^{\text{MgHL}} (30)$	1.7 ±0.3	2.6 ±0.1	1.7 ±0.1
$\log K_f^{\text{CaL}}$	3.55±0.05	3.67±0.02	2.38±0.02
$\log K_f^{\text{CaHL}}$	1.84±0.04	2.10±0.06	1.64±0.07
$\log K_f^{\text{MnL}}$	5.34±0.05	5.25±0.06	3.15±0.04
$\log K_f^{\text{MnHL}}$	2.57±0.05	2.97±0.06	1.6 ±0.2
$\log K_f^{\text{TlL}}$	2.63±0.07	2.62±0.04	-----
$pK_1$	1.7 ±0.1	2.18±0.04	2.26±0.04
$pK_2$	3.59±0.02	4.94±0.02	4.63±0.02
$pK_3$	7.56±0.02	8.14±0.02	7.75±0.02





is entropy stabilized and enthalpy destabilized, with the entropy term dominating. These studies, together with similar studies using magnesium, have shown that entropy stabilization, or the chelate effect, is the most likely mechanism which explains complex stability. Studies on PAA, PFA, and 3-PPA led to the conclusion that there may be a correlation between the complexing ability of these ligands and their biological activity.



APPENDICES



APPENDIX A

THE GENERAL USE OF THE NON-LINEAR CURVE  
FITTING ROUTINE KINFIT4



THE GENERAL USE OF THE NON-LINEAR CURVE  
FITTING ROUTINE KINFIT4

A.1. Scope of KINFIT4 Usage

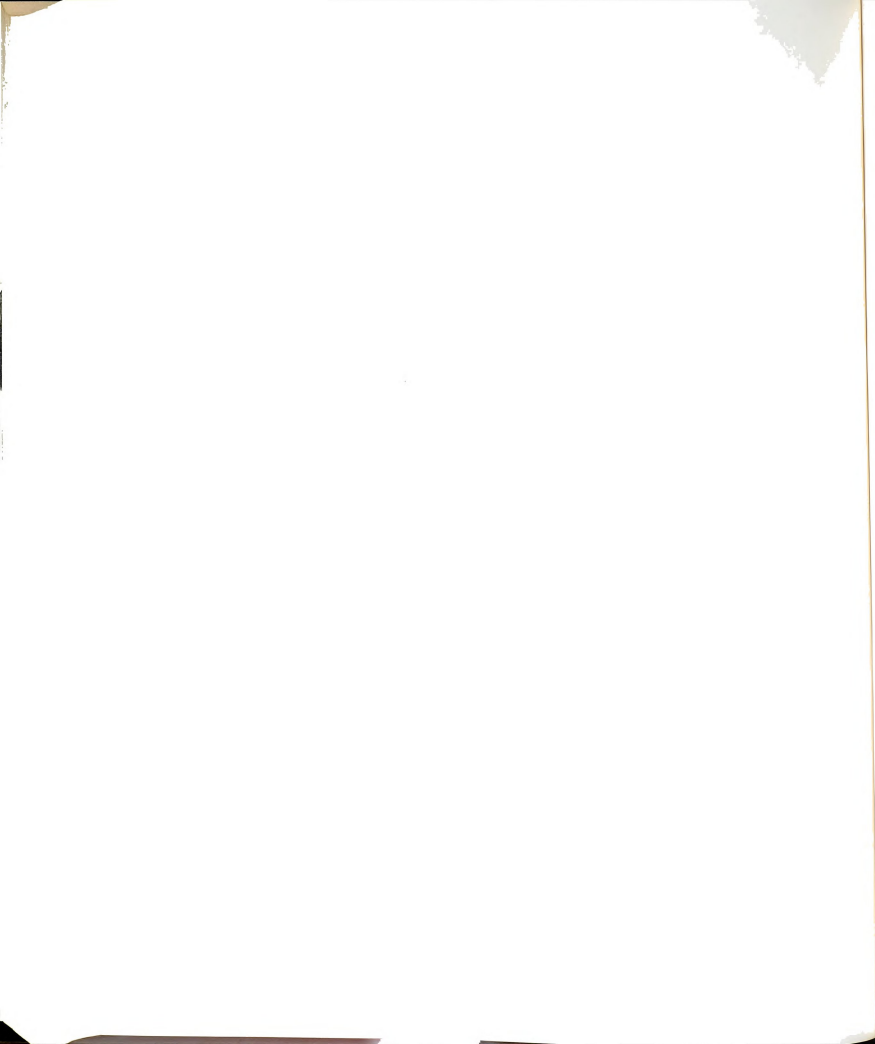
The program KINFIT4 was used to curve fit the data for all linear relationships (Lingane equation, calibration data, van't Hoff plots, thermodynamic  $K_f$  plots, etc.) as well as some non-linear relationships (some calibration curves, the Buck equation, etc.). The experimentally determined quantities were expressed in such a manner that one quantity was always expressed as a function of the other, e.g.,

$$y = f(x) \qquad (1)$$

with the function  $f(x)$  containing the unknown parameters to be determined by a computer fit. The resultant calculation of the unknowns was accompanied by such statistical data as the standard deviation of a given calculated value, the coupling (correlation) between the calculated values, and a plot of the actual data vs that calculated from the computed unknowns.

A.2. Data Input

For a more complete summary of the data input instructions, see Reference (204).





A.2.1. Equation Card / 6X,74A

This card describes the relationship between experimentally measured variables and is of the form

$$\text{CALC} = f(\text{XX}(1)) \quad (2)$$

A.2.2. Residual Calculation Card / 6X,74A

This card is of the form

$$\text{RESID} = \text{CALC} - \text{XX}(2) \quad (3)$$

where XX(2) is the dependent variable from Equation (2).

A.2.3. Control Card / 1015 NOPT, IMETH, ITMAX, IWT,  
IRX, ISMIN, IPLT, NCST,  
TEST, KVAR

Unless specified, all values are set at the default zero. Only those quantities which were not set at the default will be mentioned.

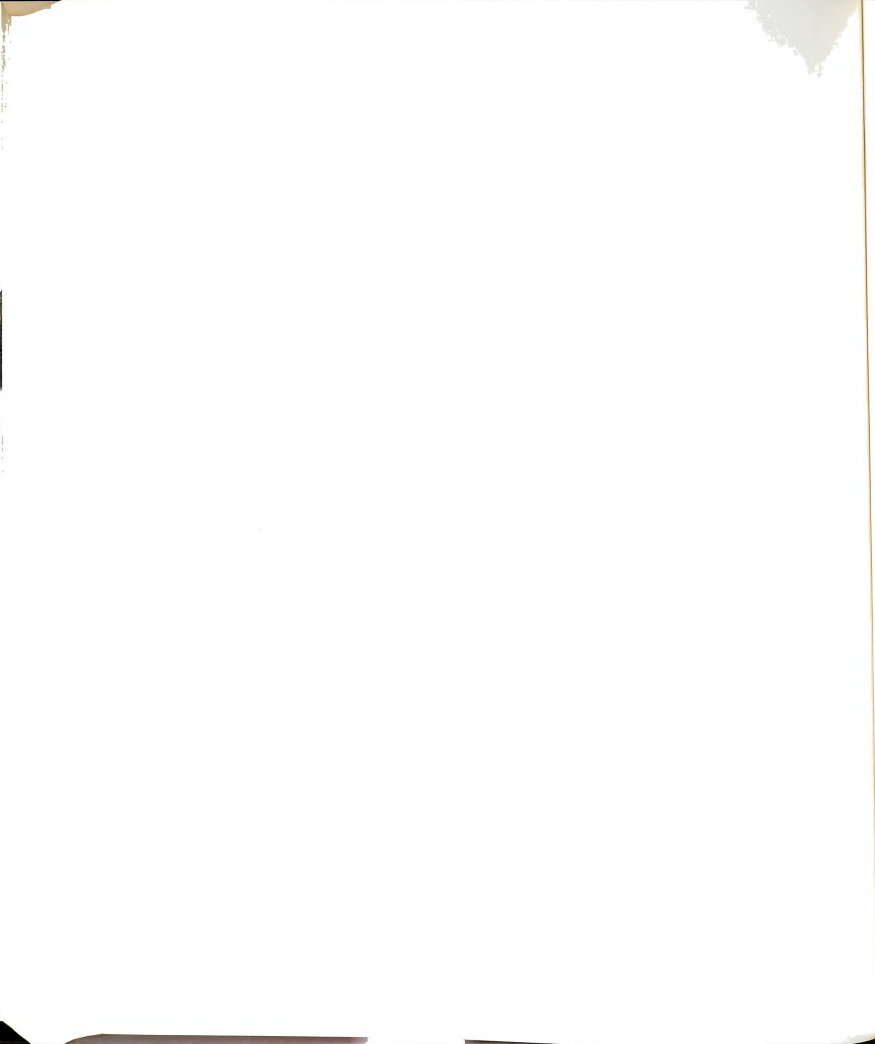
NOPT is the number of data points.

ITMAX is the maximum number of iterations permitted if convergence is not attained.

TEST is the convergence tolerance.

## A.2.4. Descriptive Title / 70A

## A.2.5. Constant Card / 8E10.5 CONST(1)



A.2.6. Initial Estimate Card / 8F10.5 U(i)

A.2.7. Data / 8E10.5 XX(1), <sup>2</sup>(1), XX(2), <sup>2</sup>(2)

A.2.8. Blank Card

A.2.9. <sup>6</sup><sub>7</sub><sup>8</sup><sub>9</sub>



APPENDIX B

DATA REDUCTION OF A POTENTIOMETRIC TITRATION FOR  
THE DETERMINATION OF COMPLEX FORMATION  
CONSTANTS USING THE COMPUTER  
PROGRAM MINIQVAD



DATA REDUCTION OF A POTENTIOMETRIC TITRATION FOR THE  
DETERMINATION OF COMPLEX FORMATION CONSTANTS USING  
THE COMPUTER PROGRAM MINIQAD

B.1. The Scope of MINIQAD

The computer program MINIQAD is a versatile program which enables the user to determine simultaneously up to 20 unknown formation constants with five reactants from potentiometric data. The program can accommodate up to three known concentrations (the pH, free metal ion concentration, free ligand concentration, etc.) determined from potentiometric data.

The equations describing the equilibria involved are of the form



with a formation constant of

$$K_f = [A_a B_b C_c] / [A]^a [B]^b [C]^c \quad (2)$$

In the specific case of complexation with PAA, all equilibria can be described in terms of the free metal ion concentration,  $[M]$ , the concentration of the free deprotonated ligand,  $[L]$ , and the hydrogen ion concentration,  $[H]$ , with the complex concentration calculated by the program. Hence, the formation constants for equilibria (1) and (2) from Part III, Section 3.1.1.





$$K_f(\text{ML}) = [\text{ML}]/[\text{M}][\text{L}] \quad (3)$$

and

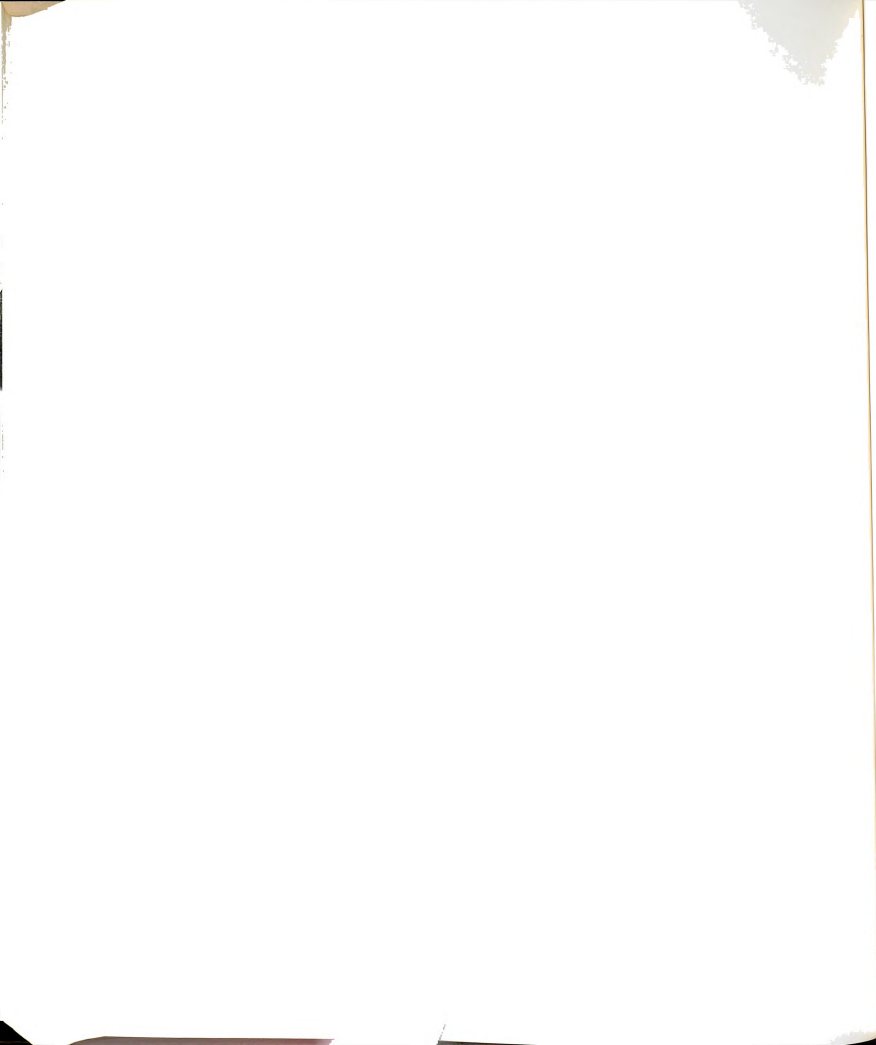
$$K_f(\text{MHL}) = [\text{MHL}]/[\text{M}][\text{H}][\text{L}] = K_f(\text{MHL})/K_3 \quad (4)$$

where  $K_3$  is the third acidity constant for the ligand. The acidity constants are written as cumulative  $\beta$ 's, i.e.,

$$K_2 = [\text{H}_2\text{L}]/[\text{H}]^2[\text{L}] \quad (5)$$

The computer program will accept the stoichiometric coefficients of the reactants for all equilibria involved. Along with initial estimates (or values obtained from other sources) for the respective formation constants. The user then has the option of refining the formation constants or holding them constant. In the PAA study, the acidity constants were known (158), leaving the complex formation constants to be determined by Equations (3) and (4). Both the pH and the free calcium ion concentration were monitored potentiometrically, while the total ligand concentration was known. Each data point input to the program consisted of a pH and volume of ligand added.

The program was modified (158) to include the KINFIT4 program described in Appendix A. This program is a general purpose non-linear curve fitting routine that was used to calculate the slope, intercept, and residual calcium from calibration data for the calcium ion selective electrode.



The data were fit to the equation

$$E_{\text{obs}} = b + M \log [(C_a^{+2})_f + R] \quad (6)$$

where  $E_{\text{obs}}$  is the observed emf,  $b$  is the intercept,  $m$  the slope,  $(Ca^{+2})_f$  the free calcium concentration, and  $R$  a residual to account for non-linearity in the calibration curve at low concentrations.

## B.2. Data Input Format for MINIQVAD

### B.2.1. KINFIT Calibration Input

B.2.1.1. Control card/8I5, F10.0, I5/see Appendix A, Section

B.2.1.2. Descriptive title/20A4

B.2.1.3. Initial Estimates/8F 10.5

This card will contain the initial estimates of the slope, intercept, and residual.

B.2.1.4. Data/8F 10.5/log  $(Ca^{+2})_f$ ,  $\sigma_{Ca}$ , Emf,  $\sigma_{\text{emf}}$

The data are input as the log of the calcium ion concentration, its estimated variance, the emf, and its estimated variance. The program internally converts the log of the concentration to a concentration, which is then used



in Equation (6). There are two data points  $(X, \sigma_x, Y, \sigma_y)$  per card.

B.2.1.5. Blank card

B.2.1.6. 789 card

B.2.2. MINIQUAD Titration Data Input

B.2.2.1. Descriptive title/20A4

B.2.2.2. Control Card/8I5/LARS, NK, N, MAXIT,  
IPRIN, NUMBEO, NCO, I COM

LARS indicates the data points to be used in the calculation of an unknown formation constant: LARS = 1 means all points are used, LARS = 2 every other point, LARS = 3 every third point, etc.

NK is the total number of formation constants input, both refined and constant.

N is the number of unknown formation constants to be calculated.

MAXIT is the maximum number of iteration cycles to be performed.

IPRIN will allow the monitoring of the program at each iteration. A value of 1 will print the results at each iteration, 2 will also print each data point and its residuals, while 0 is the default with no monitoring done.

NUMBEO is the total number of reactants for a system.

123456789

NCO is the number of free concentrations unknown.

ICOM will allow the elimination of spurious results. A value of 0 will include all results and a value of 1 will eliminate a point if the normal equation matrix is not positive definite at this point.

B.2.2.3. Temperature compensation/3F10.6, 8X,  
I2/TEMP, ADDTEMP, ALPHA, NOTAPE

TEMP is the temperature of the bulk solution in °C.

ADDTEMP is the titrant temperature in °C

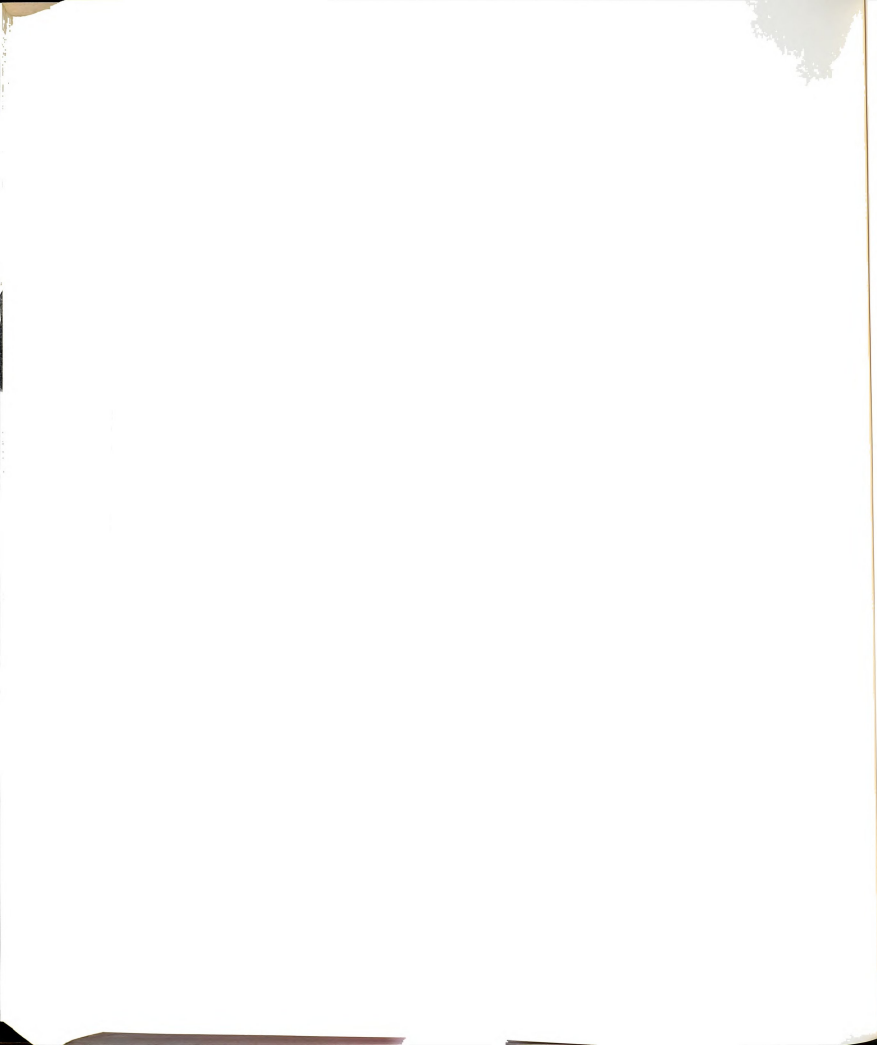
ALPHA is the coefficient of cubical expansion for the solvent in °C<sup>-1</sup>.

NOTAPE interfaces KINFIT4 to MINIQAD. NOTAPE = 1 reads the m and b values from the KINFIT4 program, while NOTAPE = 0 will use values given by EZERO and SLOPE.

B.2.2.4. Formation constant cards/F10.6, 7I5/  
BETA(I), JPOT(I), JQRC(J,I), KEY(I)

The formation constants are input in the form  $B_i = \text{BETA}(I) \cdot 10^{\text{JPOT}(I)}$

The JQRC(J,I) values are the stoichiometric coefficients of the i<sup>th</sup> species with the formation constant  $B_i$ . While the order is arbitrary, the reactants which are measured potentiometrically must come last. In the case of a mono-protonated Ca-PAA complex, the input would be 1 1 1





where the first number is the stoichiometric coefficient of the ligand L, the second of the measured calcium ion, and the third of the measured hydrogen ion concentration.

KEY(I) indicates if the value is to be refined (=1) or if it is a constant (=0).

B.2.2.5. Control Card/12I5/NMBE, JNMB(I), NC,  
JP(I)

NMBE is the number of reactants in the equilibria.

The JNMB(I) values are the integers assigned to those reactants. The equilibria in Section C.2.2.4 would have the reactants labeled

1        2        3

NC is the number of unknown free concentrations at any given point in the titration. This can be calculated by  $NMBE - NCO = NC$  where NCO is the number of electrodes.

JP contains the reactants (as numbered in JNMB) which will be processed further by the subroutine STATS. This subprogram will calculate the relative percentages of those reactants specified by JP and print them out at each point in the titration curve.

B.2.2.6. Reactant titles/5A10/REACT(I)

REACT contains the names of the reactants in the order specified by JQRO(I).



## B.2.2.7. Electrode parameters/4I5/JEL(I), JCOUL

JEL is the number of electrons transferred at each electrode. When pH values are to be read, JEL = 0. The values are given in the same order (lowest number first) as in JQRO(I).

JCOUL specifies a coulometric titration if JCOUL = 1 (no volume change). Dilutions will be calculated if JCOUL = 0.

B.2.2.8. Concentrations/8F10.6/TOTC(I), EZERO(I),  
ADDC(I), VINIT

TOTC(I) is the initial millimoles of species I in the order of JQRO(I).

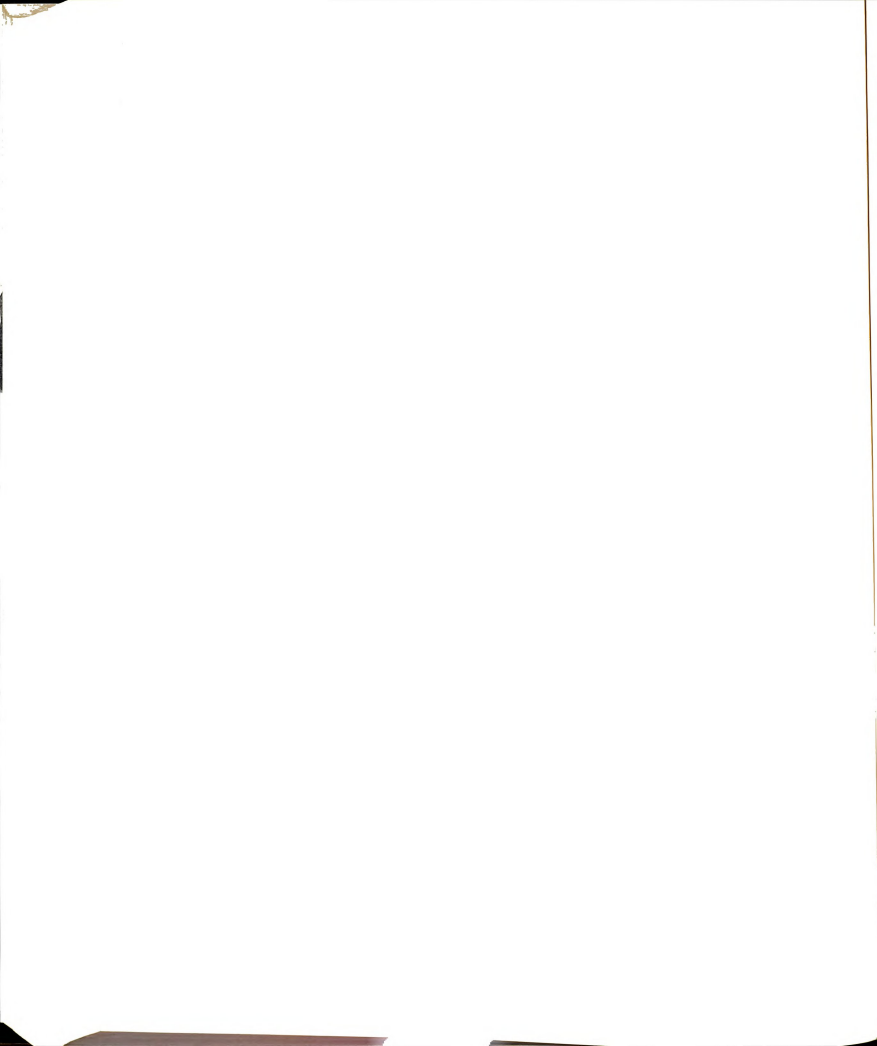
EZERO(I) is the intercept of a calibration plot for the  $i^{\text{th}}$  electrode (ignored if JEL(I) = 0).

ADDC(I) is the concentration of the titrant solution. In all cases, a number must be entered for each species, even if it is zero.

VINIT is the initial volume of the solution in milliliters.

## B.2.2.9. Slope/8F10.6/SLOPE(I)

Slope (I) contains the slope from a calibration curve for the  $i^{\text{th}}$  electrode (ignored if JEL(I) = 0).



B.2.2.10. Data input/I5, 8F8.3/LUIGI, TITRE(I),  
EMF(I).

LUIGI is a data marker for the end of a data set.

If LUIGI = 0, the next card is read. Another data set to follow is indicated by LUIGI = 1. LUIGI = 2 that the data are from coulometric measurements, with current and fractional efficiency read instead of an experimental point. LUIGI < 0 signals the end of all data sets.

TITRE is the volume titrant added (or the time of current passage in sec).

EMF is the measured potential (or pH) for each electrode.

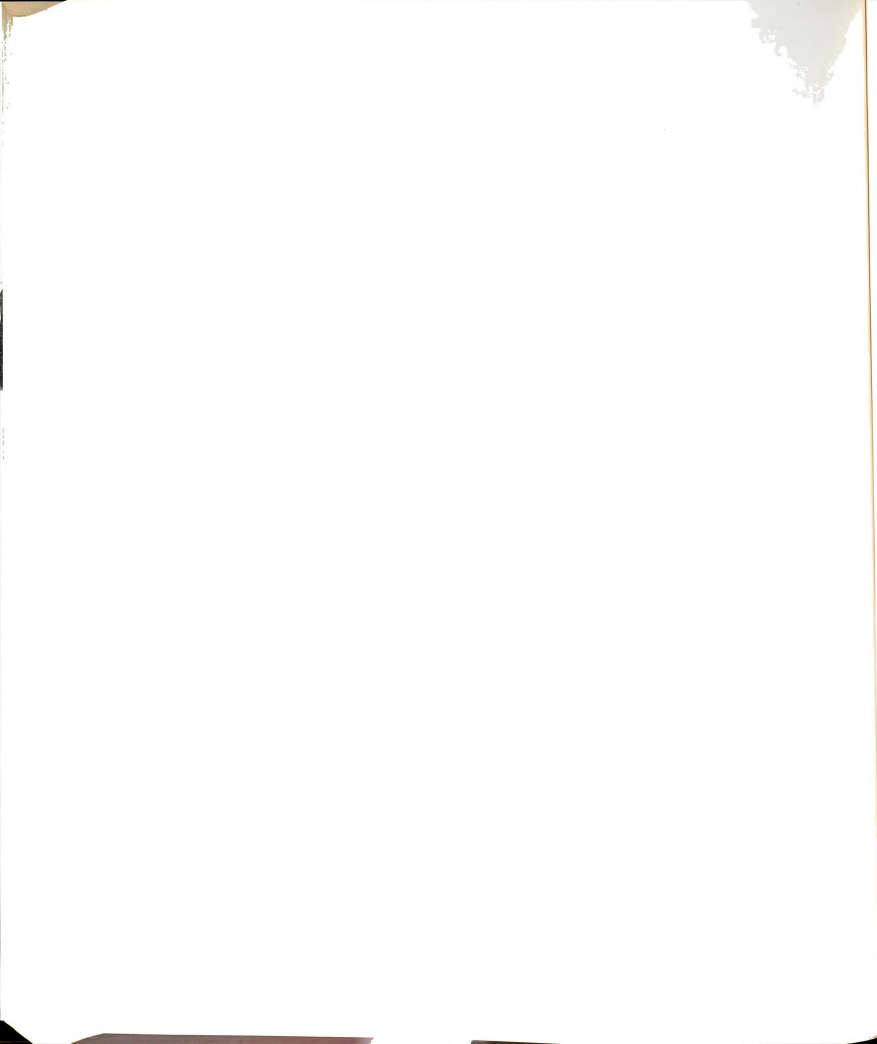
B.2.2.11. Statistics/I5/JPRIN

JPRIN controls the statistical output as follows:

JPRIN	Statistical Analysis	Tables	Graphs
0	no	no	no
1	yes	no	no
2	yes	yes	no
3	yes	no	yes
4	yes	yes	yes

B.2.2.12. Termination/I5/NSET

NSET = 1 for another set of formation constants, NSET = 0 for another complete set of data, and NSET = -1 for the



termination of a run.

B.2.2.13.  $78_9$

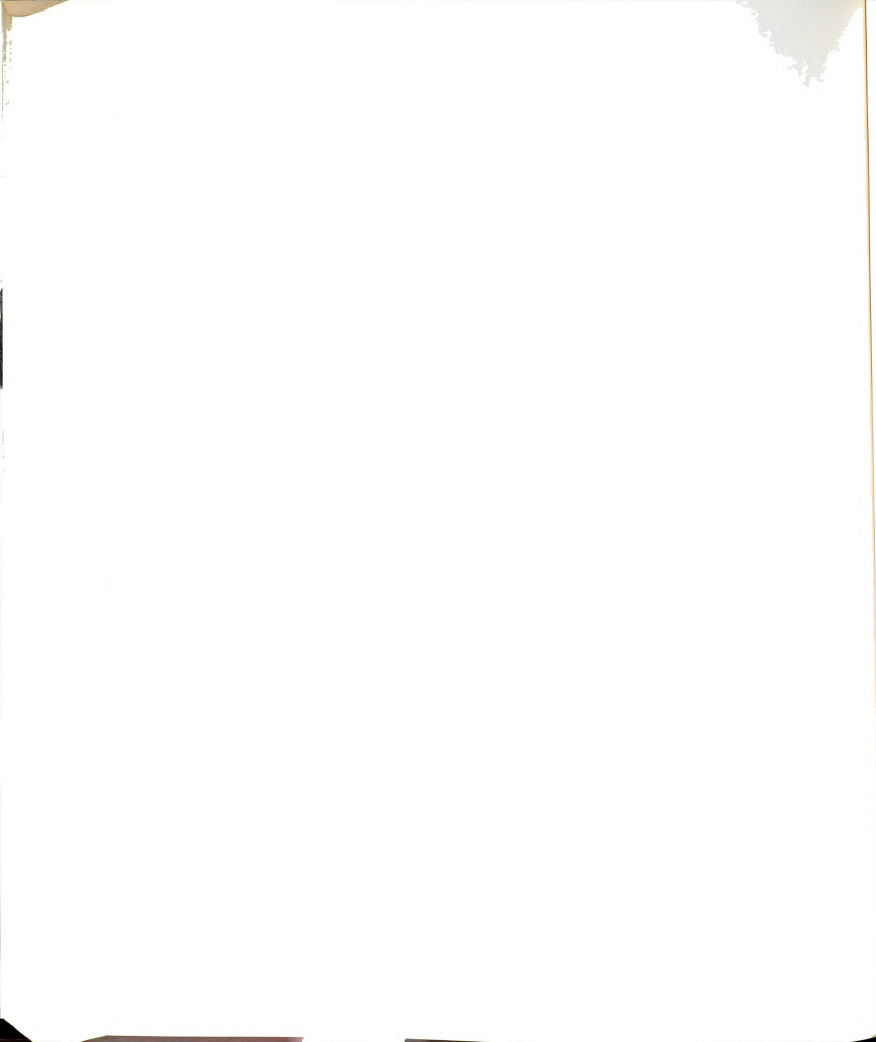
B.2.2.14.  $678_9$





APPENDIX C

THE USE OF THE PROGRAM FARM2.TSK FOR THE  
DETERMINATION OF MONOPROTONATED PAA-CALCIUM  
FORMATION CONSTANTS FROM POTENTIOMETRIC DATA



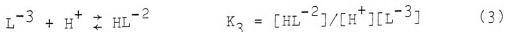
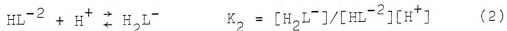
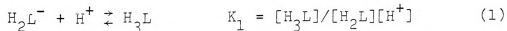
THE USE OF THE PROGRAM FARM2.TSK FOR THE  
DETERMINATION OF MONOPROTONATED PAA-CALCIUM  
FORMATION CONSTANTS FROM POTENTIOMETRIC DATA

C.1. Scope of FARM2.TSK

The program FARM2.TSK is a limited-utility computer program designed to solve repetitive formation constant calculations based on potentiometric data. The program evolved to fill the need for the calculation of mono-protonated PAA-calcium formation constants from potentiometric data. The program MINIQUAD was found to be unsuitable for these calculations. The program will solve five simultaneous equilibrium equations to yield an exact solution for the mono-protonated formation constant (with the deprotonated complex input as a known value) and the resulting standard deviation of that value.

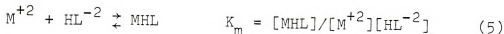
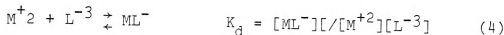
C.2. Program Derivation

PAA is a triprotic acid symbolized by  $H_3L$  in its completely protonated form. The three acid equilibria are



When PAA complexes with a metal ion, two forms usually arise





The  $K_1$  is such that this equilibria may be ignored above a pH of 4, resulting in the mass balance equations

$$[L]_{\text{total}} = [H_2L^{-}] + [HL^{-2}] + [L^{-3}] + [MHL] + [ML^{-}] \quad (6)$$

$$[M]_{\text{total}} = [M^{+2}] + [MHL] + [ML^{-}] \quad (7)$$

Subtracting (7) from (6) gives

$$[L]_T - [M]_T + [M^{+2}] = [H_2L^{-}] + [HL^{-2}] + [L^{-3}] \quad (8)$$

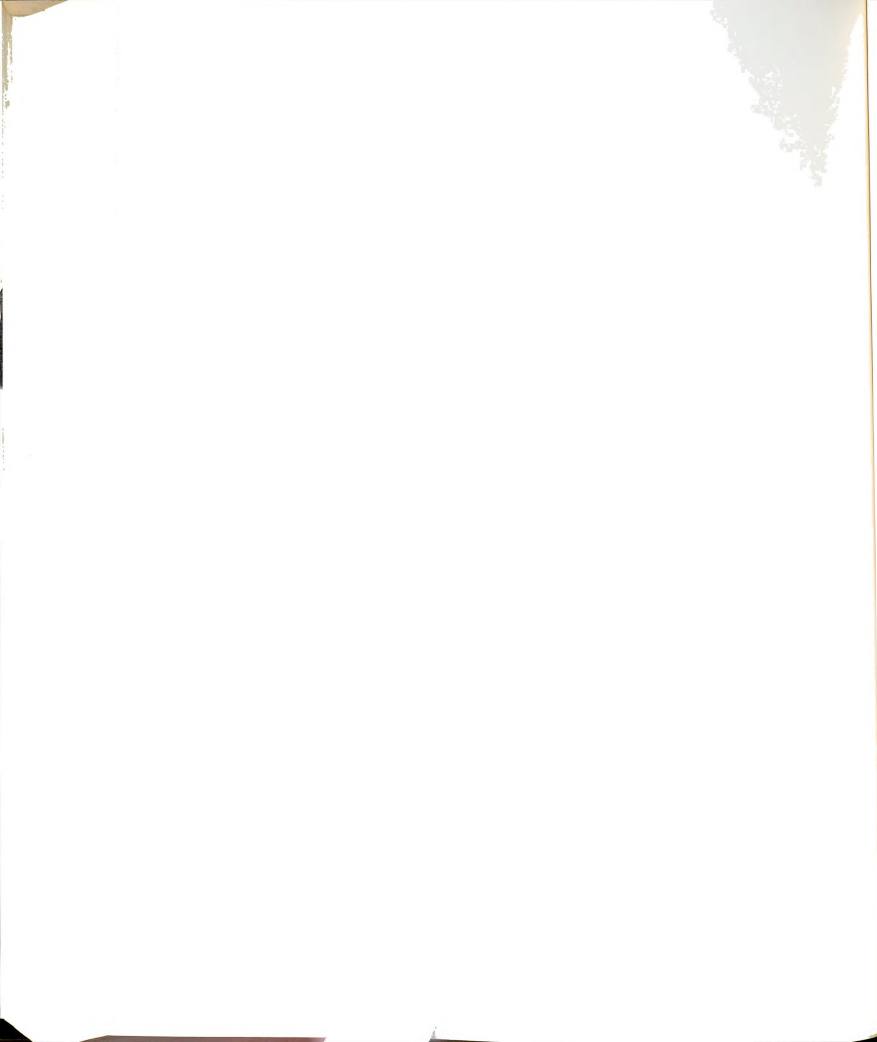
The right hand side may be restated in terms of only [HL] from Equations (2) and (3) to yield

$$\frac{[L]_T - [M]_T + [M^{+2}]}{K_3[H^{+}]} = K_2[H^{+}][HL^{-}] + [HL^{-}] + [HL^{-}]/K_3[H^{+}] \quad (9)$$

or

$$[HL] = \frac{([L]_T - [M]_T + [M^{+2}])}{(K_2[H^{+}] + 1/K_3[H^{+}] + 1)} \quad (10)$$

From Equation (4) the concentration [ML] is



$$[ML] = K_d[M^{+2}][L^{-3}] \quad (11)$$

and from (3)

$$[ML] = K_d[M^{+2}][HL^{-2}]/K_3[H^+] \quad (12)$$

Then from Equation (7)

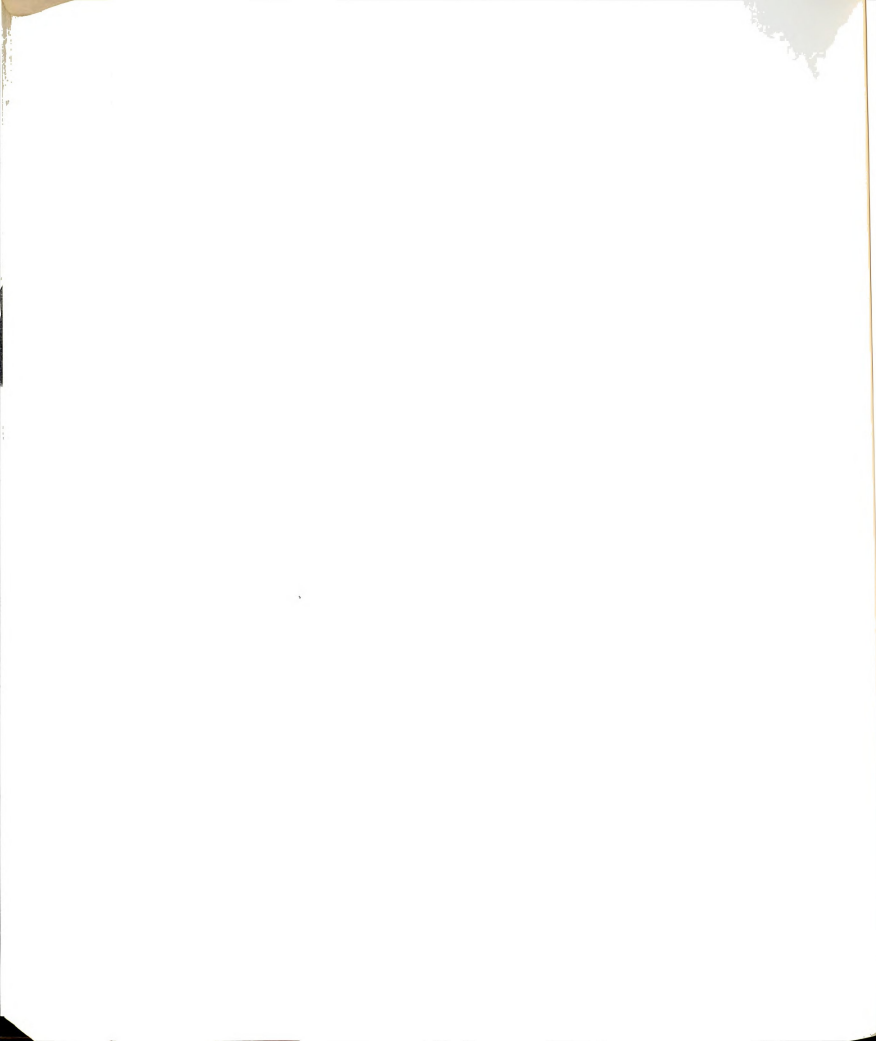
$$[M]_T = [M^{+2}] + K_d[M^{+2}][HL^{-}]/K_3[H^+] + [MHL] \quad (13)$$

or

$$[MHL] = [M]_T - [M^{+2}] - K_d[M^{+2}][HL^{-}]/K_3[H^+] \quad (14)$$

The concentration  $[M^{+2}]$  was known at any given point in the titration from emf data, with the pH (and hence the  $[H^+]$ ) also measured at each point. Since  $K_3$ ,  $K_2$ , and  $K_d$  were known, as well as the total amount of ligand and metal ion, the equations were exactly solvable at each point. The average  $K_m$  was then calculated over all the data points, with the standard deviation calculated for this average.

C.3. Data Input File - the data file was created, named, and edited using the programs RX1 (202) and TECO (203). The reader is referred to these for further information.





C.3.1. Descriptive title

C.3.2. Control Data/F15.7/SLOPE, INTERCEPT, RESID,  
TOTM, CONCL

SLOPE, INTERCEPT, and RESID were the values derived from a KINFIT4 plot of the calibration data (see B.1.).

TOTM was the total mmoles of metal ion, while CONCL was the concentration of L in molarity.

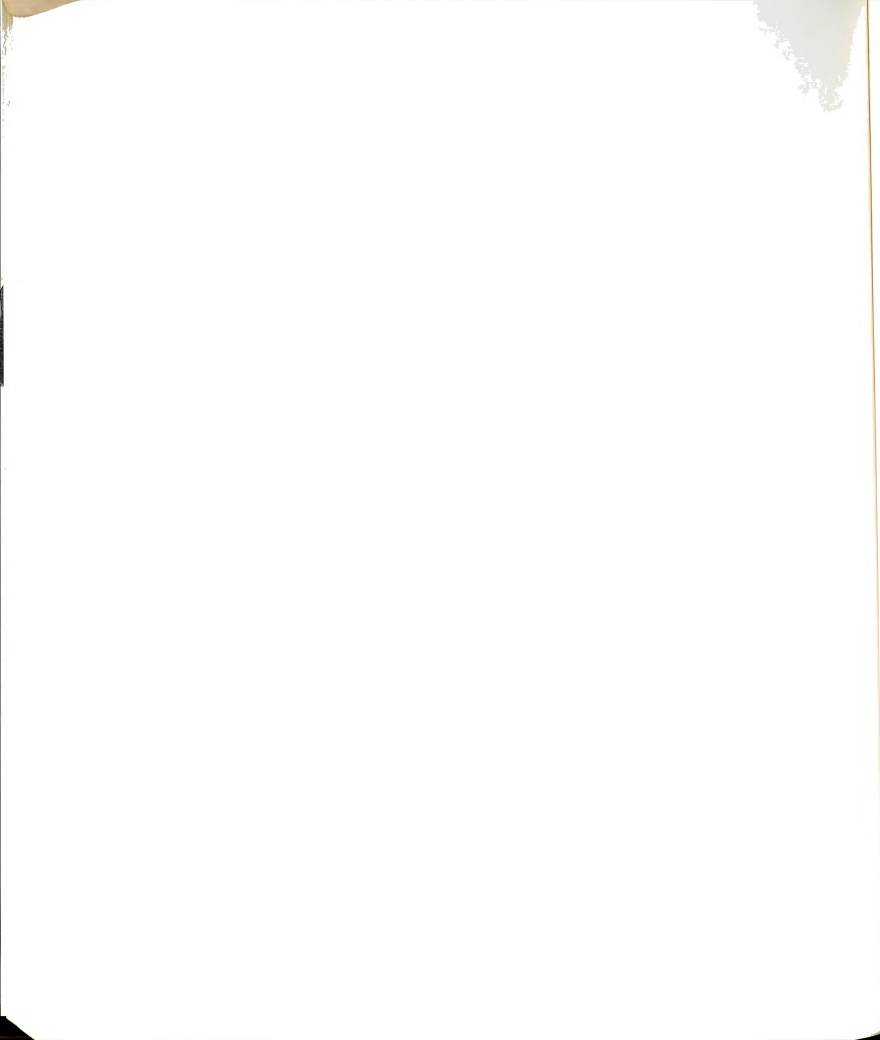
C.3.3. Data/F15.5/MLL, EMF, PH

MLL was the milliliters ligand, EMF the measured emf, and PH the measured pH.

C.4. FARM2.TSK

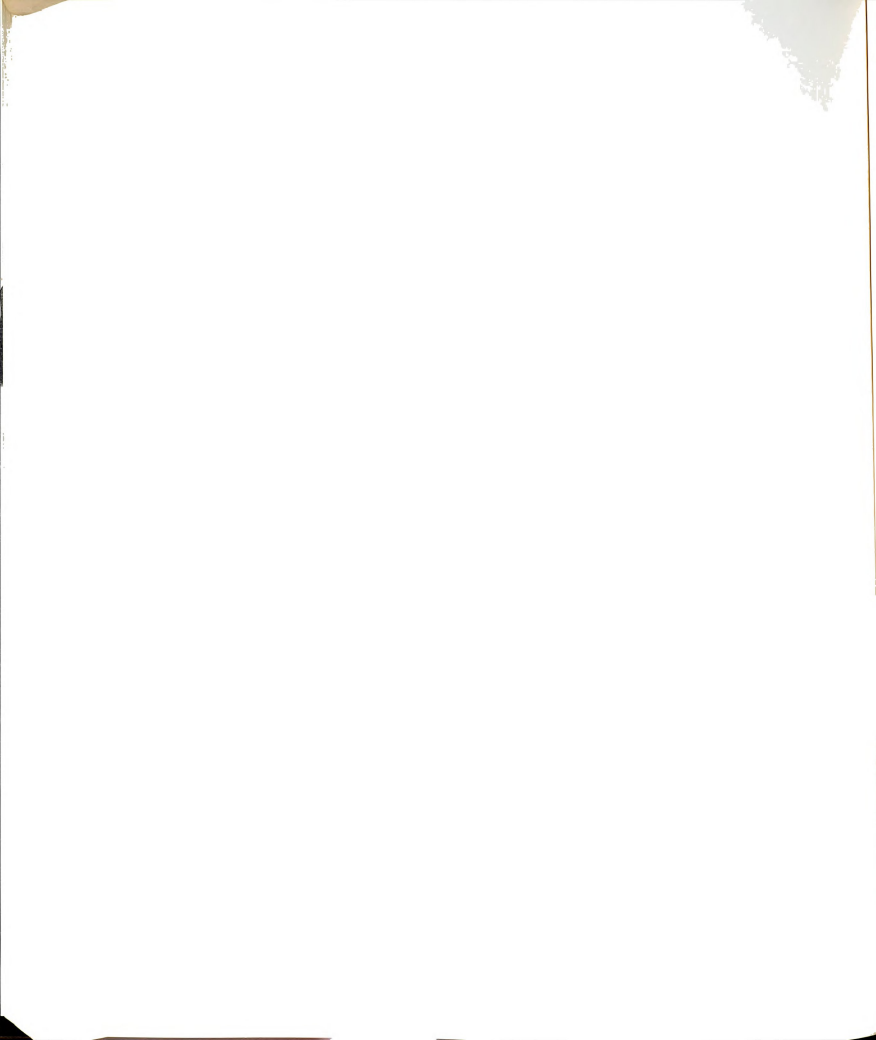
The program FARM2.TSK was then run. Upon the inquiry "input file?", the file name created in C.3.2. was given. When "output file?" appeared, the desired name of the output file was given.

The program may be modified through FARM2.FTN to suit a particular purpose. The file is then compiled and task built to give a new FARM2.TSK.



APPENDIX D

SOME CROWN AND CRYPTAND COMPLEX FORMATION CONSTANTS  
WITH MANGANESE (II) ION DETERMINED BY  
ELECTRON SPIN RESONANCE



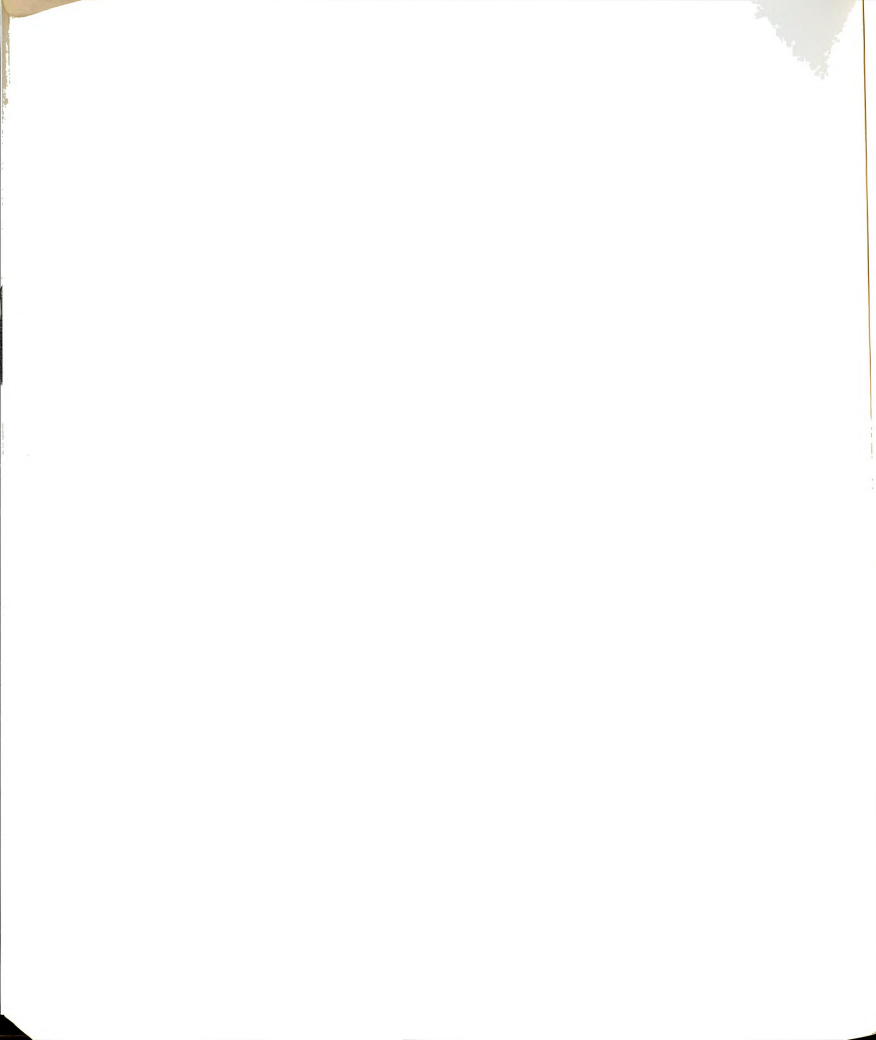
SOME CROWN AND CRYPTAND COMPLEX FORMATION CONSTANTS WITH  
MANGANESE(II) ION DETERMINED BY ELECTRON SPIN RESONANCE

D.1. Crown Complexes with Manganese (II) Ion.

The complexation properties of the crown ethers 12C4, 15C5, and 18C6 (Figure 1) with manganese (II) ion were studied using electron spin resonance. The data were collected following the procedures outlined in Sections 2.2.1. and 2.3.1.

There was found to be no significant formation of a complex within the experimental error. This was evidenced by no change in the intensity, linewidth, or saturation properties of the free manganese (II) ion resonance upon the addition of the ligand. This behavior was exhibited even when the mole ratio of ligand to metal was as high as 10:1.

Since the error in the measurement of the free manganese ion concentration was estimated at  $\pm 4\%$ , approximately 4% of manganese could complex with no effect on the signal intensity (it was probable that there would be no effect on the linewidth or saturation properties either). With a total concentration of manganese  $10^{-3}$  M and a ligand concentration of  $10^{-2}$  M, this puts an upper limit of approximately 4 for the formation constants of 12C4, 15C5, and 18C6 with manganese. That is, if a complex exists, which is doubtful, it would be very weak.

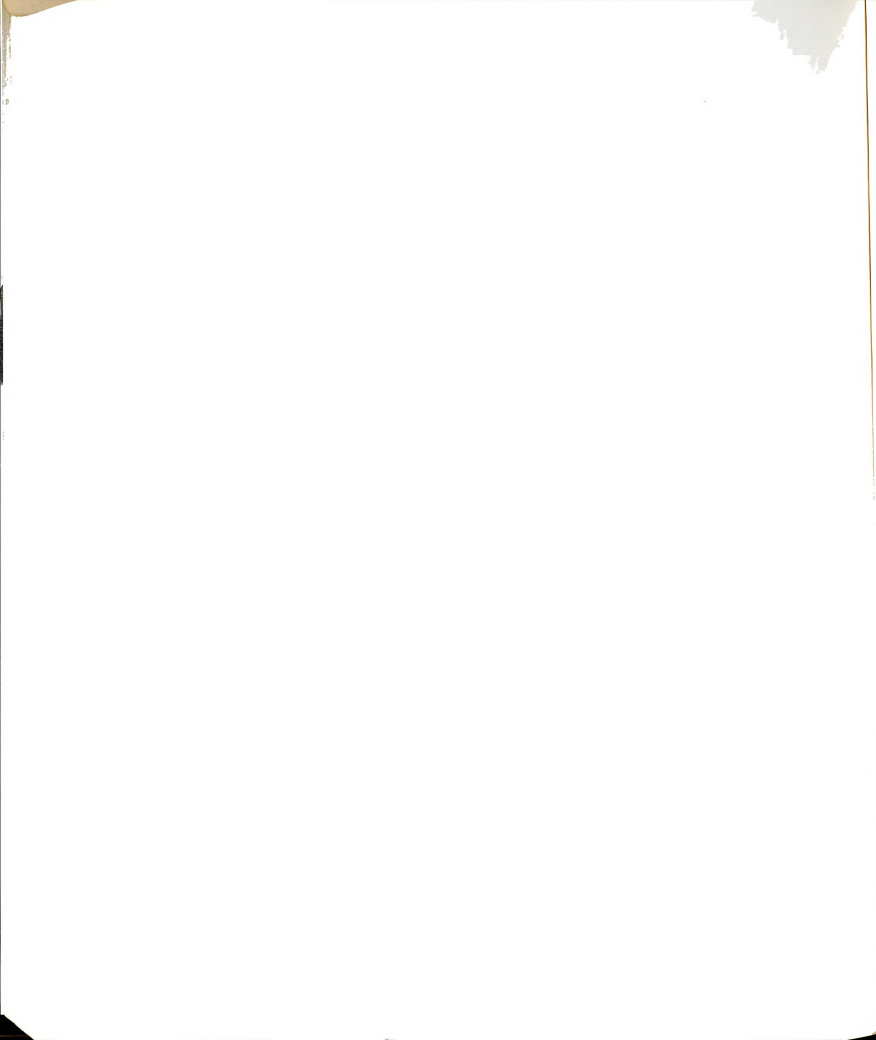


## D.2. Cryptand Complexation with Manganese (II) Ion

The complexation of C211 (Figure 1) with manganese (II) ion was also studied. The experimental procedures were as outlined in 2.2.1 and 2.3.1 with one exception. It was found that the manganese (II) ion oxidation is greatly enhanced by the addition of the cryptand (the rate is dependent on the ligand concentration). However, this problem was alleviated by degassing the solution with deoxygenated nitrogen (183) for 15 minutes prior to the addition of the ligand. In this manner, the oxidation of manganese (II) ion was negligible over the course of the experiment. Such behavior (oxidation enhancement) has been observed previously (26), although not specifically for manganese.

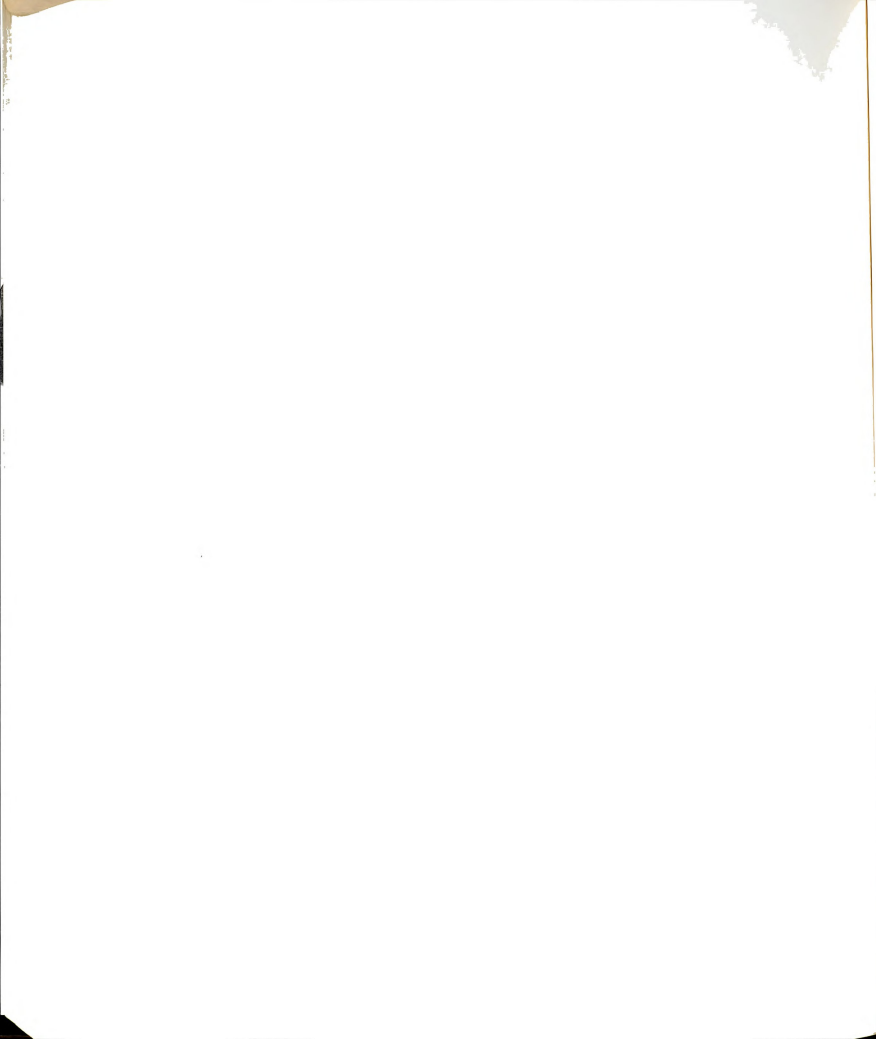
The cryptand C211 is a very strong base, with a  $pK_1(BH^+)$  of 11.3 and a  $pK_2(BH_2^{+2})$  of 8.1 (14). The pH of the solution was adjusted to 8.5 to partially deprotonate the ligand. The formation constant was then found to be  $\log K_f = 1.6 \pm 0.1$ . This value is comparable to formation constants obtained for other divalent cations (28). The presence of complexation would tend to indicate that the oxidation of manganese (II) ion is occurring through an intermediate complex. The cryptand would tend to stabilize a higher oxidation state for manganese, with subsequent oxide formation upon decomplexation.

Hence, it has been shown that electron spin resonance for manganese (II) ion is a versatile technique. Both

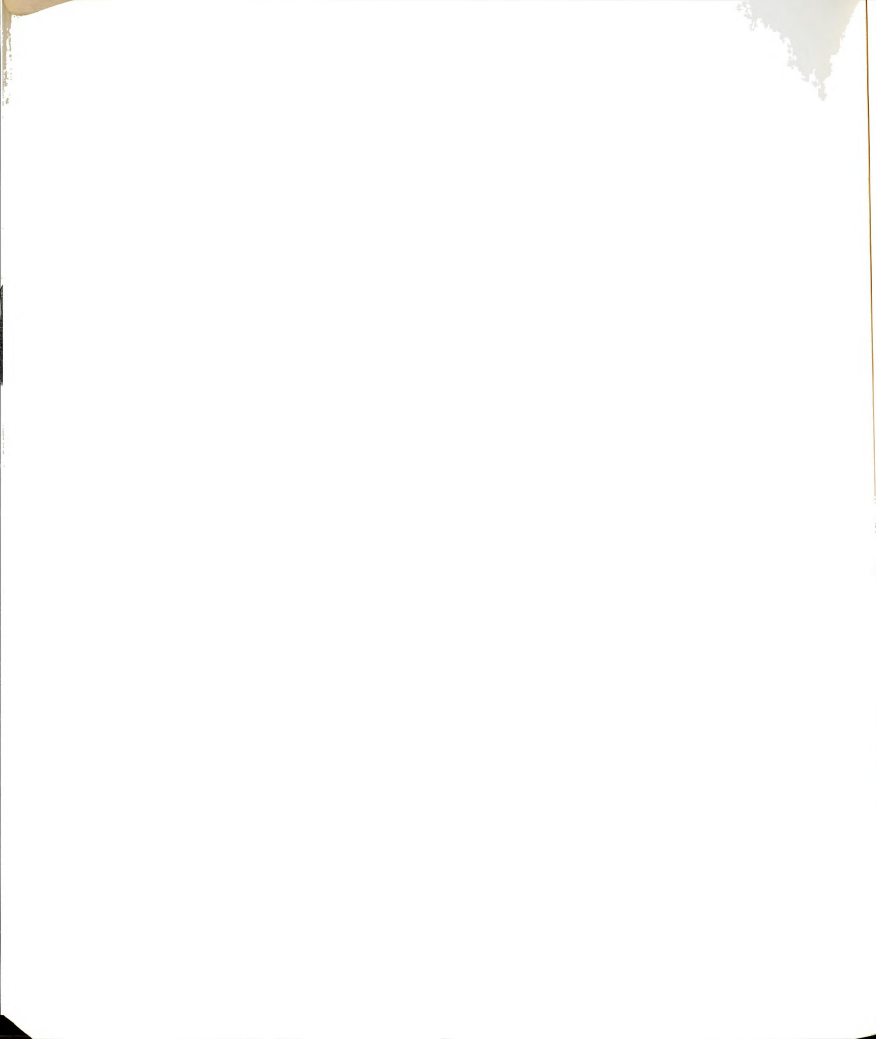




protic and aprotic ligand complexation systems may be studied using this technique, which should lead to increased interest in the complexation properties of this biologically important ion.

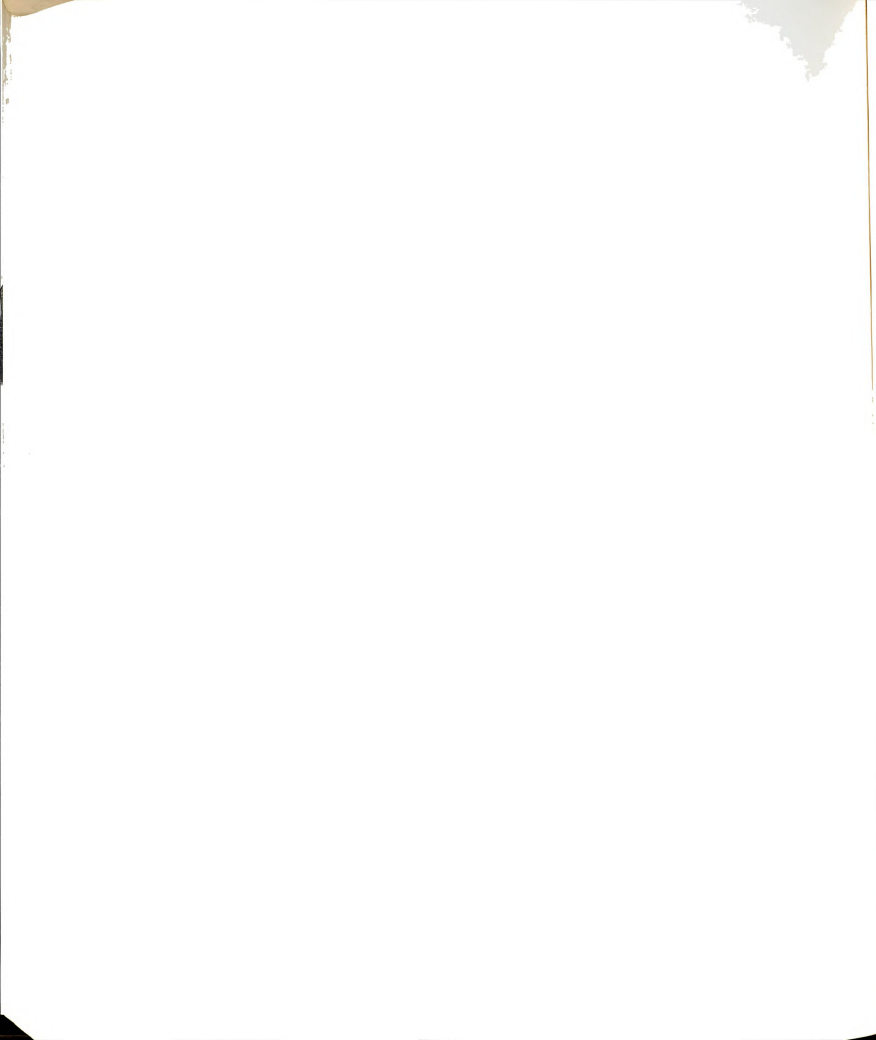


BIBLIOGRAPHY

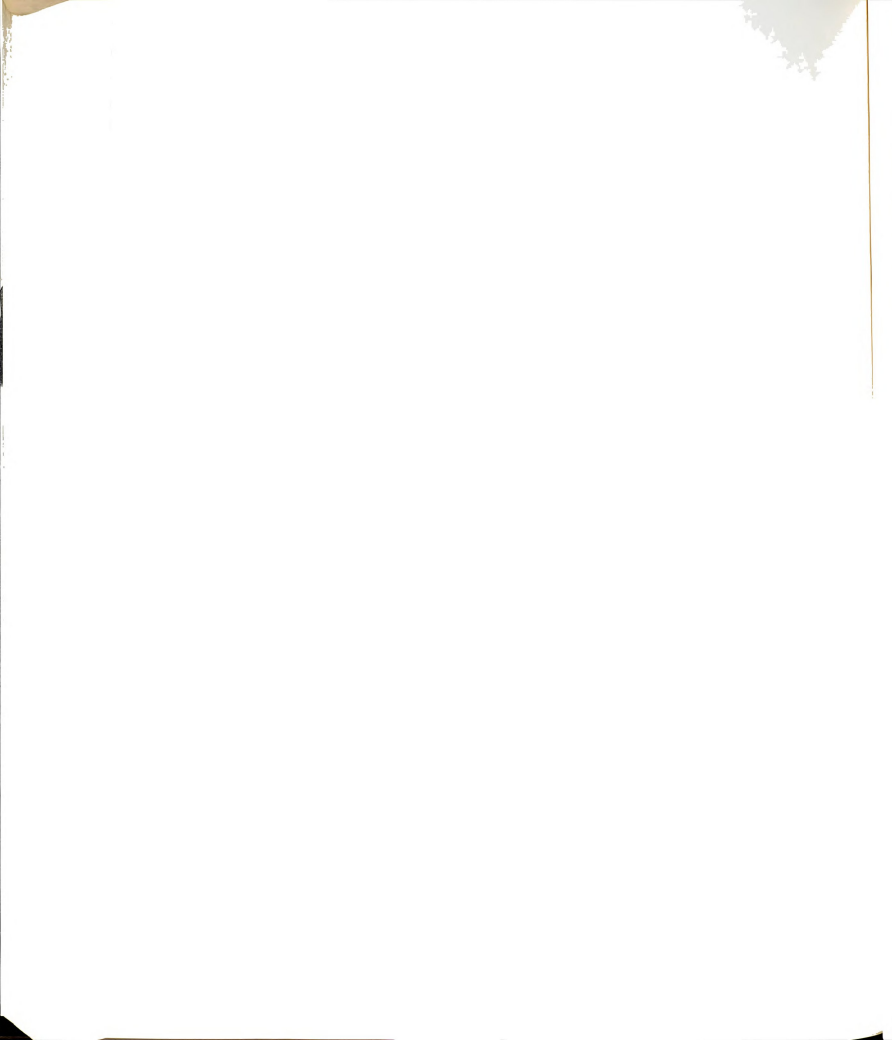


## BIBLIOGRAPHY

1. C. D. Jeffries, *Phys. Rev.* 90, 1130 (1953).
2. R. G. Bryant, *JACS*, 91, 1870 (1969).
3. H. E. Bleich, A. G. Redfield, *J. Chem. Phys.*, 11, 5405 (1971).
4. J. F. Jacquin t, W. T. Wenckebach, M. Goldman, A. Abragam, *Phys. Rev. Lett.*, 32, 1096 (1974).
5. O. Lutz, A. Schwenk, A. Uhl, *Z. Naturforsch*, 28A, 1534 (1973).
6. *Ibid*, 30A, 1122 (1975).
7. P. Grundevik, M. Gustavsson, I. Lindgren, G. Olsson, L. Robertsson, A. Rosen, S. Suanberg, *Phys. Rev. Lett.*, 42, 1528 (1979).
8. P. Robertson, Jr., R. G. Hiskey, K. A. Koehler, *J. Biol. Chem.*, 253, 5880 (1973).
9. J. Parello, H. Lilja, A. Cave, B. Lindman, *FEBS Lett.*, 87, 191 (1978).
10. P. Reimarsson, J. Parello, T. Drakenburg, H. Gustavsson, B. Lindman, *FEBS Lett.*, 108, 439 (1979).
11. H. C. Marsh, P. Robertson, Jr., M. E. Scott, K. A. Koehler, R. G. Hiskey, *J. Biol. Chem.*, 254, 10268 (1979).
12. C. J. Pedersen, *JACS*, 89, 2495 (1967).
13. C. J. Pedersen, *JACS*, 89, 7017 (1967).
14. I. M. Kolthoff, *Anal. Chem.*, 51(5), IR, (1979).
15. D. A. Skoog, D. M. West, "Fundamentals of Analytical Chemistry", New York, Holt, Rinehart & Winston, (1969).
16. R. T. Myers, *Inorg. Nucl. Chem. Lett.*, 16(6), 329 (1980)

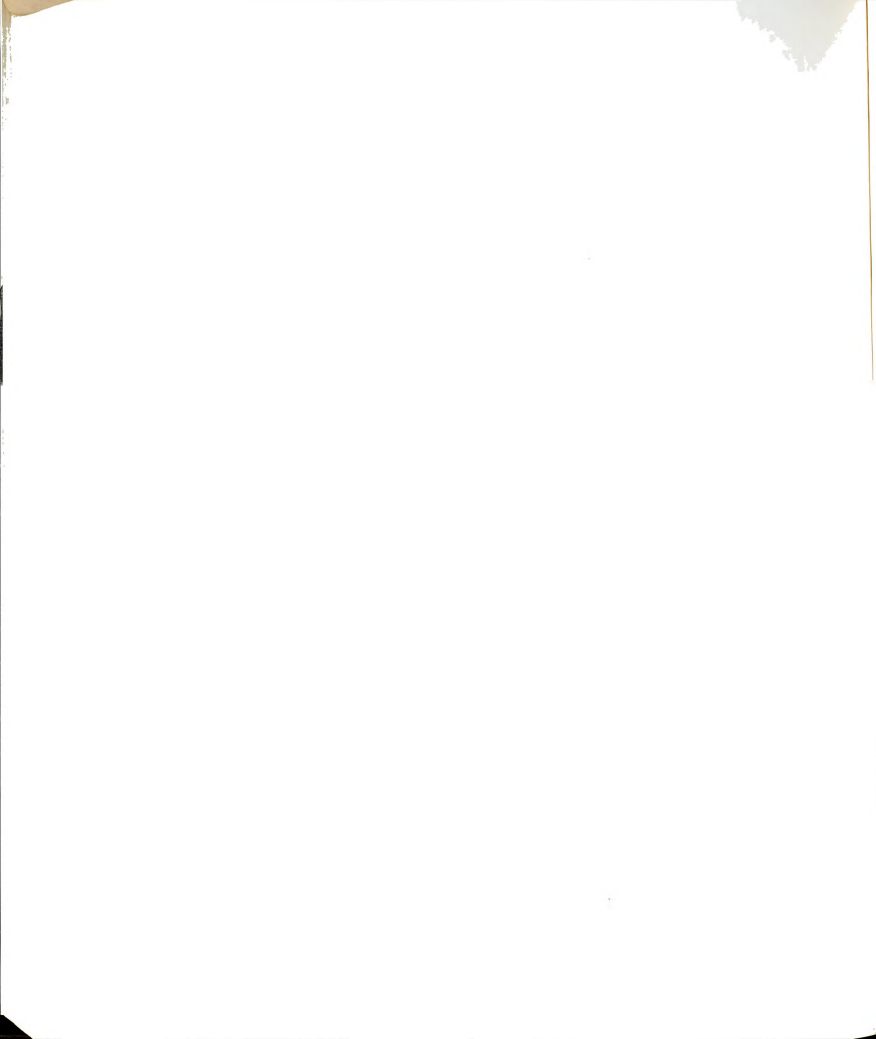


17. F. Smetana, A. I. Popov, J. Solut. Chem., 9, 183 (1980).
18. J. D. Lin, A. I. Popov, JACS, to be published.
19. R. M. Izatt, R. E. Terry, B. L. Haymore, L. D. Hansen, N. K. Dalley, A. G. Avondet, J. J. Christensen, JACS, 98, 7620 (1976)
20. J. D. Lamb, R. M. Izatt, C. S. Swain, J. J. Christensen, JACS, 102, 475 (1980).
21. J. D. Owen, J. Chem. Soc., Dalton Trans., 10, 1418 (1978).
22. T. P. Singh, R. Reinhardt, N. S. Poonia, Inorg. Nucl. Chem. Lett., 16(5), 289 (1980).
23. R. R. Hendrixson, M. P. Mack, R. A. Palmer, Toxicol. Appl. Pharmacol., 44(2), 263 (1978).
24. J. J. Christensen, D. J. Eatough, R. M. Izatt, Chem. Rev., 74, 351 (1974).
25. R. M. Izatt, R. E. Terry, D. P. Nelson, Y. Chan, D. J. Eatough, J. S. Bradshaw, L. D. Hansen, J. J. Christensen, JACS, 98, 7626 (1976).
26. P. B. Choek, Proc. Nat. Acad. Sci., US, 69, 1939 (1972).
27. J. D. Dunitz, P. Seiler, Acta. Crystallogr., B30, 2750 (1974).
28. G. A. Melson, edit., "Coordination Chemistry of Macrocyclic Compounds", Plenum Press, New York (1979).
29. R. M. Izatt, J. J. Christensen, edit., "Synthetic Multidentate Macrocyclic Compounds", Academic Press, New York (1978).
30. R. M. Izatt, J. J. Christensen, edit., "Progress in Macrocyclic Chemistry", John Wiley & Sons, New York (1979).
31. J. Christensen, R. M. Izatt, Science, 174, 459 (1971).
32. L. I. Chudinova, Izv. Vyschikh. Uchebn. Zavedenii, Khim. i Khim. Tekhnol, 5, 357 (1962).
33. G. W. Gokel, D. J. Cram, C. L. Liotta, H. P. Harris, F. L. Cook, J. Org. Chem., 39, 2445 (1974).

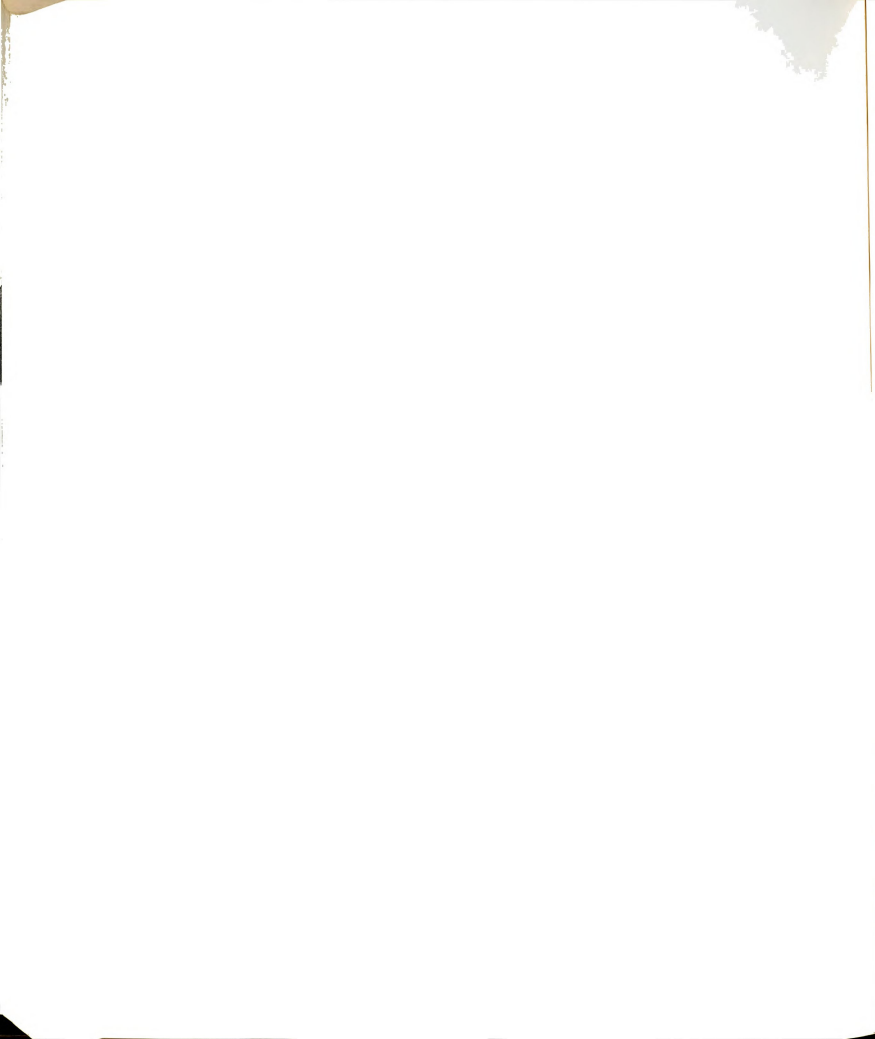




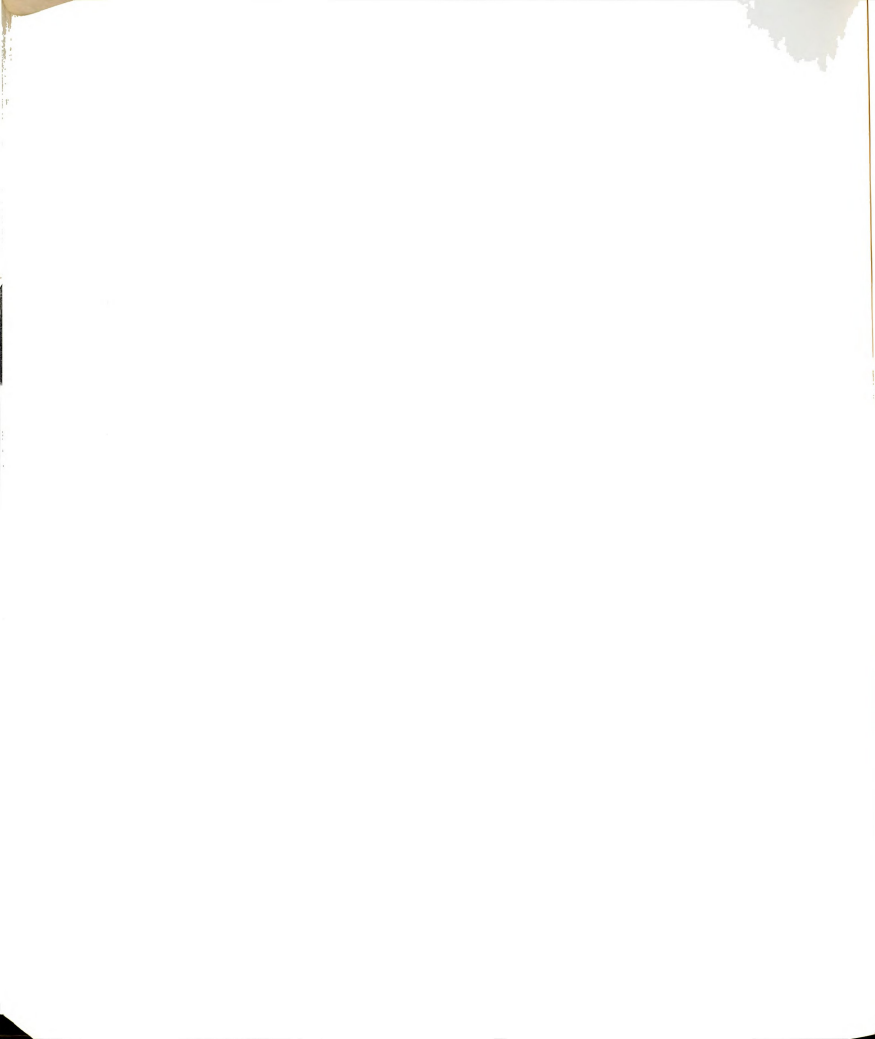
34. P. Nylén, Ber., 57B, 1032 (1924).
35. P. Nylén, Ber., 59B, 1119 (1926).
36. G. J. Templeman, A. L. Van Geet, JACS, 94, 5578 (1972).
37. D. H. Live, S. I. Chan, Anal. Chem., 42, 791 (1970).
38. J. L. Dye, V. A. Nicely, J. Chem. Educ., 48, 443 (1971).
39. P. Gans, A. Sabatini, A. Vacca, Inorg. Chim. Acta., 18, 237 (1976).
40. A. I. Popov, Pure Appl. Chem., 51, 101 (1979).
41. P. Lazlo, Angew. Chem., Int. Ed., 17, 254 (1978).
42. R. G. Pearson, JACS, 85, 3533 (1963).
43. V. Gutman, E. Wyckera, Inorg. Nucl. Chem. Lett., 2, 257 (1966).
44. G. C. Benson, A. R. Gordon, J. Phys. Chem., 13, 470 (1945).
45. A. A. Noyes, K. G. Falk, JACS, 34, 454 (1912).
46. R. E. Hester, R. A. Plane, J. Phys. Chem., 40, 411 (1964).
47. H. Sadek. R. M. Vuoss, JACS, 76, 5897, 5905 (1954).
48. S. Winstein, E. Clippinger, A. H. Fainberg, G. C. Robinson, JACS, 76, 2597 (1954).
49. M. S. Greenburg, R. L. Bodner, A. I. Popov, J. Phys. Chem., 77, 2449 (1973).
50. V. Mayer, V. Gutman, Structure and Bonding, 12, 113 (1972).
51. P.-H. Heubel, A. I. Popov, J. Solut. Chem., 8, 283 (1979).
52. M. Herlem, A. I. Popov, JACS, 94, 1431 (1972).
53. C. Deverell, R. E. Richards, Molec. Phys., 16, 421 (1969).
54. J. M. Ceraso, Ph.D. Dissertation, Michigan State University, East Lansing, MI (1975).



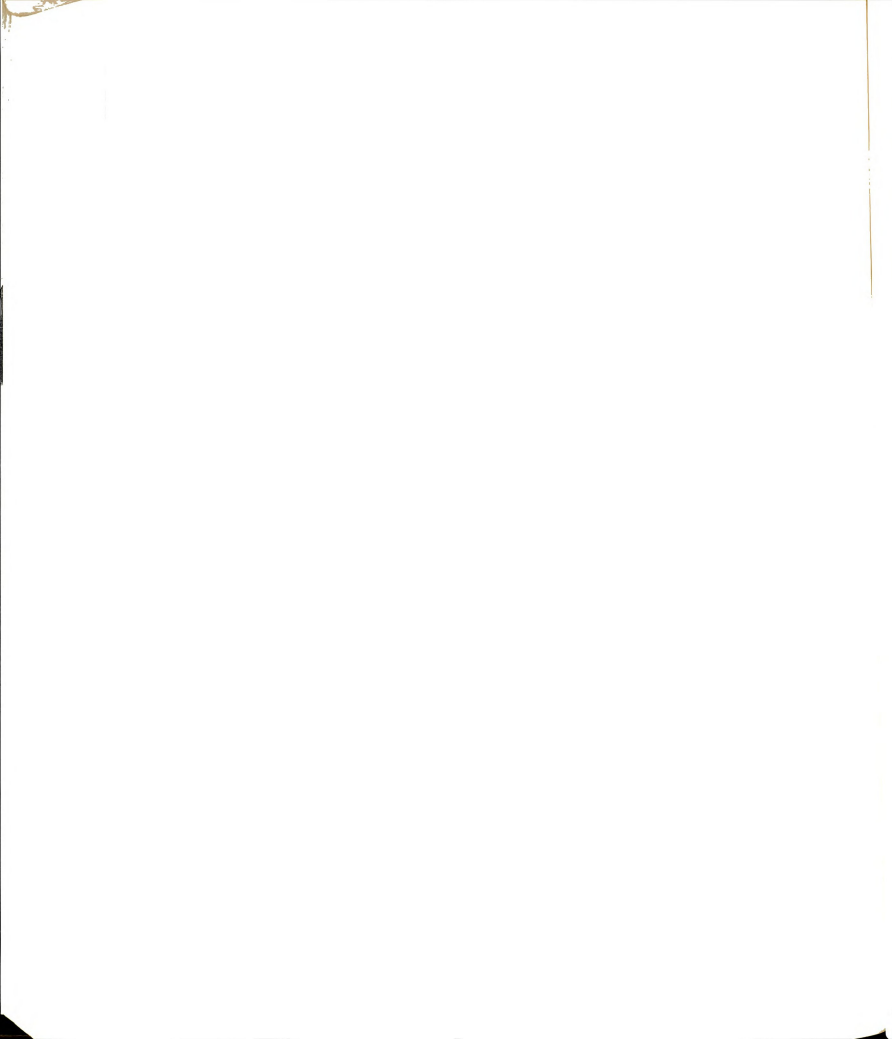
55. P. van Rysselberghe, R. M. Fristrom, J. Amer. Chem. Soc., 67, 608 (1945).
56. T. C. Farrar, E. D. Becker, "Pulse and Fourier Transform NMR", Academic Press, New York (1971).
57. M. St. J. Arnold, K. J. Packer, Molec. Phys., 10, 141 (1966).
58. R. H. Erlich, A. I. Popov, J. Amer. Chem. Soc., 93, 5620 (1971).
59. J. S. Shih, A. I. Popov, Inorg. Nucl. Chem. Lett., 13, 105 (1977).
60. H. Hoviland, J. A. Ringseth, T. S. Brun, J. Solut. Chem., 8, 779 (1979).
61. J. Dale, P. O. Kristiansen, Acta. Chem. Scand., 26, 1471 (1972).
62. Bjerrum, N., and E. Larsson, Z. Phys. Chem., 127, 358 (1927).
63. Oiwa, I. T., Sci. Rpt. Tohoku Univ. First Ser., 41, 129 (1957).
64. Alexander, R., and W. E. Waghorne, Aust. J. Chem., 31, 1181 (1978).
65. Izmaylov, N. A., and V. V. Aleksandrov, Zh. Fiz. Khim., 31, 2619 (1957).
66. Feakins, D., and P. Watson, J. Chem. Soc., 4734 (1963).
67. DeLigny, C. L., and M. Alfenaar, Rec. Trav. Chim., 84, 81 (1965).
68. Buckingham, A. D., Disc. Faraday Soc., 24, 151 (1957).
69. DeLigny, C. L., H. J. M. Denessen, and M. Alfenaar, Rec. Trav. Chim., 90, 1265 (1971).
70. Bax, D., C. I. DeLigny, and M. Alfenaar, Rec. Trav. Chim., 91, 452 (1972).
71. Salomon, Mr., J. Phys. Chem., 74, 2519 (1970).
72. Salomon, M., J. Electrochem. Soc., 118, 1609 (1971).
73. Pleskov, V. A., Usp. Khim, 16, 254 (1947).



74. Kolthoff, M. and F. C. Thomas, *J. Phys. Chem.*, 69, 3049 (1965).
75. Nelson, I. V., Iwamoto, R. T. *Anal. Chem.*, 33, 1795 (1961).
76. Koepp, H. M., H. Wendt, and H. Strehlow, *Z. Elektrochem.*, 64, 483 (1960).
77. Popovych, O., *Crit. Rev. Anal. Chem.*, 7, 73 (1970).
78. Kim, J. I., *J. Phys. Chem.*, 82, 191 (1978).
79. Alexander, R., A. J. Parker, J. H. Sharp, and W. E. Waghorne, *J. Amer. Chem. Soc.* 94, 1148 (1972).
80. Bates, R. G., *J. Electroanal. Chem.* 29, 1 (1971).
81. Parker, A. J., and R. Alexander, *J. Amer. Chem. Soc.*, 90, 3313 (1968).
82. Popovych, O., *Treatise in Anal. Chem.* (2nd ed), 1, 711 (1978).
83. Parker, A. J., *Chem. Rev.*, 69, 1 (1969).
84. Kolthoff, I. M., *Pure Appl. Chem.*, 25, 305 (1971).
85. Popovych, O., *Anal. Chem.*, 38, 558 (1966).
86. Grunwald, E., G. Baughman, and G. Kohnstam, *J. Amer. Chem. Soc.*, 82, 5801 (1960).
87. Alexander, R. and A. J. Parker, *J. Amer. Chem. Soc.*, 89, 5549 (1967).
88. Coetzee, J. F., and W. R. Sharpe, *J. Phys. Chem.*, 75, 3141 (1971).
89. Caruso, J. A., and N. Salch, *J. Solut. Chem.*, 8, 197 (1979).
90. Caruso, J. A., and J. Rosenfarb, *Can. J. Chem.*, 54, 3492 (1976).
91. Caruso, J. A., and T. L. Buxton, *J. Amer. Chem. Soc.*, 96, 6033 (1974).
92. Popov, A. I., and R. E. Humphrey, *J. Amer. Chem. Soc.*, 81, 2043 (1959).
93. Kim, J. I., *J. Phys. Chem.*, 82, 191 (1978).

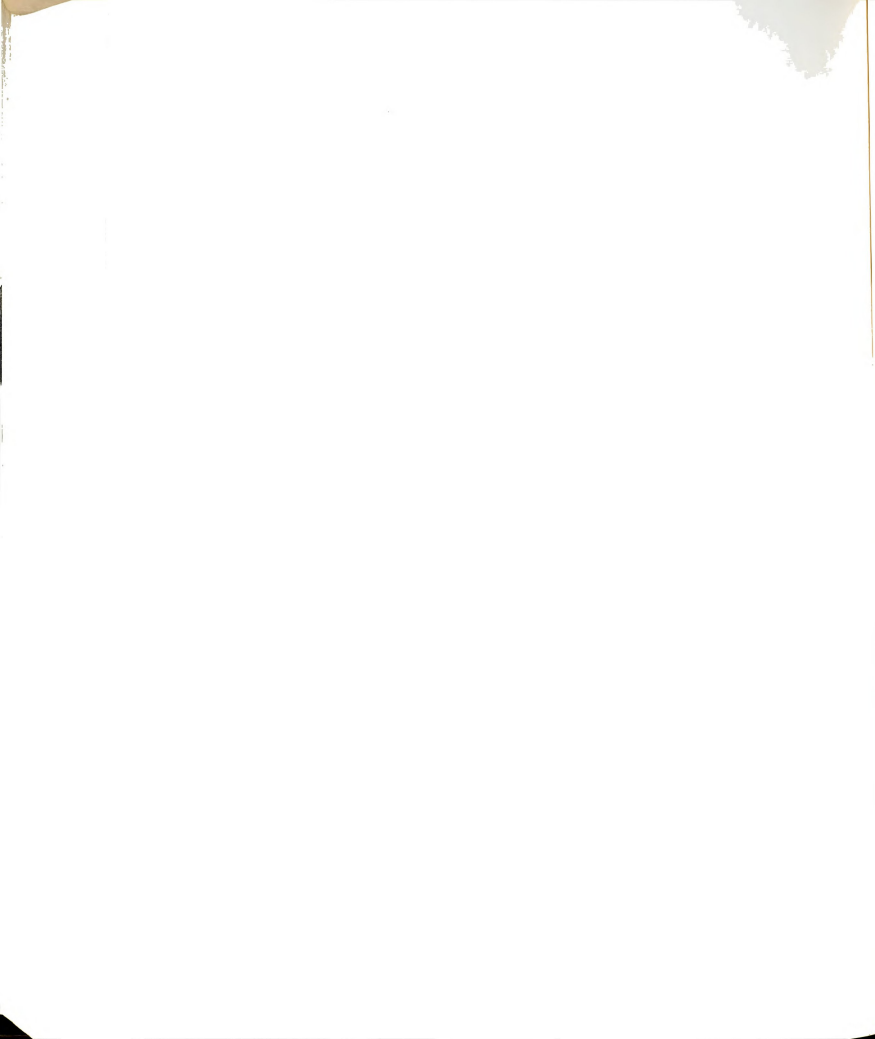


94. Kim, J. I., Z. Phys. Chem., 113, 129 (1978).
95. Kim, J. I., A. Cecal, H.-J. Born, and E. A. Gomaa, Z. Phys. Chem., 110, 209 (1978).
96. C. Treiner, Can. J. Chem. 55, 682 (1977).
97. R. A. Pierotti, Chem. Rev. 76, 717 (1976).
98. Abraham, M. H., and A. Nasehzadeh, Can. J. Chem., 57, 71 (1979).
99. Kolthoff, I. M., and M. K. Chantooni, J. Amer. Chem. Soc., 93, 7104 (1971).
100. Kolthoff, I. M., and M. K. Chantooni, J. Phys. Chem., 76, 2024 (1972).
101. Cox, B. G., R. Natarajan, W. E. Waghorne, J. C. S. Fara. I, 75, 1780 (1978).
102. Fuchs, R., C. P. Hagan, J. Phys. Chem., 77, 1797 (1973).
103. Kundo, K. K., A. K. Das, J. Solut. Chem., 8, 259 (1979).
104. Cox, B. G., R. Natarajan, W. E. Waghorne, J. C. S. Fara. I, 75, 86 (1979).
105. Cox, B. G., W. E. Waghorne, and C. K. Piggot, J. C. S. Fara I, 75, 227 (1979).
106. Friedman, H. I., J. Phys. Chem., 71, 1723 (1967).
107. Jones, E. D., E. A. Vehling, J. Chem. Phys., 36, 1691 (1962).
108. Dharmatti, S. S., H. E. Weaver, Phys. Rev., 84, 367 (1951).
109. Balimann, G., Doc. Thesis, Zurich (1977).
110. Balimann, G., and P. S. Pregosin, J. Mag. Reson. 26, 283 (1977).
111. Crutchfield, M. M., C. H. Dungan, J. H. L. Letcher, V. Mark, J. R. VanWazer, "Topics in Phosphorous Chemistry," Vol. 5, Interscience Publishing, New York (1967).





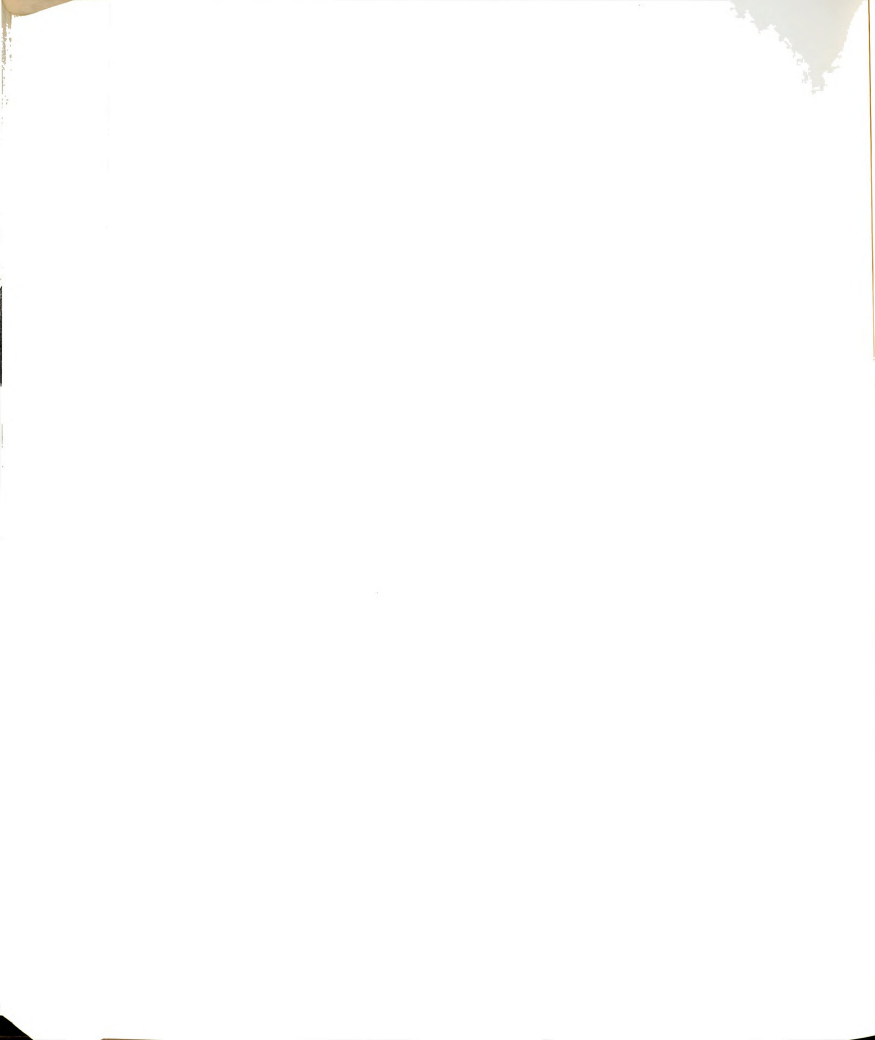
112. Mavel, G., Rep. NMR Spectroscopy, 5B, 1 (1973).
113. Nixon, J., A. Pidcock, Ann. Rep. NMR Spectroscopy, 2, 345 (1969).
114. Llinas, J. R., E.-J. Vincent, G. Peiffer, Bull. Soc. Chim. France, 3209 (1973).
115. Grim, S. O., W. McFarlane, E. F. Davidoff, T. J. Marks, J. Phys. Chem., 70, 581 (1966).
116. Latscha, H. P., Z. Naturforsch, 23b, 139 (1968).
117. Schmidpeter, A., H. Brecht, Inorg. Nucl. Chem. Lett. 4, 563 (1968).
118. Koole, N. J., A. J. DeKonig, M. J. A. DeBie, J. Mag. Reson. 25, 375 (1977).
119. Wilkie, C. A., J. Mag. Reson. 33, 127 (1979).
120. Sadtler Research Lab., Inc., Carbon-13 NMR, 4111 C (1978).
121. Sadtler Research Lab, Inc, Proton NMR 15520M,6505M (1973).
122. Wiegart, F. J., J. D. Roberts, J. Amer. Chem. Soc. 91, 4940 (1969).
123. Axelson, D. E., A. J. Oliver, C. E. Holloway, Org. Mag. Reson, 5, 255 (1973), 6, 64 (1974).
124. Hall, L. W., D. W. Lowman, J. D. Odom, Inorg. Chem. 14, 580 (1974).
125. Odom, J. D., L. W. Hall, P. D. Ellis, Org. Mag. Reson 6, 360 (1974).
126. Gragg, B. R., W. J. Layton, W. J. Niedenzu, J. Organomet. Chem., 132, 29 (1977).
127. Mazurek, M., T. M. Mallard, P. A. J. Gorin, Org. Mag. Reson, 9, 193 (1977).
128. Laitinen, A. A., W. E. Harris, "Chemical Analysis", McGraw-Hill Book Co., New York (1975).
129. Nelson, G. L., G. C. Levy, J. D. Cargieli, J. Amer. Chem. Soc. 94, 3089 (1972).



130. Onak, T. P. H. Landersman, R. E. Williams, J. Shapiro, *J. Phys. Chem.*, 63, 1533 (1959).
131. Noeth, H., H. Vahrenkamp, *Chem. Ber.* 99, 1049 (1966).
132. Thompson, R. J., J. C. Davies, *Inorg. Chem.*, 4, 1465 (1965).
133. Shipkowitz, N. L., R. R. Bower, R. N. Appell, C. W. Nordeen, L. R. Overby, W. R. Roderick, J. B. Schleicher, A. M. VonEsch, *Appl. Microbiol.*, 26, 264 (1973).
134. L. R. Overby, E. E. Robishaw, J. B. Schliecher, A. Rueter, N. L. Shipkowitz, J. C.-H. Mao, *Antimicrob. Ag. Chemother.*, 6, 360 (1974).
135. T. D. Brock, "Biology of Microorganisms", Prentice-Hall, Inc., New Jersey (1974).
136. B. W. Fox, *J. Antimicrob. Chemother.* 3, Suppl. A, 23 (1977).
137. T. H. Maugh, II, *Science*, 192, 128 (1976).
138. R. J. Klein, A. E. Friedman-Kien, *Antimicrob. Ag. Chemother.* 7, 289 (1975).
139. H. G. Adams, E. A. Benson, E. R. Alexander, L. A. Vontver, M. A. Remington, K. K. Holmes, *J. Infect. Des.* 133 (Suppl.): A151-A159 (1976).
140. E. L. Goodman, J. P. Luby, M. T. Johnson, *Antimicrob. Ag. Chemother.*, 8, 693 (1975).
141. A. E. Friedman-Kien, A. A. Fondak, R. J. Klein, *J. Invest. Dermatol.*, 66, 99 (1976).
142. D. D. Gerstein, C. R. Dawson, J. O. Oh, *Antimicrob. Ag. Chemother.*, 7, 285 (1975).
143. R. F. Meyer, E. D. Vernell, H. E. Kaufman, *Antimicrob. Ag. Chemother.*, 9, 308 (1976).
144. J. F. Fitzwilliam, J. F. Griffith, *J. Infect. Des.*, 133, Suppl. A221 (1976).
145. S. S. Leinbach, J. M. Reno, L. F. Lee, A. F. Isbell, J. A. Boezi, *Biochemistry*, 15, 426 (1976).
146. J. Roboz, R. Suzuki, G. Bekesi, R. Hunt, *Biomed. Mass Spectrom.*, 4, 291 (1977).

147. B. A. Bopp, C. B. Estep, P. J. Anderson, Fed. Proc. 36, 939 (1977).
148. T. R. Herrin, J. S. Fairgrieve, R. R. Bower, N. L. Shipkowitz, J. Mao, J. Med. Chem., 20, 660 (1977).
149. L. F. Lee, K. Nazerian, S. S. Leinbach, J. M. Reno, J. A. Boezi, J. Natl. Cancer Instit., 56, 823 (1976).
150. J. M. Reno, L. F. Lee, J. A. Boezi, Antimicrob. Ag. Chemother., 13, 188 (1978).
151. P. Nylen, Z. Anorg. Allg. Chem., 235, 33 (1937).
152. S. Warren, M. R. Williams, J. Chem. Soc. (B), 618 (1971).
153. L. L. Burger, J. Phys. Chem., 62, 590 (1958).
154. A. A. Elesin, A. A. Zaitseve, S. S. Kazakova, G. N. Yakovlev, Radiokhimiya, 14, 541 (1972).
155. A. A. Elesin, A. A. Zaitseve, S. S. Kazakova, G. N. Yakovlev, Nucl. Sci. Abstr., 28, 18030 (1973).
156. J. Mao, E. Robishaw, Biochemistry, 14, 5475 (1975).
157. H. Stunzi, D. D. Perrin, J. Inorg. Biochem., 10, 309 (1979).
158. P.-H. C. Heubel, Ph.D. Thesis, Michigan State University, E. Lansing, MI (1978).
159. J. W. Ross, Science, 156, 1378 (1967).
160. B. Collier, Anal. Chem., 42, 1443 (1970).
161. A. Shatkay, Anal. Chem., 39, 1062 (1967).
162. G. A. Rechnitz., Chem. & Eng. News, 12 June, 146 (1967).
163. C. R. Powley, R. F. Geiger, Jr., T. A. Nieman, Anal. Chem., 52, 705 (1980).
164. F. S. Nakayama, B. A. Rasnick, Anal. Chem., 39, 1022 (1967).
165. G. A. Rechnitz, Z. F. Lin, Anal. Chem., 40, 696 (1968).
166. G. A. Rechnitz, T. M. Hsev, Anal. Chem., 41, 111 (1969).

167. J. I. Watters, S. Kalliney, R. C. Machen, 31, 3823 (1969).
168. M. S. Mohan, G. A. Rechnitz, J. Amer. Chem. Soc., 94, 1714 (1972).
169. Y. S. Kim, G. M. Padilla, Anal. Biochem., 89, 521 (1978).
170. A. Craggs, C. J. Moody, J. D. R. Thomas, Analyst., 104, 961 (1979).
171. J. Townsend, Nature, 173, 1090 (1954).
172. R. G. Hayes, R. J. Myers, J. Chem. Phys., 40, 877 (1964).
173. J. B. Flato, Ph.D. Thesis, New York University, New York, New York (1968).
174. J. R. Bard, J. O. Wear, Z. Naturforsch, 26b, 1091 (1971).
175. G. P. Vishnevskaya, F. M. Gumerov, O. A. Nardid, V. A. Moiseevi Z. H. Strukt. Khim., 19, 1020 (1978).
176. L. Burlamacchi, E. Tiezzi, J. Mol. Struct., 2, 261 (1968).
177. R. E. Blankenship, K. Sauer, Biochim. Biophys. Acta., 357, 252 (1974).
178. R. Basosi, N. Niccolai, E. Tiezzi, G. Valensin, J. Amer. Chem. Soc., 100, 8047 (1978).
179. R. Basosi, F. Laschi, E. Tiezzi, G. Valensin, J. Chem. Soc., Far. Trans. I, 72, 1505 (1976).
180. R. S. Levy, J. L. Villafranca, Biochemistry, 16, 3293 (1977).
181. M. K. Green, G. Kotowycz, Can. J. Biochem., 57, 995 (1979).
182. R. N. Armstrong, H. Kondo, J. Granot, E. T. Kaiser, A. S. Mildaun, Biochemistry, 18, 1230 (1979).
183. L. Mietes, "Polarographic Techniques", Interscience New York (1965).
184. F. A. Cotton, G. Wilkinson, "Basic Inorganic Chemistry" John Wiley & Sons, New York (1976).



185. M. J. Weaver, F. C. Anson, *J. Electroanal. Chem.*, 65, 737 (1975).
186. R. C. Weast (Ed.), "CRC Handbook of Chemistry and Physics", CRC Press, Cleveland, (1975).
187. Orion Research Publication, Form 93-20/9710 (1979).
188. A. Sabatini, A. Vacca, P. Gans, *Talanta*, 21, 53 (1974).
189. A. K. Grzybowski, S. S. Tate; S. P. Datta, *J. Chem. Soc. (A)*, 241 (1970).
190. R. H. Stokes, R. A. Robinson, *J. Amer. Chem. Soc.*, 70, 1870 (1948).
191. J. Kielland, *J. Amer. Chem. Soc.*, 59, 1675 (1937).
192. V. M. Goldschmidt, *Nor. Vidensk. Akad. Oslo Skr. Math. Nat. Kl.*, No. 2 (1926).
193. E. L. Yee, J. Tabib, M. J. Weaver, *J. Electroanal. Chem.*, 96, 241 (1979).
194. J. M. Kolthoff, J. J. Lingane, *Polarography, Inter-science*, New York (1952) 2nd ed.
195. R. P. Buck, *J. Electroanal. Chem.*, 5, 295 (1963).
196. H. S. Harned, E. B. Owen, "The Physical Chemistry of Electrolyte Solutions", Reinhold Publishing Corp., New York (1958) 3rd ed., page 165.
197. O. W. Moe, L. G. Butler, *J. Biol. Chem.*, 247, 7308 (1972).
198. O. W. Moe, L. G. Butler, *J. Biol. Chem.*, 247, 7315 (1972).
199. J. A. Boezi, *Pharmacol. Ther.*, 4, 231 (1979).
200. O. W. Moe, L. G. Butler, *J. Biol. Chem.*, 247, 7303 (1972).
201. G. Schwarzenbach, *Helv. Chem. Acta.*, 35, 3244 (1952).
202. Chemistry 838, Unit RX-1, Michigan State University, East Lansing, MI (1980).
203. Chemistry 838 TECO, Michigan State University, East Lansing, MI (1980).

204. J. L. Dye, V. A. Nicely, F. Tehan, R. Cochran, J. Leckey, KINFIT<sup>4</sup>, Michigan State University, E. Lansing, MI (1977).







MICHIGAN STATE UNIVERSITY LIBRARIES



3 1293 03056 3484